PHD

The role of alpha7 nicotinic receptors in reinstatement of drug-induced conditioned place preference

Coccia, Giulia

Award date:
2022

Awarding institution:
University of Bath

The role of alpha7 nicotinic receptors in reinstatement of drug-induced conditioned place preference

Maria Giulia Coccia

A thesis submitted for the degree of Doctor of Philosophy

University of Bath

Department of Pharmacy and Pharmacology

September 2022

To Alisha

ACKNOWLEDGEMENTS

This work was performed under the supervision of Dr. Chris Bailey, Prof. Sue Wonnacott and Prof. David Heal with financial support from University of Bath, RenaSci and DevelRX Nottingham, UK.

My first thanks go to my supervisors, their guide and continuous feedback throughout my PhD have been essential in achieving this important goal. In particular, thanks Chris for helping me with patch-clamp and to be a fantastic mentor who every PhD student should have. Also, thanks a lot Sue for being an excellent supervisor too and for giving me brilliant advice, food for thoughts and for listening to my PhD troubles! Finally, thanks to Dave and Sharon for your suggestions and support, both intellectual and financial, we definitely need to meet up again. I want to thank the 4 South staff, in particular Martin and Lesley for their help and technical advice during my experiments, and for trying so hard to overcome my strong Italian accent.

Thanks to all the members of the Bailey Lab, in particular Sam for being a very good ephys teacher but also a great friend and thank you Sammy to have me brought to the Lake District in my first year! Also, thanks a lot to Eloise for being a fantastic friend and for helping me with very complicated spreadsheets. Thanks to all the fellas from the 2.48 PhD office, it has been a pleasure to share the office with them, thanks for all the laughs, emotional support and fun that we used to have.

I should say *grazie* to my Italian friends in Bath. In particular, thanks to Andrea and Davide for having so much fun together and for helping me with the Vespa. Also, thanks to Antonietta e Marco for hosting Fra and I, and my suitcases, during my last days in Bath, I am still waiting for you here in Milan! Finally, thanks to Luca and Claire for all the fantastic adventures around the UK.

Many thanks to my parents, Gianna and Augusto, for always being my cornerstone and for supporting myself no matter what, also thank you guys for shipping big boxes full of Italian groceries! Thanks to my friend from Rome and Roccantica because you were always with me, even if a bit far!

Finally, I really want to thank Francesco for making this life experience special. Thank you for your love, support, surprises, and just for making me happy every day… *Je cu' tte ce so' rimast' asott'*, and I cannot wait to see what the future holds for us.

TABLE OF CONTENTS

LIST OF FIGURES

CHAPTER 1: INTRODUCTION

CHAPTER 2: MATERIALS AND METHODS

CHAPTER 3: THE ROLE OF α7NACHRS IN MODULATING HEROIN- AND COCAINE-INDUCED REINSTATEMENT AND THEIR IMPACT ON C-FOS EXPRESSION

CHAPTER 4: INVESTIGATION OF PRE- AND POST-SYNAPTIC EFFECTS OF α7NACHRS IN VENTRAL AND DORSAL HIPPOCAMPUS

CHAPTER 5: HOW DO α7NACHRS MODULATE POST-SYNAPTIC CHANGES IN VENTRAL CA1 DURING THE REINSTATEMENT OF A HEROIN-CPP ?

CHAPTER 6: HOW ARE THE PROJECTING AREAS OF THE VHIP INVOLVED IN HEROIN-INDUCED REINSTATEMENT? A NEURONAL-TRACING STUDY

CHAPTER 7: DISCUSSION AND CONCLUDING REMARKS

LIST OF TABLES

LIST OF ABBREVIATIONS

ACh Acetylcholine

AChE Acetylcholinesterase

aCSF Artificial cerebrospinal fluid

AMPA(R) 2-Amino-3-(3-hydroxy-5-methyl-isoxazol-4-yl)propanoic acid (receptor)

ANOVA Analysis of variance

ATP Adenosine triphosphate

BLA Basolateral amygdala

CA1 Cornu ammonis regions 1

CA2 Cornu ammonis regions 2

CA3 Cornu ammonis regions 3

CaMKII Ca^{2+}/calmodulin-dependent protein kinase II - IV

cAMP Cyclic adenosine monophosphate

ChAT Choline acetyltransferase

CNS Central nervous system

CPP Conditioned place preference

CREB cAMP response element-binding protein

CTB Cholera Toxin B

D-AP5 (2R)-amino-5-phosphonovaleric acid

DA Dopamine

DAPI 4′,6-diamidino-2-phenylindole

dCA1 Dorsal cornus ammonis 1

DG Dentate gyrus

dHIP Dorsal hippocampus

DHβE Dihydro-beta-erythroidine

EGTA Ethylene glycol tetraacetic acid

ERK Extracellular signal–regulated kinases

EPSC Excitatory postsynaptic current

FG Fluorogold

$GABA_AR$ Gamma-aminobutyric acid receptor

GECIs Genetically encoded calcium indicators

GFP Green fluorescent protein

GluR- glutamate receptor

GPCR G-protein coupled receptor

GTP Guanosine triphosphate

HEPES Hydroxyethyl piperazineethanesulfonic acid

IEGs Immediate early genes

i.p Intraperitoneal

IL Infralimbic

IPSC Inhibitory postsynaptic current

LDT Lateral dorsal tegmental

LTD Long term depression

LTP Long term potentiation

mAChR Muscarinic acetylcholine receptors

MAPK Mitogen-activated protein kinase

mGLuR Metabotropic glutamate receptor

MK-801 Dizocilpine

MLA Methyllycaconitine

mPFC Medial prefrontal cortex

mRNA Messenger ribonucleic acid

MS medial septum

MSN Medium spiny neuron

NAc Nucleus accumbens

NAc Shell Nucleus accumbens Shell

nAChRs Nicotinic acetylcholine receptors

NBQX (2,3-dioxo-6-nitro-7-sulfamoyl-benzo[f]quinoxaline)

NMDA(R) N-methyl-D-aspartate (receptor)

NMDG N-methyl-D-glucamine

NBM Nucleus basalis of Meynert

PAM Positive allosteric modulators

PBS Phosphate buffered saline

PFA Paraformaldehyde

PFC Prefrontal cortex

PKA Protein kinase A

PL Prelimbic cortex

PNU-120596 N-(5-Chloro-2,4-dimethoxyphenyl)-N'-(5-methyl-3-isoxazolyl)-urea

PNU-282987 N-(3R)-1-Azabicyclo[2.2.2]oct-3-yl-4-chlorobenzamide

PPR Paired-pulse ratio

PPT pedunculopontine tegmental nuclei

QX-314 N-(2,6-Dimethylphenylcarbamoylmethyl) triethylammonium

RI Rectification index

SA Self-administration

s.c Subcutaneous

SEM Standard error of the mean

sEPSC spontaneous excitatory post-synaptic currents

SI Substantia innominata

sIPSC Spontaneous inhibitory post-synaptic currents

SN Substantia nigra

STD Short-term depression

vCA1 Ventral cornus ammonis 1

VDB Vertical limb of the diagonal band of broca

VGCC Voltage-gated calcium channel

vHIP Ventral hippocampus

VTA Ventral tegmental area

ABSTRACT

The cholinergic system in the central nervous system is profoundly implicated in cognition, learning and memory. The ventral hippocampus (vHIP) plays a key role in associative memory, in which acetylcholine (ACh) contributes to modulating neurotransmission and synaptic plasticity. Data from our lab have previously shown that inhibition of alpha7 nicotinic acetylcholine receptors (α7nAChRs) in vHIP via the selective antagonist methyllycaconitine (MLA) specifically attenuated morphine-induced reinstatement in a drug-seeking model. However, the specific action by which α7nAChRs regulate drug-related memories in vHIP is poorly understood. The aim of this work was to understand how α7nAChRs in vHIP modulate heroin- and cocaine-induced reinstatement using conditioned place preference (CPP), a Pavlovian paradigm of drug-seeking. 7-9 week old C57BL/6J male mice underwent CPP using either heroin or cocaine as the rewarding drug. Following acquisition and extinction, mice were pre-treated with either saline or MLA (4 mg/kg) prior to heroin- or cocaine-induced CPP reinstatement. MLA inhibited reinstatement of heroin CPP, but not cocaine CPP. The mechanisms of this effect were explored via immunofluorescence for c-Fos expression, a marker of neuronal activation involved in synaptic modifications. After reinstatement of heroin CPP, MLA significantly decreased c-Fos expression in vHIP but not in dorsal hippocampus (dHIP). Subsequently, patch-clamp electrophysiological experiments aimed to explore how α7nAChRs modulate the hippocampal network revealed that α7nAChRs are post-synaptically located in both vHIP and dHIP of naïve mice. Moreover, 8-9 weeks old c-Fos-GFP mice, expressing GFP fluorescent protein in c-Fos neurons, underwent heroin-CPP, and electrophysiological experiments were performed to explore mechanisms of synaptic plasticity after heroin-primed reinstatement and how MLA could affect those mechanisms. Finally, a retrograde tracing experiment was performed to understand how the projecting areas of the vHIP are involved in heroin-induced reinstatement, by performing brain infusions of retrograde tracers and subsequent co-labelling with c-Fos neurons, defining the major target areas of the vHIP. This thesis demonstrates that α7nAChRs modulate heroin-associated memories selectively in vHIP, where those receptors are post-synaptically located.

CHAPTER 1
INTRODUCTION

Relapse is one of the major issues for individuals suffering from drug addiction. The neural mechanisms underlying this phenomenon are various and extremely complex, and they still need to be fully understood. Drug-context associations underpin relapse-like behaviours, which are one of the major issues of this psychopathology. Thus, the aim of this thesis was to investigate the role of α7nAChRs in ventral hippocampus (vHIP) in a model of drug-seeking behaviour, namely conditioned place preference (CPP), after its extinction. In this thesis heroin and cocaine conditioned place preference in mice have been performed, to study the impact of the drug-associated memories on relapsing drug-seeking behaviour. Immunofluorescence was used to detect the expression of the immediate early gene c-Fos, a marker of neuronal activation, and patch-clamp electrophysiological experiments have been performed to characterise functional α7nAChRs in hippocampus.

1.1 Psychopathology of drug-addiction: an overview

1.1.1 Motivation, learning and memory

"The urge to transcend self-conscious self-hood is, as I have said,
a principal appetite of the soul."
Aldous Huxley, "The Doors of Perception"

All organisms, including humans, have an intrinsic need to approach positive stimuli and avoid negative ones, and this has an evolutionary function. The nervous system coordinates the selection of the strategies, aimed to advance or escape from such stimuli, which depends on complex interactions between organism and environment. In this adaptive behaviour, the value of the rewarding or negative stimuli is strongly identified, as well as their predictive cues, leading the individuals to the desired outcomes. Behaviour is widely influenced by motivational salience, which consists

of the power of relevant or arousing stimuli to provoke an attentional or behavioural change, leading to the individual to focus on the surrounding stimuli (Puglisi-Allegra & Ventura, 2012). The association between emotionally salient events and the environmental stimuli induce the formation of highly enduring memories which can strongly affect behaviour. However, in some pathological circumstances highly salient memories are experienced intrusively leading the individual to maladaptive outcomes, developing psychopathologies. An example of this condition is drug addiction, in which environmental stimuli or discrete cues paired with drug effects acquire the ability to trigger intense drug desire that leads to drug-taking and drug-seeking behaviours (Robinson & Berridge, 1993; Childress et al., 1999; Everitt et al., 2001; Shalev et al., 2002). In Pavlovian terms, motivational properties of an unconditioned stimulus are transferred to a stimulus initially neutral that becomes a conditioned stimulus able to evoke a conditioned response. Unconditioned stimuli with a positive valence are defined as "rewarding", where reward is experienced as "making things better" and, therefore, pursued (Berridge & Robinson, 2003).

1.1.2 The three theories of drug-addiction

As elegantly defined by White (2011), "reward" generally refers to a phenomenon which induces a pleasant or emotionally positive experience. In other words, reward is thought of as an event that fosters behaviour when this event is contingent with the behaviour itself, becoming a synonymous of reinforcement (White, 2011). This assumption is important to understand the different theories of addiction, which are aimed to explain the complexity of the neurocircuitry of this disorder. The common postulate is that the extended drug use induces several types of neuroadaptations underlying the more serious and long-lasting stages of this psychopathology.

In their theory, Koob and Le Moal (1997) support the idea that prolonged access to a drug of abuse causes a pathological shift from the hedonic state, provoked by the rewarding effect of the drug, to a dysregulation of brain reward system, which results in experiencing dysphoria and anxiety when the access to drug is prevented, and loss of control over drug-intake (Koob & Le Moal, 1997). In other terms, the drug-use affects the reward system, compromising the ability of the individual to maintain homeostasis over changes. The authors hypothesised that the main cause of this "hedonic shift" can be found in enhanced sensitivity and counteradaptation of the

brain reward system, involving a dysregulation of the mesolimbic dopamine (DA) and the opioid and stressor hormone functions. Thus, according to this theory, this hedonic shift provokes loss of control over drug use through mesocorticolimbic brain circuits that are involved in compulsive behaviour.

On the other hand, Robinson and Berridge (1993) suggest an "incentive sensitisation" theory of addiction, according to which the drug of abuse affects several brain areas, specifically the ones involved in modulating the incentive motivation and reward for natural appetitive stimuli. According to this theory, the chronic use of drug implies that the motivational and rewarding properties of the drugs are transferred to the contextual stimuli, making the individual enduringly hypersensitive to them. Importantly, those drug-associated cues are responsible for the switch for drug "liking", present during the initial state of the pathology, to drug "wanting", characterising the compulsive patterns of drug-seeking behaviour (Robinson & Berridge, 1993).

Everitt and Robbins (2005) hypothesised that drug-induced neural modifications sustain the persistence of drug addiction though the formation of "habits" in the form of aberrant stimulus-response learning, sustained by the instrumental learning (Everitt & Robbins, 2005). In other words, those habits lead to compulsive behaviours, defined as the maladaptive persistence of drug-seeking behaviours despite the negative consequences (Dalley et al., 2011), with alteration of cortical activity leading to reductions in behavioural control and decision-making skills (Jentsch & Taylor, 1999). Importantly, some other theories have focused on the role of the prefrontal cortex (Goldstein & Volkow, 2002) or of the cellular memory induced by drug consumption, responsible for synaptic adaptations induced by drug-intake (Nestler, 2013).

All of those theories investigate different features of the psychopathology of drug-addiction, and they have had a crucial impact on the direction that drug-addiction research has taken, even if none of them should be interpreted as definitive. In fact, drug-addiction is a complex and multi-factorial disorder, in which organism-environment interactions, individual differences, type of drugs of abuse, coping and resilience skills, and comorbidity with other psychopathologies

dynamically interact. Hence, to enlarge scientific knowledge about each of those aspects and integrating new findings with old and new addiction theories is a crucial strategy to better understand this pathology and improve the quality of life of addicts.

1.1.3 Social impact of drug-addiction

Drug addiction is a chronic, relapsing neuropsychiatric disorder and a major public health issue which affects societies in terms of health care, families, criminality and accidents. According to the Diagnostic and Statistical Manual of Mental Disorders (DSM-5), of the American Psychiatry Association, human addiction is characterised by compulsive drug-seeking and taking behaviour, despite the negative consequences, physical and psychological problems related to use and craving. This disorder has also been conceptualised in a range, from mild to severe, depending on the number of symptoms manifested. More broadly, drug-addiction is characterised by the following phases: occasional use, recreational use, regular use, and addiction (Koob, 2017). Frequent drug-use and addiction are major public health problems. In fact, it has been reported that 3.5-7% of the world's population aged 15-64 tried an illicit drug at least once in 2012, and approximately 33 million drug users worldwide abuse opioid drugs (UNODC, 2014). The abuse of synthetic opioids, such as fentanyl, keeps rising, reaching more than 56,516 overdose deaths reported in the USA in 2020 (Source: CDC WONDER). Hence, due to the severe consequences of drug abuse disorders on society, the impact of this pathology is monitored and constantly studied.

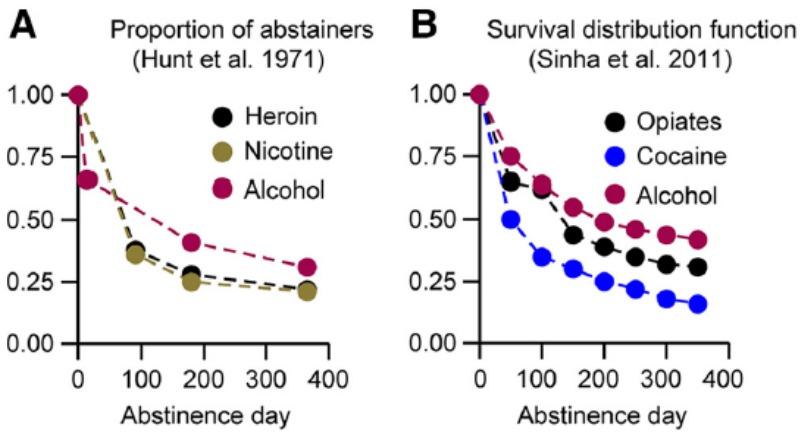

Figure 1.1 - Relapse rates in 1971 and 2011 – (**A**) Relapse rates from addiction programs and (**B**) relapse to drug use in addiction clinics (Dong et al., 2017)

One of the major issues of this disorder is the high rate of relapse in drug-addicts, which remained unchanged in the last 40 years, reinforcing the classic definition of drug-addiction as a chronic, relapsing disorder (Leshner, 1997). In fact, as reported in Figure 1.1, with opioids, relapse rates to first reuse are approximately 60% after 3 months and 80% after 12 months of abstinence.

1.1.4 Animal models of drug-seeking

Pre-clinical research provides a variety of sophisticated animal models of drug-addiction, essential to understanding more in depth the neurobiology and neuropharmacology of this psychopathology. Conditioned place preference (CPP) and intravenous drug-self administration (SA) are the most common techniques to study several features of drug-addiction, such as the rewarding effects of the drug, extinction of conditioned responses and relapse prevention. Those behavioural tasks investigate different aspects of a complex psychiatric disorder, both presenting advantages and limitations and this is the reason why results from these approaches should be interpreted as "complementary", rather than in opposition. CPP, based on Pavlovian learning, is normally performed under strictly controlled experimental conditions in rodents, primates and humans (Cunningham et al., 2006; Tzschentke, 2007; Childs & de Wit, 2009). Specifically, animals are exposed to an apparatus having two initially neutral contexts, which are characterised by different texture, spatial stimuli, odours or lighting and so on (Tzschentke, 2007). In general, animals are exposed, or "conditioned", to one of the two arenas after an injection of a drug of interest, while the day after the other compartment will be associated with an injection of saline as a control (Figure 1.2). After the training, which consists of a few conditioning sessions, animals are allowed to freely explore both compartments in a drug-free state, and the preference for one of the two compartments is assessed. If a drug has rewarding effects, the animal should spend more time in the drug-paired side and, in accordance, several drugs of abuse, such as opiates or cocaine, normally induce CPP (Swerdlow et al., 1989). This procedure is a useful, non-invasive and low cost behavioural task to evaluate the drug-related associations, induced by the rewarding properties of the drug itself (Bardo & Bevins, 2000). In addition, pharmacological or genetic manipulations can be performed to test if those affect the CPP, in terms of alteration in the associative leaning and incentive salience toward the conditioned stimulus. However, CPP can be difficult to interpret if the animals

show a previous preference for one compartment before the conditioning training, and, importantly, the nature of this model does not allow any voluntary learning or choice. On the other hand, there is a widely used variant of CPP where the less favoured compartment is paired with the rewarding stimulus, yielding valid results.

In contrast, in SA animals actively learn an operant behaviour, such as lever press or nose spoke, to obtain a drug of abuse though an intravenous catheter. In general, the drug delivery is predicted by a light and/or a tone, and these become drug-associated stimuli (Schuster & Thompson, 1969). This behavioural task can be used to model human craving for the majority of the drugs of abuse. SA is generally thought a better model for human addiction, as it is volitional and contingent, crucial aspects for developing addiction. However, this approach presents some limitations. Because of the nature of this paradigm, the animal receives the drug under the effect of the drug itself, leading to an increase of lever pressing, and the surrounding environment of the animal is depleted, in which the major stimulus for the animal is the lever pressing itself. Moreover, SA is a highly invasive approach, requiring surgery and long-term maintenance of a catheter, coupled with single housing, making it difficult to translate to a typical human condition.

Thus, even if CPP might be considered as a simpler model, it is an excellent paradigm to study the drug-related memories and their impact in inducing relapse. For example, in this thesis, where one aim is to understand how α7nAChRs modulate drug-seeking behaviour, specifically in the ventral portion of the hippocampus, where those reward-related associations are stored and reactivated. Furthermore, CPP has the advantage over SA, to test animals in drug-free state, reducing the impact of locomotor sensitisation or tolerance; it can be used as an experimental model of reward-learning and aversion. Finally, it can be used not only for the study of the reward itself but also the extinction and the relapse, or reinstatement, of the conditioned responses.

Thus, in the present thesis, CPP has been used as a model of relapse of drug-associated conditioned responses, as important mechanism which takes part in the onset of addiction.

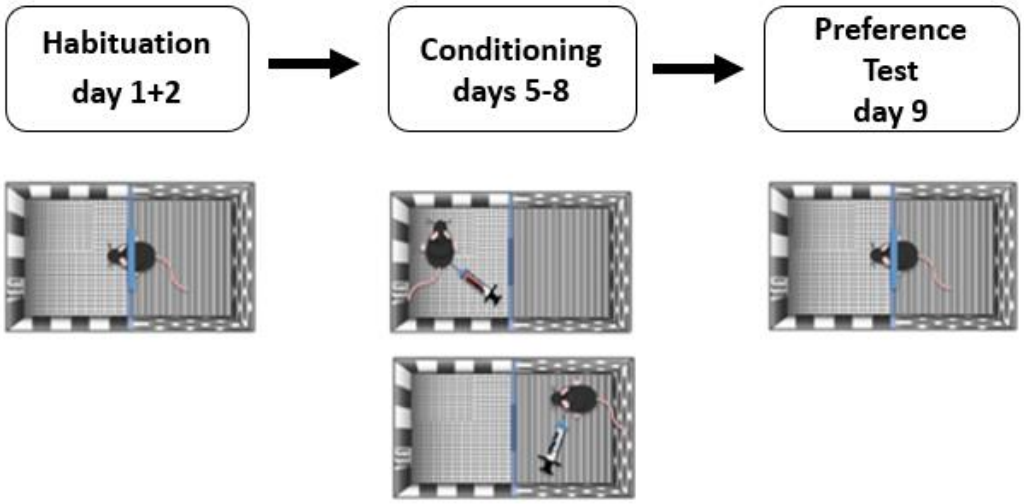

Figure 1.2 – The general protocol for the acquisition of conditioned place preference in mice - During the habituation session (day 1+2) mice freely explore the apparatus for 15 minutes in each day, to obtain a baseline and assess any possible prior preference or avoidance. In the conditioning phase (day 5-8) mice are administered daily, alternating doses of either saline or drug dose and confined in either side of the CPP box separated by guillotine door. On day 9 animals are once again allowed to explore the apparatus in drug-free state. The time spent during habituation and performance test is recorded by Ethovision software**.**

1.2 Exploring the neurocircuitry of drug-related memories and behaviours

The dopaminergic system, involving dopaminergic neurons in the ventral tegmental area that project to the nucleus accumbens, has been characterised as the reward circuit for years (Salamone & Correa, 2012). This pathway involves several brain regions, such as prefrontal cortex, amygdala, hippocampus and other brain areas. All of these so called "brain reward regions" (Russo & Nestler, 2013) are inter-connected in complex ways, through different neurotransmitter pathways, such as dopamine, glutamate and GABA (Figure 1.3).

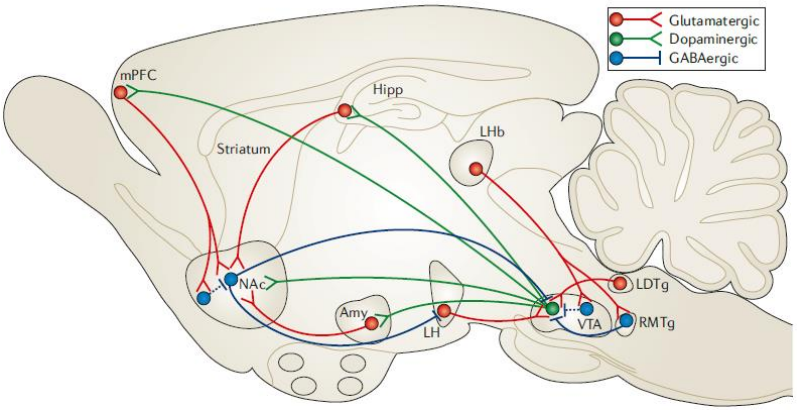

Figure 1.3 – Simplified scheme of the brain pathway for reward processing - Major dopaminergic, glutamatergic and GABAergic connections to and from the ventral tegmental area (VTA) and nucleus accumbens (NAc) in the rodent brain. The primary reward circuit involves dopaminergic projections from the VTA to the NAc, which release dopamine in response to reward-associated stimuli. There are also GABAergic projections from the NAc to the VTA. Moreover, NAc receives dense innervation from glutamatergic monosynaptic circuits from the medial prefrontal cortex (mPFC), hippocampus (Hipp) and amygdala (Amy), as well as other regions. The VTA receives such inputs from the lateo-dorsal tegmentum (LDT), lateral habenula (LHb) and lateral hypothalamus (LH), not treated in the main text. These glutamatergic inputs regulate of reward-related perception and memory (Russo & Nestler, 2013)

In this section, the main brain pathways involved in reward processing and their reciprocal interaction will be discussed, highlighting also the role of other non-conventional reward systems.

1.2.1 Reward system and the dopaminergic hypothesis

For years, the mesocorticolimbic dopamine (DA) has been the focus for the study of the neural basis of drug-addiction. In general, all drugs of abuse have the power to increase DA release in the nucleus accumbens (NAc), either directly involving the

dopaminergic neuron in the ventral tegmental area (VTA) or indirectly through other systems (Wise, 2008). Early studies showed that dopaminergic depletion, induced by 6-OHDA infusion in those areas, microinjections of dopamine antagonists, or D1 and/or D3 receptor knockout mice all decreased reward-seeking behaviours (Smith et al., 1985; Koch et al., 2000; Karasinska et al., 2005). Phasic firing of DA neurons is essential for processing reward and to establish long-term associations between rewarding effects of the drug and predictive stimuli, while tonic DA release modulates motivation and arousal (for review, see Wise & Robble, 2020). Specifically, DA neurons in the VTA project to the NAc. This brain area has been defined as "limbic–motor interface" at which motivation- and emotion-related processing is connected with the motor system (Mogenson et al., 1980). It is also directly involved in processing reward and goal-directed behaviours sustained by salient stimuli (Salamone & Correa, 2012). The DA input in NAc and in dorsal striatum induces GABA release in those areas, sustaining motivation and reinforced behaviours, but also processing aversive stimuli (for review, see Pignatelli & Bonci, 2015). The dorsal striatum also receives DA afferents from the substantia nigra (SN) and this interplay is responsible for transforming the persistent reward signals into goal-directed behaviours, which over time become less responsive to the rewarding properties of the goal.

DA neurons from the VTA also project to hippocampus and amygdala (Lisman & Grace, 2005; Lutas et al., 2019), which regulate emotional and memory associations, and to several subregions of the PFC (for review, see Lammel et al., 2014), modulating salience attribution and inhibitory control, all contributing in the development of drug-addiction, from the first rewarding experience to chronic drug-intake.

The dopaminergic hypothesis represents a good attempt in explaining the complexity of reward system, and it has driven for years very interesting research, with consequent important findings in the field. However, it remains too simplistic and there are some findings reporting contrasting results with this hypothesis (for review, see Salamone & Correa, 2012). Overall, it is well accepted that mesolimbic DA plays an important role in motivation, goal-directed behaviours and in processing reward-associated cues. However, several studies have demonstrated that both the block of

DA receptors or inhibition of DA synthesis do not always compromise the euphoria, normally associated with rewarding experiences (fore review, see Salamone & Correa, 2012). Interestingly, it has been recently studied that D2 antagonists do not block either SA of opiates or their associated cues (Heal & Smith, 2021). Therefore, DA transmission is not necessarily involved in the acute rewarding or psychoactive effects of opiate (Heal & Smith, 2021). Hence, the DA transmission might not be the main neural actor in processing the pattern of effects of the drug under investigation, as it will be better explained in section 1.2.8.

Although reward research has mainly addressed to the study of dopamine (Ikemoto, 2010), there other brain pathways and neurotransmitters that need to be integrated in understanding the neurocircuitry of reward and addiction.

1.2.2 Beyond the dopaminergic hypothesis, what is the role of acetylcholine?

Acetylcholine (ACh) is released throughout the mammalian nervous system, and it modulates attention, cognition, memory formation, awake-sleep cycles and reward. In the Central Nervous System (CNS), ACh mediates neuronal excitability, synaptic release of neurotransmission and coordinates firing groups of neurons (for review, see Picciotto et al., 2012). There is a wide body of evidence investigating the role of cholinergic system in reward. For example, silencing ACh interneurons in NAc decreased the cocaine-CPP, while activating these cells did not have effect in potentiating a place preference (Witten et al., 2010). Optogenetic activation of ACh interneurons in NAc provoked an inhibitory post-synaptic current mediated by $GABA_A$ receptor, while their silencing induced an increase in firing rate, demonstrating an important interplay between those two systems (Witten et al. 2010). In addition, other optogenetic studies reported that the inputs from the VTA to ACh interneurons in the NAc are selectively GABAergic and the activation of those, with the concomitant inhibition of ACh interneurons firing, improved associative learning related to aversive stimuli (Brown et al., 2012). As reviewed by Kaneda (2019), cholinergic neurons in the latero-dorsal tegmental nucleus (LDT), another key area for reward processing, contributes to induce synaptic adaptations underlying addictive behaviours (Kaneda, 2019).

Overall, ACh interneurons in the NAc are believed to play a key role for modulating associations between drugs and contextual cues that lead to relapse of drug-seeking and taking behaviour (Exley & Cragg, 2008).

The cholinergic septal-hippocampal pathway importantly contributes to memory storage and reactivation, including drug-related memories, also via the α7nAChR, a homomeric, ion channel highly expressed in the hippocampus (see section 1.3). Therefore, the aim of this thesis is to better clarify the role of hippocampal α7nAChR in reward-associated memories.

1.2.3 Long-term potentiation as a correlate of drug-related memory

Exposure to drugs of abuse changes the brain, whether they are self-administered or not (Luscher & Malenka, 2011), and induce development of memory traces of drug experience (Wise & Koob, 2014), suggesting that those mechanisms are associative and synapse specific (Hyman et al., 2006). Thus, it is essential to understand the cellular and molecular mechanisms underlying the encoding of drug-memories and how those memories can lead to relapse.

Glutamatergic excitatory transmission and its receptors play an essential role in this process and is responsible for the complex phenomena of synaptic plasticity or "metaplasticity" (for review, see Chiamulera et al., 2021). Long-Term Potentiation (LTP) and Long-Term Depression (LTD) increases or weakens synaptic strength, respectively by modifying neural circuitry in response to changes in neural stimulation, by altering gene and protein expression. Those changes are sustained by alterations in glutamatergic receptors, on the post-synaptic site. In particular, calculating the ratio between amino-3-hydroxy-5-methyl-4-isoxazole propionic acid receptor (AMPAR)-mediated synaptic currents, that are tetrameric ionotropic glutamate receptors mediating fast excitatory transmission, and N-methyl-D-aspartate receptor (NMDAR)-mediated synaptic currents of a population of stimulated synapses is a normalization procedure to measure the synaptic strength and it is independent of factors such different preparations or the number of synapses that are activate (Kauer & Malenka, 2007).

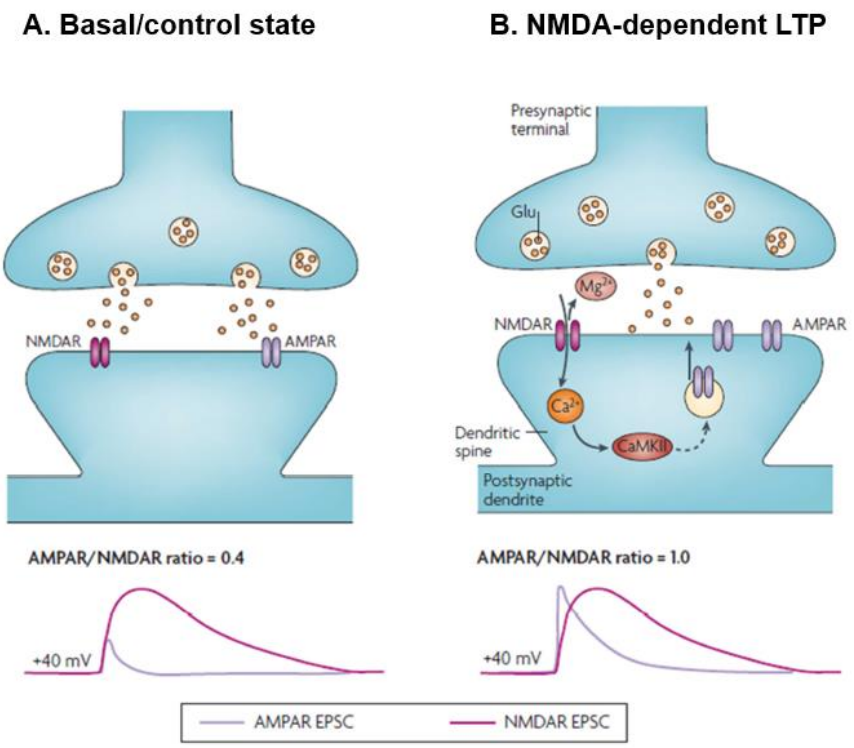

Figure 1.4 – Schematic diagram of AMPA and NMDA changes in basal state (A) and during NMDA-dependent LTP (B) – Sustained glutamate release from the pre-synaptic (**A**) induces depolarisation of the post-synaptic terminal through the activation of AMPAR, resulting in the Mg^{2+} block removal form NMDAR and subsequent Ca^{2+} influx. The intracellular Ca^{2+} activates CaMKII that, via downstream cascades, induces insertion of AMPA into the postsynaptic membrane, leading to an increase in AMPA receptor density at the synapse (**B**), measurable as an increase in AMPA/NMDA ratios. This results in the strengthening of the synapse. Below are shown examples of AMPA/NMDA currents and their ratios during A and B, when the excitatory post-synaptic current (EPSC) is measured at +40mV, in order to measure both AMPA and NMDA currents. (Adapted from Kauer & Malenka, 2007).

There are several types of LTP (Kauer & Malenka, 2007), however this section will focus on the most widely investigated, in particular in addiction-related topics, which is the NMDA-dependent LTP. This form was first found in the hippocampus (Rosenblum et al., 2002), but it has been also demonstrated that this LTP occurs in other brain regions, such as NAc, VTA and cortex (van Huijstee & Mansvelder, 2014). It requires activation of the post-synaptic AMPAR, by pre-synaptic glutamate release, which induces membrane depolarisation and the subsequent Mg^{2+} block removal from the NMDAR, allowing Ca^{2+} entrance in the post-synaptic compartment. The increase of the intracellular Ca^{2+} levels activate several signalling

cascades, including many protein kinases, such as the calcium/calmodulin-dependent protein kinases (CaMKII) (Malenka & Nicoll, 1999), which contributes to triggering trafficking of AMPAR to the post-synaptic membrane. This effect leads to an increase of the synaptic strength, with no change in numbers of NMDAR (Malenka & Nicoll, 1999). LTP maintenance requires protein synthesis, within few hours, and it has been shown that this phenomenon is accompanied by visible growth of dendritic spines and associated post-synaptic densities (Harris, 2020).

It has been shown that LTP in the CA1 region of the hippocampus, widely involved in learning and memory, was impaired after the extinction of a morphine-CPP but restored during the morphine-primed induced reinstatement, suggesting the importance of this mechanism in drug-memory maintenance (Portugal et al., 2014). Moreover, an *in vivo* electrophysiological work reported that glutamatergic LTP at hippocampal ventral subiculum to the NAc Shell is facilitated in rats following re-exposure to the morphine-paired side during the post-conditioning test (Li et al., 2017).

1.2.4 Hippocampal formation and its role in memory

The importance of the hippocampus in episodic learning and memory, in both animals and humans, is well established. In experimental settings, synaptic plasticity in this brain area has been largely studied for its role in putative information-storage (Neves et al., 2008). The hippocampus consists of different interconnected internal regions, and several cell types. The four major sub-areas, namely cornu ammonis 1 (CA1), CA2, CA3 and dentate gyrus (DG), have a well-defined laminar organisation, where the cell bodies are tightly grouped in a C-shaped arrangement, having projections terminating on different regions of the dendritic tree (Figure 1.4; Neves et al., 2008). In this area there are different types of neural cells, such as pyramidal neurons, granule cells and inhibitory interneurons, constituting microcircuits which are coordinated in time for processing and storage of information (Cutsuridis & Wennekers, 2009). According to Fuchs and colleagues (2017), the intrahippocampal information processing starts from the entorhinal cortex (EC), through the perforant pathway, and passes either through the dentate gyrus and CA3 to the CA1, via Shaffer Collaterals, or directly to the CA1, while the extrahippocampal connections occur via the subiculum and via direct connections from CA areas (see Figure 1.5 (Fuchs et al.,

2017)). The CA1 subregion is the output of the hippocampus, and it has been recognised as essential for contextual memory formation (Daumas et al., 2005).

Nevertheless, those internal circuit forms the classical hippocampal loops and they have been subjected to several experimental manipulations for synaptic plasticity studies.

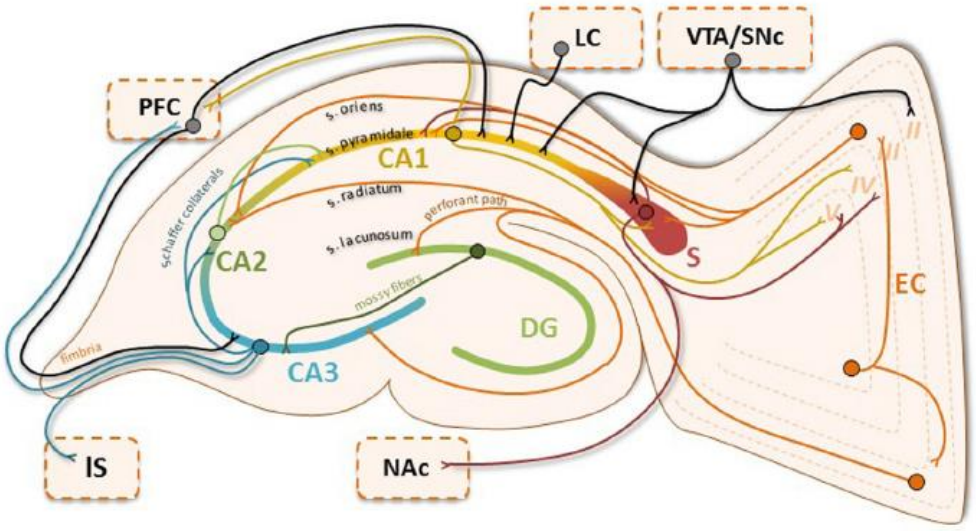

Figure 1.5- Laminar organization of the hippocampal formation and its interconnection – A sagittal section of the hippocampus. Intrahippocampal information processing occurs primarily along the entorhinal cortex (EC, brown) → dentate gyrus (DG, green) → cornu ammonis (CA)3(blue)→CA1(yellow), EC→CA3→CA1, EC/CA3→CA2→CA1, and EC-CA1 functional circuits. Extrahippocampal communication occurs primarily via the subiculum (S; red), EC, and via direct connections with CA areas (for example lateral septum (lS), prefrontal cortex (PFC), locus coeruleus (LC). Dopamine input from the ventral tegmental area (VTA) and substantia nigra pars compacta (SNc) ends primarily in the EC, S, and CA1. Hippocampal laminae (i.e., stratum (s.) oriens, pyramidale, radiatum, and lacunosum) are also described (Fuchs et al., 2017).

The medial septum highly projects to the hippocampus and this pathway is mainly composed by GABAergic and cholinergic afferents, which are implicated in cognitive functions. More specifically, medial septal cholinergic terminals project to all regions of the hippocampus, targeting the stratum oriens of CA1 and CA3 subfields, where synaptic contacts are established with dendrites of pyramidal cells, as well as cell bodies and dendrites of GABAergic and somatostatin-containing interneurons and dentate granule cells (reviewed in Teles-Grilo Ruvio & Mellor, 2013). Hence, this anatomical organisation allows the cholinergic system to modulate

rhythmic activity and interact with other neurotransmitters, through the activation of its receptors in hippocampus.

The hippocampus is also known to be involved in spatial memory. The discovery of place cells in the dorsal hippocampus (O'Keefe & Dostrovsky, 1971; O'Keefe & Speakman, 1987) and evidence that hippocampal lesions impair spatial memory have driven this concept (Morris et al., 1982). Even though the role of the hippocampus in spatial and declarative memory (Cave & Squire, 1991) has been well established, there is also evidence of the involvement of this area in emotional memory (Kim & Fanselow, 1992). Hence, it is possible that the hippocampus modulates different types of memory, depending on distinct intrahippocampal circuits (Strange et al., 2014).

The anatomical position of the hippocampal formation allows the regulation of mesocorticolimbic and nigrostriatal dopamine (Fuchs et al., 2017), implying that the hippocampus can have a role in reward-related memories. Interestingly, it has been found that acute cocaine application increased hippocampal LTP in the CA1 (Stramiello & Wagner, 2010). Moreover, hippocampal cAMP response element-binding protein (CREB), Extracellular signal–regulated kinases (ERK), and GluR1-containg AMPA, all factors playing a critical role in synaptic plasticity, and consequently LTP formation, were increased after a cocaine-CPP (Tropea et al., 2008). This evidence demonstrates that acute cocaine provokes hippocampal plasticity and activation of cellular cascades inducing LTP, which may promote the formation of the maladaptive drug-context memories. Importantly, hippocampal function could result in drug-context-triggered cravings and drug seeking as initial cocaine use which develops in cocaine addiction and chronic cocaine intake.

It has been found that chronic morphine and heroin can compromise hippocampus-dependent spatial learning in Morris water maze (Means et al., 1996 ; Tramullas et al., 2008). On the other hand, there are also studies showing that rodents can successfully learn opiate-induced CPPs, suggesting that normal drug-context association occurs when induced by the reinforcing effects of the opiates (Kutlu & Gould, 2016)

Although the hippocampus is often thought of as a single, entire brain area, it may not act as a unitary structure, but it can instead be thought as functionally distinct along the dorso-ventral axis (Moser & Moser, 1998). In the next section the functional difference between dorsal hippocampus and ventral hippocampus will be explored.

1.2.5 Ventral and Dorsal hippocampi are functionally different

From an anatomical point of view, distinct hippocampal circuits are segregated along the dorsoventral axis. Early studies suggested that the dorsal hippocampus (dHIP) is more involved in spatial learning (Moser et al., 1995), while lesions in the ventral hippocampus (vHIP) altered emotional behaviour (Henke, 1990). This distinction depends on how dHIP and vHIP are connected to other brain regions. In fact, the greatest density of the place cells coding spatial location are contained in the CA1 of the dHIP (Jung et al., 1994), which sends sequential and feed-forward projections to the dorsal part of subiculum (reviewed in Fanselow & Dong, 2010). The cells contained in the dorsal subiculum are responsible for encoding head position in space (Taube, 2007). The most pronounced projections from the dorsal CA1 and subiculum to the PFC are to the retrosplenial and anterior cingulate cortices in rats (Van Groen & Wyss, 2003; Cenquizca & Swanson, 2007) implicated in the cognitive processing of visuospatial information and memory processing (Frankland et al., 2004; Jones & Wilson, 2005) and environmental exploration, also defined as spatial navigation in rats (Harker & Whishaw, 2004). In addition, the dorsal subiculum, but not the ventral, projects to the medial and lateral mammillary nuclei and the anterior thalamic complex (Kishi et al., 2000), two brain regions implicated in navigation (Taube, 2007). This evidence demonstrates that the dHIP and its connections mediate cognitive process such as learning, memory, navigation, and exploration.

On the other hand, the vHIP has direct projections to the olfactory bulb and other primary olfactory cortical areas (Cenquizca & Swanson, 2007) and those connections may be implicated in depression-like symptoms (Wang et al., 2007). The ventral CA1 (vCA1) and subiculum are interconnected with the extended amygdala, which also shares connectivity with olfactory sensory input, but also with infralimbic cortex (IL), prelimbic cortex (PL), and insular cortex (Chiba, 2000; Jones & Wilson, 2005; Hoover & Vertes, 2007). The connection between vHIP and bed nucleus of stria

terminalis (BNST), an amygdalar nucleus, may be critical for understanding the neuroendocrine alteration associated to psychiatric disorders, as the BNST sends afferents to the hypothalamic nuclei (Dong & Swanson, 2006). The vHIP is connected to the amygdala (Pitkänen et al., 2000) and this pathway plays a role in Pavlovian fear conditioning (Fanselow & Poulos, 2005). Moreover, the vCA1 directly projects to the NAc shell, and this relationship with the NAc is also relevant to reward processing or goal-directed actions (Royer et al., 2010; Ruediger et al., 2012). Hence, this evidence suggested that the functional difference between dHIP and vHIP depends on the respective connections with other brain areas.

Several behavioural studies over the years have explored and characterised the functional distinction between dHIP and vHIP, increasing the evidence that the vHIP is more involved in reward-related memories. For example, it has been found that morphine-associated contextual memories increased synaptic plasticity in vHIP, and the authors suggested that this change could underlie context-induced relapse (Alvandi et al., 2017). Furthermore, data from our lab showed that morphine-induced reinstatement, in a CPP model, produced an increase in AMPA binding in ventral, but not in dorsal CA1 (dCA1), highlighting the importance of this sub-region in drug-seeking behaviours (Wright et al., 2019). It has been demonstrated that in a rat model of alcohol dependence vulnerability, LTP in the vHIP, but not in dHIP, was decreased, highlighting the role of this sub-region in regulating addictive behaviours (Almonte et al., 2017).

In the next sections the role of hippocampus in reinstatement-like behaviours, focusing on the impact of cues and drug-priming in this phenomenon, will be discussed.

1.2.6 Drug-primed induced reinstatement

Reinstatement of a conditioned response, such as drug-seeking, through an injection of the same drug used for conditioning is believed to be a reliable model of relapse (Shalev et al., 2002; Shaham et al., 2003). In the CPP model of reinstatement, an extinguished drug-induced CPP is recovered, or re-activated, after a priming injection of the conditioning drug and so re-inducing the preference for the drug-paired side. The effect of a priming dose of morphine to reinstate the morphine-CPP

has been widely demonstrated (Ventura et al., 2005; Hearing et al., 2016; Wright et al., 2019), as well as cocaine induced-reinstatement in mice (Maldonado et al., 2007; Singh & Lutfy, 2017; McReynolds et al., 2017).

However, over the years, the hippocampus has gained a lot of attention for its role in modulating drug-related memories. For example, it has been shown that morphine-primed reinstatement of CPP in mice was associated with a significant enhancement in LTP in the dorsal hippocampus (Portugal et al., 2014). On the other hand, Wright et al. (2019) found that inhibition of α7nAChRs in vHIP, but not in dHIP, prevented priming-induced reinstatement of a morphine CPP (Wright et al., 2019). Moreover, the vHIP has been shown to process cue-induced reinstatement of cocaine seeking in SA administration models (Rogers & See, 2007; Ramirez et al., 2009). Thus, this evidence suggests that the ventral portion of the hippocampus may have a major role in processing the drug-induced reinstatement.

1.2.7 Cue-induced reinstatement

Early studies found that that environmental context associated with drug taking could trigger relapse in humans (O'Brien et al., 1992). This finding led to a large number of preclinical models showing the influence of drug-conditioned contexts or cues on relapse-like behaviours. Specifically, the cues used are presumed correlates of the environmental cues shaped when addicts, both humans and rodents, repeatedly take drugs, which trigger craving. In other words, conditioned stimuli, such as environmental cues or contexts, can be defined as "motivational magnets" which drive to reward seeking and even consumption (Berridge & Robinson, 2003).

The hippocampus has an important role in the formation and maintenance of drug-context associations (Childress et al., 1999), because of its involvement in learning, memory and reward. For example, it has been found that the dHIP processes context-induced reinstatement of cocaine-seeking (Fuchs et al., 2007; Xie et al., 2010). Interestingly, in a multi-disciplinary study, Luo et al. (2011) used electrophysiology, neuronal tracing, reversible inactivation, and 'disconnection' approach to demonstrate a role for projections from the CA3 dorsal hippocampus area to VTA, via the lateral septum, in context-induced reinstatement of cocaine seeking (Luo et al., 2011). On the other hand, the vHIP has also been implicated in

cue-induced reinstatement. Lasseter et al. (2010) found that inactivation of the vHIP, but not dHIP or DG, decreased context-induced reinstatement in a cocaine-SA model (Atkins et al., 2008; Lasseter et al., 2010).

Thus, both dorsal and ventral portions of the hippocampus are implicated to be critical for context-induced reinstatement of drug-seeking.

1.2.8 Different drugs, different circuits

Depending on the molecular targets and their pharmacological effects, drugs of abuse recruit additional neurotransmitters and brain pathways. There are several pharmacological classes and subclasses of drugs of abuse, this section will focus however on the neural mechanisms of heroin and cocaine, as CPP experiments using those two drugs have been performed in this thesis.

The main target of most opioid drugs, such as heroin, is the μ opioid receptor (μOR), which regulates the addictive properties of opioids. The main characteristic of these compounds is their capability to induce euphoria, analgesia, sedation, and/or respiratory depression, and ability to induce tolerance and dependence. The neuronal adaptations underlying the chronic opioid consumption are the loss of μOR in coupling to its cellular effectors, adaptation in the intracellular signalling and general changes in synaptic plasticity (Christie, 2008).

Cocaine, a potent psychostimulant deriving from the coca plant, produces several effects when consumed, such as euphoria, pleasure, loss of behavioural control and compulsive responses to drug-related cues (Nestler, 2005). Unlike opioids, cocaine directly interacts with the dopamine system by inhibiting DA reuptake into the pre-synaptic site, blocking the DA transporter (DAT), promoting DA accumulation in the synaptic cleft, producing sustained activation of dopaminergic receptors. However, it has been also highlighted that cocaine pharmacology might be more complex than generally thought, proposing DAT "inverse agonism" as an alternative mechanism to explain cocaine pharmacology (Heal et al., 2014).

Differences between heroin and cocaine addiction are also reflected in behaviour. In particular, a series of interesting work from Badiani and colleagues emphasises this

difference. They first found that cocaine self-administration was higher in rats not residing in the test chambers, defined as non-resident rats, in comparison to rats living in the test chamber, namely resident rats. However, the opposite trend was found for animals self-administering heroin, stressing the role of the environment as a crucial factor influencing opiate and psychostimulant drug taking (Celentano et al., 2009). In a similar study authors found that this finding was extendable also to drug-seeking behaviours. In fact, all resident and non-resident rats acquired heroin and cocaine SA, but cocaine priming reinstated cocaine-seeking only in non-resident rats, whereas heroin priming reinstated heroin-seeking only in resident rats (Montanari et al., 2015). These findings highlight fundamental differences between psychostimulant and opioid reward, showing a specific phenotype for each drug of abuse.

ACh, acting via α7nAChRs, has been shown to modulate rewarding effects of both heroin and cocaine (Zanetti et al., 2006; Palandri et al., 2021 Pastor et al., 2021). Hence, the effect of α7nAChRs in the reinstatement of both cocaine- and heroin-CPPs was investigated.

1.2.9 The importance of the Immediate Early Gene c-Fos

As yet, the interaction between different neurotransmitters and brain areas, during drug-related behaviours or memories, have been discussed. What are the mechanisms occurring downstream?

Immediate Early Genes (IEGs) have been widely used as indirect markers of neuronal activity and the most commonly used for this aim are c-Fos and Erg1. They stimulate transcription factors in modulating neuronal physiology by regulating the gene expression at downstream level. In this section, only the properties of c-Fos will be explored.

The IEG c-Fos, and its protein derivate Fos and mRNA, are commonly used in addiction research as markers of behaviourally-activated neurons. C-Fos can be found in many neuronal types in the CNS, such as glutamatergic, GABAergic MSNs and interneurons, monoaminergic, spinal cord and neurosecretory neurons, as well as in glia and astrocytes (for review, see McReynolds et al., 2018). Under basal conditions, c-Fos activity is weakly detectable in most brain regions. However, c-Fos

can be rapidly stimulated by various external stimulations such as drug-taking and seeking behaviours, stress, inflammation, neuroendocrine and neuropeptide signalling, depolarisation, neurotransmission, neurotrophic factors and intracellular Ca^{2+} levels increase (reviewed in Cruz et al., 2015 and McReynolds et al., 2018). Moreover, once activated, c-Fos expression peaks between 1 and 3 hours, accumulating in the nucleus.

According to Cruz (2015), the c-Fos promoter is activated by drug-related behaviours mainly by calcium-dependent activation of the ERK/MAPK pathway, which plays a key role in coordinating glutamatergic and DA systems (Cahill et al., 2014). Neuronal stimulation begins with Ca^{2+} influx from, for example, the activation of AMPA and NMDA receptors, as well as from a variety of voltage-gated calcium channels (VGCC), which activates calcium-dependent molecules such as Ras-GRP. This protein activates Ras/Raf kinase pathway that phosphorylates and activates ERK/MAPK complex, which phosphorylates the transcription activator Elk-1, via ribosomal S6 kinase (RSK), involved in signal transduction, and so the cAMP response element-binding (CREB), on the c-Fos promoter. Moreover, also the calcium-dependent CaM kinase IV can rapidly phosphorylate CREB, resulting faster than ERK/MPAK pathway (for review see Cruz et al., 2015). In addition, cAMP/PKA signalling, via G-protein-coupled receptors (GPCRs), also contributes to c-Fos promoter activation (Figure 1.6). Importantly, CREB is expressed in many brain regions, mainly in NAc and hippocampus, and it can activated by drugs of abuse and learning mechanisms (Tully et al., 2003 Kandel, 2012; Nestler, 2005).
Interestingly, neurons expressing c-Fos are thought to encode learned associations, such as those that play a key role in addiction. Those sparsely distributed sets of neurons are called neuronal ensembles, which are neuronally represented by 1-3% of neurons in a specific brain region, and for a specific behaviour, such as heroin or cocaine seeking (Bossert et al., 2011; Cruz et al., 2014). Moreover, c-Fos can be co-localized with other markers to characterize differential patterns of neuronal activation following an experimental manipulation (McReynolds et al., 2018).

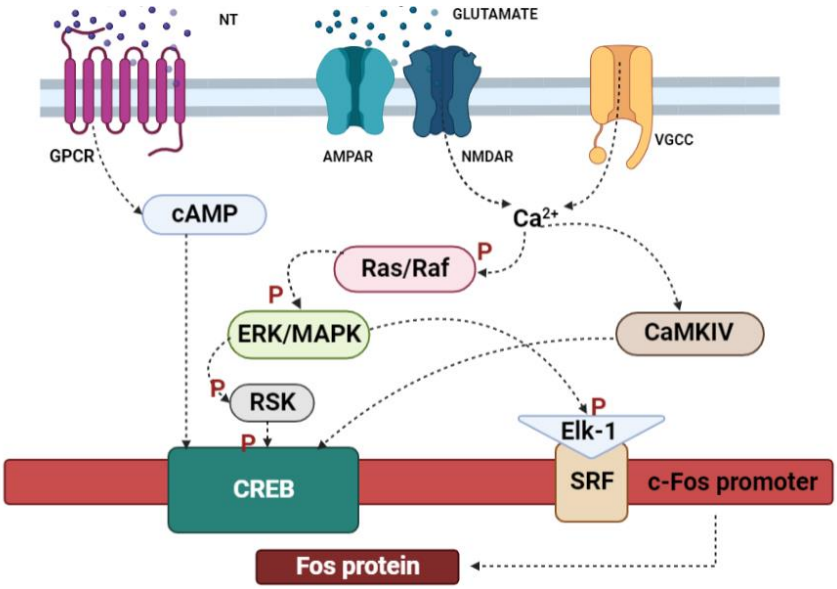

Figure 1.6 – Model of signalling cascades activating c-Fos expression in brain's behaving animals – The Ca^{2+} influx through NMDAR and VGCC, because of strong action potentials, induces phosphorylation and activation of ERK/MAPK complex via Ras/Raf pathway. ERK/MAPK activation provokes phosphorylation of Elk-1 that is associated with serum response factor (SRF) and phosphorylation of CREB via ribosomal S6 kinase (RSK). Elk-1/SRF and CREB are transcription factors that, when phosphorylated, can induce transcription of the coding sequence for c-Fos and translation of its protein. C-Fos can be used as markers of strongly activated neurons. cAMP activation though GPCRs and calcium-dependent pathways such as CaMKIV also contribute to c-Fos protein translation. (Adapted from Cruz et al., 2015)

c-Fos expression is relatively easy to measure through immunohistochemistry or immunofluorescence, and supplies good spatial resolution, providing patterns of activated cells during a specific behaviour. Thus, in this work c-Fos expression has been investigated to study the effect of the α7nAChRs during drug-induced reinstatement.

1.3 Cholinergic α7 nicotinic receptors modulate reward, learning and memory

1.3.1 Cholinergic system in the central nervous system

The cholinergic system is extremely implicated in cognition, learning and memory. Through distinct neural innervations, located in the basal forebrain and the brainstem area, the system modulates neural activity among several brain regions. ACh can be also defined as a neuromodulator due to its power in modulating neurotransmission, which is not purely excitatory or inhibitory. In fact, interacting with glutamate or

GABA respectively (Ito & Schuman, 2008), ACh can therefore modifying the state of one or more neurons and its response (Picciotto et al., 2012). Cholinergic transmission interacts with dopaminergic, noradrenergic and serotonergic systems, modulating readiness of the basal forebrain and reward (Sarter et al., 2009; Livingstone & Wonnacott, 2009). Furthermore, ACh is thought to strengthen neuronal loops and cortical pathways during learning processes, by potentiating the action of feed-forward afferent inputs to the cortex and so integrating sensory information (Hasselmo, 2006). More broadly, the main characteristic of ACh is to modulate pattern of neurons in response to environmental changes.

Cholinergic projections innervate distal and proximal areas from two primary areas, the pedunculopontine (PPT) and LDT areas and the basal forebrain complex (BF) complex (for review, see Picciotto et al., 2012). Specifically, the BF includes the medial septum (MS), the vertical limb of the diagonal band of Broca (VDB), and the nucleus basalis of Meynert, and the substantia innominate in the rodent brain (Paul et al., 2015). Cholinergic projections from those areas innervate several brain regions, in both cortical and limbic regions, including the hippocampus (Mesulam et al., 1983; Gallagher & Colombo, 1995). The septo-hippocampal pathway, which begins from the MS and VDB, is the main pathway of the cholinergic system and more extended innervation to the hippocampus. In particular, lesion, tracing and immunocytochemical studies within this tract, revealed that the MS is connected to the hippocampus via the fimbria and dorsal fornix (Teles-Grilo Ruivo & Mellor, 2013). Early studies showed that the CA1 and DG of the dHIP receive projections from the VDB, while those areas in the vHIP receive inputs from both MS and VDB (McKinney et al., 1983; Nyakas et al., 1987). Overall, these cholinergic projections are believed to be implicated in memory, arousal and other cognitive processes (Figure 1.7).

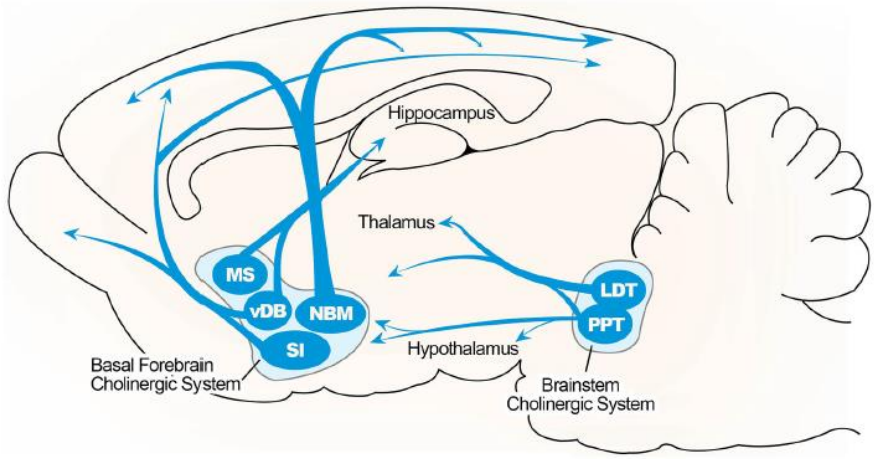

Figure 1.7 - Brain map of the basal forebrain cholinergic pathway - Cholinergic innervation consist of medial septum (MS), vertical limbs of diagonal band of Broca (VDB), nucleus basalis of Meynert (NBM) and substantia innominate (SI), projecting to the hippocampus, thalamus, olfactory bulb and cortical regions. Cholinergic protomesencephalon included pedunculopontine (PPT) and laterodorsal tegmental areas (LDT), projecting to midbrain, thalamus, hypothalamus and BS (Paul et al., 2015)

The cholinergic system, at basal forebrain projections to the hippocampus level, is also characterised by both "wired" and "volume" transmissions (Sarter et al., 2009). As elegantly summarised by Teles-Grilo Ruivo and Mellor (2013), "wired" neurotransmission is characterised by acetylcholine being released from axonal terminals at synaptic sites, resulting in post-synaptic ion channel activation. This synaptic release of acetylcholine is regulated by the catalytic action of the enzyme acetylcholinesterase (AChE). In "wired" ACh transmission, following axonal terminal depolarisation, ACh is released and can bind to both nicotinic and muscarinic cholinergic receptors (see 1.4.2) and it is rapidly hydrolysed by AChE, resulting in choline and acetate. Choline is taken back into the terminal by high-affinity choline transporters to be re-synthesised into acetylcholine by the enzyme choline acetyltransferase (ChAT). On the other hand, "volume" transmission refers to when ACh is released axonally, but away from nerve terminals. In this type of chemical communication, presynaptic cholinergic active zones are not adjacent to defined post-synaptic densities and activate extra-synaptic cholinergic receptors (Zoli et al., 1999). Consequently, neurotransmission is not regulated by ACh degradation by AChE, with ACh reaching the extracellular space and activating

extra-synaptic nicotinic and muscarinic receptors (for review, see Teles-Grilo Ruivo & Mellor, 2013).

1.3.2 Cholinergic receptors: focus on α7 nicotinic ACh receptors

The action of ACh in the brain is mediated by a large variety of pre-, post- and extra-synaptic cholinergic receptors, contributing to both cortical and hippocampal function. Specifically, ACh is the endogenous ligand of ionotropic nicotinic acetylcholine receptors (nAChRs) and metabotropic muscarinic acetylcholine receptors (mAChRs). Although mAChRs can largely affect neurotransmission and excitability in many brain regions, this section will mainly focus on nAChRs, and specifically on the α7 subtype, which are largely expressed in the hippocampus, and their role in modulating reward-related learning and behaviours.

Generally, nAChRs are widely expressed throughout brain (Figure 1.8) and their responses to endogenous ACh and choline, and to exogenous nicotine, are involved in a number of physiological processes and pharmacological effects. From a structural point of view, nAChRs are cys-loop cationic ligand-gated channels, composed of five subunits which define either a heteromeric or homomeric receptor (Figure 1.9) and its consequent localisation and pharmacological properties. nAChRs in the CNS are formed from a portfolio of α- and β-subunits (α2–α10 and β2–β4), the differential association of which confers distinct functional and structural properties to the resultant subtypes the receptor (Dajas-Bailador & Wonnacott, 2004). Such subunits have a large extracellular N-terminal domain involved in ligand binding, three hydrophobic transmembrane regions (M1–M3), a large intracellular loop, a fourth transmembrane region (M4) and a short extracellular C-terminal. In particular, the extracellular N-terminal contains: two cysteine residues (Cys 128, 142, Torpedo α1 subunit numbering), separated by 13 amino acids, form a disulphide bond to create a loop that has been implicated in the transduction of agonist binding into channel opening (Sine & Engel, 2006; Bouzat, 2012). Mutagenesis and photoaffinity labelling experiments have highlighted the relevance of 4 aromatic residues (Tyr 93, Trp 149, Tyr 190, Tyr 198, Torpedo numbering), consistent with 3 polypeptide loops of the α subunit (loops A–C) contributing to the principal agonist binding site (Bouzat, 2012). For example, it has been demonstrated that the α7 subunit can

combine with the β2, forming the α7β2, nAChR, localised in BF cholinergic neurons (Azam et al., 2003).

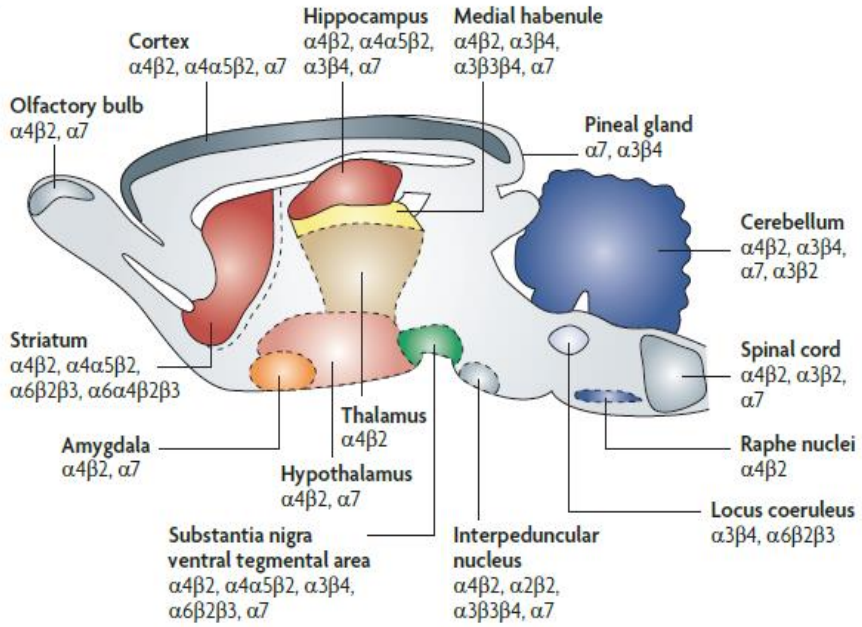

Figure 1.8 - nAChRs expression in the CNS – The various assemblies of nicotinic acetylcholine receptor subtypes are broadly distributed in the brain (Taly et al., 2009).

The functional response of nAChRs is defined by the conformational state of the channel: resting, activated and desensitised state. For example, for α7nAChRs binding with an antagonist, such as α-bungarotoxin, leads to the resting state; while binding with a positive allosteric modulator (PAM), such as PNU-120596, sustains the activated state, in the co-presence of the agonist, by preventing desensitisation, allowing cations to enter via the pore, and long-term exposure and binding of an agonist, sustains the desensitised state (Letsinger et al., 2021). The acute effect of ACh consists of fast opening, in the microsecond to millisecond range, of the channel that is permeable to Na^+, K^+ and less frequently Ca^{2+} ions (Taly et al., 2009**)**. However, the permeability to Ca^{2+} varies depending on the specific subtype of nAChRs (McKay et al., 2007; Fayuk & Yakel, 2007). The already mentioned homomeric α7 subtype is characterised by an elevated permeability to calcium (Fucile, 2004), which is comparable to that of the NMDAR (Uteshev, 2012). Fluorescent calcium indicators allow estimation of the Ca^{2+} permeability of nAChRs, by relying on the simultaneous recording of fluorescence signals and transmembrane

current and requiring perfect voltage control of the cell and the absence of the calcium-induced calcium release (CICR) from the endoplasmic reticulum (ER). In this way, the percentage of the total current flowing can be calculated through a given ion channel that is carried by calcium ions, the so-called "fractional calcium current" can be measured (Shen & Yakel, 2009). The entrance of calcium into the cell induces several cellular events, such as excitability, exocytosis, motility, apoptosis, and transcription, which is elicited by interacting with thousands of proteins and their downstream effectors (Dajas-Bailador & Wonnacott, 2004; Cheng & Lederer, 2008). Thus, due to its unique properties, α7 nAChRs are responsible for regulating synaptic events involved in learning and memory, which is one of the reasons why these receptors are the focus of this thesis.

Another important and distinctive feature of α7nAChRs is their ability to quickly desensitise. For instance, as highlighted by Bouzat and colleagues (2008) ACh-induced currents decay very rapidly in the presence of ACh, in macroscopic current recordings from cell cultures. However, it is important to consider how fast the receptors returns to the open state after the infusion of the agonist, as this temporal window impacts on the response at the synaptic level, where the presence of the agonist is temporary. Thus, by performing a protocol involving the double application of a 150 ms-pulse of 1 mM ACh, it was found that desensitised α7nAChRs are able to recover in the absence of agonist with a time constant of ~1 s (Bouzat et al., 2008). In this framework, a correlation between reported rise times or current decay time constants and solution exchange rates in these receptors, in cell cultures, has been investigated (Pesti et al., 2014). Specifically, when the solution exchange rates were faster, the respective onset and offset kinetics were as well. On the other hand, as the solution exchange is rate limiting, the intrinsic kinetics of α7 cannot be properly determined, suggesting a possible reason why the reported desensitised rates for α7nAChRs show great variability and include values ranging from the sub-millisecond to the second range (Pesti et al., 2014).

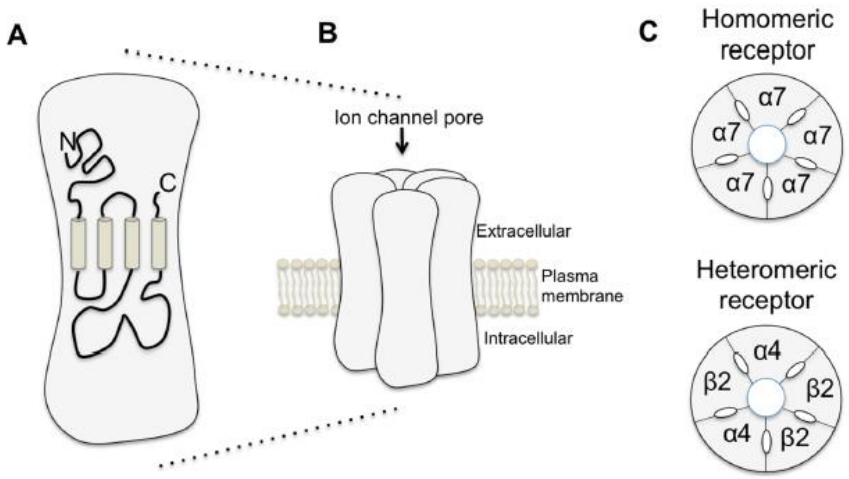

Figure 1.9 - The Structure of the nAChR – (**A**) Schematic diagram of the structure of nAChR subunit, showing the N and C terminus, the membrane extent regions and the complex cytoplasmic loop between M3 and M4. (B) The organisation of the subunits to form a receptor. (**C**) Subunit arrangement is specific to each subtype, either homomeric or heteromeric, having two different subunit types. (Gotti & Clementi, 2004).

Overall, desensitisation in nAChRs is implied in many cellular functions, such as neuroprotection, modulation of synaptic plasticity, and regulation of the neurotransmitter release (Wang and Sun 2005; Placzek et al., 2009). In particular, the fast desensitisation and brief open duration could be responsible for avoiding cell excitotoxicity caused by increased intracellular Ca^{2+}, provoked by overstimulation, since α7 is, among nAChRs, the one that shows the highest Ca^{2+}/Na^{+} permeability ratio (Bouzat et al., 2018).

1.3.3 Hippocampal α7nAChRs

The hippocampus has the highest density of α7nAChRs (Orr-Urtreger et al., 1997). The distribution of mRNA for α7nAChRs, as well as binding sites for α-bungarotoxin (α-BTX), which labels α7nAChRs, are widespread throughout the dentate gyrus, CA3 and CA1 regions (Sudweeks and Yakel, 2000; Fabian-Fine et al., 2001; Adams et al., 2002). Within this area, α7nAChRs are located on presynaptic and postsynaptic sides at both glutamatergic and GABAergic terminals (Fabian-Fine et al., 2001). Their potential for modulating the excitatory and inhibitory oscillations is therefore profound.

The development of genetically encoded calcium indicators (GECIs) has provided the possibility to directly monitor neuronal activities, by measuring changes in cytoplasmic calcium levels, at either the synaptic or network level. Moreover, differently coloured GECIs have provided excellent tools to distinguish presynaptic and postsynaptic components at the same time, facilitating our understanding of the coordinated activities that mediate synaptic plasticity (Zhao et al., 2011; Tian et al., 2012). Specifically, α7nAChRs, by interacting with the glutamatergic system (Cheng & Yakel, 2015), induce glutamate release and the consequent signalling cascades underlying mechanisms of synaptic adaptations. In fact, in a hippocampal glutamatergic synapse, the propagation of an action potential induces the depolarisation of the pre-synaptic terminal, where VGCCs provoke an increase of intracellular calcium, able to induce the exocytosis of synaptic vesicles containing neurotransmitter. However, this mechanism can be strongly amplified by activation of pre-synaptic α7nAChRs, and several findings support this concept. In fact, studies from both spontaneous and evoked glutamatergic synaptic transmission showed that presynaptic α7nAChRs mediated enhancement of glutamate release (reviewed in Cheng & Yakel, 2015). Interestingly, Cheng and Yakel (2014) reported that activation of α7nAChRs at presynaptic sites, via protein kinase A (PKA) activation, enhances synaptic efficiency of hippocampal mossy fibre transmission, by using brain slice electrophysiology in mice (Cheng & Yakel, 2014). Consistent with these findings, it has been demonstrated that activation of α7nAChRs could directly trigger glutamate release from mossy fibre terminals (Sharma et al., 2008) and the application of choline on hippocampal synaptosomes induced a significant glutamate release (Zappettini et al., 2010). Moreover, an interesting finding from Huang and colleagues (2010) reported that nicotine induced a strong enhancement of firing in extracellular recordings in vivo from CA3 pyramidal neurons, inducing glutamate transmission. This release was blocked by the selective α7 antagonist methyllicaconitine (MLA), highlighting the importance of these receptors in regulating neurotransmission (Huang et al., 2010).

Overall, as these receptors have been found on both inhibitory GABAergic interneurons (reviewed in Griguoli et al., 2013), and excitatory pyramidal neurons, it is possible to suppose that they could provoke amplification of weak inputs on pyramidal cells directly by activation of their postsynaptic α7nAChRs or indirectly

by inhibition, or disinhibition, of GABAergic interneurons that directly synapse onto pyramidal cells (Ji & Dani, 2000; Ji et al., 2001).

Taking into account the above-mentioned properties of α7nAChRs, it is worth exploring their contribution in modulating synaptic plasticity.

1.3.4 α7nAChRs regulate hippocampal LTP

The effect of α7nAChRs' activation on synaptic plasticity has been suggested to depend on the timing of their activation and stimulation on glutamatergic synaptic currents. When α7 nAChR agonists were bath perfused, the activation of α7 nAChRs facilitated the induction of LTP (Hunter et al., 1994), and enhanced both early and late LTP (Kroker et al., 2011) in the CA1 of ventral hippocampal region, in rats. More recently, by using optogenetic approaches, it has been possible to evaluate the effect of the specific cell-type and temporally precise stimulation of cholinergic inputs to the hippocampus. Yakel's lab investigated how the activation of endogenous cholinergic inputs could regulate hippocampal synaptic plasticity, in mice. The authors found that α7nAChRs mediated two forms of hippocampal synaptic plasticity with a timing precision in the millisecond (ms) range. In particular, when the cholinergic input to the CA1 hippocampal region was activated 100 ms prior to activation of the Schaffer collateral (SC) pathway, this induced an α7nAChR- dependent form of LTP. On the other hand, cholinergic activation only 10 ms earlier to activation of the SC pathway, provoked an α7nAChR-dependent short-term depression (STD) that was mediated primarily through the presynaptic inhibition of glutamate release (Gu & Yakel, 2011). In addition, the same group showed that both presynaptic and postsynaptic sites can thus coordinate presynaptic and postsynaptic activities to induce timing-dependent synaptic plasticity, precisely, either LTP or STD, in mice hippocampus slices. (Gu et al., 2012). Finally, interesting evidence from Ma and colleagues (2014) demonstrated that in aged α7nAChR KO mice, both evoked synaptic field potentials and LTP were significantly reduced in hippocampal CA3-CA1 synapses, compared to wild type mice, suggesting that α7nAChRs are necessary for inducing cholinergic modulation of LTP (Ma et al., 2014).

Hence, targeting α7nAChR can be a useful strategy to explore how these receptors takes part in the dynamics of hippocampal synaptic plasticity and how α7 contribute to learning and memory.

1.3.5 α7nAChRs in learning and memory

Neuronal nicotinic receptors play a critical role in memory function in both humans and experimental animals (Levin, 2013). In fact, α7nAChRs have gained a lot of attention for its role in memory processing.

There is evidence that α7nAChRs activation may underlie neuronal activity in brain areas implicated in attention and working memory. In fact, it has been found that acute administration of the selective α7 agonist A-582941 induced an increase in mRNA expression of c-Fos and the cytoskeletal protein Arc, in a dose-dependent manner, in mPFC of juvenile rats, and the α7nAChRs antagonist MLA reversed those effects (Thomsen et al., 2008). MLA is a selective competitive α7 antagonist, a norditerpenoid alkaloid isolated from *Delphinium* seeds (Ward et al., 1990; Blagbrough et al., 1994). α7nAChRs play a critical role in enhancing episodic memory tasks. Both objective and social recognition tests, in animals experiencing mnemonic deficits, are improved by α7 agonists such as EVP-6124 or RG3487, before, immediately after, or post-training (Koenig et al., 2009; Wallace et al., 2011). These data suggest that activation of α7nAChRs is involved in acquisition, consolidation and retrieval. It has been found that administration of the full α7nAChR agonist, SEN12333, improved the performance during the object recognition task in mice with cognitive deficits induced by MK-801 and scopolamine, NMDA and muscarinic receptor antagonists respectively (Roncarati et al., 2009). Moreover, acute administration of the full α7nAChR agonist SSR180711 improved recognition memory in rat and mouse after a 24 and 48 hours, respectively. Such an effect was not observed in α7 knock-out mice and was prevented in animals given the antagonist MLA (Roncarati et al., 2009). Interestingly, it has been reported that SSR180711 can work as a cognitive enhancer, as its administration restored the performance in the latent inhibition model, in rats treated with MK-801 or amphetamine, highlighting the role of α7nAChRs in fostering learning and cognition (Barak et al., 2009). α7nAChRs are also involved in modulating sensory gating. The selective agonist

PNU-282987 enhanced the auditory sensory gating damaged by amphetamine (Hajos et al., 2005)

Several compounds that cannot activate the receptors themselves but can potentiate the response of an agonist, such as endogenous ACh, known as positive allosteric modulators, have been also investigated as possible cognitive enhancers, such as PNU-120596 (Hurst et al., 2005), NS1738 (Timmermann et al., 2007) and SB-206553 (Dunlop et al., 2009). It has been recently shown that the α7 positive allosteric modulator AVL-3288 ameliorated contextual fear conditioning and water maze tasks in rats experiencing brain injury, improving also hippocampal synaptic plasticity (Titus et al., 2019). Hippocampal infusion of choline immediately after training for inhibitory avoidance (IA) task improved the performance. However, administration of the antagonist MLA produced a memory impairment, suggesting that α7nAChRs receptors are involved consolidation of an IA task in mice (for review, see Blake et al., 2014). Moreover, when MLA was administered immediately after memory reactivation, memory reconsolidation was impaired in mice trained either with a mild or a high footshock (Boccia et al., 2010), suggesting that MLA effects were long lasting. The blockade of α7 by MLA produced an antidepressant like-effect in stressed mice and it also decreased hippocampal c-Fos expression in male mice treated with the reversable inhibitor of AChE physostigmine, highlighting the role of hippocampal α7 in emotional responses (Mineur et al., 2018).

1.3.6 α7nAChRs in reward

For years, the study of nAChRs has been oriented on tobacco dependence. A variety of nAChRs can be found on VTA DA neurons (Figure 1.8). When activated by nicotine they enhance DA release in NAc Shell, which leads to development of nicotine addiction (Balfour, 2004). An early study showed that mice lacking the β2 subunit did not present the classical effects elicited by nicotine, such as nicotine-induced DA release in the NAc and nicotine-induced increases in the firing rate in DA neurons, highlighting the importance of the β2 subunit in nicotine addiction (Picciotto et al., 1998). Furthermore, high-affinity nAChRs can incorporate further subunits, including β3, α6, or α5 subunits, with the resulting nAChR subtypes playing discrete and dissociable roles in the excitatory actions of nicotine on DA transmission (for review, see Wills et al., 2022).

Nicotine, via activation of nAChRs, may also modulate the endogenous cholinergic component of reward from other drugs of abuse. As reviewed by Berrendero and colleagues (2010) acute administration of nicotine induced the release of opioid peptides, as well as changes in their expression. In fact, they reported that acute administration of nicotine produced an increase in metenkephalin and dynorphin, in the mouse striatum (Berrendero et al., 2010), suggesting the presence of an interplay between nicotinic and opioid receptors. Moreover, the homomeric α7nAChRs may also modulate the cannabinoid rewarding effects. In fact, selective systemic administration of the α7nAChR antagonist MLA prevented the reinforcing effects of Δ9- tetrahydrocannabinol (THC), reduced SA of the synthetic cannabinoid CB1 receptor agonist WIN55,212-2 and decreased THC-induced dopamine elevations in the shell of the NAc, demonstrating a critical role of α7nAChRs of modulating the rewarding effects of cannabinoids (Solinas et al., 2007).

1.3.7 α7nAChRs in reinstatement and contribution to the field by research at the University of Bath

The role of α7nAChRs in reinstatement models is not fully understood. Our lab and others contributed to enlarge the knowledge about the selective mechanism of α7nAChRs in reinstatement. In fact, there is evidence supporting a role for α7nAChRs in this phenomenon. For example, Feng and co-workers (2011) found that systemic administration of MLA (4 mg/kg, subcutaneously), 20 minutes before morphine-primed induced reinstatement of CPP, significantly decreased the morphine-CPP in BALB/c mice. This is the first work to suggest the interaction between α7nAChRs and the opioid system, even if the brain circuits underlying reinstatement were not investigated. Another attempt is from Secci and colleagues (2017) who explored the action of a kynurenine 3-monooxygenase (KMO) inhibitor, Ro 61-8048 to elevate kynurenic acid levels in the brain, as kynurenic acid is believed to behave as a negative allosteric modulator of α7nAChRs. Briefly, the authors used Ro 61-8048 to study its role in the reinforcement and reinstatement of nicotine and cocaine self-administration in rats and squirrel monkeys. Their results showed that Ro 61-8048 inhibited nicotine self-administration in rats and monkeys, but not cocaine in monkeys in a dose-dependent manner. In addition, they found that the selective α7nAChR PAM PNU-120596 re-induced this response in monkeys, but not

in rats, suggesting additional mechanisms to the downregulation of α7nAChRs may modulate self-administration (Secci et al., 2017).

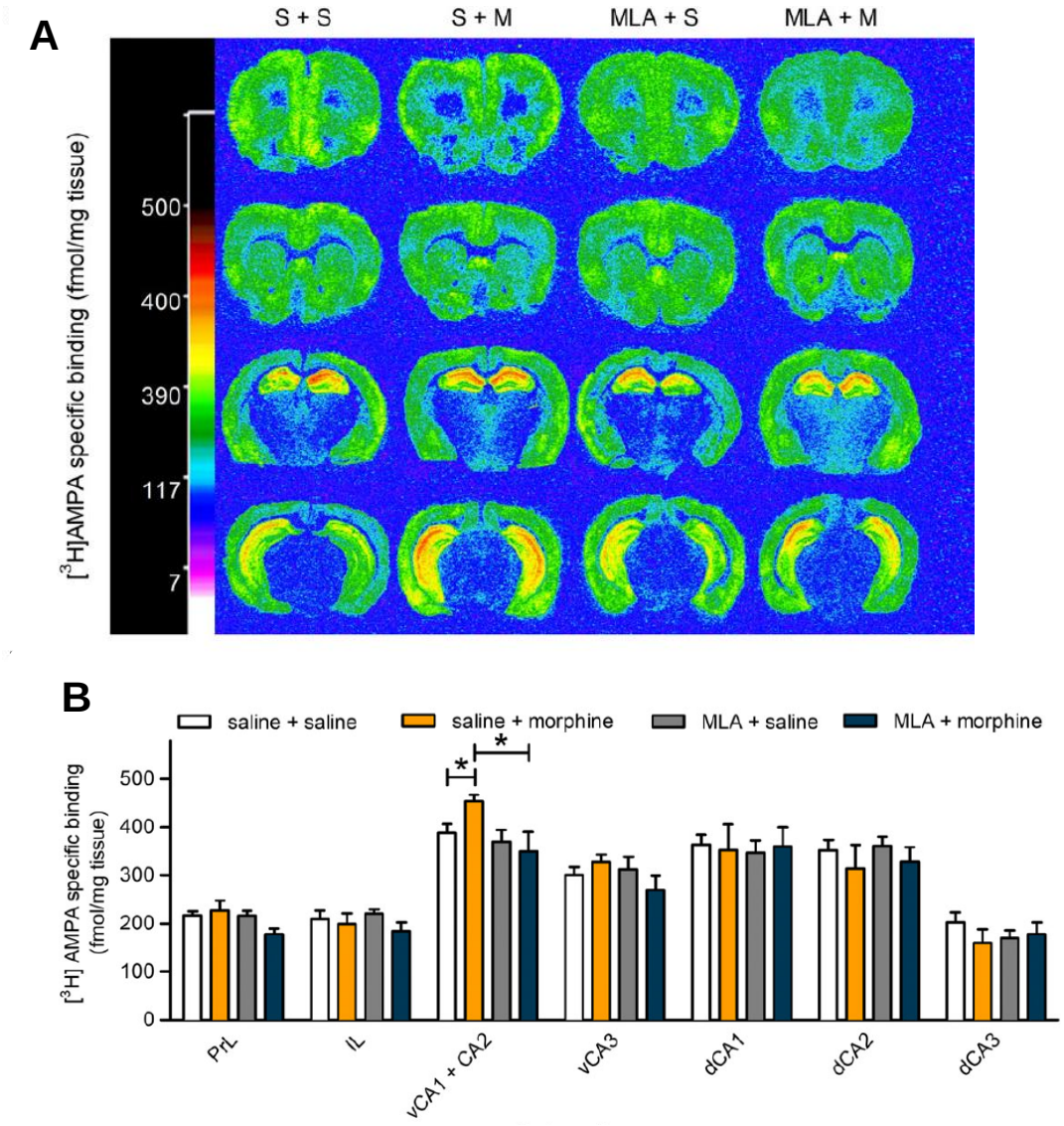

Figure 1.10 – Autoradiography results from Wright et al., 2019 –Effect of morphine-CPP reinstatement, in the presence and absence of MLA, on AMPA receptor binding in mouse brain. Mice underwent morphine-CPP reinstatement, and their brains were prepared for autoradiography. Four experimental group were tested: SALINE+SALINE (S+S), SALINE+MORPHINE (S+M), MLA+SALINE (MLA+S), MLA+MORPHINE (MLA+M) (**A**) Representative [3H]-AMPA binding density autoradiogram of binding following either MLA pre-treatment or morphine-primed reinstatement. Images are of coronal sections of the mPFC (top, bregma 1.94 mm), striatum (second row, bregma 1.42 mm), dorsal hippocampus (third row, bregma -1.22 mm) and ventral hippocampus (bottom, bregma -3.08 mm). (**B**) Quantitative AMPA receptor binding shown for mPFC regions, namely prelimbic cortex (PL), infralimbic cortex (IL); ventral hippocampus (vCA1+CA2, vCA3), dorsal hippocampus (dCA1, dCA2, dCA3). Adapted from Wright et al. (2019).

Our lab has been focused for years on the study of nicotinic and opioid receptors and recent published findings complement and extend Feng's work. Wright and colleagues (2019) reported that inhibition of α7nAChRs by MLA selectively inhibited morphine-primed reinstatement, when give systemically to C57BL/6J mice, and locally infused in vHIP in Wistar rats (Wright et al., 2019). Importantly, the same study showed that MLA had no effect on either the acquisition, expression, reconsolidation or extinction stages of CPP (Wright et al., 2019). These findings are remarkable and suggest a possible selective role of α7nAChRs in the reinstatement of morphine-CPP. Moreover, they also found a significant increase in [^{3}H]-AMPA binding (Figure 1.10 A), but not [^{3}H]NMDA binding, only in the vHIP after morphine-primed reinstatement of CPP, in comparison to other brain regions, such as sub-areas of PFC, NAc or VTA, involved in drug-seeking behaviours (Figure 1.10 B).

This increase of AMPA receptor binding could be interpreted as indirect evidence of LTP induction and the drug-related memory evoked by the priming dose of morphine during reinstatement. However, systemic treatment with MLA prior to morphine-induced reinstatement blocked this increase in [^{3}H]-AMPA binding (Figure 1.10A and B), consistent with α7nAChR modulation of the LTP underlying reinstatement, specifically in the vHIP. The autoradiography approach, unfortunately, cannot distinguish cell surface insertion from intracellular expression of receptors, so it is impossible to firmly state that the increase of AMPA receptors is related to a change in synaptic plasticity. Therefore, one of the aims of this thesis was to overcome the limitations of this approach.

Researchers at the University of Bath went on to show that rats systemically pre-treated with MLA, 20 minutes before heroin challenge, did not show reinstatement of the heroin-CPP in rats, suggesting the α7nAChR are also involved in processing heroin-related memories (Palandri et al., 2021). On the other hand, systemic administration of MLA did not prevent reinstatement of heroin-seeking in a SA model, induced by heroin priming and the presentation of drug-paired cues (Palandri et al., 2021). CPP and SA investigate different components of drug-addiction, it is possible that the α7nAChR are more implicated in context-drug associations rather than habit-like behaviours, therefore reporting different effects across different reinstatement models.

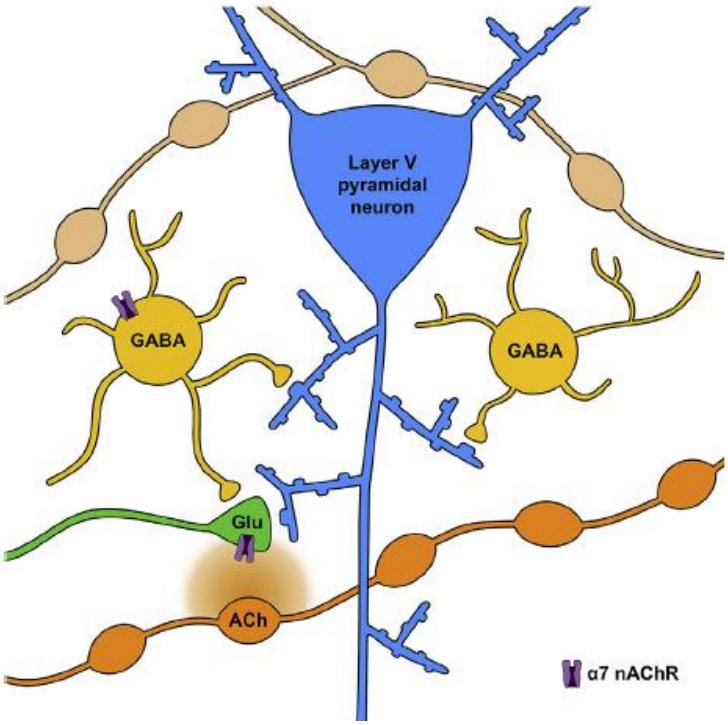

Figure 1.11 - Layer V pyramidal neurons are dynamically regulated by prelimbic α7nAChRs – Schematic model of the potential locations of α7nAChRs and the interaction between glutamatergic, GABAergic and cholinergic systems in layer V of PL. α7nAChRs are shown on the terminal of a glutamatergic afferent (green) and on cell bodies of inhibitory interneurons (yellow). Thus, α7nAChRs are able to influence both the excitability and inhibition of layer V pyramidal neurons (blue). Tonic endogenous ACh selectively targets α7nAChRs on glutamatergic terminals, suggesting close proximity to tonically active boutons en passant (orange). In contrast, GABAergic interneurons bearing α7nAChRs are either more distant from cholinergic fibres, or localised close to tonically inactive varicosities (brown) (Udakis et., 2016).

Insights into the synaptic contributions of α7nAChR have come from an electrophysiological study from our lab that showed that activation of α7nAChR located on glutamatergic terminals and cell soma of GABAergic interneurons increased excitation and inhibition, respectively, in layer V of the prelimbic cortex (Figure 1.11 (Udakis et al., 2016)). Specifically, the PAM PNU-120596, increased spontaneous excitatory events, an effect that was subsequently enhanced by inhibition of the enzyme AChE. In contrast, α7nAChR modulation of inhibitory signalling required the concomitant action of the agonist PNU-282987 and PNU-120596. These data suggest that α7nAChRs can bi-directionally modulate network activity in the PL, depending on the magnitude and localisation of α7 activation (Udakis et al., 2016). This finding highlights the role of α7nAChRs in modulating neurotransmission and the excitatory and inhibitory network of PL. Do α7nAChRs have the same regulative action in hippocampus? Hence, all this evidence, including limitations of previous studies, possible interrelations, and unanswered questions, led up to this project and its aims.

1.3 Aims of this thesis

Data from our lab explained in the previous sections suggest that α7nAChRs have a role in opioid-related memories, as their block inhibits reinstatement of both morphine- and heroin-CPP and that this action may depend on α7nAChRs' role in modulating neurotransmission and synaptic plasticity. The general focus of this thesis is to understand the role of α7nAChRs on the mechanisms underlying the heroin- and also cocaine-CPP, in order to explore the interplay between α7nAChRs and psychostimulants. Thus, the aims of this thesis were to:

- **Study the contribution of α7nAChRs in heroin- and cocaine-primed reinstatement of the CPP, in mice**

  The mouse CPP design was used to compare the role of α7nAChRs in heroin- and cocaine-CPP, extending the findings of Wright et al. (2019) and Palandri et al. (2021).

- **Investigate the role of functional α7nAChRs in hippocampus**

  The hippocampus is a key area for episodic memory and α7nAChRs are abundantly expressed within this area (Wallace & Porter, 2011). Due to their

role in modulating synaptic plasticity, I aimed to gain greater understanding in their action in regulating excitatory and inhibitory transmission in both dHIP and vHIP, in order to verify possible differences in α7nAChR distribution or function across those sub-regions.

- **Explore the neuronal activation, using c-Fos expression, in vHIP after the drug-primed induced reinstatement**

  Investigating the c-Fos expression in vHIP, but also in dHIP, as a control, and NAc Shell, BLA and PL, as the main projecting areas of the vHIP, was relevant to understand the role of the post-synaptic α7nAChR in modulating intracellular signalling associated with memory reactivation.

- **Optimise and study synaptic changes underlying the heroin-primed induced reinstatement and the effect of MLA on them**

  The autoradiography data from Wright et al (2019) cannot be directly interpreted as changes in synaptic plasticity. Hence, by performing patch-clamp recordings after heroin-primed induced reinstatement, AMPA/NMDA ratios were studied in order to test the hypothesis that the memory reactivation involves α7nAChR action.

- **Optimise and explore the involvement of the vHIP projecting areas during heroin-induced reinstatement and how α7nAChRs are involved in this process**

  In the last part, the involvement of the main projecting areas of the vHIP, namely PL, NAc Shell and BLA, during the heroin primed induced-reinstatement was examined in mice pre-treated with SALINE and MLA, by performing a retrograde tracing study and co-labelling with c-Fos activated neurons.

These Aims were undertaken to better understand the role of α7nAChRs in the memory events encapsulated in CPP reinstatement.

CHAPTER 2: MATERIALS AND METHODS

2.1 Animals and housing

All experiments were performed in accordance with Home Office project licence held under 'ASPA' 2012 and approved by the University of Bath's ethical review process. All animals were housed in groups of four, except animals that underwent surgery which were housed singly post operatively, in a behavioural holding room with controlled temperature (24 ± 2 ºC), humidity (50-60%), and a 12:12h light-dark cycle (lights on: 07.30h - 19.30h), with *ad libitum* access to food and water. For behavioural experiments, mice were allowed to acclimate to laboratory conditions for at least 3 days before the procedure during which they were handled daily in the experimental room. Weekly cage cleaning was conducted by the experimenter, immediately after behaviour on test days, allowing two days of recovery before the next stage of the protocol.

To carry out this project, two different strains of mice have been used, according to the aim of the study. Naïve (4 weeks old) male C57BL/6 mice were used for electrophysiological experiments (see Chapter 3). Adult (7-8 weeks old) male C57BL/6 mice were used for behavioural experiments (see Chapter 4), while 8-10 weeks old male c-Fos-GFP mice were necessary to perform the experiment described in Chapter 6. c-Fos-GFP mice were originally purchased from Jackson Laboratories (Bar Harbor, Maine, USA) and bred in-house from heterozygous males mated with wild type C57BL/6 females (Charles River UK).

2.2 Genotyping

Polymerase chain reaction (PCR) was used to genotype c-Fos-GFP mice from ear notch biopsy samples, collected from 3-week old male and female mice. For the DNA extraction, 75 µl of alkaline lysis reagent (25 mM NaOH, 0.2 mM disodium EDTA, pH 12) was set in the heat block at 95°C for 20 minutes. After heating, samples were

cooled at 4°C followed by adding 75µl of neutralising reagent (40 mM Tris-HCl, pH 5) into each sample (Truett et al., 2000). Once DNA was extracted, samples were processed for PCR, by using Taq DNA polymerase with standard Taq (Mg^{2+}-free) buffer kit (New England Biolabs, M0320S), dNTP mix (10 mM) (Thermo Fisher Scientific, R0191) and previously designed gene specific primers (Sigma-Aldrich, UK; summarised in Table 1). Specifically, 2.5 µl 1x standard Taq (Mg-free) buffer (containing 10 mM Tris-HCl, 50 mM KCl, pH 8.3), 2 µl $MgCl_2$ (1.5 mM) solution, 0.5 µl dNTPs (10 mM), 2.5 µl GFP forward primer (10µM), 2.5 µl GFP reverse primer (10µM), 1.25 µl β-actin forward primer (10µM), 1.25 µl β-actin reverse primer (10µM), 0.25 µl Taq polymerase, 8.25 µl RNase-free water and 4 µl DNA sample were added in each PCR tube. All the tubes were placed in a PCR machine (MJ Research, PCT-200) with the following reaction cycling conditions: 95 °C for 30 seconds (denaturation), 40 cycles of 95 °C for 15 seconds (denaturation), 60 °C for 30 seconds (annealing), 68 °C for 30 seconds (extension), followed by 68 °C for 5 minutes for final elongation. Samples were loaded with PCR loading dye and transferred on a 1% agarose gel with SYBR™ Safe Stain (1:10,000, Thermo Fisher Scientific) under 100V for 45 minutes. DNA bands were exposed to UV and visualised with Bio-Rad ChemiDoc.

Primer	Sequences 5'-3'	Size
β-Actin	**Forward:** CTAGGCCACAGAATTGAAAGATCT	324
	Reverse: GTAGGTGGAAATTCTAGCATCATCC	324
GFP	**Forward:** AAGTTCATCTGCACCACCG	173
	Reverse: TCCTTGAAGAAGATGGTGCG	173

Table 2.1 - The genetic sequences of forward and reverse primer sequences for β-actin (internal positive control) and GFP (transgene).

2.3 Electrophysiology experiments in naïve mice

2.3.1 Brain slice preparation

Male C57BL/6 mice 4 weeks old were anaesthetised via intraperitoneal injection of 160 mg/kg ketamine and 20 mg/kg xylazine and decapitated. The brains were quickly removed and immediately submerged into ice-cold solution containing (in mM): 20 NaCl, 2.5 KCl, 1.6 NaH_2PO_4, 7 $MgCl_2$, 85 sucrose, 25 D-glucose, 60 $NaHCO_3$, and

0.5 $CaCl_2$, and saturated with 95% O_2 / 5% CO_2. A razor blade was used to remove the anterior frontal cortex and the whole cerebellum, leaving a brain section containing midbrain and hippocampi. For the vHIP, horizontal slices (~bregma -3.2) 250 μm thick were produced using a vibratome (DTK-1000, DSK), while for dHIP brains were sliced coronally (~bregma 1.94). The brain slices were separated with a razor blade and then incubated at 32 °C for 30 min in artificial cerebrospinal fluid (aCSF) containing (in mM): 125 NaCl, 2.5 KCl, 1.2 NaH_2PO_4, 1.2 $MgCl_2$, 11.1 D-glucose, 21.4 $NaHCO_3$, 0.5 $CaCl_2$ saturated with 95% O_2/ 5% CO_2. Finally, slices were kept at room temperature until being placed in the recording chamber.

2.3.2 Whole-cell patch-clamp recordings

In both vHIP and dHIP, recordings were made from pyramidal cells in the stratum pyramidale of the CA1. Slices were submerged in a chamber receiving a constant flow of 2-3 ml/min aCSF, saturated with 95% O_2/ 5% CO_2 at 32°C. Slices were visualised using oblique optics on an Olympus BX51WI upright microscope. Recording electrodes with 3-5 MΩ tip resistance were fabricated using a micropipette puller (Sutter-instruments, P-97) and filled with an intracellular recording solution containing (in mM): 120 caesium methanesulphonate, 10 NaCl, 10 HEPES, 0.5 EGTA, 5 QX-314 bromide, 2 Mg-ATP, 0.25 Na-GTP, with an osmolarity 275 mOsm/L, pH 7.4 adjusted with CsOH and junction potential ~12 mV. Whole cell voltage-clamp recordings were amplified and filtered at 2 kHz using an Axopatch 200B amplifier (Axon Instruments) and digitised at a sampling rate of 10 kHz using a Digidata 1440a (Axon Instruments). Voltage steps from -60 mV to 0 mV were performed to obtain both excitatory and inhibitory post-synaptic currents.

2.3.3 Drugs

Methyllycaconitine (MLA), PNU-120596 and PNU-282987 were purchased from Abcam. MLA was dissolved in Milli-Q distilled water to obtain 100 μM concentration, while PNU-120596 and PNU-282987 were diluted in DMSO at the concentrations of 10 μM and 300 μM respectively. All other drugs and compounds were purchased from Sigma Aldrich.

2.3.4 Data analysis

All data from whole-cell voltage-clamped electrophysiological experiments were acquired using WinEDR and WinCP recording software (University of Strathclyde) and analysed off-line. Data points from traces were exported from WinEDR and graphically plotted using GraphPad Prism (Version 10). The inward currents induced by the α7 stimulation were quantified through expression of the magnitude of evoked current over time. Spontaneous EPSCs and IPSCs were detected using a threshold of between 2-10 pA and manually inspected to remove false events. The inter-event interval was used as a measure of post-synaptic event frequency over one minute. For the cumulative frequency, the same number of events were taken for each cell so as not to distort results towards cells with higher frequencies. One-Way Repeated Measure ANOVA or Friedman Test were performed with p values adjusted for multiple comparisons. Significant differences from control were presented as asterisk and assigned when $p<0.05$.

2.4 Conditioned place preference

2.4.1 Apparatus

The apparatus (MED Associates, UK) consisted of two-compartment shuttle boxes (Ugo Basile, Gemonio, Italy), containing 15 cm square arenas, separated by a guillotine door, with different texture and patterns. One arena consisted of grey walls and a metal floor with circular holes, the other had striped walls and square holes. Experiments were performed between 9:00h and 18:00h under dim white light and animals were weighed daily before drugs administration. During all preference test sessions, the animal had free access to both compartments; the time that the animal spent in each compartment and their locomotor activity (distance travelled in centimetres, cm) were recorded using EthoVision XT version 7.0 (Noldus Information Technology, Wageningen, The Netherlands) tracking software. The acquired digital signal was then processed by the software to extract the "time spent" in seconds (sec) in the two arenas of the apparatus.

2.4.2 Drugs

All drugs were dissolved in sterile sodium chloride solution (0.9%, Hameln pharmaceuticals, Gloucester, UK) and filter sterilised using 0.45 μm syringe filters

(Millipore). Mice were intraperitoneally (i.p.) injected with heroin, cocaine, or saline, while MLA was given subcutaneously (s.c.); all given using a volume of 10 mL/kg. Cocaine and MLA aliquots were stored at -20 C° for up to one month, while heroin aliquots were freshly prepared every day. Heroin hydrochloride (McFarlan Smith, UK) was injected at 2 mg/kg for conditioning and 1 mg/kg for reinstatement, while MLA was injected at 4 mg/kg, as previously reported by Wright and colleagues (Wright et al., 2019). Cocaine Hydrochloride (Sigma-Aldrich) was administered i.p. at doses of 15 mg/kg and 7.5 mg/kg for conditioning and reinstatement respectively, as shown by Singh & Lutfy, 2017.

2.4.3 Experimental procedure

The CPP procedure (Wright et al., 2019) consisted of six different phases: Habituation (1x15 minute session/day for 2 days); Conditioning (1x40 minute trial/day for 4 days), Acquisition test (1x15 minute trial), Extinction (1x30 minute trial/day for 4 days) Extinction test (1x15 minute trial) and Reinstatement (1x30 minute trial). The whole protocol and the steps used for each experiment are shown in Figure 2.1. Before starting the experiment, mice were weighed and handled in the CPP room, during the three previous days, in order to reduce stress and facilitate the output of the experiment.

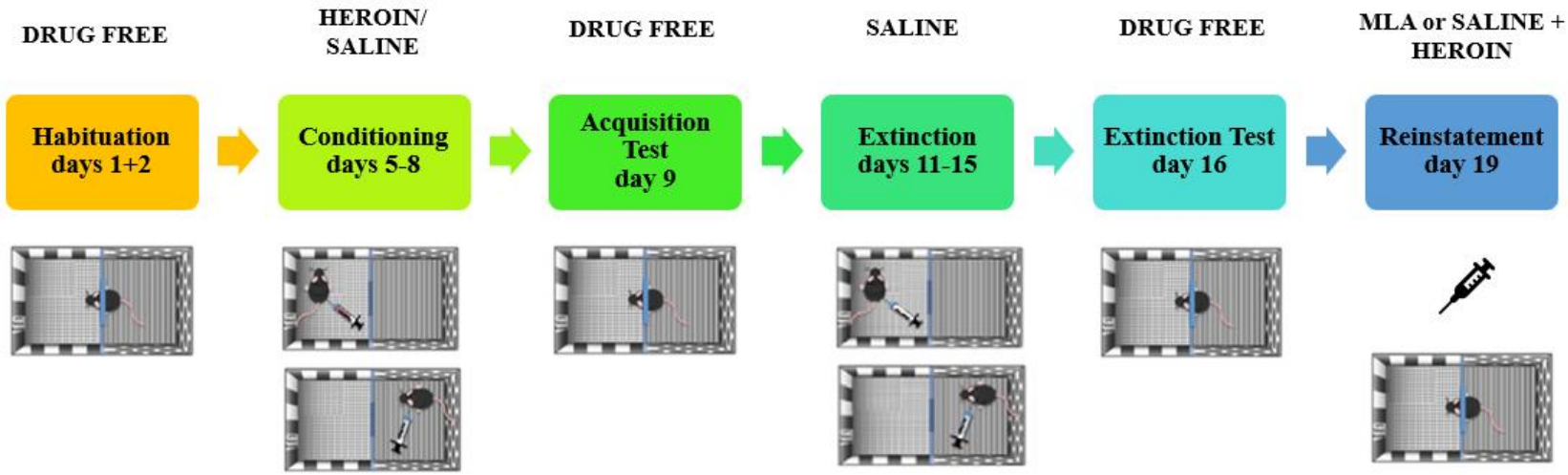

Figure 2.1 - Diagram of the heroin CPP – Experimental protocol of the heroin-CPP, from the habituation to the drug-induce reinstatement, specifying type of treatment, duration in days and type of stimulation.

2.4.3.1 Habituation

During the first two days of the experiment (Figure 2.1) animals were placed in the CPP boxes and allowed to freely explore both arenas for 15 minutes, described in section 2.5.1. Meanwhile, the software tracked the time spent in each compartment and the total distance moved in order to determine any initial preference to one of the compartments. Data obtained from the two days of habituation were averaged to define treatment groups in a pseudo-randomised trial, namely numerical sequences statistically random, but having been generated by a totally deterministic and repeatable process, for a counterbalanced design, in which half of the subjects were conditioned to the grey-wall arena and the other half to the striped-wall arena. Animals showing a preference score of > 200 or > -200 seconds were excluded from the experiment.

2.4.3.2 Conditioning

From day 5 (see figure 2.1), mice received a daily i.p. injection either saline (0,9%) or heroin (2 mg/kg) or cocaine (15 mg/kg), depending on the type of the experiment (for heroin-CPP and cocaine-CPP). Daily treatments, namely the drugs and saline, were assigned using counterbalanced design, in which half of the animals were drug-paired with one compartment type and the other half were drug-paired with the other compartment type and the order of heroin, or saline presentation was also counterbalanced. The same experimental design was used for the cocaine CPP experiments. After the injections, mice were confined to their paired compartment for 40 minutes and on the following day, those that received drug were then administered saline in the other compartment and *vice versa*. This alternation was repeated over the four days. Thus, mice were given two injections of drug and two of saline, throughout the conditioning phase. Locomotor activity was recorded during each session.

2.4.3.3 Acquisition test

The day after the last conditioning day, animals were allowed to explore both arenas for 15 minutes, by removing the guillotine door. Time spent in each chamber was recorded and the number of seconds spent in each side was used to assess the preference. Specifically, an initial Student's t test, between the time spent in the drug-

paired compartment during habituation and preference test to verify the acquisition of the preference and before moving to the next phase.

2.4.3.4 Extinction test

Mice received daily i.p. injections of saline (0.9%) for four consecutive days and were confined to the previously drug-paired compartment on the first and third day and to the previously saline-paired one on the second and fourth day (Figure 2.1).

2.4.3.5 Reinstatement

On reinstatement day (see Figure 2.1), mice were assigned to MLA or saline treatment groups by using a pseudo-randomisation model. Subjects were pseudo-randomised so that preference scores from the Habituation, Acquisition test, and Extinction tests had similar averages between the two reinstatement treatment groups, while retaining balance with respect to cage numbers, CPP box numbers, and which side of the box the animal was conditioned to. Moreover, the experiment was performed according to a "blinded" protocol. Experimental groups received a subcutaneous injection of either saline (0.9%) or MLA (4 mg/kg) 20 minutes before heroin- or cocaine-primed reinstatement, in their home cages. To induce reinstatement, a priming dose of the drug used during conditioning was administered via i.p. injection to induced reinstatement. Mice were then allowed to explore the apparatus for 30 minutes, while time spent in each compartment and distance travelled were recorded. Ninety minutes after the beginning of the reinstatement test (Cruz et al., 2014; Ziminski et al., 2018), mice were killed, and brains taken either for subsequent immunohistochemical experiments (see Section 2.6) or brain slice electrophysiological experiments (see Section 2.7).

2.4.4 Data analysis

All CPP data are presented as mean ± standard error of the mean (SEM). Time spent in seconds and distance travelled in cm were acquired via camera and analysed with Ethovision XT version 7. The preference scores are displayed as time spent in the drug-paired compartment - 450 seconds, namely half of the test time.

Statistical outlier, across each phase of the CPP, were identified via Grubb's test and excluded where appropriate, revealing a total of one outlier out of forty-seven. Reinstatement results were analysed in consecutive 15 minute time-bins, however, the last 15 minutes appeared more reliable, as in previous work from our lab (Wright

et al., 2019; Palandri et al 2021). Behavioural analyses were performed with One-Way ANOVA Repeated Measures with Dunnett's *post hoc* test, comparing habituation and post-extinction to the preference test, and Student's t-test unpaired to evaluate the effect of MLA and SALINE on the drug-induced reinstatement. Significant differences from control were assigned when $p<0.05$.

2.5 Single-injection experiment

This experiment was aimed to examine any acute effect of drug on c-Fos expression (section 2.6). Male C57BL/6 6-7 weeks old mice were treated as on the heroin-CPP reinstatement day, but without any behavioural manipulation or exposure to CPP apparatus. Treatment groups are explained in the following table:

Pre-treatment (s.c.)	Treatment (i.p.)	Group name
SALINE 0.9%	SALINE 0.9%	S+S
SALINE 0.9%	HEROIN 4 mg/kg	S+H
MLA 4 mg/kg	SALINE 0.9%	M+S
MLA 4 mg/kg	HEROIN 1mg/kg	M+H

Table 2.2 - Experimental groups for the single-injection trial.

Mice were firstly pre-treated with either saline or MLA and returned to their home cages. Twenty minutes later, animals received an i.p. injection of saline or heroin and were again returned to their home cages for the following 90 minutes. Mice were then killed, and brains sectioned for immunohistochemistry (see section 2.6).

2.6 Immunofluorescence for c-Fos detection

2.6.1 Perfusion fixation and sectioning

Following CPP or single injections (sections 2.4 and 2.5) animals were anaesthetised with 4% pentobarbital and cardio-perfused with 0.1M PBS and 4% paraformaldehyde (PFA) and the brains removed. Cardiac perfusion was performed by anaesthetising the animals, opening the chest cavity. The ribcage was cut and

removed to expose the heart and to make a cut with scissors on the right atrium. A 26-gauge syringe needle, connected to a peristaltic pump with a flow rate of 4 mL/min, was inserted into the left ventricle and the ice-cold PBS was washed through. Systemic blood washout was considered successful when the liver became clearer, and death confirmed with the cessation of breathing and cardiac arrest; then the animal was perfused with 4% PFA until the body was rigid. The brains were extracted, and the fixation process was considered to have worked if the brain appeared pale white. Samples were stored in 4% PFA for the following 1-2 days and then transferred to 30% sucrose in PBS with 0.1% azide solution and stored in the fridge until further use.

Brains were sectioned to give 40 μm coronal slices in cold 0.1M PBS using a vibratome, in order to obtain the following brain regions, also shown in Figure 2.2: PL (bregma 2.8), NAc Shell (bregma 1.34), dCA1 and BLA (bregma 1.94) and vCA1 (bregma -3.2), according to the mouse brain atlas (Paxinos & Franklin, 2004). From every brain, 5-6 slices were taken for each brain region and kept in a 24 well plate containing 0.1M PBS.

For the single-injection experiment (see section 2.5) brains were sliced horizontally to better detect the vCA1.

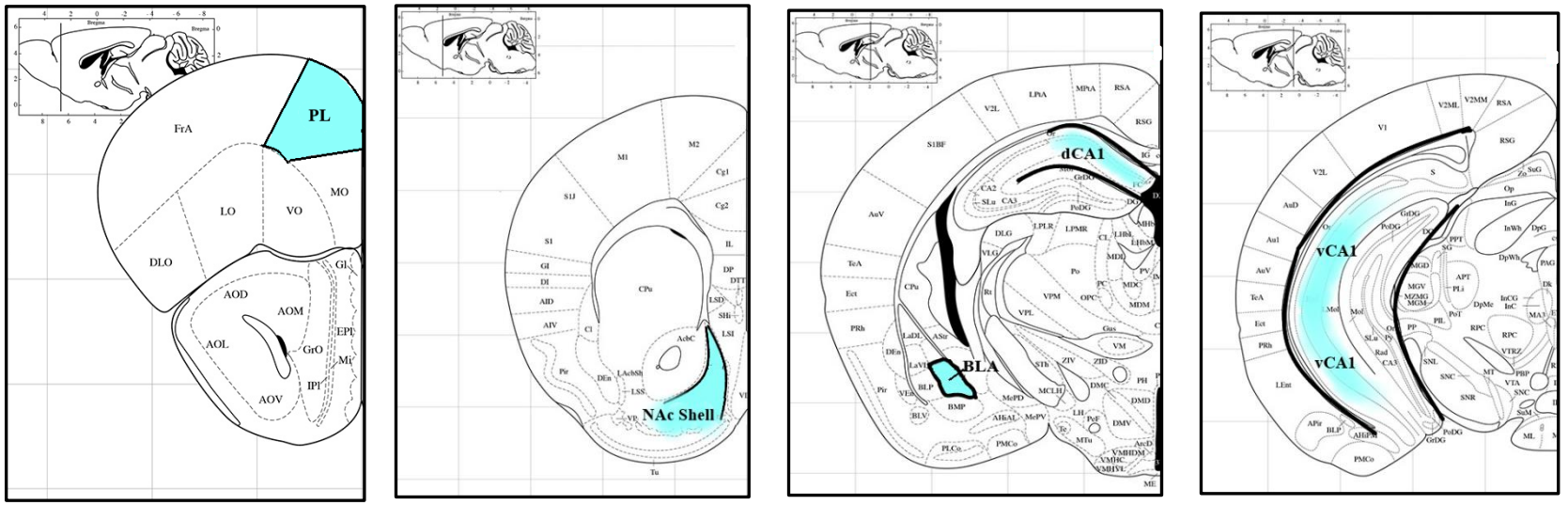

Figure 2.2 – Coronal sections and bregma points for immunofluorescence – The light blue parts indicate in which point of the brain sections were exactly take for immunofluorescence. In mm: PL (2.8), NAc Shell (1.34), dCA1(1.98) and BLA (-1.34), vCA1 (-3.2) (figure adapted from Paxinos & Franklin, 2004)

2.6.2 Staining for c-Fos and Neun

After the slicing procedure, brain sections were incubated, on a shaker, for two hours at room temperature in a blocking PBS solution containing 0.1% Triton X-100 and 5% donkey serum. Hereafter, slices were incubated at 4°C with the following primary antibodies: c-Fos (9F6) rabbit (Cell Signalling, mAb #2250, 1:1000), and chicken Anti-Neun (Merk, ABN91, 1:500) to detect c-Fos positive nuclei and neuronal cells respectively. The following day, slices were washed four times with 0.1 M PBS (15 minutes each wash); the slices were then incubated with the secondary fluorescent antibodies: goat anti-Rabbit IgG (H+L) Alexa Fluor 568 (Thermo Fisher Scientific, 1:500) and Alexa Fluor 488 ab150169 (Abcam, 1:1000) for two hours at room temperature, on a shaker. Finally, brain tissues were washed four times over 2 hours and mounted with Vectashield Mounting Media (Vector Laboratories) on microscope slides, which were subsequently acquired by using a Leica Fluorescent Microscope, equipped with three filter cubes: 'Filter Cube A (DAPI)': Excitation: 340-380 nm / dichromatic mirror: 400 nm / suppression filter 425 nm; 'Filter Cube L5 (GFP)': Excitation: 480/40 nm / dichromatic mirror: 505 nm / suppression filter: 527/30; 'Filter Cube N2.1 (rhodamine): Excitation: 515-560 nm / dichromatic mirror: 580 nm / suppression filter 590 nm.

2.6.3 Cell quantification and statistical analysis

Images were analysed using FIJI-ImageJ and c-Fos positive nuclei calculated as cells/mm^2 (Ziminski et al., 2018), by dividing the number of the nuclei, automatically calculated by the software, per the slide area. A total of 2-3 images were averaged within the same area for each subject. Statistical analysis was performed by Student's t-test paired, where the SALINE and MLA treated groups were compared for each brain region. Brain slices from the single injection experiment were analysed via One-Way ANOVA and Bonferroni's *Post hoc* test for multiple comparisons. Data were analysed using GraphPad Prism version 9.3.1.

2.7 Electrophysiology experiments in heroin-CPP trained mice

2.7.1 Brain slice preparation

cFos-GFP mice (8-11 weeks old) first underwent reinstatement of heroin CPP (see Section 2.4). 90 minutes after the beginning of the reinstatement test, mice were anaesthetised with 160 mg/kg ketamine and 20 mg/kg xylazine and then cardio-perfused with ice-cold NMDG-based recovery solution (Sieburg et al., 2019) containing (in mM): 93 NMDG, 2.3 KCl, 1.2 NaH_2PO_4, 30 $NaHCO_3$, 20 HEPES, 25 D-glucose, 12 N-acetyl-L-cysteine, 2 sodium ascorbate, 3 sodium pyruvate, 10 $MgSO_4$, 0.5 $CaCl_2$, giving an osmolarity of approximately 330 mOsm/L adjusted to pH 7.4 with HCl and saturated with 95% O_2 / 5% CO_2. As explained in 2.3.1, coronal cuts were made with a razor blade to remove the anterior frontal cortex and the whole cerebellum, obtaining a brain section containing midbrain and hippocampi. The brain was then placed in a falcon tube containing NMDG recovery solution and carried to the building where electrophysiological experiments took place. Brains were then sliced in ice-cold saturated NMDG recovery solution to obtain 250 μm horizontal slices of vHIP (-3.2). Finally, slices were transected to separate the hemispheres and the CA3 removed in order to avoid any excitatory reverberation following electrical stimulation. Slices were then placed into a slice-holder containing aCSF saturated with 95% O_2 / 5% CO_2 at 32ºC for 30 minutes and then stored at room temperature for the rest of the experiment.

2.7.2 Whole-cell patch clamped recordings

As reported in section 2.3.2, slices were transferred to the recording chamber and submerged in aCSF, and neurons localised using oblique optics on an Olympus BX51WI upright microscope. c-Fos positive neurons were identified through the fluorescent Olympus U-RF-LT mercury lamp attached to the BX51WI microscope. For evoked responses, a Teflon coated bipolar stimulating electrode (tip separation 75 μm) was placed in the proximity of the stratum radiatum of the CA1 of the vHIP. The stimulation consisted of a square wave of 150μs duration at a frequency of 0.1Hz. Stimuli were induced using WinWCP software via a constant-current stimulation isolation unit (DS2A, Digitimer). For paired-pulse recordings, twin pulses (inter-pulse interval: 50 ms) were applied, however, pulses were switched to single pulse before the application of the drugs. The recording electrode consisted of a pulled glass pipette

with an electrical resistance of 3-5 MΩ and filled with: intracellular recording solution containing: (in mM): 0.1 spermine, 120 Caesium Methanesulphonate, 10 NaCl, 10 HEPES, 0.5 EGTA, 5 QX-314 bromide, 2 Mg-ATP, 0.25 Na-GTP, with an Osmolarity of 275 mOsm/L, pH 7.4 adjusted with caesium hydroxide (CsOH) and junction potential ~12 mV. At the beginning of each recording, a stimulus-response (I-V) curve was generated to find the sub-maximum response, and a stimulation value (constant current) that gave a response equal to ~75% of the maximum was used for the duration of the experiments.

2.7.3 Drugs

All the compounds for this experiment were purchased from Hello Bio (Bristol). Drugs were diluted and dissolved as follows: spermine 100 mM in water, picrotoxin 50 mM in DMSO, D-AP5 50 mM in water, NBQX disodium salt 10 mM in water.

2.7.4 Data analysis

Recordings were obtained by stimulating Schaeffer Collateral inputs to generate evoked EPSCs and using a combination of voltage-steps to +30 mV and selective NMDA receptor antagonists to isolate the AMPA and NMDA receptor components of the EPSCs (see Chapter 5, Figure 5.6). AMPA/NMDA current ratios were obtained through two different types of analyses. Firstly, the NMDAR current at +30 mV was found by subtracting the AMPAR-only current at +30 mV (in the presence of D-AP5) from the composite AMPAR+NMDAR current at +30 mV then compared with the AMPAR current at -60 mV. Secondly, the NMDAR current at +30 mV was found by recording the composite AMPAR+NMDAR current at a timepoint where the AMPAR component had decayed to zero (60 ms) and compared with the AMPAR current at -60 mV.

The AMPAR rectification curves were generated by averaging 2-3 stimulations at -60, 0, +30 mV in the presence of D-AP5. The rectification index (RI) was calculated by dividing the EPSC amplitude at -60 mV by the one at +30 mV.

Paired-pulse ratios (PPRs) were obtained by recording from paired stimulations (50ms apart), at -60mV, and dividing the second EPSC peak by the first one.

One-Way ANOVA Repeated Measures was performed to investigate any significant difference.

2.8 Brain surgery: infusions of retrograde tracers

2.8.1 Experimental design

Before the surgery procedure, male C57BL/6, 6-7 weeks old, underwent CPP for heroin with habituation, conditioning and extinction, including preference test and extinction test. Heroin (2 mg/kg i.p.) or saline (0.9%) were administered on alternate conditioning days during conditioning and only saline was given during the extinction (as reported in section 2.4.3). Subjects were pseudo-randomised for treatments balanced according to the preference score across habituation, preference test and extinction test and underwent surgery for infusion of three dyes, counterbalanced across regions (PL, NAc Shell and BLA) between different animals. After the surgeries and the subsequent recovery, mice were treated with MLA (4 mg/kg s.c.) or saline (0.9% s.c.) and, 20 minutes later, given an injection of a priming-dose of heroin (1 mg/kg) and tested for the primed-induced reinstatement.

2.8.2 Infusions of retrograde tracers

Surgeries were performed between extinction and reinstatement phases. Mice were anaesthetised with isoflurane (induction 4%, maintenance, 2-3%, Baxter, UK). The animal was quickly placed into the stereotaxic apparatus and put on a heated blanket to maintain a consistent body temperature during the procedure. The skull was then exposed and gently scraped to identify the bregma. Once the bregma was viewable and the skull was assessed to be completely flat and straight, anterior-posterior (A-P), medium-lateral (M-L) and dorsal-ventral (D-V) coordinates were taken. The skull was then drilled in the points which corresponded to the coordinates relative to bregma and the infusion needle was inserted in: PL (AP +2.8, ML ± 4.8, DV 0.5), NAc Shell (AP +1.34, ML ± 0.5, DV -4,7), BLA (AP -1.60, ML ± 3.32, DV -4.9). Cholera Toxin Subunit B conjugated with Alexa Fluor 488 and Cholera Toxin Subunit B conjugated with Alexa Fluor 660 (CTB 488 and 660, Biotium) 0.5%, dissolved in 0.1 M PBS, and Fluorogold (FG, Fluorochrome) 2%, dissolved in 0.9% saline were used. Each tracer was backfilled in a 35 bevelled NanoFil stainless steel needle (WPI), connected with a tubing to a 10 µl NanoFil syringe (WPI). Tracers were infused through an automated

syringe infusion pump (Harvard apparatus) with a flow rate of 0.1 µl/min for 5 minutes and allowed to diffuse for an additional 5 minutes before the retraction of the infusion needle. Once the brain infusions were completed, the skull was cleaned, and the incision sutured. Local antibiotic solution was applied in proximity of the stitches. Mice were rehydrated with saline (0.9%, s.c.) and given a systemic antibiotic (Clamooxyl LA, Pzifer, 15 mg/mL, s.c.) and post-operative pain analgesia (Caprieve 25 mg/kg, s.c.). Operated animals were allowed to recover in a clean and heated cage under constant supervision, until the animal was able to walk around the cage. Mice were single-housed for three days, and the weight was measured daily, to ensure there was not any rapid weight loss, while analgesia was administered for three days following the surgery. The recovery time, including the three days of post-op care was one week at least. A time-window of 2-7 days was also necessary to allow CBT and FG to express themselves (Lanciego & Wouterlood, 2020; Saleeba et al., 2019) Thereafter, mice were group-housed and allowed to recover until the beginning of the reinstatement phase. As reported in 2.6, mice were perfused 90 minutes after the beginning of the test and brains treated for immunofluorescence and co-labelling with retrograde tracers. For detecting FG, CTB 488 and c-Fos stained neurons a Leica Fluorescent Microscope was used, while a Zeiss Confocal Microscope was necessary for acquiring the CTB 660 infected neurons.

2.8.3 Data analysis

As reported in section 2.6, mice were perfused 90 minutes after the beginning of the reinstatement test and brains treated for immunofluorescence and co-labelling with retrograde tracers.

To examine the co-labelling of c-Fos expression and CTB 488, CTB 660 and FG in the CA1 of the vHIP from different brain regions, c-Fos neurons and retrograde-tracer-labelled neurons were counted with FIJI-ImageJ (see 2.7.3). The percentage overlap was the calculated as: ((CTB 488)/c-Fos)*100), ((CTB 660)/c-Fos)*100), ((FG/c-Fos)*100), as previously reported (Roy et al., 2017).

CHAPTER 3
THE ROLE OF α7nAChRs IN MODULATING HEROIN- AND COCAINE-INDUCED REINSTATEMENT AND THEIR IMPACT ON c-FOS EXPRESSION

3.1 Introduction

In clinical settings, drug-context associations represent the one of the main reasons for failure of strategies oriented to prevent drug-seeking, leading to relapse (Napier et al., 2013). In animal models, stimuli conditioned to the motivational properties of the drugs of abuse make the individual susceptible to drug-seeking behaviour, despite negative consequences (Vanderschuren & Everitt, 2004), and resistant to extinction-like therapies (Bouton, 2014). In fact, the initial or acute use of drugs of abuse can induce the establishment of maladaptive memories (Van Der Meer & Redish, 2011) and these become very enduring. Hence, the aim of this chapter was to investigate the role of α7nAChR in modulating drug-associated memories in both heroin- and cocaine-CPP, as a model of drug-seeking.

In pre-clinical scenarios, different behavioural paradigms are used to study several features of those maladaptive drug-context associations and how they can elicit drug-seeking behaviours. As discussed in section 1.1.4 of Chapter 1, conditioned-place preference (CPP) is a Pavlovian behavioural model which allows the evaluation of the conditioned reward produced by different types of stimuli (Tzschentke, 2007), representing an viable approach to study the motivational properties of the drugs (Aguilar et al., 2009).

The CPP model has been largely used to study the acquisition itself. However, the use of this paradigm can be extended to study extinction and reinstatement, which can be defined as an experimental model of relapse of drug-seeking in rodents. According to this approach, the CPP must be extinguished and then reinstated through different factors, such as exposure to priming doses of drugs, which is the phenomenon

investigated here, discrete or contextual stimuli or stressors (Shaham et al., 2003). In general, it is possible to consider the challenge dose of the drug as successful in inducing reinstatement, if there is a significant difference with preference scores from the pre-conditioning, or habituation, and extinction. Moreover, the presence of the drugs of abuse during the reinstatement session reduces the possibilities of a competing extinction process during the memory reactivation. Thus, the administration of a priming dose of the drug given during the training can reinstate the preference for the drug-paired compartment, expressed as a re-approach to the contextual stimuli. Specifically, the persistent memory of the rewarding effects of the drugs, re-activated by the drug-priming induced reinstatement, motivates subjects to seek the contextual cues related to that reward (Perry et al., 2014).

On the other hand, CPP presents some limitations. For example, subjects may develop an initial considerable preference or avoidance for one arena over the other, affecting the acquisition of the conditioning. Specifically, when one of the compartments is "highly preferred" during the habituation, the preference may not be boosted by the conditioning phase, while a prior avoidance for one side could be considered as a "less aversive" after the conditioning, but not truly preferred (Napier et al., 2013). A way to overcome those issues is to perform a balanced unbiased procedure and so reduce the impact of an initial trend on the interpretation of results. Moreover, the CPP approach does not allow a dose-response curve definition, reducing its utility when the value of a drug has to be measured during conditioning (Napier et al., 2013). However, this thesis is focused on the role of α7nAChRs in modulating reinstatement of drug-associated memories, demonstrating that the preference has been already acquired and extinguished.

As reported in Chapter 1, nicotinic receptors have been studied not only for their role in nicotine addiction, but also for their interaction with the endogenous opioid system, particularly in respect of drug-memory associations. Importantly, data from our lab showed that the selective antagonist of α7nAChRs MLA selectively blocked the reinstatement of a morphine- and heroin-CPP, even if the mechanism by which this action occurs still needs clarification (Feng et al., 2011; Wright et al., 2019; Palandri et al., 2021). In particular, in the work from by Wright et al. (2019), only when MLA

was locally infused in vHIP, but not in dHIP or in mPFC, was morphine-induced reinstatement blocked, highlighting the relevance of α7nAChRs in vHIP for drug-related memories.

The impact of nAChRs on cocaine-associated effects has been also explored. For instance, the reinforcing effect of cocaine was inhibited by microinjections of MLA in VTA, in a model of intracranial self-stimulation (ICSS) of cocaine in the lateral hypothalamus, suggesting that α7nAChRs may modulate rewarding effects of cocaine (Panagis et al., 2000). Furthermore, it has been reported that micro-infusions of MLA, but not the α4β2 antagonist DhβE, in VTA or NAc enhanced the levels of cocaine-induced DA release in NAc, in a microdialysis experiment, indicating a role of α7nAChRs in mediating mesolimbic dopaminergic activity (Zanetti et al., 2007). In particular, α7nAChRs have been shown to be relevant for cocaine-related memories. A recent work investigated the effect of local infusions MLA in mPFC on the acquisition, consolidation, and expression of a cocaine-CPP, showing that α7nAChRs in mPFC are required for acquisition and retrieval but not consolidation of the cocaine-CPP (Pastor et al., 2021). In addition, an interplay between α7nAChRs and the dopaminergic system in rat prefrontal cortex has been demonstrated (Livingstone et al., 2010). This evidence suggests that there is an interaction between α7nAChRs and cocaine-associated effects, but the role of the vHIP in these processes is still to be clarified. Furthermore, there is no literature about the action of α7nAChRs in modulating cocaine-induced reinstatement. In fact, the interest in cocaine addiction has focussed mainly on mesolimbic DA transmission and as mentioned in Chapter 1 (section 1.2.8), and interaction between α7nAChRs and cocaine will be therefore investigated, to explore a possible novel mechanism underlying cocaine-associated memories.

Taken together, these findings highlight a potential role for α7nAChRs in modulating reward-related memories, in particular the ones related to opioids and cocaine. This has prompted the hypothesis that their actions on this type of memory can be found downstream, sustaining mechanisms of drug-related memories reactivation. Findings from our group have shown that MLA can selectively block reinstatement in morphine- and heroin-CPP in rats (Wright et al., 2019; Palandri et al., 2021). The

ability of MLA to selectively block α7nAChRs on the reinstatement of the heroin-CPP in mice and on the cocaine-CPP have now been investigated for the first time.

The presence of post-synaptic α7nAChRs has been demonstrated and reported in Chapter 4. Hence, it can be hypothesised that when activated by the cholinergic input coming from the medial septum, α7nAChRs allow Ca^{2+} entrance, activating the ERK/MAPK pathway that directly stimulates the c-Fos promoter CREB and so translation of c-Fos protein (Cruz et al., 2015). It has been shown that c-Fos expression correlates with learning, performance and memory retrieval (Gallo et al., 2018). Hence, this brings to the hypothesis that the blockade of α7nAChRs by MLA could also decrease c-Fos expression, as a correlate of neuronal activation during drug-induced reinstatement. The aim of the experiments described in this chapter was to investigate the involvement of the vHIP in this process, as it has been found to have a selective role in morphine-induced reinstatement (Wright et al., 2019). Thus, to study the relevance of the ventral hippocampal α7nAChRs, in respect of the CPP-reinstatement, c-Fos expression in vHIP has been explored. In addition, the c-Fos expression in dHIP was also measured, to verify the selective role of vHIP in re-activating this type of memories. The dHIP is more involved in "spatial memory" and has been employed as a reference control brain region (see Chapter 1, section 1.3.3). Finally, the effect of MLA before drug-induced reinstatement also in the projection areas of the vHIP, such as PL, NAc Shell and BLA, was evaluated, to define a possible network modulated by α7nAChRs during drug-induced reinstatement. The effect of MLA in heroin-treated naïve mice has been evaluated, to identify a possible *per se* on neuronal activation induced by this drug.

In the next section the different phases of the heroin-CPP will be shown. At first, baseline, acquisition of the preference for the heroin-paired side and its extinction have been analysed, reporting that the CPP was successful. Next, animals have been pseudo-randomised and so assigned in the two treatment groups, namely SALINE and MLA, and tested for the heroin-primed induced reinstatement.

3.2 Results

3.2.1 Habituation, acquisition and extinction of the heroin-CPP

As reported in Chapter 2 (section 2.4), the CPP procedure consisted of six different phases: habituation, conditioning, acquisition test, extinction, extinction test and reinstatement (1x30 minute trial). Briefly, after obtaining baseline preference measurements, in which no drugs were administered, C57BL/6 male mice underwent the conditioning phase, where daily i.p. injections of either 2 mg/kg heroin or 0.9% saline were given to mice which were then confined into their paired compartment for 40 minutes. The day after the last conditioning day, animals were allowed to explore both arenas for 15 minutes, by removing the guillotine doors. Once that the acquisition of the preference was assessed, mice underwent the extinction phase, where they received daily i.p. injections of saline (0.9%) for four consecutive days and confined to the drug-paired side on the first and third day and to the saline-paired one on the second and fourth day.

All the testing sessions were recorded by Ethovision XT 7 and the number of seconds spent in each side was used to assess the presence of the preference. Locomotor activity in cm was also acquired and analysed during each session.

As reported below, mice acquired the preference for the heroin-paired side and its extinction, which is fundamental for the continuation of the experiment to the reinstatement phase.

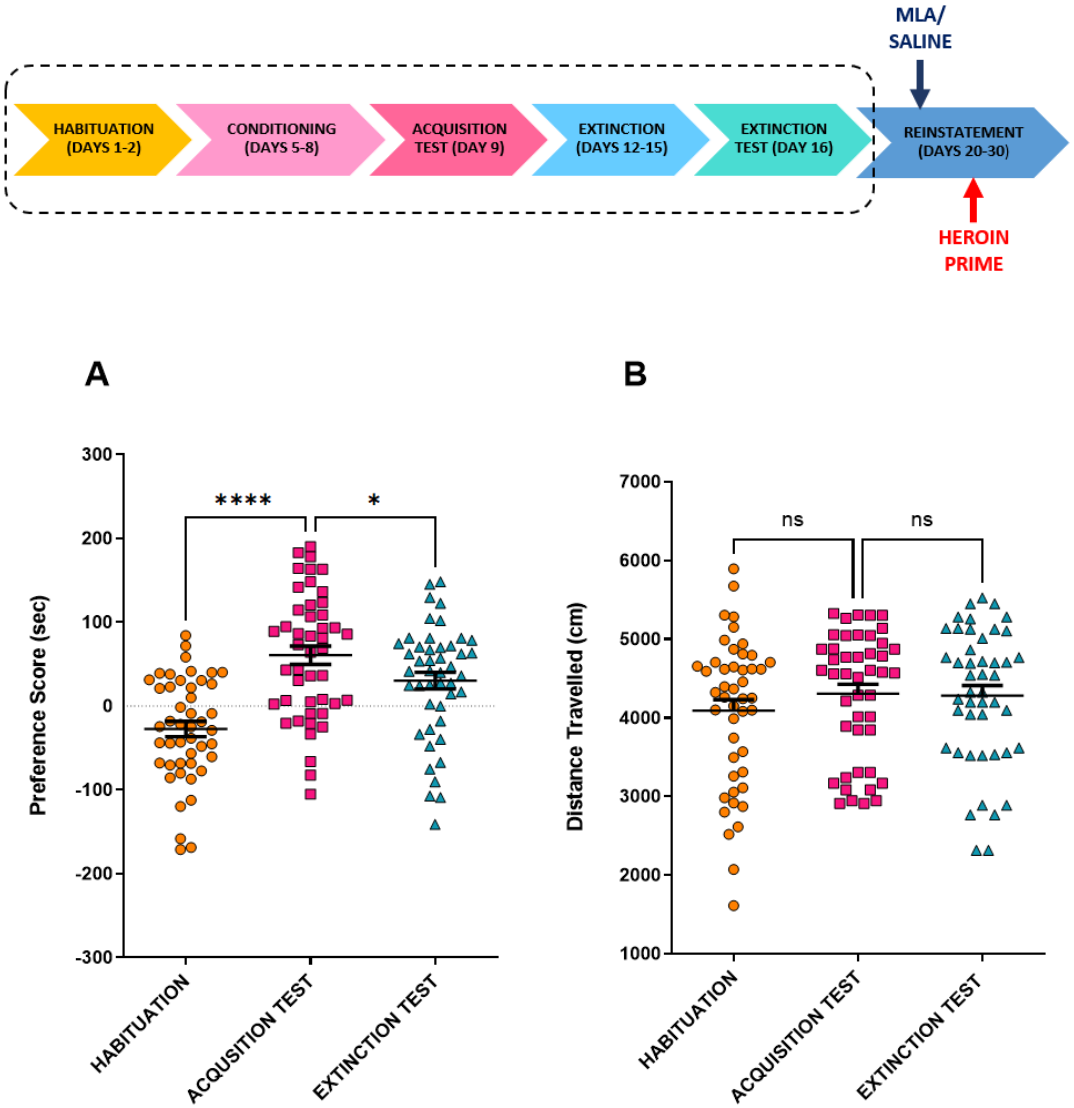

Figure 3.1– Preference scores and locomotor activity on the stages of the heroin-CPP in mice - Above, experimental timeline of the heroin-CPP including all the phases and days. (**A**) Preference scores expressed in seconds across the habituation to obtain a baseline (average from day 1 and day 2), acquisition of the preference (day 9) for the heroin-paired side, induced by a daily injection of heroin 2 mg/kg given in one compartment, and saline (0.9% i.p.) in the other one, alternately for 4 days; and extinction (day 16), which consisted of daily saline injections (0.9% i.p.) in both compartments alternately, for 4 days. During the habituation, acquisition test and extinction test, mice were allowed to freely explore the apparatus. Overall, mice significantly acquired the preference for the heroin-paired compartment, which was then significantly extinguished in comparison with acquisition test. Preference Score is expressed in seconds (sec). One-way ANOVA with Dunnett's Multiple Comparison Test (*post hoc* analysis preference test vs habituation and acquisition test vs extinction), p****<0.0001, p*<0.5. n=46. (**B**) Total distance travelled (cm) along the CPP apparatus during habituation, preference test and extinction. The analysis of the locomotor activity reported no significant difference across the CPP phases. One-way ANOVA with Dunnett's Multiple Comparison Test (*post hoc* analysis preference test

vs habituation and preference test vs extinction), n=46. Data All test sessions were performed in drug free state and tracked via Ethovision XT. Data points are individual mice responses with mean ± SEM overlaid.

In the first part of the CPP, all mice first explored the apparatus during the habituation, in order to assess any prior preference or avoidance for one or the other compartment. Two mice out of 48, showing a preference score lower than 200 seconds during the habituation have been excluded from the experiment. Once the baseline was acquired, mice underwent the conditioning session, to induce the preference for the heroin-paired compartment, which was then significantly attenuated during the extinction phase. These data show that, on average, mice did not show preference for the heroin-paired compartment during the habituation. Instead, in the acquisition test, mice spent on average 86 sec (S.E.M±10.7) longer in the heroin-paired side, developing a significant increase for the heroin-paired arena. Importantly, these results are combined from three different experiments, over which the effect of the 2 mg/kg heroin to induce preference was consistent, demonstrating that this dose of heroin was effective in inducing the drug-context association. Thus, even if some subjects showed negative preference scores, the entire cohort exhibited an overall increase in preference in comparison to the scores from habituation.

Mice showed a significant difference between the scores from acquisition and extinction test, with an overall trend showing a significant attenuation of the preference score, demonstrating that the extinction training was successful (Figure 3.1A). Moreover, as shown in Figure 3.1B, there was no difference in locomotor activity, across habituation, preference test and extinction tests. These data suggest that the relative changes in the preference score, across the experimental phases were not provoked by changes in the exploratory behaviour.

In summary, these results indicate that the heroin dose of 2 mg/kg used during the conditioning produced CPP in mice. This behaviour could also be extinguished, which is an essential step to proceed to reinstatement. Thus, the CPP was considered successful, and the experiment progressed studying the impact of the effect of MLA on the heroin-primed reinstatement, and so the involvement of α7nAChR in this phenomenon.

3.2.2 The effect of MLA on heroin-primed induced reinstatement

Before proceeding with the reinstatement phase, mice were pseudo-randomised and assigned to the treatment groups, namely SALINE and MLA to guarantee that the preference scores during habituation, acquisition test and extinction test were all balanced, in order to avoid any possible bias in the interpretation of results (for more details see Chapter 2, section 2.5.3.5). Figure 3.2 shows the preference scores during the habituation, acquisition test and extinction test for mice distributed to treatments groups. In this case, Student's t-test (unpaired) showed no difference in the preference scores between treatment groups. In addition, the spread of data points between groups was comparable, confirming that the study was balanced Once mice were pseudo-randomly distributed to either SALINE, which was the control group, or MLA group, the experiment was progressed to the reinstatement phase.

Twenty minutes prior to the heroin-primed reinstatement, mice were administered saline or MLA (4 mg/kg s.c.). At the present, there are no studies investigating heroin-primed reinstatement of heroin CPP in mice. However, it has been shown that 2 mg/kg heroin is an effective dose to induce the acquisition CPP in C57BL/6J mice (Bailey et al., 2010; Figure 3.1). Thus, the heroin-induced primed reinstatement was performed by using 1 mg/kg, because a lower dose of the drugs can reinstate the responses elicited by the injection of the conditioning drug (Shalev et al., 2002). Moreover, the MLA dose of 4 mg/kg, given s.c, has been already found effective on drug-induced reinstatement in both mice and rats, by experiments performed in our research group (Wright et al., 2019; Palandri et al., 2021) and others (Feng et al., 2011).

Results of both preference score and locomotor activity during the heroin-induced reinstatement are displayed below, in Figure 3.2 C and D.

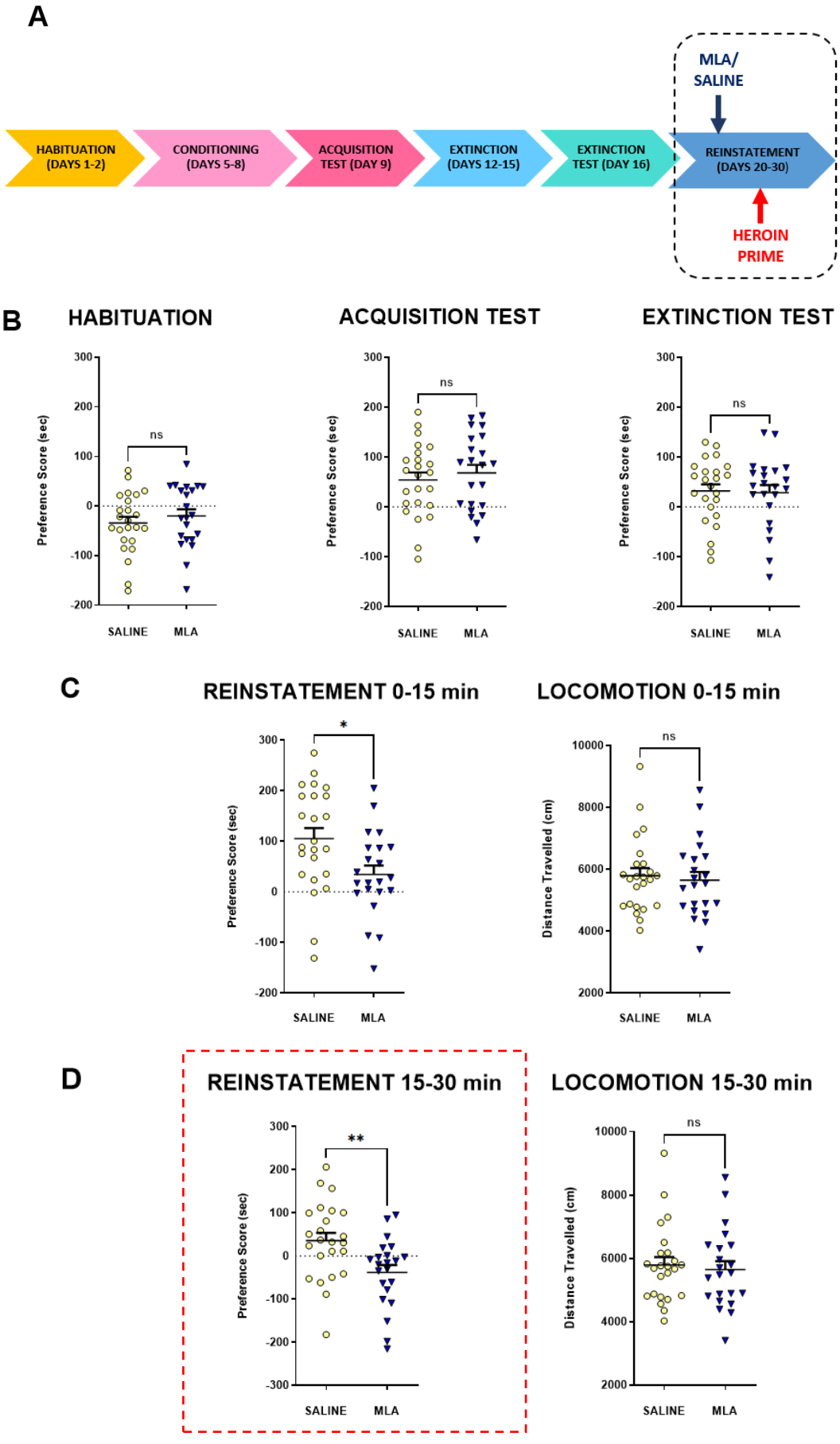
A
HABITUATION (DAYS 1-2)
CONDITIONING (DAYS 5-8)
ACQUISITION TEST (DAY 9)
EXTINCTION (DAYS 12-15)
EXTINCTION TEST (DAY 16)
REINSTATEMENT (DAYS 20-30)
MLA/ SALINE
HEROIN PRIME
B
HABITUATION
ACQUISITION TEST
EXTINCTION TEST
Preference Score (sec)
ns
SALINE
MLA
C
REINSTATEMENT 0-15 min
LOCOMOTION 0-15 min
*
Distance Travelled (cm)
D
REINSTATEMENT 15-30 min
LOCOMOTION 15-30 min
**

Figure 3.2 - Pseudo-randomisation of preference scores during habituation, acquisition test and extinction test of SALINE and MLA groups and preference score and locomotion from SALINE and MLA groups during the heroin-primed induced reinstatement – (**A**) Time-line of the heroin-CPP, with emphasis on the reinstatement phase. (**B**) Mice were split in two balanced treatment groups, across habituation, acquisition test and extinction test, using the pseudo-randomisation design. Unpaired Student's t-test revealed no difference between assigned groups across the experimental sessions, demonstrating that the treatments groups were balanced and not biased. SALINE=24; MLA=22. (**C**) Preference scores (sec) and Distance travelled (cm) during heroin-primed reinstatement of SALINE and MLA treatment groups. Twenty minutes before the heroin-primed reinstatement, mice were given either SALINE (0.9%, s.c.) or MLA (4 mg/kg, s.c.) and returned to the home cage until the beginning of the test. Mice were the administered a challenge injection of heroin (1 mg/kg, i.p.) and let explore the apparatus for 30 minutes. This amount of time was split in two time-bins of 15 minutes each (C and D), where only the second one was considered as more reliable. As reported in C, SALINE group reported a significant preference for the heroin-paired compartment in comparison with MLA treated group in which the preference score was attenuated. Unpaired Student's t-test, *$p<0.05$ SALINE=24, MLA=22. On the right, total distance travelled (cm) across the CPP compartments during the reinstatement test, no difference between groups was reported. Unpaired Student's t-test, SALINE=24, MLA=22. (**D**) Similar to C, SALINE group reported a significant preference for the heroin-paired compartment in comparison with MLA treated group in which the preference score was attenuated. The red, dashed rectangle emphasises the effect of MLA on the second time-bin of reinstatement. Unpaired Student's t-test, **$p<0.05$ SALINE=24, MLA=22. On the right, total distance travelled (cm) across the CPP compartments during the reinstatement test, no difference between groups was reported. Unpaired Student's t-test, SALINE=24, MLA=22. Data points represent individual mice with mean±SEM overlaid.

Animals pre-treated with SALINE before heroin-primed reinstatement showed a significant increase in the time spent in the heroin-paired side, compared with the MLA group, where the preference score was significantly lower (Figure 3.2 C&D). Hence, these results demonstrate that heroin 1 mg/kg (i.p.) was effective in inducing reinstatement of the heroin-CPP and that the systemic administration of MLA (4 mg/kg, s.c.) attenuated the drug-seeking behaviour reported by SALINE controls. The MLA pre-treatment, before reinstatement, was effective in both time-bins, in the second part (Figure 3.2 D) the effect was however statistically clearer. Moreover, the MLA pre-treatment did not affect locomotion (Figure 3.2 C&D), demonstrating that the difference reported in the preference score is not provoked by a general inhibitory effect of MLA affecting the explorative behaviour.

Together these data suggest that α7nAChRs play a role in modulating drug-related memories. The advantage of administering the MLA systemically is that it is a more translatable approach and much less invasive than brain infusions. This was the first time in which the effect of MLA was tested in the priming-induced reinstatement of the heroin-CPP in mice. However, the disadvantage of the systemic administration of MLA is that it is impossible to identify the brain areas more involved in the behaviour under investigation. Hence, in the next part of the experiment, we explored *ex vivo* c-Fos expression, in the vHIP in the first instance, to understand if the behavioural inhibition induced by MLA correlated with a decrease in neuronal activation underlying reinstatement in this area. c-Fos expression in dHIP, PL, NAc Shell and BLA was also examined, to understand the impact of MLA before heroin-induced reinstatement on the projection areas of the vHIP, which are also implicated in mediating drug-related associative memories.

3.2.3 MLA selectively decreased c-Fos expression in vHIP during heroin-primed reinstatement

Ninety minutes after the beginning of the reinstatement test, mice were transcardically perfused with 4% PFA and brains removed and sectioned for immunofluorescence, as reported in Chapter 2, section 2.6. At first, it was necessary to understand if the vHIP is particularly recruited during heroin-induced reinstatement, in accordance with the findings of Wright and colleagues (2019). On the other hand, to confirm the selective action of the α7nAChRs vHIP in regulating reinstatement behaviour, c-Fos expression in dHIP was evaluated, as well as in the projection areas of the vHIP, namely PL, NAc Shell and BLA, in both SALINE and MLA-treated mice.

The quantification of the c-Fos expression in vHIP, dHIP, PL, NAc Shell and BLA, in SALINE and MLA treatment groups, is reported below.

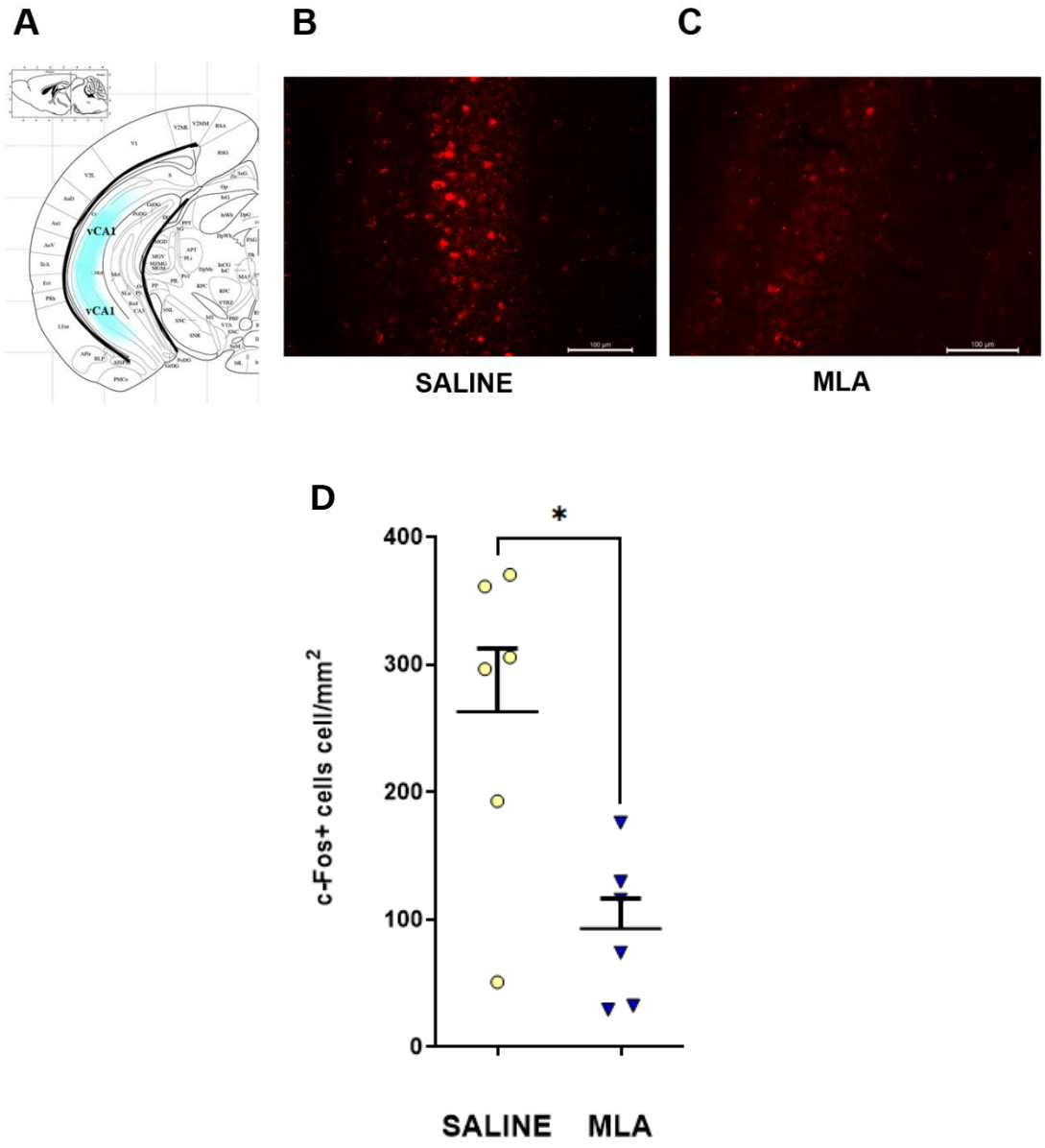

Figure 3.3 - The effect of SALINE and MLA on c-Fos expression in vHIP and quantification of c-Fos+ cells/mm^2 in vHIP in mice after heroin-primed reinstatement – (**A**) Relative bregma point (-3.2 mm) of the vCA1 (light blue shadow). On the right, representative images of the vCA1 of mice treated with SALINE (**B**) and MLA (**C**) before the heroin-primed induced reinstatement. (**D**) Administration of MLA (4 mg/kg) prior to heroin (1 mg/kg)-primed reinstatement significantly reduced c-Fos expression in vHIP compared to animals administered saline prior to heroin-primed reinstatement. Cells quantification has been performed through FIJI ImageJ (SALINE: n=6; MLA: n=6; *p<0.05, Student's t-test). Data points represent quantification of how many sections/slices from individual mice with mean±SEM overlaid.

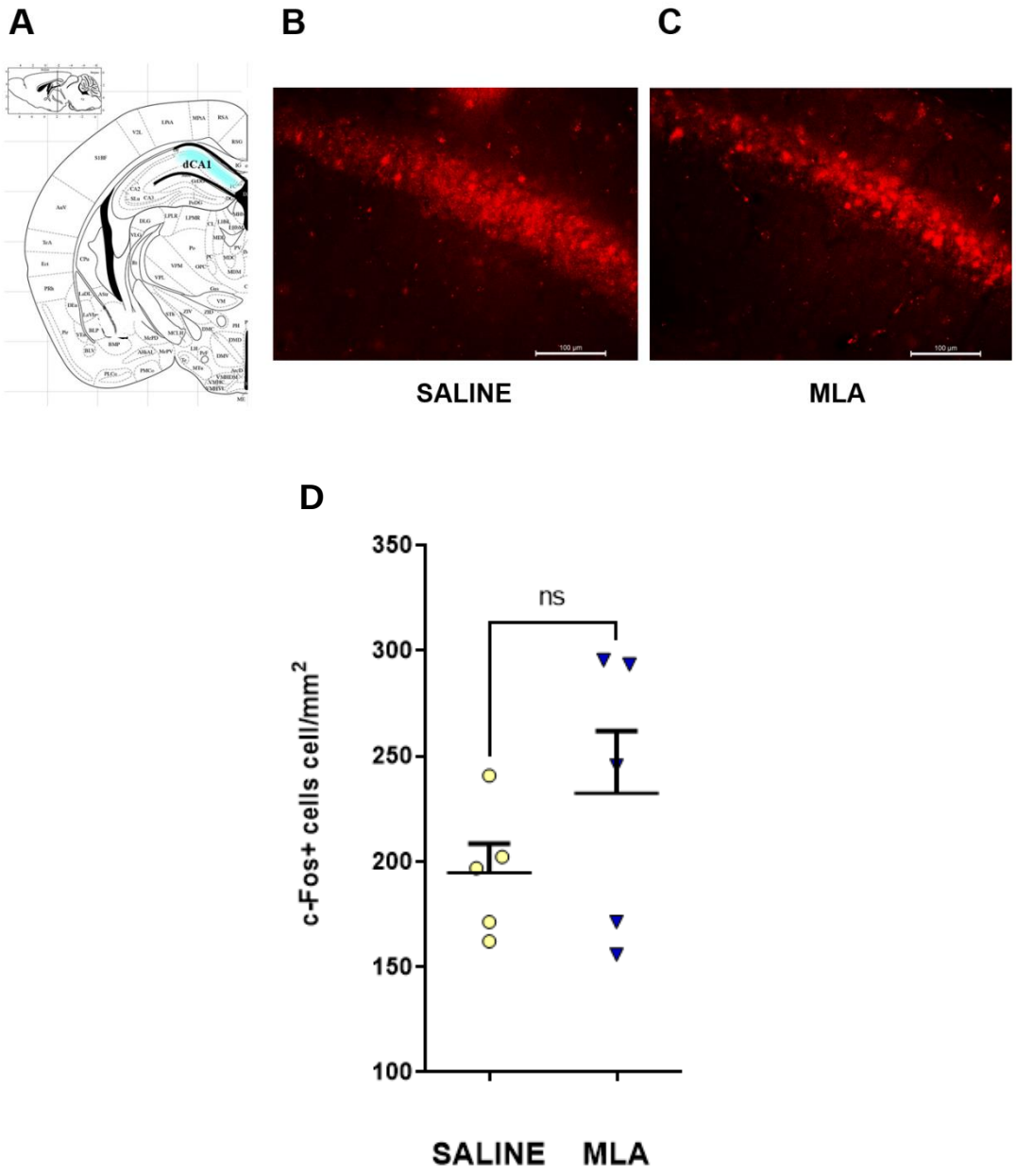

Figure 3.4 - The effect of SALINE and MLA on c-Fos expression in dHIP and quantification of c-Fos+ cells/mm^2 in dHIP in mice after heroin-primed reinstatement – (**A**) Relative bregma point (-1.98 mm) of the dCA1 (light blue shadow). On the right, representative images of the dCA1 of mice treated with SALINE (**B**) and MLA (**C**) before the heroin-primed induced reinstatement. (**D**) Administration of MLA (4 mg/kg) prior to heroin (1 mg/kg)-primed reinstatement did not significantly reduce c-Fos expression in dHIP compared to animals administered saline prior to heroin-primed reinstatement (SALINE: n=5; MLA: n=5; Student's t-test).

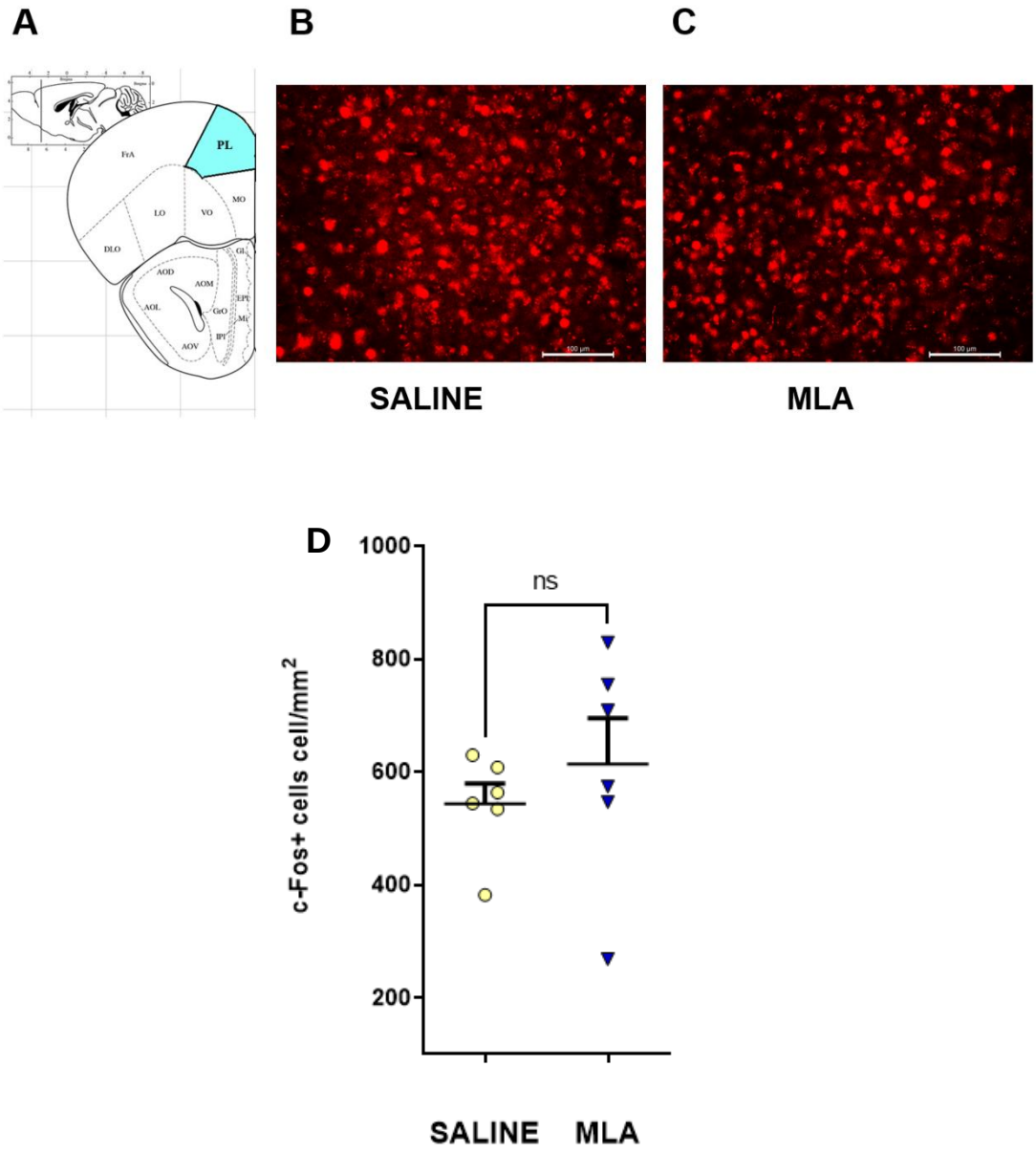

Figure 3.5 - The effect of SALINE and MLA on c-Fos expression in PL and quantification of c-Fos+ cells/mm^2 in PL in mice after heroin-primed reinstatement – (**A**) Relative bregma point (2.8 mm) of the PL (light blue shadow). On the right, representative images of the PL of mice treated with SALINE (**B**) and MLA (**C**) before the heroin-primed induced reinstatement. (**D**) Administration of MLA (4 mg/kg) prior to heroin (1 mg/kg)-primed reinstatement did not significantly reduce c-Fos expression in PL compared to animals administered saline prior to heroin-primed reinstatement (SALINE: n=6; MLA: n=6 Student's t-test).

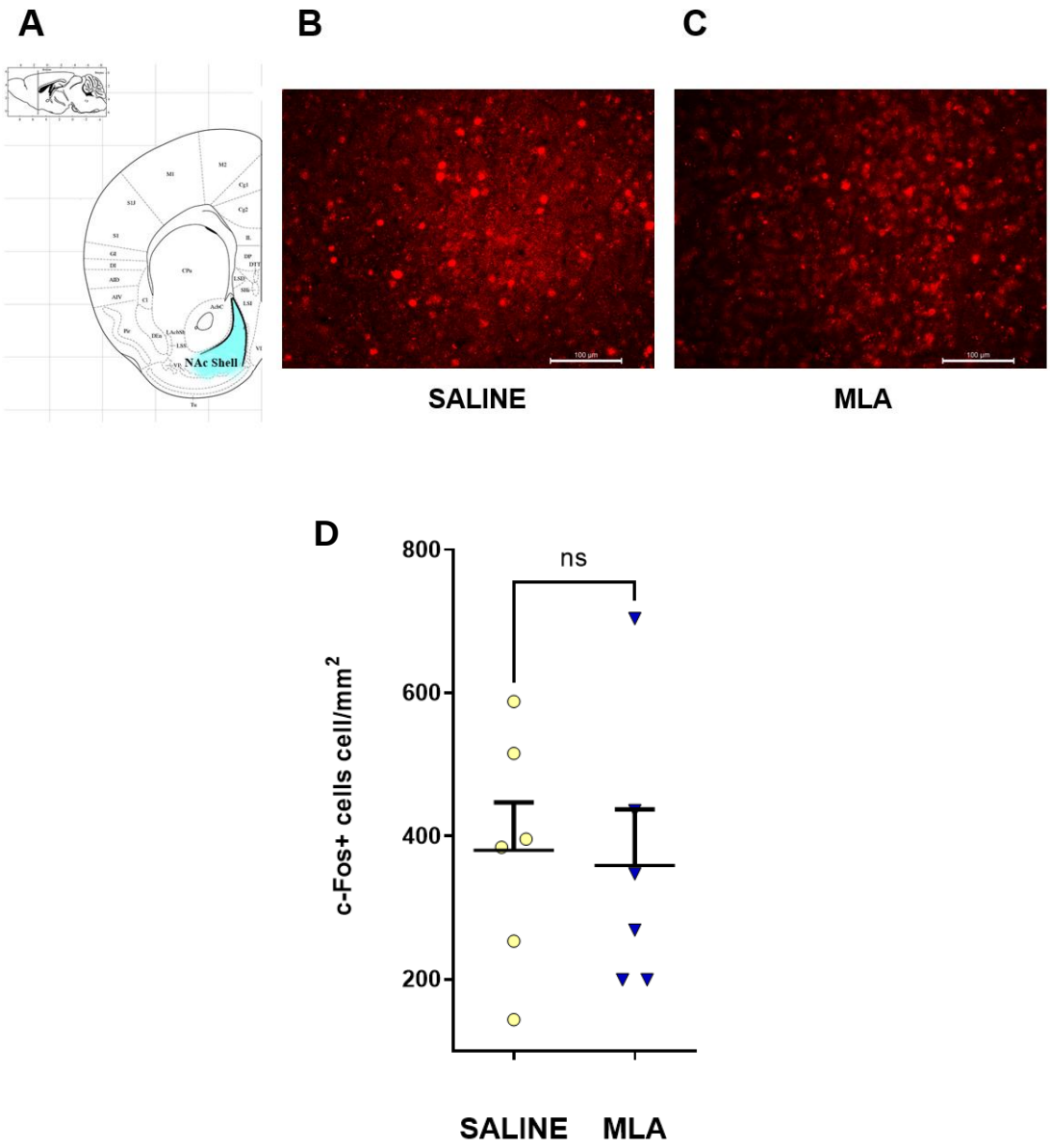

Figure 3.6 - The effect of SALINE and MLA on c-Fos expression in NAc Shell and quantification of c-Fos+ cells/mm^2 in NAc Shell in mice after heroin-primed reinstatement – (**A**) Relative bregma point (1.34 mm) of the NAc Shell (light blue shadow). On the right, representative images of the NAc Shell of mice treated with SALINE (**B**) and MLA (**C**) before the heroin-primed induced reinstatement. (**D**) Administration of MLA (4 mg/kg) prior to heroin (1 mg/kg)-primed reinstatement did not significantly reduce c-Fos expression in NAc Shell compared to animals administered saline prior to heroin-primed reinstatement (SALINE: n=6; MLA: n=6 Student's t-test).

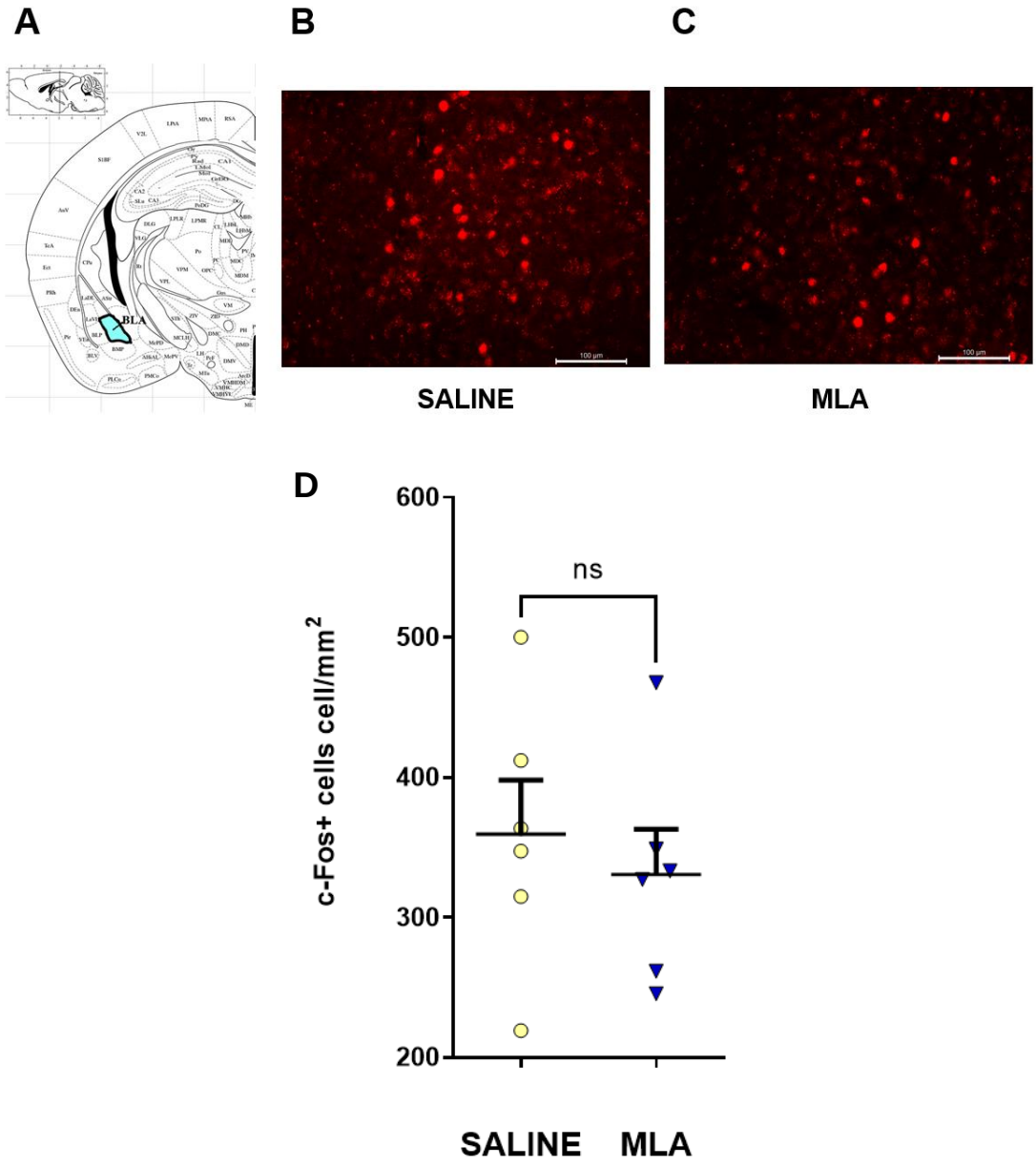

Figure 3.7 - The effect of SALINE and MLA on c-Fos expression in BLA and quantification of c-Fos+ cells/mm2 in NAc Shell in mice after heroin-primed reinstatement – (**A**) Relative bregma point (-1.60 mm) of the BLA (light blue shadow). On the right, representative images of the NAc Shell of mice treated with SALINE (**B**) and MLA (**C**) before the heroin-primed induced reinstatement. (**D**) Administration of MLA (4 mg/kg) prior to heroin (1 mg/kg)-primed reinstatement did not significantly reduce c-Fos expression in NAc Shell compared to animals administered saline prior to heroin-primed reinstatement (SALINE: n=6; MLA: n=6 Student's t-test).

Figure 3.3 shows that the systemic MLA injection (4 mg/kg, s.c.) significantly reduced c-Fos expression in the CA1 of the vHIP ($p=0.011$) after heroin-primed CPP reinstatement, consistent with the selective involvement of α7nAChRs within this area

in the modulation of heroin-primed reinstatement. On the other hand, the quantification of c-Fos expression in the dCA1 reported no statistical difference between SALINE and MLA treated mice (Figure 3.4). Moreover, c-Fos activation was not affected in PL, NAc Shell and BLA by the administration of MLA, suggesting that α7nAChRs in these brain regions are not specifically involved in the modulation of heroin-primed induced reinstatement (Figures 3.5, 3.6, 3.7). These results are consistent with what was reported previously from our lab. In fact, the administration of MLA before the heroin-induced reinstatement significantly reduced the AMPAR binding in the ventral CA1, but not in dorsal CA1, PL, NAc Shell or BLA (Wright et al., 2019), suggesting a selective role for α7nAChRs in vHIP in processing primed-induced reinstatement.

The main evidence of this chapter is that MLA decreased c-Fos expression only in vHIP, during the reinstatement of the heroin-CPP. Thus, the aim of the next experiment was to understand if this effect is *a priori* or is correlated instead to the behavioural inhibition of drug-induced reinstatement reported in section 4.2.2.

3.2.4 MLA does not reduce c-Fos expression per se

The previous section demonstrated that inhibition of α7nAChRs by the selective antagonist MLA prior to heroin-primed reinstatement reduced c-Fos expression only in vHIP. However, it is possible that the effect of MLA in vHIP could have been *a priori*, and so acting at the basal, physiological level rather than specifically on memory reactivation. In such a scenario, MLA would reduce c-Fos expression in this area, producing less neuronal activation and also inducing behavioural inhibition, leading to a behavioural impairment. Hence, the aim of the present experiment was to test if MLA could decrease c-Fos expression *per se* after the administration of non-contingent heroin, affecting neuronal activation in absence of drug-conditioning, extinction and the subsequent reinstatement. To do so, we investigated whether there is an increase in c-Fos expression in vHIP after non-contingent administration of heroin, and if this is inhibited by MLA.

Naïve mice were treated as on the reinstatement day but without any prior drug treatment and no behavioural testing: a single dose of MLA (4 mg/kg) or saline was delivered s.c. and after 20 minutes mice received an i.p. injection of saline or heroin (1 mg/kg). Hence, mice were divided into the following experimental groups: saline control (SALINE+SALINE, S+S), saline heroin (SALINE+HEROIN, S+H), MLA control (MLA+SALINE, M+S) and MLA heroin (MLA+HEROIN, M+H). After i.p. injections of either saline or heroin, mice were returned to their home cage. Ninety minutes later, animals were sacrificed, and brain sections taken for immunolabelling of c-Fos in the vHIP. In contrast to the previous experiments, brains were sliced horizontally, rather than coronally, to better locate the CA1 of vHIP, as described in Chapter 2, section 2.5.

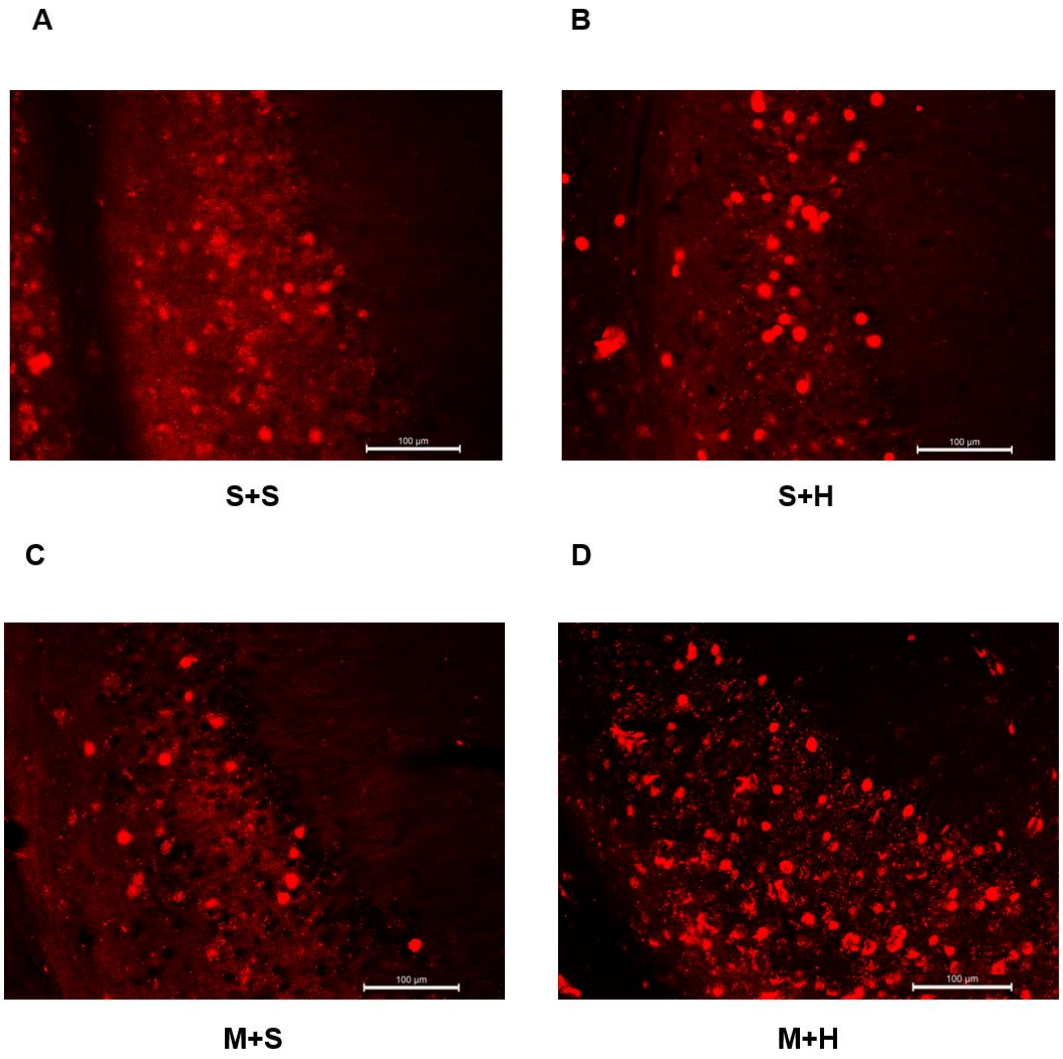

Figure 3.8 – c-Fos expression in the ventral CA1 across single-injection treatments – Representative images of the ventral CA1, horizontally sliced, of mice treated with (**A**) SALINE+SALINE (S+S); (**B**) SALINE+HEROIN (S+H); (**C**) MLA+SALINE (M+S); (**D**) MLA+HEROIN (M+H)

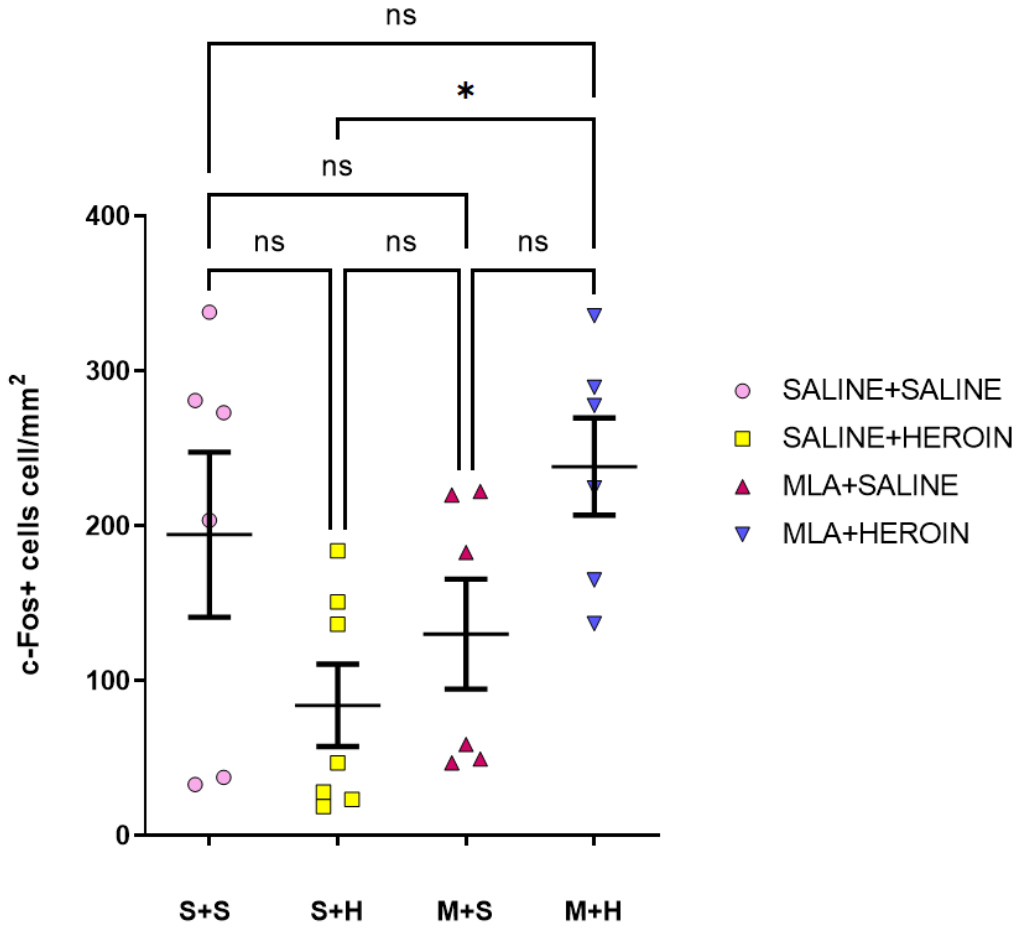

Figure 3.9 – c-Fos expression in vHIP and the effect of SALINE and MLA in naive mice given a single injection of heroin or SALINE –Mice were given single injections of SALINE or MLA (4 mg/kg; M) 20 minutes prior to a single injection of SALINE or HEROIN (1 mg/kg). Administration of MLA and heroin (M+H) significantly increased c-Fos expression in comparison to S+H group, while there is no statistical difference in comparison with S+S and M+S groups. S+S = 6; S+H = 7; M+S= 6; M+S M+H= 6; *p<0.05, One-Way ANOVA with Bonferroni's Multiple Comparison Test. Data points represent individual mice with mean±SEM overlaid.

As shown in Figures 3.8 and 3.9, the prior administration of MLA either before heroin or saline, did not decrease c-Fos activation in the ventral CA1. Specifically, S+S and M+S treatments did not have any effect on c-Fos expression in naïve mice. Interestingly, a statistically significant difference was reported on c-Fos expression in

ventral CA1 between S+H and M+H treatments groups. Heroin alone (S+H) did not increase c-Fos expression in vHIP. However, c-Fos activation was higher when HEROIN was given after MLA and not SALINE, which contrasts with what reported in section 3.2.2. Hence, this experiment demonstrates that MLA does not inhibit c-Fos expression *per sé* or specifically heroin-induced c-Fos expression, confirming also that MLA specifically decreases c-Fos expression during heroin-induced reinstatement, rather than a direct effect of MLA on the expression of this marker.

Thus, these results support the interpretation of the reinstatement experiment (Figure 3.8) that MLA specifically inhibits the neuronal activity underlying the reactivation of salient memories.

Taken together, these results support the hypothesis that α7nAChRs play a crucial role in heroin-primed induced reinstatement, modulating drug-seeking behaviour and the underlying neuronal activation. On the other hand, MLA does not impact on c-Fos expression *a priori*, confirming their crucial role during memory reactivation. The next step is to understand if this action of α7nAChRs can be extended to other drugs of abuse, such as cocaine, or if it is specific for opioid-related memories. Hence, in the next section the role of α7nAChRs on cocaine-primed induced reinstatement and the subsequent c-Fos expression are investigated.

3.2.5 Habitation, acquisition and extinction of the cocaine-CPP, a pilot study

The following experiment was the first, performed by our research group, to investigate the effect of MLA on reinstatement induced by a non-opioid drug, in this case cocaine, was tested on C-57 BL/6 mice. The aim of this study was to explore if MLA could have actions on other drugs of abuse classes, in this case a psychostimulant, extending the previous and current findings on the role of α7nAChRs in vHIP in mediating drug-context associations.

This experiment consisted of the same experimental procedure reported in 3.2.1. Briefly, C-57 BL/6 male mice underwent the conditioning phase, where daily i.p. injections of either 15 mg/kg cocaine or 0.9% saline were given to mice which were then confined into their paired compartment for 40 minutes. The cocaine dose was

chosen based on similar studies (McReynolds et al., 2017; Singh and Lufty, 2017). On the following day, mice that received cocaine were then administered saline and confined to the opposite side of the apparatus and vice-versa, for four days. The day after the last conditioning day, animals were allowed to explore both compartments for 15 minutes. Once the acquisition of the preference had been assessed, mice underwent the extinction phase, where they received daily i.p. injections of saline (0.9%) for four consecutive days and were confined to the drug-paired side on the first and third day and to the saline-paired one on the second and fourth day. In this experiment, all the testing sessions were recorded by Ethovision XT 7, measuring preference scores and locomotor activity across habituation, acquisition test and extinction test, as reported below.

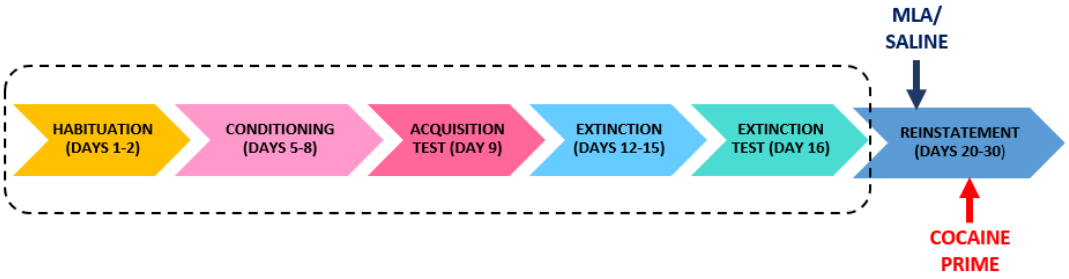

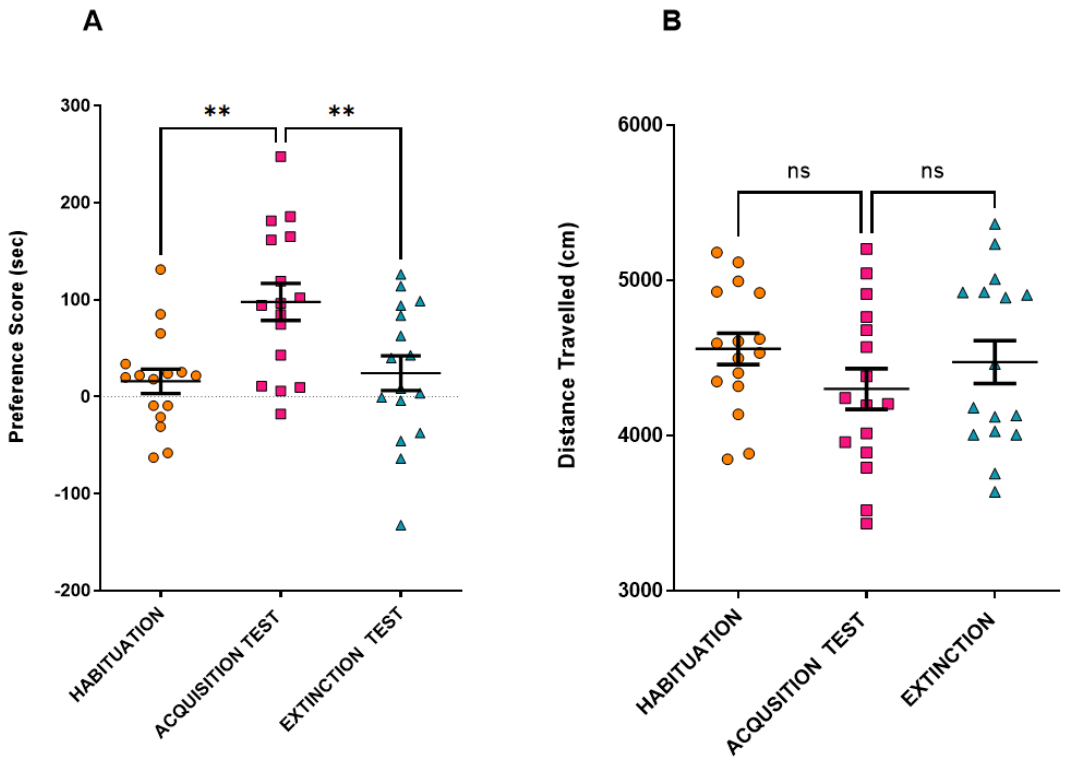

Figure 3.10 – Preference scores and locomotor activity on the stages of the cocaine-CPP in mice - Above, experimental timeline of the cocaine-CPP including all the phases and days. (**A**) Preference scores expressed in seconds across the habituation to obtain a baseline (average from day 1 and day 2), acquisition of the preference (day 9) for the heroin-paired side, induced by a daily injection of cocaine 15 mg/kg given in one compartment, and of saline (0.9% i.p.) in the other one, alternately for 4 days; and extinction (day 16), which consisted of daily saline injections (0.9% i.p.) in both compartment in both compartments alternately, for 4 days. During the habituation, acquisition test and extinction test, mice were allowed to freely explore the apparatus. Overall, mice significantly acquired the preference for the cocaine-paired compartment, which was then significantly extinguished in comparison with acquisition test. Preference Score is expressed in seconds (sec). One-way ANOVA with Dunnett's Multiple Comparison Test (*post hoc* analysis preference test vs habituation and acquisition test vs extinction), p**<0.5. n=16. (**B**) Total distance travelled (cm) along the CPP apparatus during habituation, preference test and extinction. The analysis of the locomotor activity reported no significant difference across the CPP phases. One-way ANOVA with Dunnett's Multiple Comparison Test (*post hoc* analysis preference test vs habituation and preference test vs extinction), n=16. Data All test sessions were performed in drug free state and tracked via Ethovision XT. Data points are individual mice responses with mean ± SEM overlaid.

Mice acquired cocaine CPP, with scores significantly above their baseline preferences, and this preference was successfully extinguished. In addition, mice did not show any previous preference for the cocaine-paired side during the habituation. Animals significantly preferred the cocaine-paired side after conditioning (Figure 3.10). Hence, the CPP was deemed successful, and the experiment progressed to the reinstatement phase. No exclusions were made for this experiment.

Mice did not show any difference in the locomotor activity, which was measured during habituation, preference test and extinction test and in drug-free state (Figure 3.8 B). Thus, the changes in the preference scores across the different CPP-phases were not due to alterations in the locomotion.

In conclusion, these results demonstrated that the cocaine dose of 15 mg/kg, used during conditioning, effectively induced the CPP, which was then extinguished with saline. Hence, in the next part of the experiment we studied the role of α7nAChRs in processing cocaine-primed induced reinstatement in C-57 male mice.

3.2.6 Does the MLA affect the cocaine-primed induced reinstatement and neuronal activation?

Consistent with the heroin-CPP protocol, before proceeding with the reinstatement phase, mice were pseudo-randomised and assigned to the treatment groups SALINE and MLA, to guarantee that the preference scores during habituation, preference test and extinction test were all balanced. Figure 3.11 B shows the preference scores during the habituation, acquisition test and extinction test for mice distributed to treatments groups. In this case, Student's t-test (unpaired) showed no difference in the preference scores between treatment groups. In addition, the spread of data points between groups was comparable, confirming that the study was balanced.

Once mice were pseudo-randomly distributed to either SALINE, which was the control group, or MLA group, the experiment progressed to the reinstatement phase. Twenty minutes prior to the cocaine-primed reinstatement, mice were administered saline or MLA (4 mg/kg s.c.). There are several studies about cocaine-primed induced reinstatement. For this experiment, cocaine 15 mg/kg and 7.5 mg/kg doses were used for inducing conditioning and reinstatement respectively, as successfully reported by others (McReynolds et al., 2017; Singh & Lutfy, 2017). The dose of 7.5 mg/kg was therefore used for this experiment and the effect of the α7nAChRs blockade on cocaine-induced reinstatement, and the subsequent c-Fos expression, was explored.

Results of pseudo-randomisation, preference score and locomotor activity during the cocaine-induced reinstatement are displayed below, in Figure 3.11 C.

A

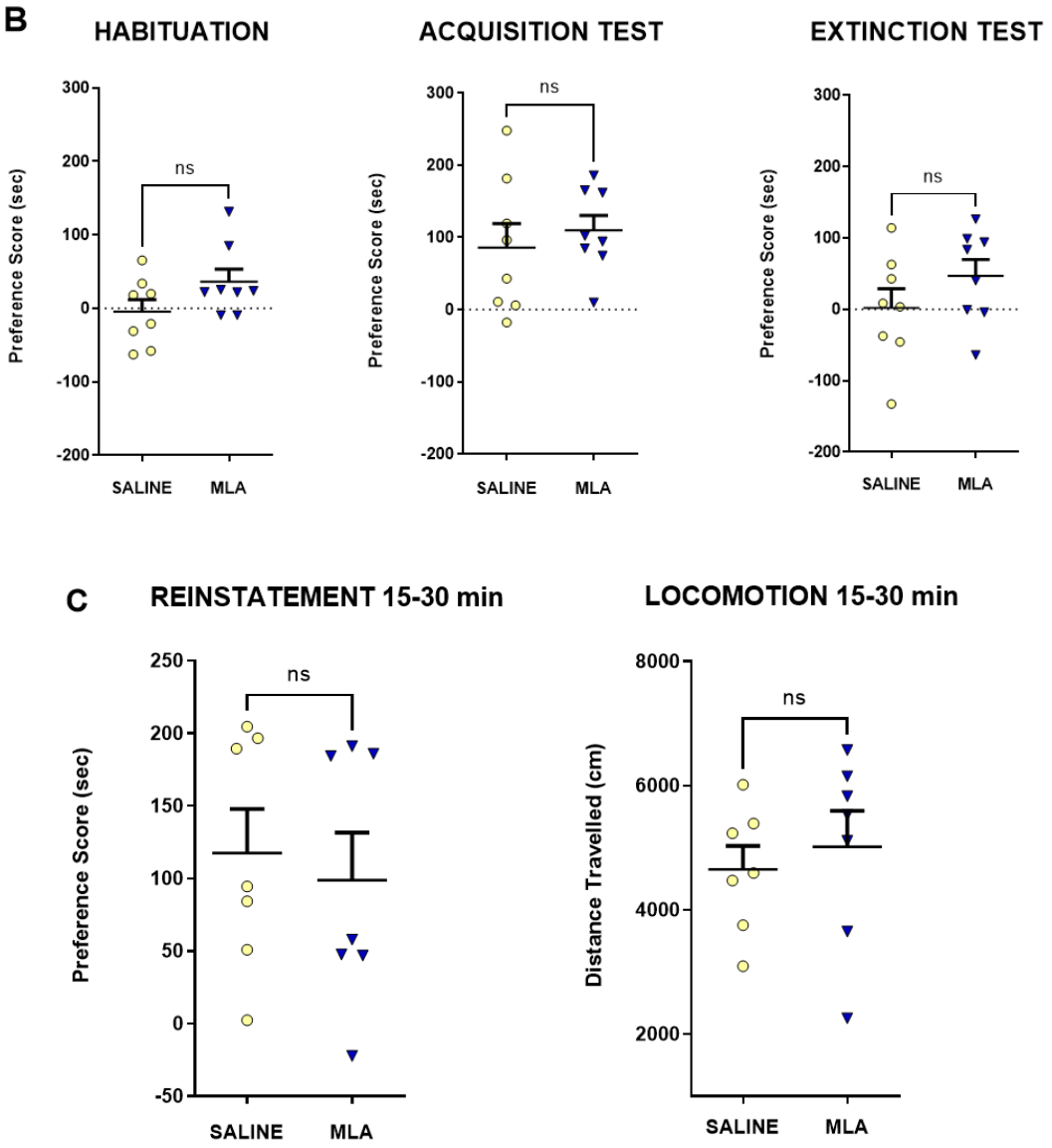

Figure 3.11 - Pseudo-randomisation of preference scores during habituation, acquisition test and extinction test of SALINE and MLA groups and preference score and locomotion from SALINE and MLA groups during the cocaine-primed induced reinstatement – (**A**) Time-line of the cocaine-CPP, with emphasis on the reinstatement phase (**B**) Mice were split in two balanced treatment groups, across habituation, acquisition test and extinction test, using the pseudo-randomisation design. Unpaired Student's t-test revealed no difference between assigned groups across the experimental sessions, demonstrating that the treatments groups were balanced and not biased. SALINE=8; MLA=8. (**C**) Preference scores (sec) and Distance travelled (cm) during cocaine-primed reinstatement of SALINE and MLA treatment groups. Twenty minutes before the cocaine-primed reinstatement, mice were given either SALINE (0.9%, s.c.) or MLA (4 mg/kg, s.c.) and returned to the home cage until the beginning of the test. Mice were the administered a challenge injection of cocaine (15 mg/kg, i.p.) and allowed to explore the apparatus for 30 minutes. Unpaired Student's t-test reported no significant

difference between treatment groups during the cocaine-induced reinstatement. SALINE=8, MLA=8. On the right, total distance travelled (cm) across the CPP compartments during the reinstatement test, no difference between groups was reported. Unpaired Student's t-test, SALINE=8, MLA=8. Data points represent individual mice with mean±SEM overlaid.

Student's t-test (unpaired) showed no difference in the preference scores between treatment groups, confirming that the experiment was correctly balanced (Figure 3.11 B). Figure 3.11 C shows that mice treated with MLA before cocaine-primed reinstatement of CPP did not attenuate the preference for the cocaine-paired chamber. This result cannot be addressed to a persistent memory trace of the conditioning, as the preference was significantly extinguished (Figure 3.10).

In order to evaluate a possible effect of MLA on c-Fos expression, mice were cardio-perfused with 4% PFA 90 minutes after the beginning of the test, as described in section 3.2.3 for the heroin-CPP. However, the immunofluorescence for c-Fos staining was performed just in vHIP, as α7nAChRs play a key role selectively within this area, as reported in section 3.2.3.

c-Fos expression was not affected in MLA treated subjects, reporting similar values of SALINE controls (Figure 3.12). According to those preliminary results, α7nAChRs in vHIP may not be involved in processing cocaine-induced reinstatement. However, some factors need to be considered. First, the sample size for the CPP was relatively small in comparison to the heroin-CPP (n=41). Second, as only single cocaine doses were used here for conditioning and reinstatement, it is possible that they are too high, masking any effect MLA might have on cocaine-seeking behaviour and the consequent c-Fos expression in vHIP. Thus, at this stage, it is not possible to generate a clear argument about the role of α7nAChRs in cocaine-induced reinstatement, although there are indications that MLA does not inhibit cocaine-primed cocaine CPP, unlike the effect seen for heroin CPP. As no effect in vHIP was observed, no further analyses of c-Fos expression in other brain areas, or a single-injection experiments, have been performed.

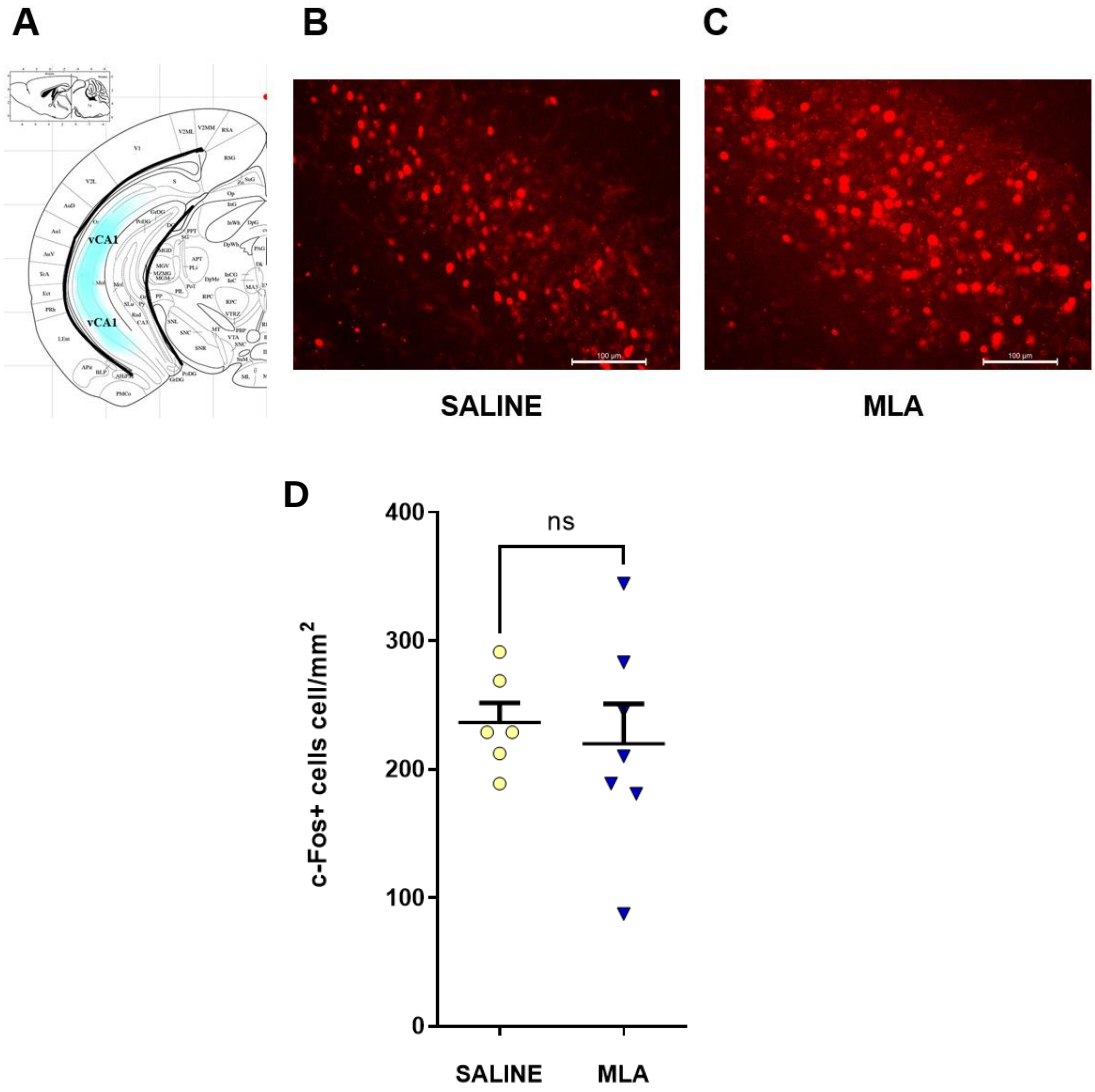

Figure 3.12 - The effect of SALINE and MLA on c-Fos expression in vHIP and quantification of c-Fos+ cells/mm^2 in vHIP in mice after cocaine-primed reinstatement – (A) Relative bregma point (-3.32 mm) of the vCA1 (light blue shadow). On the right, representative images of the vCA1 of mice treated with SALINE (**B**) and MLA (**C**) before the cocaine-primed induced reinstatement. (**D**) Administration of MLA (4 mg/kg) prior to heroin (1 mg/kg)-primed reinstatement did not significantly reduce c-Fos expression in vHIP compared to mice treated with saline prior to cocaine-primed reinstatement. Cells quantification has been performed through FIJI ImageJ (SALINE: n=6; MLA: n=7; Student's t-test). Data points represent quantification of how many sections/slices from individual mice with mean±SEM overlaid.

In conclusion, this is a key new finding with important implications about CPP-reinstatement. Future experiments with a lager sample size, or using a lower dose of cocaine, will be useful to understand if α7nAChRs are involved in modulating cocaine-induced reinstatement.

3.3 Discussion

The main findings of this chapter are that administration of MLA before heroin-primed reinstatement of CPP decreased drug-seeking behaviour and c-Fos expression that was selective for the vHIP, while the same treatment did not affect cocaine-induced reinstatement and subsequent c-Fos expression. Moreover, MLA did not affect cFos expression in vHIP *per se*.

3.3.1 α7nAChRs modulate heroin-induced reinstatement in mice

Although there have been many studies investigating morphine-primed CPP reinstatement, to date, there have been no studies investigating heroin-induced reinstatement of CPP in mice. Therefore, we validated the heroin doses of 2 mg/kg and 1 mg/kg which effectively induced conditioning and reinstatement respectively. There are few studies about the heroin-induced reinstatement in rats, where a heroin dose of 1 mg/kg was used (Leri & Rizos, 2005; Palandri et al., 2021). However, according to Nair (2016), if a dose of a drug is effective in a rat, doubling the dose in a mouse should give the same effect (Nair & Jacob, 2016). In this study, the dose of 2 mg/kg induced a good preference for the heroin-paired side, reporting significantly higher scores during the preference test compared to habituation and extinction test. Moreover, there was no significant difference in the preference score reported during habituation and extinction test, demonstrating that the extinction training performed was effective. It is worth noting that the extinction is not the mere oblivion of the trace but a new and active learning processes (Bouton, 2004). Hence, the memory trace underlying the conditioning was not deleted, but overwritten by the extinction learning which attenuated the motivational properties of the heroin-associated context. In fact, a lower dose of heroin (1 mg/kg) before reinstatement was sufficient to induce the drug-seeking behaviour in SALINE controls. This phenomenon can be interpreted as the reactivation of the salient memory associated to the rewarding effects of the drug and it is triggered by the challenge dose of heroin, leading the animals to spend more time in the drug-paired arena. Moreover, animals were tested under the effect of drug, potentiating the drug-related memory.

The main results from this chapter demonstrated that MLA inhibited the heroin-primed CPP-reinstatement. This evidence is in accordance with previous

findings from our lab for both morphine- and heroin-CPP in rats (Wright et al., 2019; Palandri et al., 2021) and with another study (Feng et al., 2011) reporting that MLA inhibits morphine-primed CPP reinstatement in mice. To date, those are the only studies demonstrating that MLA, an α7nAChRs antagonist, is effective against the reinstatement of other drugs of abuse only during reinstatement (Wright et al., 2019; Palandri et al., 2021).

To perform this set of experiments we used MLA 4 mg/kg, according to other evidence demonstrating its efficacy in both mice and rats (Feng et al., 2011; Wright et al., 2019; Palandri et al., 2021). It has been shown that lower doses of MLA (1 and 3 but not 10 mg/kg) decreased locomotory activity in mice (Chilton et al., 2004). However, the authors did not report the change rate in locomotion over time, without defining if this decrease was constant or transient during the task. We observed no effect of MLA on the distance travelled during the heroin-primed reinstatement test, which is consistent with the findings of Wright and colleagues (2019).

3.3.2 α7nAChRs regulate neuronal activity underlying heroin-induced reinstatement

As reported in section 3.2.3 MLA decreased c-Fos expression in ventral, but not in dorsal, CA1 during the heroin-primed reinstatement. Wright and colleagues (2019) showed that brain infusions of MLA were effective in blocking morphine-induced reinstatement in rats only when infused in vHIP, but not in dHIP or mPFC. This is in accordance with the findings reported in this thesis. In fact, c-Fos was significantly less expressed in MLA-treated mice, in comparison to SALINE controls, only in vHIP, while dHIP, PL, NAc Shell and BLA were not affected by MLA, in respect of c-Fos activation. These results highlight the importance of *α*7nAChRs in vHIP in modulating heroin-primed reinstatement. c-Fos is widely recognised to be activity-dependent, modulating learning, performance and neuronal ensembles, which can be activated by recall (for review, see Gallo et al., 2018). Hence, different magnitude of c-Fos activation across the hippocampal formation here reported might confirm that vHIP and dHIP play different roles in memory and emotion (Fanselow & Dong, 2010).

Previous data from autoradiography experiments (Wright et al., 2019) showed that AMPA binding density, but not NMDA, was affected by the systemic administration

of MLA only in the vCA1, in mice reinstated with morphine. In contrast, the AMPA density binding in dHIP, PL, NAc Shell and BLA was not affected by MLA. The nature of c-Fos expression and the AMPAR neuronal density is different and not necessarily correlated. However, both indexes are from a glutamatergic matrix, suggesting that α7nAChRs are involved in modulating the excitatory tone in the vHIP during the reinstatement of drug-induced CPP. The post-synaptic location of α7nAChRs on the pyramidal glutamatergic neurons of the vHIP, demonstrated in Chapter 4, could allow Ca^{2+} entrance into the cell, facilitating the activation of the c-Fos promoter. However, Chapter 4 also revealed that α7nAChRs are postsynaptic also in the dHIP, but the block of α7nAChRs by MLA did not affect c-Fos expression in this area. This result suggests that vHIP and dHIP play different roles and the neural basis of this distinction will be further discussed in Chapter 7.

Importantly, the possible *a priori* effect of MLA on vHIP activity, has been evaluated during the control experiment reported in Section 3.2.4, demonstrating that administration of MLA before a single non-contingent dose of heroin does not reduce c-Fos expression in naïve mice. This result suggests that α7nAChRs in vHIP selectively modulate heroin-induced reinstatement of CPP. Conversely, the M+H group showed a significant increase in c-Fos expression ($p=0.035$), in comparison to S+H group, which is in contrast with what reported in section 3.2.3, where MLA-treated mice showed a significantly lower c-Fos activation in vHIP, during heroin-CPP reinstatement. Interestingly, S+S treatment induced a higher c-Fos expression in vHIP, in comparison with S+H-treated mice. However, this is in contrast with early studies reporting that a challenge of heroin in drug-sensitised rats induced an increase in c-Fos mRNA expression in the basal ganglia (Pontieri et al., 1997). An Unpaired Student's t-test was performed between the two groups and no significant difference was reported ($p=0.078$). Future experiments aimed to enlarge the sample size will clarify those results.

3.3.3 MLA does not prevent cocaine-induced reinstatement and its neuronal activation

MLA given to mice before cocaine-primed reinstatement did not block the place preference and the subsequent c-Fos expression. However, the argument that α7nAChRs are selectively involved in opioid-related memories should be taken as first

interpretation cautiously. It is possible that the priming cocaine dose of 7.5 mg/kg used to elicit reinstatement was too high, provoking a too robust response and masking any possible effect of MLA, on both behaviour and c-Fos expression. Alternately, it has been shown that, using a conditioning cocaine dose of 15 mg/kg, a challenge cocaine dose of 0.93, 1.87 and 3.75 mg/kg were still effective in inducing reinstatement, (McReynolds et al., 2017). Thus, those doses could be used to prime reinstatement in future experiments.

Another possible caveat of this experiment was that the sample size for this experiment is relatively small, preventing the identification of a clear effect of MLA on drug-seeking behaviour. A second attempt to this experiment has been performed in November 2021, in order to clarify those preliminary data. Unfortunately, no data could be obtained for technical reasons, relative to animals' housing, affecting the animals' performance.

In conclusion, this work shows that α7nAChRs in vHIP play an important role in modulating heroin-primed induced reinstatement and that their action is memory reactivation specific. This appears to be a specific effect in vHIP. Furthermore, a similar effect of α7nAChR inhibition was not seen with cocaine-primed reinstatement suggesting the effect is specific to heroin-CPP.

The next chapter will study in depth the downstream mechanisms of α7nAChRs in modulating heroin-induced reinstatement by exploring their impact on synaptic plasticity in the vHIP.

CHAPTER 4
INVESTIGATION OF PRE- AND POST-SYNAPTIC EFFECTS OF α7NACHRS IN VENTRAL AND DORSAL HIPPOCAMPUS

4.1 Introduction

In the previous Chapter it has been demonstrated that inhibition of α7nAChRs, through the systemic administration of MLA, significantly decreased both heroin-induced reinstatement and c-Fos expression in vHIP, but not in dHIP. Furthermore, this evidence corroborates the data from our lab reported by Wright et al (2019), showing that the local infusion of MLA in vHIP, but not in dHIP, blocked morphine-induced reinstatement. How α7nAChRs in these sub-regions differently modulate drug-related memories is still unclear. One possibility is α7nAChRs are differently distributed across the longitudinal axis of the hippocampus. Hence, the aim of this Chapter was to explore the synaptic location of α7nAChRs in both vHIP and how those receptors modulate the excitatory and inhibitory post-synaptic events within those two areas.

It has been demonstrated that nAChRs, and in particular the α7 subtype, are expressed at excitatory synapses at both pre- and post-synaptic sites (Fabian-Fine et al., 2001; Figure 4.1), where they profoundly modulate synaptic events (Ji et al., 2001). In addition, α7 nAChRs have also been found in the pre- and postsynaptic sites of GABAergic inhibitory interneurons, where they regulate inhibitory transmission (Alkondon & Albuquerque, 2001). Thus, α7nAChRs not only directly depolarise interneurons, but they are also implicated in neurotransmission and synaptic plasticity. Specifically, α7nAChRs have been shown to enhance pre-synaptic release of both GABA and glutamate, promoting LTP (Radcliffe et al., 1999; Cheng & Yakel, 2015). The α7 contribution in modulating neurotransmitter release and cellular signalling, via volume transmission, has been extensively studied (Dajas-Bailador & Wonnacott, 2004; Dani & Bertrand, 2007).

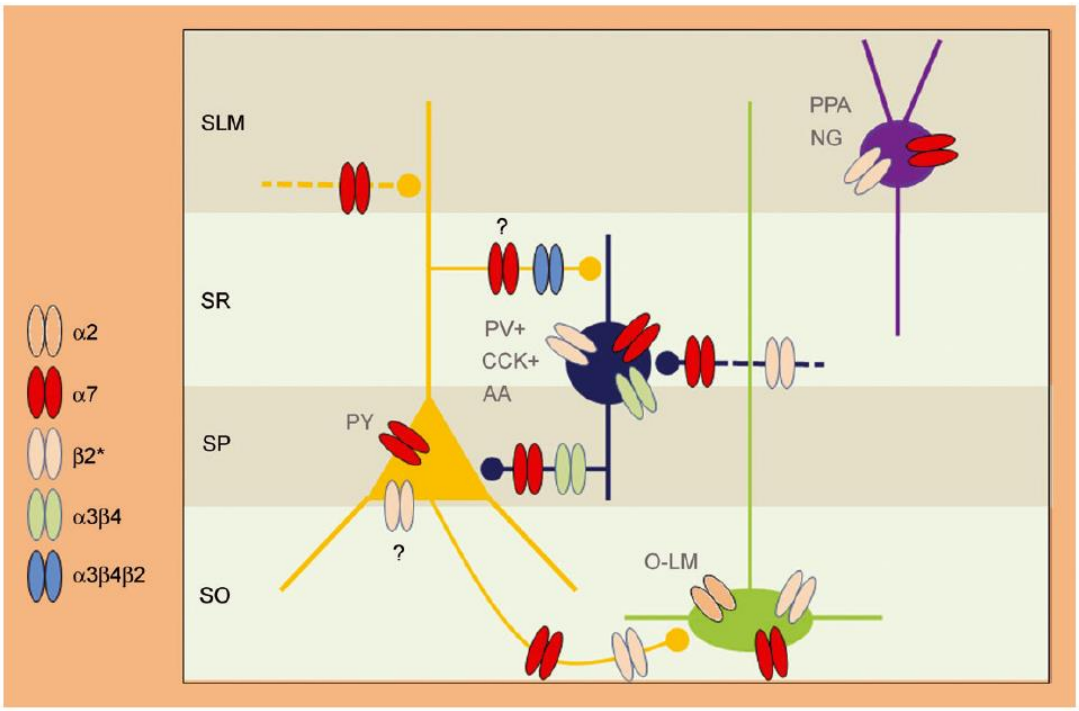

Figure 4.1 – Schematic CA1 architecture of different nAChRs subtypes on pyramidal neurons and GABAergic interneurons in the CA1 of the hippocampal formation - SLM, stratum lacunosum moleculare; SR, stratum radiatum; SP, stratum pyramidale; SO, stratum oriens; PY, pyramidal cells; PV+, parvalbumin-positive; CCK+, cholecystokinin-positive; AA, axo-axonic interneurons; O-LM, oriens-lacunosum moleculare; PPA, perforant path-associated lacunosum moleculare or lacunosum moleculare-radiatum interneurons; NG, neurogliaform cell. Dashed lines represent glutamatergic terminals from pyramidal cells (yellow) or from GABAergic interneurons (blue). α7nAChRs are predominantly expressed across the CA1, gaining a crucial role in network modulation (Griguoli et al., 2013).

As previously discussed in Chapter 1 (section 1.3.3), α7nAChRs desensitise very quickly, providing a compensatory effect able to protect cells against excessive stimulation (Shen et al., 2016). On the other hand, desensitisation can confound the investigation of the α7nAChR. Type II positive allosteric modulators (PAMs) are widely used to prevent receptor desensitisation, as these compounds increase current peak and considerably decrease current decay (Papke & Lindstrom, 2020). PAMs act as a filter, binding to the receptor at a site different from the agonist binding site and can reactivate nAChRs that have been previously desensitised by applying agonists, such as nicotine (Papke et al., 2009). Such molecules only act in the presence of the agonist, by potentiating or, more generally, modulating its response (Figure 4.2). Two different types of PAMs have been reported so far, type I PAMs which mainly enhance

agonist-induced peak currents without significantly affecting current decay, and type II PAMs, which increase peak currents and also delay the current decay rate (Bertrand & Gopalakrishnan, 2007; Chatzidaki & Millar, 2015). When applied to α7 desensitised receptors, type II but not type I PAMs are able to induce re-sensitisation after desensitised states (Andersen et al., 2016). PNU-120596, a II type of α7nAChRs PAM mediates the effect by preventing desensitization as well as enhancing agonist responses (Hurst et al., 2005; Livingstone & Wonnacott, 2009). It has been demonstrated that type II PAMs increase the open-channel duration, the number of detectable open states, the burst or cluster duration and the probability of channel opening (Hurst et al. 2005; daCosta et al., 2011; Pałczyńska et al., 2012; Andersen et al., 2013). Furthermore, it has been suggested that the underlying mechanisms require an increase in the energetic barrier for desensitisation and/or reverse some forms of desensitised states induced by agonists (Williams et al. 2011; Szabo et al., 2014; Bouzat & Sine, 2018).

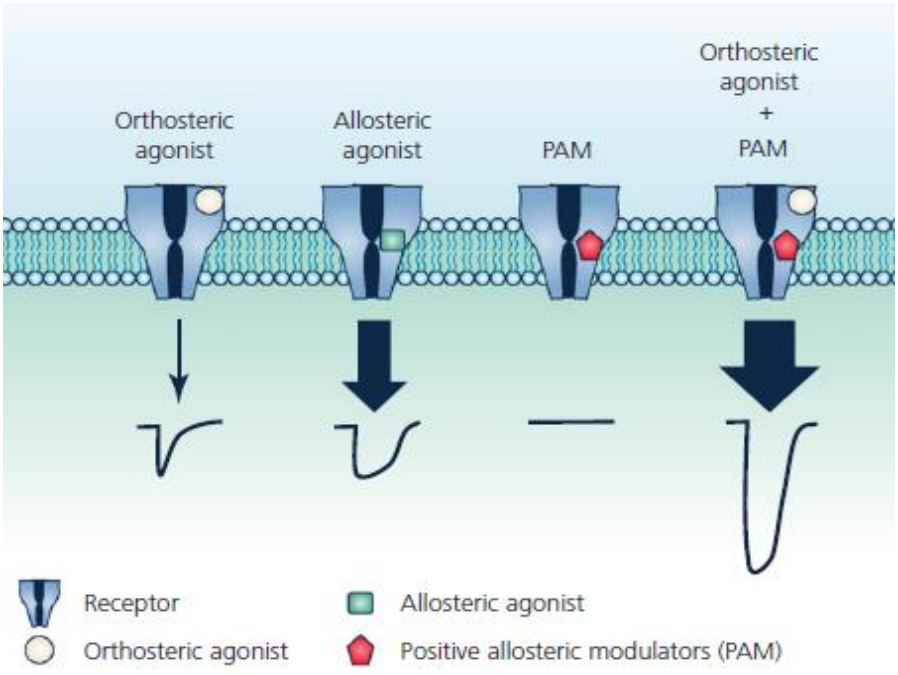

Figure 4.2 - Schematic representation of how α7 are modulated by different types of allosteric ligands – The cartoon scheme of the α7nAChRs and the sites of action which bids different compound types. The response induced by the natural agonist ACh can be increased, decreased or remain unchanged by the binding of the different types of ligands, such as agonists and modulators (adapted from Bouzat et al., 2018).

A good compound for investigating the functional properties of α7nAChRs is PNU-120596, which is also the first type II PAM to be described (Hurst et al., 2013). this PAM enhances the magnitude of the agonist-induced responses several-fold and increases the time-course of the responses by preventing desensitization processes. A considerable number of *in vitro* studies have utilised this compound to magnify the α7nAChRs response at the concentration of 10 μM in PC12 cultured cells and hippocampal slices (Dickinson et al., 2007; Kouhen et al., 2009; Grybko et al., 2011). Moreover, it has been shown that potentiation depends on the number of α7 subunits resistant to PNU-120596 and so, five predicted subunits must be sensitive to this ligand to obtain potentiation, suggesting that this PAM is highly cooperative (Corrie & Sine, 2013). Hence, PNU-120596 had the potential to be a viable tool to achieve the aim of this chapter, namely the study of the functional properties of α7.

There are several α7nAChR-selective agonists, with respect to the large variety and structural diversity of nAChRs. Functional potency of novel ligands is normally evaluated by electrophysiological recording or Ca^{2+} flux assays in recombinant nAChR subunits expressed in Xenopus oocytes or mammalian cells. Among the selective synthetic agonists of α7nAChRs, PNU-282987 has been shown to be effective in vivo, depending on the dose injected or infused. In addition, the combination of PNU-120596 and PNU-282987 activates the ERK/MAP pathway via CAMKII, leading to increases in phosphorylated CREB, a well-known transcription factor implicated in learning and memory (Gubbins et al., 2010; Besson et al., 2012; Kouhen et al., 2009).

On the other hand, the choice of α7nAChR-selective antagonists is more limited. An essential compound to perform these studies is the selective competitive α7 antagonist MLA, a norditerpenoid alkaloid isolated from delphinium seeds (Blagbrough et al., 1994) Unlike α-bungarotoxin, a strong pseudo-irreversible α7 antagonist, MLA is relatively easy reversible and it does not block muscle nAChRs, expanding its use also for in vivo experiments. Systemic and local infusions in vHIP selectively prevented the reinstatement of a both morphine-primed and heroin-primed CPPs (Wright et al., 2019; Palandri et al., 2021). However, the specific mechanism by which hippocampal α7nAChRs modulate the above-mentioned processes remains to be elucidated. Recent

work from this lab (Udakis et al., 2016) investigated how prelimbic α7nAChRs modulate synaptic plasticity and network function. It showed that the PAM, PNU-120596, increased spontaneous excitatory events, while α7 modulation of inhibitory transmission required the concomitant action of the agonist PNU-282987 and PNU-120596, which was also unaffected by AChE inhibition. These data suggest α7nAChRs can bi-directionally modulate network activity in the PL, depending on the magnitude and localisation of α7 activation (Udakis et al., 2016).

Thus, the focus of the present work is to understand how α7nAChRs modulate neurotransmission and synaptic plasticity in the vHIP, in order to clarify their functional contribution in learning and memory mechanisms that may be relevant to drug-associated learning.

4.2 Results

4.2.1 Method to simultaneously examine pre- and postsynaptic α7nAChRs

Using whole-cell patch-clamp recordings, activation of postsynaptic receptors would be observed as an inward current. To investigate presynaptic receptors, the most common method used is to record excitatory post synaptic currents (EPSCs) or inhibitory post synaptic currents (IPSCs) in isolation, using selective blockers of $GABA_A$ and glutamate receptors respectively. Conversely, a method illustrated by others (Semyanov & Kullmann, 2000) has the advantage of recording both EPSCs and IPSCs from the same neuron, with pharmacological intervention limited to stimulation of α7nAChRs, by using a voltage step protocol. As the involvement $GABA_A$ and glutamate receptor blockers are not required, this method also has the advantage of keeping the integrated network intact.

This objective is achieved using voltage steps (see Figure 4.1A). The reversal potential of chloride currents, such as the $GABA_A$ receptor, is at ~-60 mV. Therefore, at a holding potential of -60 mV only EPSCs will be recorded and seen as downward (inward) currents. On the other hand, the reversal potential of AMPA receptors is at ~0 mV, so at a holding potential of 0 mV, only IPSCs are seen, as upward hyperpolarising currents. This experimental approach has been confirmed previously by our research group (Udakis et al., 2016).

Using this approach, it is theoretically feasible to determine the influence of α7nAChR type II PAM PNU-120596 (10 μM), in combination with α7nAChR agonist PNU-282987 (300 nM) and α7nAChR antagonist MLA (100 nM) on spontaneous IPSC and EPSC from the same neuron, by repeatedly switching the holding voltage of patch-clamped cells from -60 mV to 0, as reported in Figure 4.3 A.

4.2.2. Post-synaptic currents induced by α7nAChR activation in CA1 pyramidal neurons in vHIP and dHIP

The experimental aim was to explore possible differences between dHIP and vHIP in terms of α7nAChRs distribution and density. In fact, it has been reported that α7nAChRs have been identified on the pre-synaptic, post-synaptic and extra-synaptic compartment in the entire hippocampal region (Fabian-Fine et al., 2001; Bürli et al., 2010). dHIP and vHIP are involved in different functions (Strange et al., 2014) which may be explained by the different distribution of receptors, including α7nAChRs, across the hippocampal structure. For example, Wright and colleagues (2018) reported that the infusion of the selective antagonist MLA in vHIP, but not in dHIP, prevented the reinstatement of a morphine-CPP. On the other hand, the infusion of MLA in dHIP, but not in vHIP, attenuated the inhibitory avoidance learning (Sakimoto et al., 2019), highlighting the heterogenous action of α7nAChR in hippocampus across the dorsal-ventral axis.

In the vHIP, bath perfusion of the α7nAChR PAM, PNU-120596, alone did not induce any inward current, confirming that this compound does not have any effect *per sé*. In contrast, co-application of this PAM and plus the α7 agonist, PNU-282987, produced a substantial inward current that was reversed by the subsequent application of the α7 antagonist MLA (Fig. 4.3).

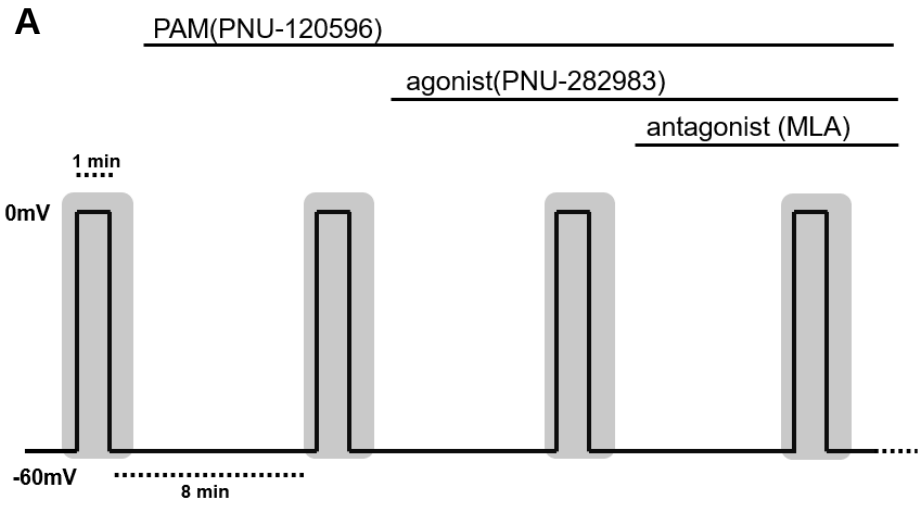
A
PAM(PNU-120596)
agonist(PNU-282983)
antagonist (MLA)
1 min
0mV
-60mV
8 min

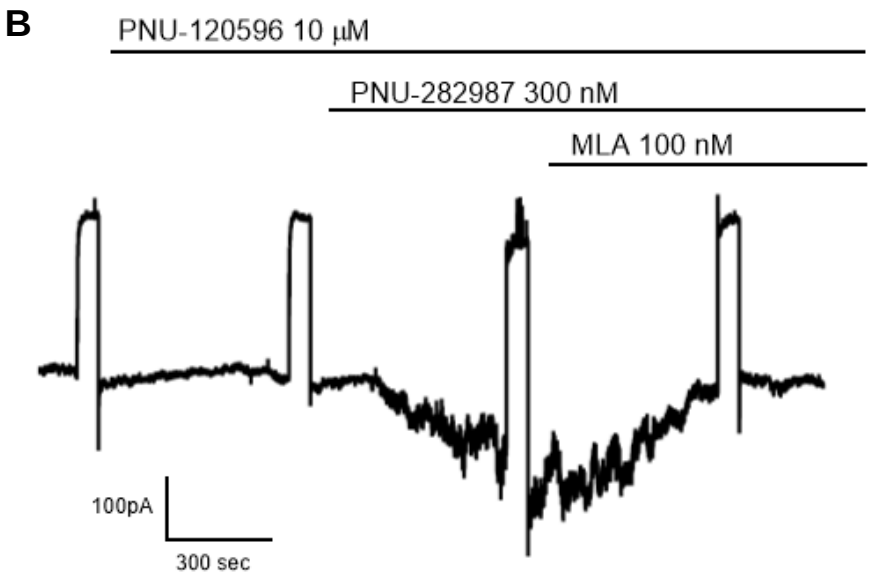
B
PNU-120596 10 μM
PNU-282987 300 nM
MLA 100 nM
100pA
300 sec

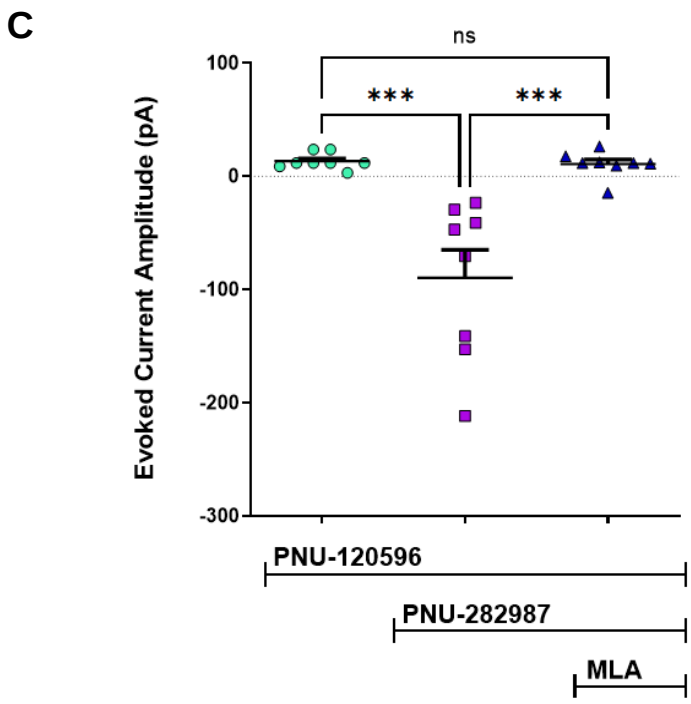

Figure 4.3 - Post-synaptic currents induced by α7nAChRs activation in CA1 pyramidal neurons in vHIP – (**A**) Representative scheme of the voltage-step protocol to record spontaneous EPSCs and IPSCs from the same neuron. The alternation of the holding voltage-clamp of the cell to the relative reversal potential makes possible to measure EPSCs and IPSCs during the stimulation of α7 nAChRs in the CA1 of vHIP. Each drug is perfused for 8 minutes during the voltage-clamp at -60 mV and for 1 minute at 0 mV. PNU-120596 (10 μM) in combination with PNU-282987 (300 nM) and MLA (100 nM) are cumulatively applied to the slice and allowed to equilibrate for 8 min before analysis of 1 min of events at -60 mV and 1 min of events at 0 mV (grey rectangles). (**B**) Representative current traces showing current changes during the above-mentioned compounds in vCA1. (**C**) α7current amplitude in pA showing that co- administration of the α7 PAM (PNU-120596 (10 μM)) and α7nAChR agonist (PNU-282987 (300 nM)) induced a significant inward current in vHIP CA1, reversed by the selective α7nAChRs antagonist MLA (100 nM). α7 PAM alone had no effect (n=8, ***p<0.001 One-Way Repeated Measures ANOVA with Tukey's *post hoc* test).

Figures 4.3 B and C demonstrate that pyramidal cells within the ventral CA1 express α7nAChRs, activation of which provokes an inward current, when the receptors are stimulated via the combined action of PAM + agonist. These data suggest that the post-synaptically located α7nAChRs might be responsible for molecular cascades, involving Ca^{2+} intracellular signalling, and inducing c-Fos promoter activation as described in Chapter 3. Therefore, the same experiment was performed in the dorsal

CA1, to determine if the difference between vHIP and dHIP in modulating reinstatement, depends on a different synaptic location of α7nAChRs.

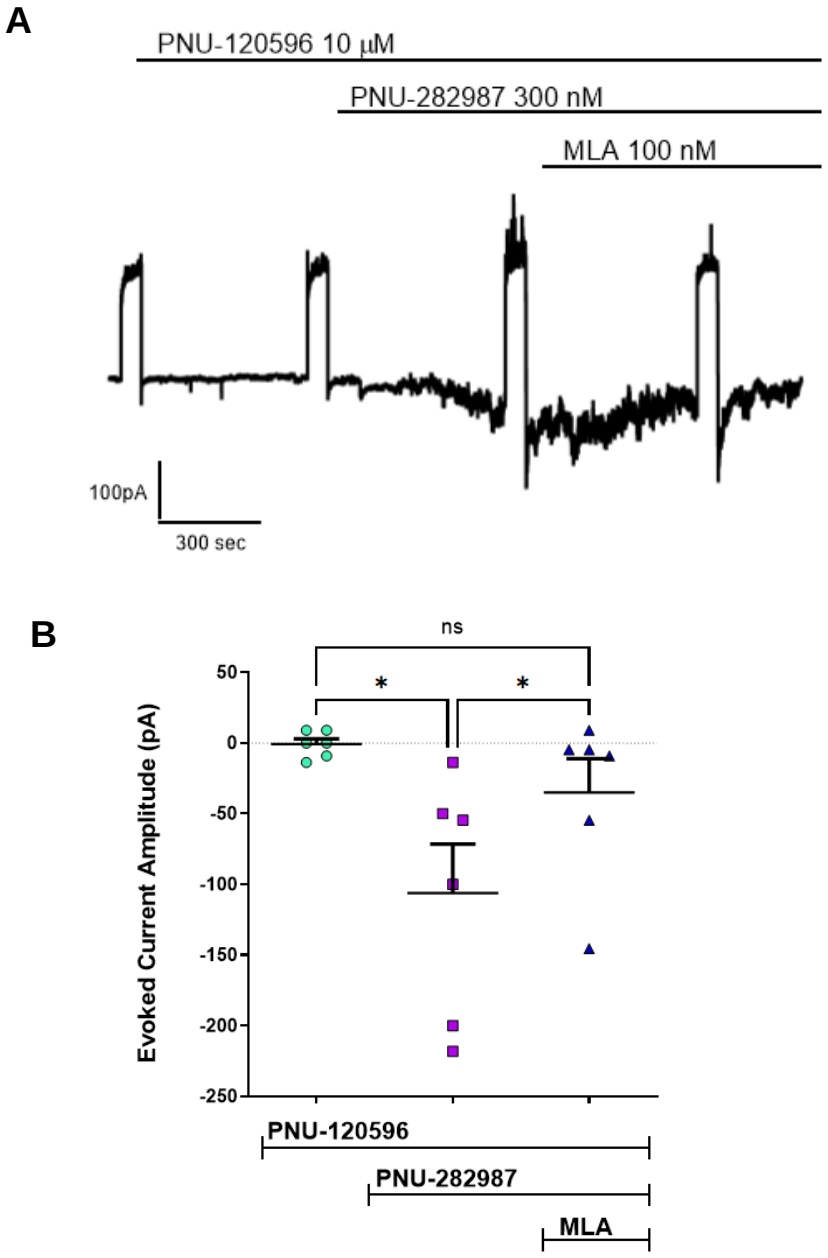

Figure 4.4 - Post-synaptic currents induced by α7nAChRs activation in CA1 pyramidal neurons in **dHIP** – Voltage clamp recording were made from pyramidal cells. Neurons were held at -60 mV and the current recorded in response to continual bath perfusion of control aCSF and then aCSF containing the α7nAChR-selective PAM PNU-120596 (10 µM), the α7nAChR PAM and selective agonist PNU-282987 (300 nM) and finally the α7nAChR PAM + agonist and with the antagonist MLA (100 nM). (**A**) Representative current traces showing current changes during the above-mentioned compounds in dCA1. (**B**) Evoked current amplitude in pA showing that co-administration of the α7 PAM

(PNU-120596 (10 μM)) and α7nAChR agonist (PNU-282987 (300 nM)) induced a significant inward current in vHIP CA1 that was, reversed by the selective α7nAChRs antagonist MLA (100 nM). The α7 PAM alone had no effect (data are presented as mean ± SEM; n=8 *p<0.05, Friedman Test with Dunn *post hoc* test; n= 6).

As shown in Figure 4.4, post-synaptically located α7nAChRs were detected in the dorsal CA1 where the induced a significant inward current when activated by the perfusion of PAM + agonist (Figure 4.4 A and B). Therefore, the different action of α7nAChRs in vHIP and dHIP during the heroin-induced reinstatement cannot be attributed to their synaptic location.

In the next section, the contribution of α7nAChRs in regulating the neuronal network in both vHIP and dHIP was investigated, by exploring the effect of their stimulation on EPSCs and IPSCs, as explained in section 4.2.1.

4.2.3 α7nAChRs modulation of spontaneous inhibitory currents in vHIP and dHIP

The initial aim of this experiment was to measure both excitatory and inhibitory post-synaptic currents from the same neuron, as described by Figure 4.3A. However, the inward current induced by the post-synaptic α7nAChRs prevented the analysis of sEPSCs, detectable when the membrane potential was hold at -60 mV. Hence, it was impossible to isolate this type of current accurately and measure the frequencies of sEPSC. On the other hand, the post-synaptic inward current did not affect the analysis of the sIPSCs (recorded at a holding membrane potential of 0 mV), which is reported in this section.

The investigation of the spontaneous inhibitory post-synaptic currents from both CA1 neurons in vHIP and dHIP revealed similar response induced by the activation of the α7nAChR, as reported by Figure 4.3A. In fact, none of the α7 treatments induced a significant effect on the IPCS frequency in vHIP or dHIP, suggesting this methodology may not be suitable for exploring these synaptic events in hippocampus.

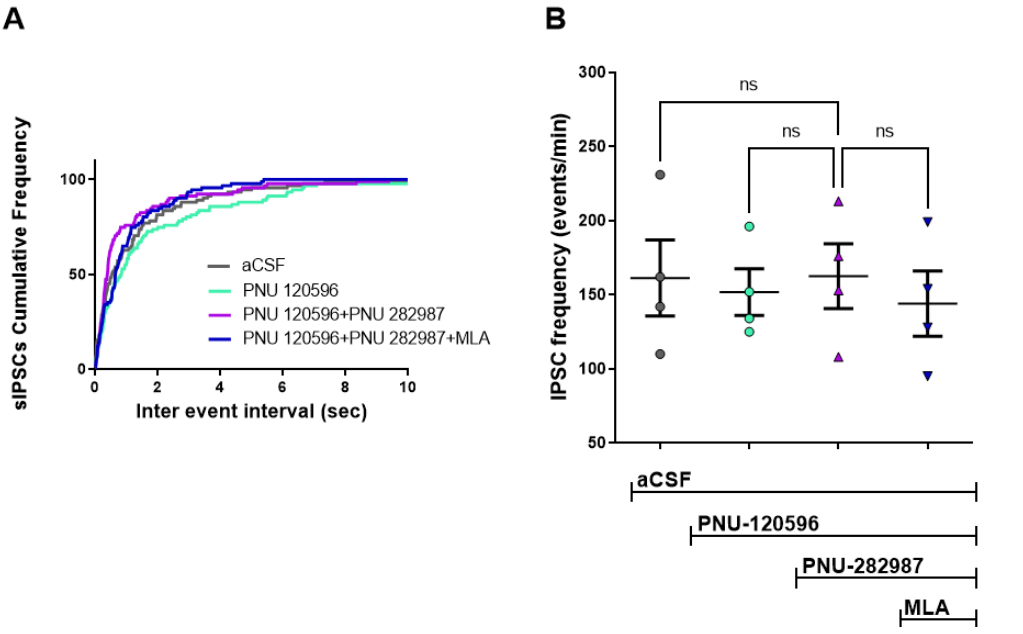
A
sIPSCs Cumulative Frequency
100
50
0
0
2
4
6
8
10
Inter event interval (sec)
aCSF
PNU 120596
PNU 120596+PNU 282987
PNU 120596+PNU 282987+MLA
B
IPSC frequency (events/min)
300
250
200
150
100
50
ns
ns
ns
aCSF
PNU-120596
PNU-282987
MLA

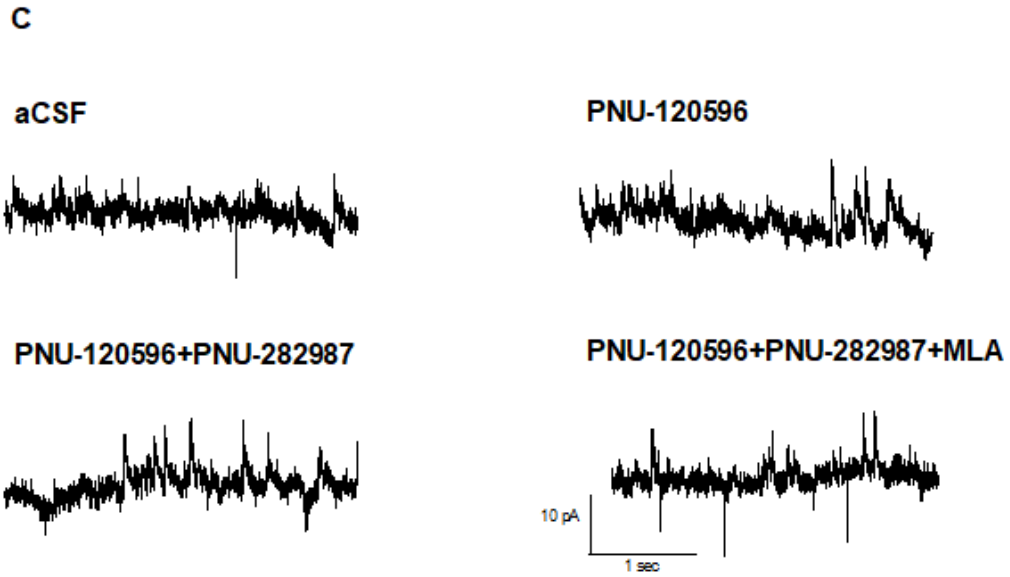
C
aCSF
PNU-120596
PNU-120596+PNU-282987
PNU-120596+PNU-282987+MLA
10 pA
1 sec

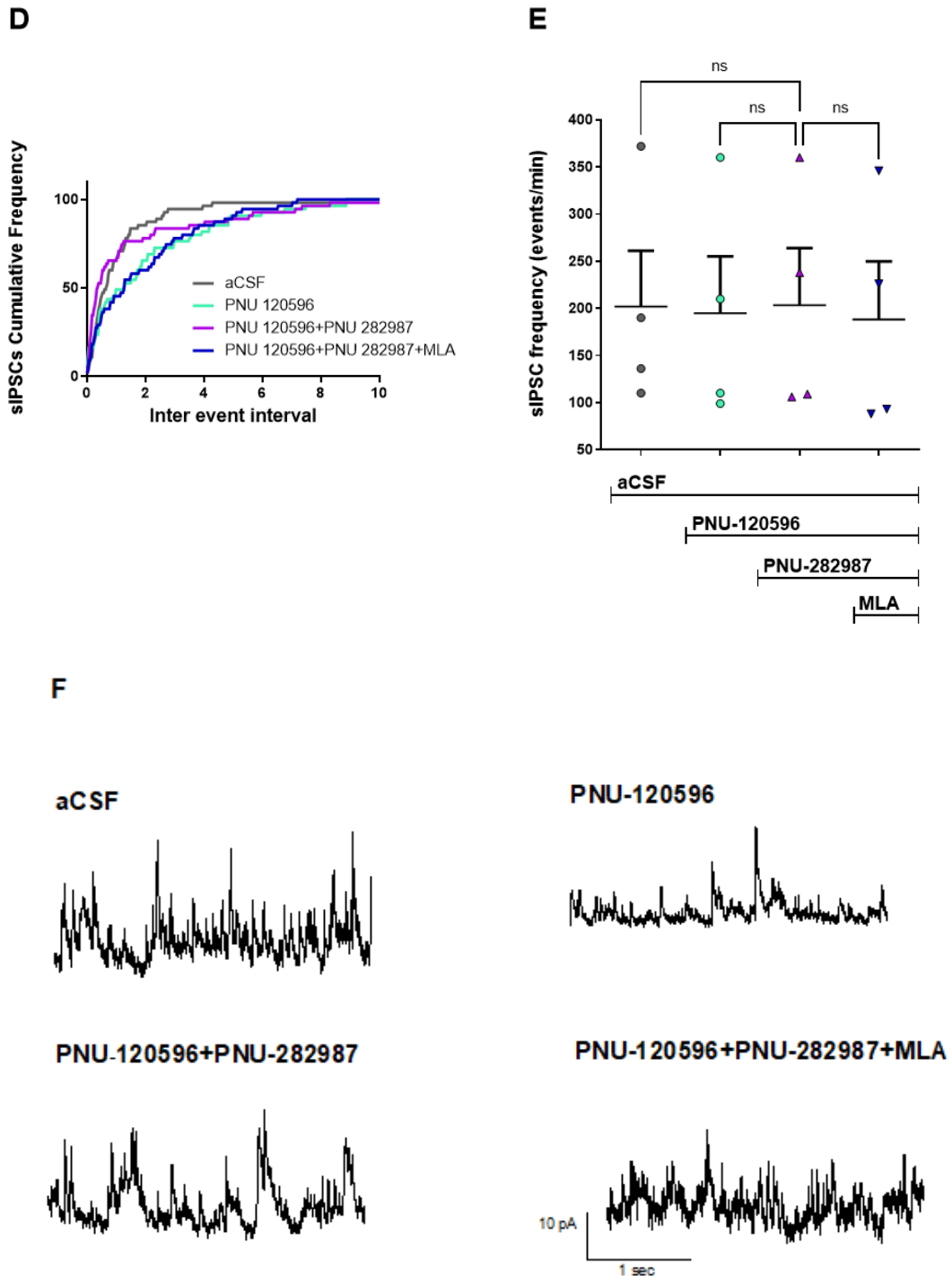

Figure 4.5 - Frequency of sIPSCs in response to α7nAChR stimulation and antagonism in vHIP and dHIP – Voltage clamping was performed in CA1 of both vHIP and dHIP. While neurons were held at 0 mV sIPSCs were recorded in response to continual bath perfusion of control aCSF and then aCSF containing the α7nAChR-selective PAM PNU-120596 (10μM), the α7nAChR PAM and selective agonist PNU-282987 (300 nM) and finally the α7nAChR PAM + agonist and antagonist MLA (100 nM). (**A**) sIPSC inter event intervals from vHIP were analysed, ranked and plotted in a cumulative

frequency trend scheme and (**B**) total events per minute were also calculated and represented as mean ± S.E.M in summary scattered plots. One-Way Repeated Measures ANOVA with *post hoc* Dunnett's Multiple Comparison Test to aCSF, n=4. (**C**) Representative current traces of sIPSC in vHIP during the application of each compound. (**D**) sIPSC inter event intervals from dHIP were analysed, ranked and plotted in a cumulative frequency trend scheme and (**E**) total events per minute were also calculated and represented as mean ± S.E.M in summary scattered plots. Friedman Test with Dunn *post hoc* test to aCSF; n=4. (**F)** Representative current traces of sIPSC in dHIP during the application of each compound

As shown from Figure 4.5 A and B, there were no significant differences between treatment groups, suggesting that the stimulation and antagonism of α7nAChRs, provoked by PNU-120596+PNU-282987 and MLA respectively, did not affect the frequencies of the sIPSC in vHIP. Moreover, similar results were reported for the IPSC recorded in dorsal CA1, as shown in Figures 4.5 D and E. The action of α7nAChRs on hippocampal GABAergic system has been largely demonstrated by others (Alkondon & Albuquerque, 2001; Griguoli et al., 2013). Hence, the methodology here used to detect the post-synaptic events in the hippocampus is almost certainly not viable for the purpose of the experiment. Possible explanations for this phenomenon will be discussed in the following section.

4.3 Discussion

The main finding of the current chapter was that α7nAChRs are post-synaptically located in the CA1 of both vHIP and dHIP. To my knowledge, this was the first time in which α7nAChRs were clearly found in the post-synaptic site and separately studied in ventral and dorsal CA1. Due to methodological artefacts, the evaluation of pre-synaptic α7nAChRs, by analysing the EPSC and IPSC, was not possible, as explained below. However, there is a large body of evidence showing that α7nAChRs in hippocampus are pre-synaptic (Fabian-Fine et al., 2001; Gu et al., 2012; Cheng & Yakel, 2014). Hence, the relevance of the post-synaptic α7, and possible alternative strategies to investigate how these receptors can modulate the hippocampal network, in both dorsal and ventral portions, will be discussed.

4.3.1 The impact of post-synaptic α7 in synaptic adaptations

As previously demonstrated, activation of post-synaptic α7nAChRs induces a fast, inward cationic current and can therefore cause amplification of weak inputs on

pyramidal cells directly by activation of their postsynaptic α7nAChRs or indirectly by inhibition of GABAergic interneurons that directly synapse onto pyramidal cells in hippocampus (Ji & Dani, 2000; Ji et al., 2001). α7nAChRs allow flux of Na^+ and K^+ ions but are also highly permeable to Ca^{2+}. In fact, activation of post-synaptic α7nAChRs induces membrane depolarisation and the initiation of several molecular cascades led by Ca^{2+} acting as a second messenger (Gotti & Clementi, 2004). Moreover, due to its Ca^{2+} permeability, α7nAChRs has been defined as a metabotropic/ionotropic receptor (Kabbani et al., 2013) binding with both Gα and Gβγ proteins the M3-M4 loop and allowing a Ca^{2+} signalling response beyond the expected time course of channel activation (Kabbani et al., 2013; King et al., 2015). The intracellular Ca^{2+} increase induced activation of CaMKII/IV and ERK/MAPK, and the sustained phosphorylation of CREB in hippocampal cell cultures (Dajas-Bailador et al., 2002), which is involved the activation of immediate early genes (IEG), such as c-Fos, an important marker of neuronal activation. Thus, the post-synaptic α7 location could be the reason, at least in part, for what was reported in Chapter 3, in which the block of α7 via MLA reduced c-Fos expression in the ventral CA1. On the other hand, the presence of post-synaptic α7nAChRs in the dHIP was also demonstrated. This suggests that α7nAChRs attenuation of the opiate-primed reinstatement of CPP and the subsequent neuronal activation do not depend on their location across the dorso-ventral axis. Possible interpretations of this finding will be discussed in Chapter 7.

4.3.2 The complexity of hippocampal network: α7nAChRs

In this experiment, a "voltage-steps" approach was used to detect and analyse both EPSCs and IPSCs (Figure 4.3A). The advantage of this methodology consists of isolating either the AMPAR or the GABAR components, using the reversal potentials of those receptors which are 0 mV and -60 mV respectively, and so detect the post-synaptic events. With this approach, a significant reduction in the use of animal numbers can be achieved, which would have not been possible with a traditional pharmacological method (see below). This technique was already used in our lab and so deemed successful for the aim of this experiment (Udakis et al., 2016). However, the results finding here differ from what Udakis and colleagues (2016) showed. In fact, the authors performed a set of experiments using the same type of approach, but in another brain region, namely PL, where α7nAChRs in the layer V of the prelimbic

cortex were found only pre-synaptically, allowing a wider investigation of the excitatory and inhibitory networks. In these experiments, the presence of the inward current, due to the post-synaptic location of α7nAChRs, prevented the analysis of the EPSCs and confounded the results for the IPSC in both vHIP and dHIP. In summary, determining on which type of neurones α7nAChRs are located and how they modulate on the hippocampal network, by measuring both the excitatory and inhibitory pyramidal synaptic events in the same recording, was not technically feasible.

In the hippocampus, α7nAChR's interaction with the excitatory glutamatergic system has been convincingly demonstrated (Banerjee et al., 2013; Cheng & Yakel, 2015). α7nAChRs expression has been found lower in the soma of primary excitatory cells, and is highly expressed at the excitatory synapses of the hippocampus (Fabian-Fine et al., 2001). It has been reported that stimulation of pre-synaptic α7nAChRs facilitates glutamate release from glutamatergic terminals in hippocampal synaptosomes and brain slices (Zappettini et al., 2010; Banerjee et al., 2012). Importantly, α7nAChRs and NMDAR receptors are co-localised on glutamatergic terminals, and the stimulation of α7nAChRs with choline fostered glutamate release via the increased levels of intracellular Ca^{2+} and the subsequent expression of NMDAR in hippocampal cell cultures (Zappettini et al., 2014). In addition, it has been also demonstrated that the modulatory effects of α7 receptors associated with glutamatergic signalling depends on the timing of α7nAChRs activation related to the glutamatergic transmission (Ge & Dani, 2005; Gu & Yakel, 2011). Hence, this substantial body of evidence confirms that α7nAChRs modulate glutamatergic transmission and its post-synaptic events, even if the hippocampal portion is dorsal or ventral is hardly ever stated.

Despite the above-mentioned issue to detect spontaneous EPSCs and so the interplay between α7nAChRs and glutamatergic system, the investigation of IPSCs was possible. Our data showed that stimulation of α7nAChRs did not induce any significant change in vHIP and in dHIP. However, these data are in contrast with the literature, as the interplay between α7nAChRs and GABAergic system has widely been demonstrated. Inhibitory interneurons substantially contribute to information processing in the hippocampus and their diversity in anatomical structure and location

underpin different functions (Freund & Buzsáki, 1996; Klausberger & Somogyi, 2008). Importantly, according to the interneuron subtype and its connection with the pyramidal cell, a single interneuron can block activity in a dendrite, alter action potential firing phase at the soma, or inhibit action potential firing at the pyramidal cell body (Miles et al., 1996).

Oriens lacunosum-moleculare (OLM) interneurons located in the stratum oriens of the CA1 express nAChRs and are critical in processing hippocampus-dependent memory formation (Haam et al., 2018; van Goethem et al., 2019). These interneurons are a subset of CA1 somatostatin-positive interneurons, and their main target is the distal dendrites of CA1 pyramidal cells in the stratum lacunosum–moleculare (SLM). In this stratum the pyramidal neurons receive excitatory inputs from the EC. OLM interneurons are characterised by a large α7nAChRs current, in comparison to other somatostatin interneurons and pyramidal cells (Gu et al., 2020). It has been found that activation of α7nAChRs inhibits the EC→CA1 pyramidal neurons pathway via direct inhibition, increasing Schaffer collateral inputs through indirect disinhibition (Leão et al., 2012). This may be due to the evidence that α7nAChRs are expressed in both pre- and post-synaptic sites of GABArgic inhibitory interneurons, regulating the inhibitory transmission (Alkondon & Albuquerque, 2001). Importantly, inhibiting α7nAChRs on the interneurons of the CA1 stratum radiatum can induce either inhibitory or disinhibitory effects on CA1 pyramidal neurons (Ji & Dani, 2000). Thus, beyond directly depolarizing interneurons, α7nAChRs also modulate synaptic transmission and plasticity, increasing presynaptic release of both glutamate and GABA (Radcliffe et al., 1999) and so promoting mechanisms of LTP (Cheng & Yakel, 2015).
However, these studies do not mention if their recordings are from either the dHIP or vHIP, therefore it remains hard to address the above mentioned α7nAChRs properties on one of the sub-hippocampal regions.

In summary. the complexity of the hippocampal inhibitory and excitatory neuronal transmissions, in respect of the α7nAChRs regulation, prevented the voltage-steps approach from detecting the EPSC and obtaining clear results from IPSC analysis. The impact of α7nAChRs on hippocampal GABAergic signalling has been widely demonstrated and the lack of effect from the α7 treatments may reflect an unexpected

methodological issue. In fact, the voltage-steps stimulation can provoke an interaction between glutamatergic pyramidal neurons and GABAergic interneurons, making it difficult to determine the effect of α7nAChRs at single neuron level. Therefore, in the next section, potential alternatives to this methodology will be described.

4.3.3 Possible alternatives "voltage-step" methodology

Patch-clamp electrophysiology is a comprehensive approach to investigate how different receptors can influence the neuron-neuron communication and the associated synaptic signalling. There are different methods to study how a defined target can affect the neuronal network under investigation. An alternative to the voltage-steps protocol is to use a bipolar tungsten stimulating electrode, stimulating according to a specific interval. For instance, when cells are clamped at -60 mV , the GABAR (IPSC) and AMPAR+NMDAR (EPSC) currents would be amplified. This stimulation-recording protocol can evoke synaptic responses predominantly from proximal inputs, such as GABAR responses from interneuron axon terminals that synapse on or close to the soma of the patched pyramidal cell, and glutamatergic responses from proximal pyramidal cell terminals (Proctor et al., 2011). In this way, it would be possible to record both IPSC and EPSC from the same cell, and so to explore the effect of PNU-12569, PNU-282987 and MLA on the hippocampal, dissected in its dorsal and ventral portions, network.

A pharmacological approach could also be applied to achieve this aim. Specifically, isolating either the GABAR component or the glutamatergic one, using a selective antagonist for each component, such as picrotoxin and NBQX respectively (Ji & Dani, 2000; Alkondon et al., 2013; for review see Stone, 2021), may help to define the α7nAChRs action of the hippocampal network, without perturbing the micro-circuit equilibrium and preventing the obtainment of clear results.

Another pharmacological method to explore α7nAChRs influence on the hippocampal network would be the block of the post-synaptic α7 receptors and to better isolate its pre-synaptic action on both GABAergic and glutamatergic cells, by detecting IPSC and EPSC respectively. Specifically, the MK-801 (dizocilpine), is widely known as a NMDA channel blocker that does not simultaneously affect AMPA or kainate

receptors. This compound is also an open channel blocker of α7 and α4β2nAChRs. MK-801 is 40 times less potent on nAChRs in comparison to NMDAR (Amador & Dani, 1991; Briggs & McKenna, 1996). However, the bath application of the MK-801 would provoke the block of both pre- and post-synaptic α7. Hence, inserting this compound into the intracellular solution, contained in the recording glass-pipette, can be a successful strategy to block the post-synaptic α7, but not the pre-synaptic α7, and so to abolish the inward current, shown in Figures 4.3 B and 4.4 A, without affecting the effects of pre-synaptic α7nAChRs (see Figure 4.6).

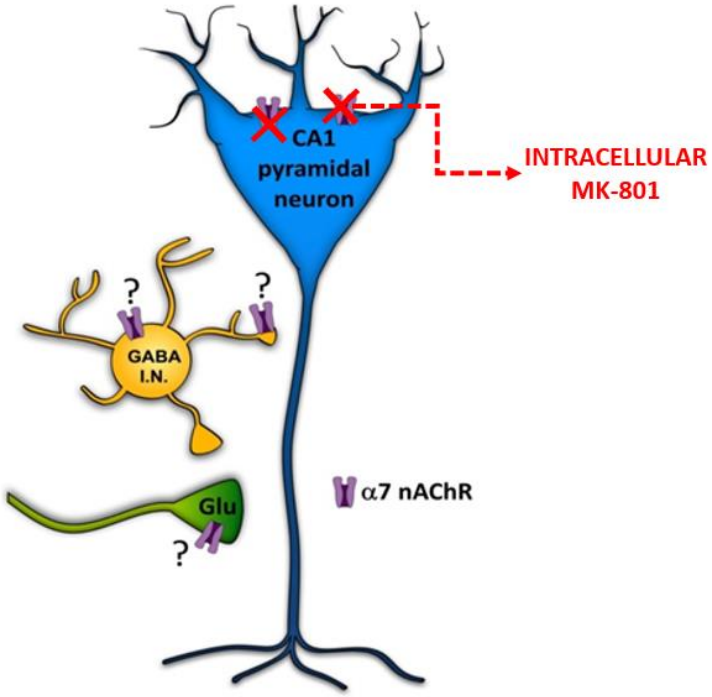

Figure 4.6 – The effect of the intracellular MK-801 on α7nAChRs in the CA1 of vHIP and dHIP- The application of the MK-801 in the intracellular solution contained in the recording pipette would allow the exploration of both EPSC (glutamatergic neurons) and IPCS (inhibitory interneurons), inhibiting the current induced by post-synaptic α7nAChRs and leaving intact the pre-synaptic compartment.

In order to perform this study, a set of optimisation experiments would be necessary, such as defining the correct concentration of the MK-801. It has been found that an intracellular concentration of 1 mM, has been reported to be effective in blocking NMDA receptors (Berretta & Jones, 1996), and it, therefore, represents a good starting point for finding the right concentration for blocking α7 (Figure 4.6). Hence, such an

approach may help us in properly investigating the action of α7nAChRs, bringing new insight into the nature of these receptors.
Overall, these data provide the first evidence that α7nAChRs are located post-synaptically in both vHIP and dHIP, and so exclude the idea that the functional differences relative, observed *in vivo*, to those two subregions, in respect to α7nAChRs, depend on some other factors rather than on the location of those. Possible interpretations are discussed in Chapter 7.

So far, it has been demonstrated in this thesis that α7nAChRs modulate neuronal activation (Chapter 3) and that they are post-synaptically located. Therefore, the next chapter is focussed on how the *in vivo* block of α7nAChRs, during the heroin-induced reinstatement, modulate synaptic plasticity in vHIP, by selectively targeting the behaviourally recruited c-Fos tagged neurons.

CHAPTER 5
HOW DO α7NACHRS MODULATE POST-SYNAPTIC CHANGES IN VENTRAL CA1 DURING THE REINSTATEMENT OF A HEROIN-CPP?

5.1 Introduction

The evidence presented in the previous chapter supported the idea that α7nAChRs in vHIP are implicated in memory recall of heroin-primed reinstatement of CPP. In fact, the systemic administration of MLA before the heroin-primed induced reinstatement reduced the drug-seeking behaviours in MLA-treated mice, in comparison to saline controls, and selectively decreased the associated c-Fos expression in vHIP. One possible explanation for this is that α7nAChRs are involved in synaptic plasticity in the vHIP, such that blocking α7nAChRs inhibits memory reactivation. c-Fos is broadly considered to be a marker of neuronal activation, although there is some evidence suggesting that c-Fos expression is relevant for the maintenance of LTP in murine hippocampus (Miyamoto, 2006).

Early studies investigated the correlation between c-Fos expression and synaptic plasticity using electrophysiological recordings, in the rat striatum and dentate gyrus, highlighting that c-Fos activation correlates with synaptic activity levels and not with action potential generation (Labiner et al., 1993; Sgambato et al., 1997). However, from these studies it is unclear whether the recorded neurons were c-Fos positive (c-Fos+) or negative (c-Fos-), since the majority of neurones are c-Fos-, it is possible that their level of synaptic activity may be below the threshold that are required to generate the action potentials necessary for synaptic plasticity to occur (Cruz et al., 2015).

Various transgenic, viral, and chemogenetic approaches, based on activation of the Fos promoter, have been used to manipulate this small subset of strongly active neurons and understand their role in learned behaviours in the addiction and fear

conditioning (Cruz et al., 2013; Ramirez et al., 2013; Warren et al., 2016). Most of these strategies used the Fos promoter to drive expression of other target proteins, such as GFP, in order to identify, manipulate and dissect the Fos-expressing neuronal ensembles (for review, see Whitaker & Hope, 2018). In fact, associative learning is underpinned by functional changes across sparsely distributed populations of neurons, commonly referred to as "neuronal ensembles," that are selected by specific stimuli during learning (Hebb, 1949).

Using the Fos promoter to introduce fluorescent transgenes, such as in c-Fos-GFP (Green Fluorescent Protein) mice, it is possible to design experiments in which sets of tagged cells are compared to the untagged ones. For instance, Barth and colleagues first performed whole cell patch-clamp recordings from both c-Fos-GFP positive and negative neurons, in order to investigate synaptic properties specifically in cortical circuits recruited by particular behaviours (Barth et al., 2004). In fact, more recent studies using this strain of mice, expressing GFP in behaviourally activated Fos-expressing neurons, reported that the set of neurons encoding learned associations show specific adaptations at glutamatergic synapses in the NAc, compared with the surrounding neurons (Koya et al., 2012; Whitaker et al., 2016). Hence, to perform the experiments reported in this chapter, c-Fos-GFP mice have been used to identify the behaviourally recruited neurons, namely the c-Fos+ ones, and to perform brain-slice electrophysiology on those neurons.

Previous research from our group showed that a single injection of MLA before morphine-primed reinstatement resulted in significantly lower AMPA, but not NMDA, binding in the CA1/CA2 of the vHIP, compared with saline controls (Wright et al., 2019). This finding suggests that α7nAChRs are implicated in modulating synaptic modifications which directly involve the glutamatergic system, highlighting their contribution to mechanisms of learning and memory. Long-term potentiation (LTP) is a common form of synaptic plasticity that involves insertion of AMPA receptors in the postsynaptic region of the synapse. Therefore, one possible interpretation of the Wright et al finding is that morphine-primed reinstatement induces LTP in CA1 of the vHIP, which is inhibited by MLA. However, there could be alternative explanations for an increase in AMPA binding, including an enhanced

assembly of receptors either intracellularly or expression nearby the extra-synaptic site (Malinow et al., 2000). Even though it has been shown that AMPA mRNA synthesis can be viewable 15 minutes after a pharmacological stimulation (90 mM KCl) in rat primary cortical cultures (Orlandi et al., 2011), *de novo* protein synthesis and potential translocation from cell body requires more time. Since mice were sacrificed 30 minutes after behavioural assessment, it is unclear whether or not the changes observed by Wright and colleagues are relative to the insertion of AMPA receptors onto the neuronal surface, and therefore indicative of synaptic plasticity.

Other studies highlighted the importance of AMPAR insertion in hippocampal neurons in context-related memories. For instance, it has been found that alterations of synaptic AMPAR expression in the hippocampus mediate morphine-induced context-dependent sensitisation (Xia et al., 2011). An increase of AMPAR, in mouse hippocampal cultured slices, acute slices and in vivo, was required for LTP induction, and selective alteration of AMPAR trafficking in dHIP inhibited fear-conditioning learning (Penn et al., 2017). Hence, looking at the AMPAR activity remains a promising approach to investigate learning-driven synaptic plasticity.

According to Stone (2021), glutamatergic receptors and nicotinic receptors, especially α7nAChRs, should not totally be thought as spatially and functionally distinct entities. In fact, the activation of α7nAChRs can alter the subunit composition of both NMDA or non-NMDA receptors, and can modify the cellular distribution and localisation of the resulting receptor (Stone, 2021). It has been shown that nicotine selectively enhanced the amplitude of AMPAR mediated current and AMPA/NMDA ratio, in the layer I of rat PFC, and this increase was inhibited by the application of MLA, an α7 selective antagonist (Tang et al., 2015). In the same work Tang and colleagues (2015) reported that nicotine increased AMPAR currents by modulating the phosphorylation activity of the GluR1 subunit, selectively, which depended on α7nAChRs (Tang et al., 2015), suggesting an interplay between α7nAChRs and AMPA currents in rat prefrontal neurons. Remarkably, hippocampal α7nAChRs located on the surface of dendrites and spines can induce clustering of AMPAR, investigated by using tagged GluA2 subunits and this activity was calcium-dependent, and involved increased

activity of the postsynaptic density protein (PSD-95) protein complex and the calcium-permeable GluR1 trafficking to the cell surface (Elnagar et al., 2018).

There are several ways to assess synaptic plasticity *ex vivo*. The investigation of the AMPA/NMDA ratio is a viable approach to measure post-synaptic changes, in terms of synaptic strength, after behavioural training. Insertion of AMPAR over the extracellular surface of CA1 neurones is widely accepted as a model of synaptic plasticity, after both in vivo and ex vivo stimulation (Pascoli et al., 2014; Park et al., 2018), whereas NMDAR expression levels remain unchanged. An increase in AMPA/NMDA ratio is taken as an indicator of synaptic plasticity-induced increase in AMPAR synaptic expression. For instance, it has been shown that inhibitory avoidance (IA) training increased AMPA/NMDA ratio in dHIP, but not in vHIP, and such synaptic change was prevented by in vivo infusion of MLA, impairing also the IA (Sakimoto et al., 2019). Moreover, Hyer and colleagues found that adolescent female rats which received a stress protocol had a decreased AMPA/NMDA-dependent current ratio compared to controls, indicating a weakening in synaptic strength in the hippocampus (Hyer et al., 2021). Thus, all these findings highlight the relevance of measuring the AMPA/NMDA ratio as an indication of synaptic plasticity, and so as a marker of long-term memory.

Synaptic strengthening has been related to an enhanced AMPAR conductance, as an increase of ionic flow through an individual ionophore (Benke et al., 1998). In fact, short-term plasticity can induce modifications in the relative permeability of AMPAR, through the insertion of calcium permeable AMPAR (CP-AMPARs), which typically consist of GluA2-lacking AMPARs, known to mediate fast excitatory synaptic transmission (Glasgow et al., 2019). In order to estimate the presence of CP-AMPAR, it is necessary to measure the rectification index (RI) of the AMPAR, namely the way in which the AMPAR conducts across different voltages. The majority of the AMPAR are Na^+ permeable but Ca^{2+} impermeable, showing a linear I-V relationship. This implies the presence of at least one GluA2 subunit in the receptor composition, where the relative mRNA-editing induces a replacement of the glutamine residue, at the Q/R site of the receptor, with an arginine residue (Sommer et al., 1991). As such a residue is positively charged, it blocks the interaction between Ca^{2+} ions and the channel pore,

preventing the cation flow through the channel. However, depending on the type of the stimulation, AMPAR GluA2-lacking but GluR1-containing can assemble, making the channel calcium-permeable. Moreover, CP-AMPAR are characterised by an inward rectification, showing a reduced outward current at more depolarised potentials (Figure 5.7), arising from fast voltage-dependent channel block by intracellular polyamines (Pellegrini-Giampietro, 2003). In fact, spermine, which is positively charged, selectively blocks CP-AMPAR because it is attracted by a negatively charged ring of carbonyl-oxygen groups present in the glutamine residues of the GluR1 and rejected by the positive arginine (Figure 5.5). Hence, the application of spermine in the intracellular solution allows the evaluation of the RI, which is the direct evidence of the potential presence of CP-AMPAR, without using any external pharmacological inhibitor.

However, it is not clear if the insertion of CP-AMPAR is transient or not (Park et al., 2018). Interestingly, it has been found that CP-AMPAR in dHIP does not impact on the neutral memory consolidation (Torquatto et al., 2019). In addition, the same work while fear memory retrieval involves CP-AMPAR activity in dHIP and BLA and that those hippocampal CP-AMPAR are crucial for memory updating (Torquatto et al., 2019). Moreover, a recent study showed that CP-AMPA provided an important contribution to excitatory transmission in the CA1 of the vHIP in the last phases of escalating cocaine-conditioning CPP model in mice, highlighting the importance of CP-AMPA in vHIP as a possible enhancer of cocaine-contextual associations (Preston & Wagner, 2021).

Lastly, the paired-pulse ratio (PPR) is another useful measurement to observe changes in synaptic strength. In fact, it indicates the probability of the presynaptic nerve terminal to release neurotransmitter. Specifically, when two pulses are paired in quick succession (typically 20–100 ms), it is thought that residual Ca^{2+} left over from the first stimulus will transiently increase the release probability upon the second stimulus and the relative peak amplitude of the two pulses is known as PPR (reviewed in Glasgow et al., 2019). On this basis, it was decided in this chapter that investigating the AMPA/NMDA ratio, RI and PPR in vHIP would facilitate assessment of any

α7nAChR-mediated changes in synaptic plasticity during the reactivation of a salient memory.

To perform this experiment, c-Fos-GFP mice underwent reinstatement of heroin-CPP as explained in (Chapter 2, section 2.4.3.4) and whole-cell patch clamp recordings were made from vHIP slices, in order to evaluate the AMPA/NMDA ratio, RI and PPR in c-Fos+ and cFos- neurons, from animals treated with either MLA or SALINE before the heroin-primed reinstatement of CPP.

5.2 Results

5.2.1 Optimisation for AMPA/NMDA ratio and Rectification Index

To carry out this study, a series of experiments were performed to optimise the protocol. Male C57BL/6J and c-Fos-GFP mice 8-10 weeks old were cardio-perfused initially with cutting ringer, then with NMDG-recovery solution, to better preserve cellular health (Ting et al., 2018).

In order to obtain both AMPA/NMDA ratio and RI from the neuron, we designed an experimental protocol which consisted of the application of different compounds to explore AMPA, NMDA and $GABA_A$ components, across different voltage steps. Specifically, recordings were made from the CA1 of vHIP slices CA3-lacking (see Chapter 2) under paired-pulse stimulation. For the first part of the recording the voltage-current relationship (I-V curve) was investigated to obtain the submaximal (50%) evoked response from the stimulated cell.

The stimulation-recording protocol provokes both glutamatergic and GABAergic post-synaptic currents (EPSC and IPSCs). Hence, in order to selectively record the glutamatergic current, which will be dissected into AMPAR and NMDA components, the GABAergic currents must be blocked. Normally, there is no GABAergic component at -60 mV, it is however detectable at 0 mV, as shown in Figure 5.1.

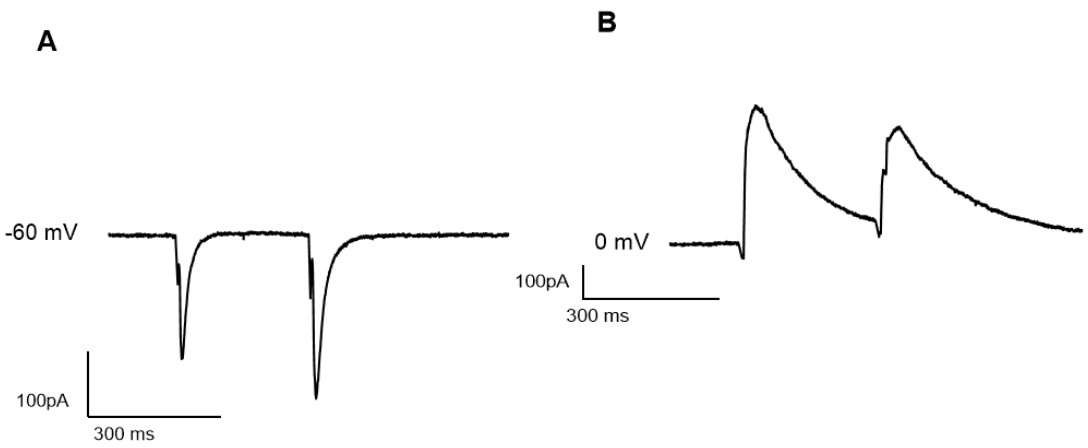

Figure 5.1 – Detection of baseline for AMPAR and $GABA_AR$ at -60 and 0 mV respectively – The neuron under investigation was stimulated at 30 mA for 150 ms. Representative current traces to detect **(A**) AMPA current at -60 mV, and (**B**) $GABA_A$ component at 0 mV, which is the reversal potential of AMPAR. No drugs were applied at this stage**.**

In order to prevent possible overlap between glutamatergic and GABAergic components and to record the RI across different voltage-steps, the GABAergic current was blocked by the application of picrotoxin 50 mM, a non-competitive $GABA_A$ antagonist (Figure 5.2). Recordings for AMPA/NMDA ratios and RI were, therefore, performed in the presence of picrotoxin, which was applied at the beginning of each experiment.

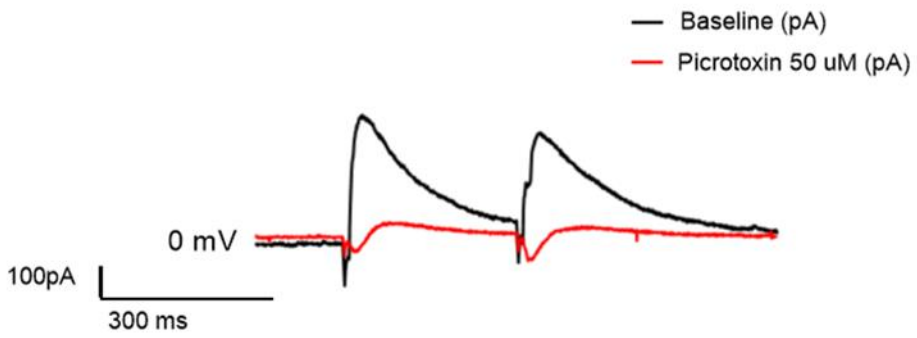

Figure 5.2 – The effect of picrotoxin on GABAergic current at 0 mV – The presence of 50 μM picrotoxin inhibited the stimulus-evoked events and, therefore, blocked $GABA_A$ receptors.

Once the $GABA_A$ component was deemed as isolated, the glutamatergic currents at -60 mV were explored. At this membrane potential the EPSC derives from the AMPAR component, as the NMDAR does not allow any ion influx, because of the

Mg^{2+} block. Therefore, to test that the current at -60 mV was purely AMPA, the effect of D-AP5, a selective antagonist of NMDAR was tested. Also, as a further control, the NBXQ 10 mM, a selective and competitive AMPAR antagonist, was applied to evaluate changes in the evoked current at -60 mV (Figure 5.3).

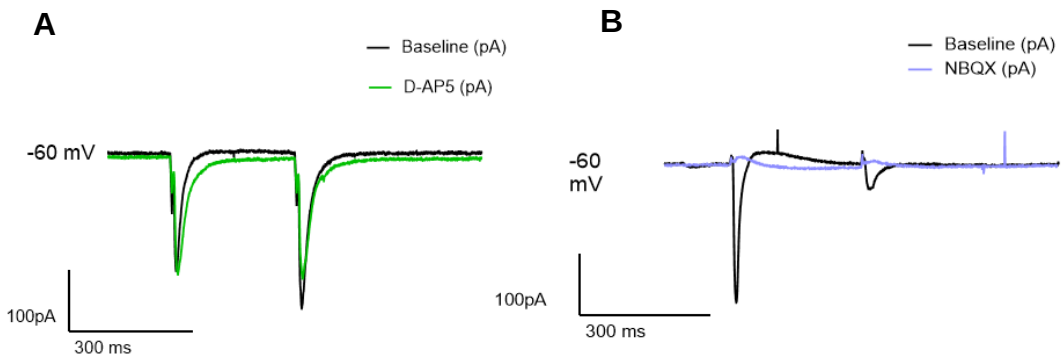

Figure 5.3 – The effect of the D-AP5 50 µM and NBQX 10 µM at -60 mV – Both AMPAR and NMDAR selective antagonists were bath-perfused when the cell was held at -60 mV. Traces represent a comparison between (**A**) baseline before the application of D-AP5 (black line) and after the effect of D-AP5 (green line) and (**B**) baseline before the application of NBQX (black line) and after the effect of NBQX (lilac line). All the traces were taken at least three minutes after the perfusion of the drug. Pairs of traces represented in A and B are taken from two different experiments.

As showed by Figure 5.3 A D-AP5 (50 µM) did not affect the EPSC measured at -60 mV, confirming that the EPSC at this holding potential is caused by activation of AMPAR not NMDAR. This was further confirmed by experiments as shown in Figure 5.3 B that confirmed that the EPSC at -60 mV was blocked by the NBQX (10 µM), confirming that the current detected at this membrane potential was mediated exclusively by AMPAR.

In contrast, when the cell is held at +30 mV, the resulting EPSC is a combination of AMPAR and NMDAR components, which is however possible to isolate from each other. As AMPAR and NMDAR currents have different time constants, the specific contribution of each receptor can be separated.

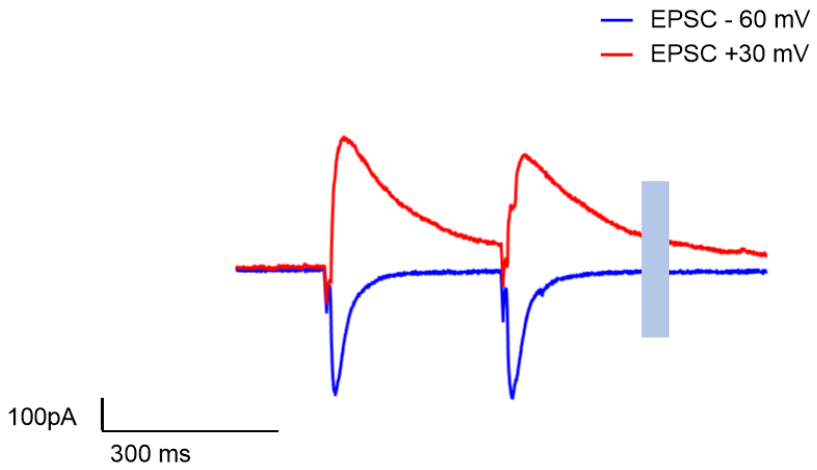

Figure 5.4 – Different time-constants of AMPA and NMDA currents – The blue line represents the EPSC at –60 mV, which is mediated entirely by AMPAR activity, while the red line defines the same EPSC at +30 mV, where both AMPAR and NMDAR components form the evoked current. Shaded rectangular areas indicate at 60 ms there is no AMPAR component left and what remains can be taken as an index of the magnitude of the slow NMDAR component.

As shown in Figure 5.4, the AMPAR-mediated current (blue line) at +60 mV decays much more rapidly than combined AMPAR/NMDAR-mediated current (red line) at +30 mV. At -60 mV, the AMPAR current shows both fast rise and decay times, with the current decaying to zero within approximately 50 ms. On the other hand, the EPSC at +30mV, which consists of AMPA and NMDAR currents, decays more slowly, as the NMDA receptor-mediated component itself decays more slowly. Therefore, it is possible to measure the EPSC (at +30 mV) at 60 ms and define it as being derived solely by the NMDAR current. As reported below (section 5.2.3), this approach to measure the NMDAR current has been used to further calculate the AMPA/NMDA ratios (Van den Oever et al., 2008).

A second method for quantifying the NMDAR component is by recording the EPSC at +30 mV and subtract the AMPAR current from the entire EPSC (Figure 5.5). As the EPSC at +30 mV is a composite of the AMPAR and NMDAR component, subtracting the AMPAR component from the EPSC leaves the NMDAR-only

component. To do this, a first entire EPSC at +30 mV was recorded and then the selective, competitive NMDA receptor antagonist D-AP5 (50 mM), to abolish the NMDAR currents was applied while EPSCs continue to be recorded. This results in the AMPAR-only component and subtracting this EPSC from the composite EPSC yields the NMDAR-only component (Figure 5.5). As well as the method outlined above, this has been used to determine both AMPAR and NMDAR components, in order to determine AMPA/NMDA ratios, as reported by others (Thomas et al., 2001; Shukla et al., 2017).

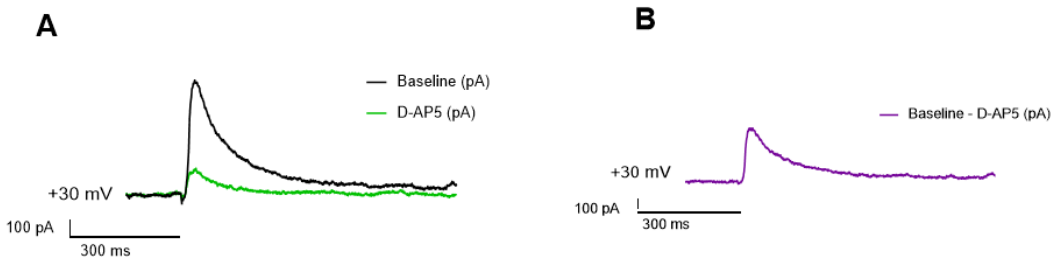

Figure 5.5 – Dissecting the +30 mV EPSC to obtain the NMDAR component – (**A**) EPSC recorded at + 30 mV, the black line represents the baseline with no drug applied, while the green line defines the effect of the D-AP5 50 µM on the baseline, where the NMDA component is completely abolished, leaving the AMPAR-only component. (**B**) The purely NMDA component can be obtained from subtracting the AMPA-only mediated current from the baseline current in which both NMDAR and AMPAR currents co-exist. Recordings were made in the presence of picrotoxin 50 µM.

To confirm that D-AP5 (at a concentration of 50 µM) fully blocks NMDARs, recordings were made at +30mV and AMPARs were blocked by NBQX (10 µM; see Figure 5.3). After recording NMDA-only EPSCs (Figure 5.6, black trace), D-AP5 (50 µM) was applied (magenta trace) which fully abolished the residual EPSC.

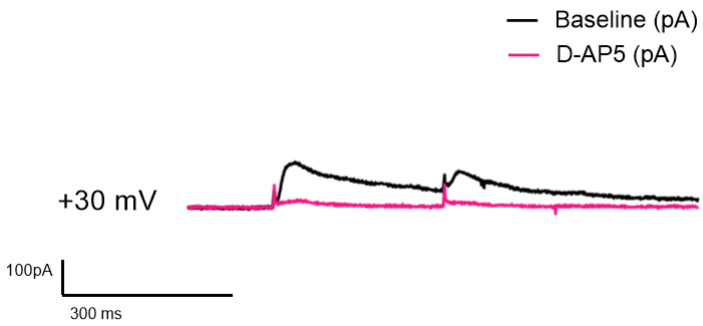

Figure 5.6 – The effect of 50 µM D-AP5 on NMDA current at +30 mV – The black line represents the baseline of an EPSC recorded at +30 mV, while the magenta line stands for the same EPSC but under the effect of the D-AP5. This recording was entirely preformed in the presence of NBQX, in order to dissect just the NMDA component. This recording was performed under the effect of picrotoxin 50 µM and NBQX 10 µM.

In addition to recording AMPA/NMDA ratios, it is possible to determine the AMPA receptor Rectification Index (RI). As outlined in the Introduction, calcium-permeable AMPA receptors (CP-AMPA) are inwardly rectifying. Therefore, changes in the relative AMPA conductance at hyperpolarized and depolarized membrane potentials can help demonstrate the presence of CP-AMPA. The inward rectification of CP-AMPARs is caused by fast voltage-dependent channel block by intracellular polyamines at depolarised membrane potentials. Therefore, in order to observe any inward rectification all experiments in this Chapter were performed by using an intracellular recording solution containing 0.1 mM spermine, the mechanism of which is explained in Figure 5.7.

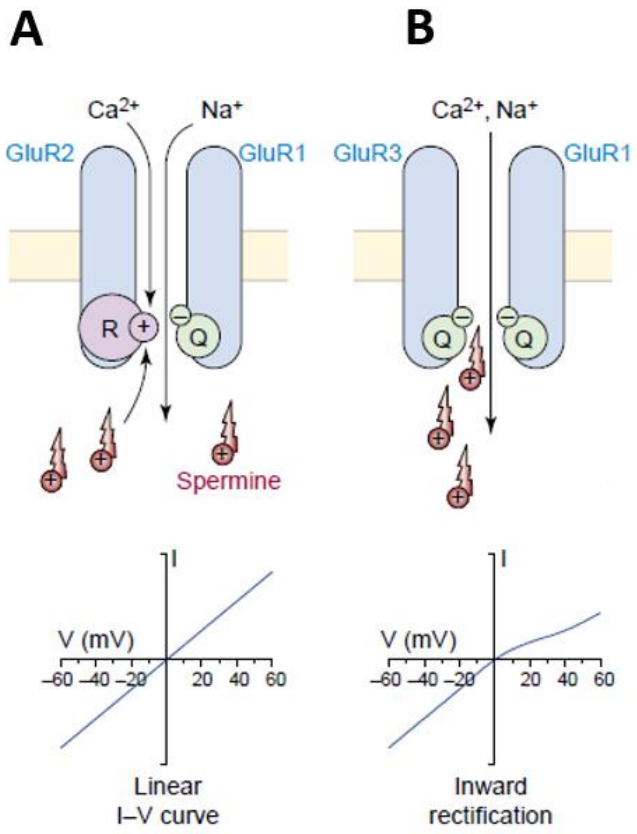

Figure 5.7 – Spermine induces inward rectification of CP-AMPAR – (**A**) AMPA receptors containing the GluR2 subunit are calcium impermeable and present a linear current-volage (I-V) relationship. The GluR2 subunit limits the entrance of Ca^{2+} ions and blockade by intracellular spermine, due to the presence of an edited positively charged arginine residue (R) rather than a glutamine residue (Q) in the region lining the selectivity pore. (**B**) GluR1/GluR3-containing AMPAR are calcium permeable, displaying an inward rectification, which arises from voltage-dependent channel block by intracellular spermine. The polar glutamine residues attract both Ca^{2+} and spermine into the channel (Pellegrini-Giampietro, 2003).

Once all the currents had been isolated and the action of compounds, at those concentrations, tested, we designed the final protocol used to detect AMPA/NMDA ratio, RI and PPR in c-Fos+ and c-Fos- neurons from c-Fos-GFP mice, after the heroin-primed CPP reinstatement (Figure 5.10). Picrotoxin (50 μM) was applied at the beginning of each recording and allowed to equilibrate for 6 minutes. AMPA/NMDA ratio and RI were obtained by comparing AMPAR and NMDAR currents across different voltages steps and during the application of above-mentioned compounds. More details about the analysis of these measures are given in the results and discussion sections. Finally, to verify that the evoked current obtained at -60 mV was

purely provoked by AMPAR activation, NBQX 10 μM was applied. This protocol scheme is graphically represented in Figure 5.8.

Due to the different decay kinetics characterising both AMPAR and NMDAR, two different methods were used to perform data analysis. As already mentioned, when AMPAR currents are recorded at hyperpolarising membrane potentials they exhibit an inward current with fast rise (2–7 ms) and decay kinetics (20–30 ms). On the other hand, the NMDAR, which is quiescent at resting membrane potential and activates only at depolarising voltages, is characterised by a slow rise (20 ms) to maximal current, and slow decay kinetics of 40-200 ms (Glasgow et al., 2019).

Here, we analysed the data using two different approaches, both measuring the AMPAR evoked current at -60 mV, under the effect of picrotoxin 50 μM, rather than at +30 mV, in order to avoid any interference due to the possible presence of CP-AMPAR. In the first approach, the NMDA component was obtained by subtracting the AMPAR current at +30 mV, over the effect of the D-AP5 50 μM, from the AMPAR+NMDAR currents present during the first voltage step (Figure 5.8) leaving the residual NMDAR current. Once the NMDAR component was isolated, the NMDAR current was considered at the peak of the curve (method A). In method B, the NMDAR component is taken as the magnitude of the composite AMPAR+NMDAR EPSC at 60 ms, by which the AMPAR component will have decayed to <5% of its maximum, and so can be taken as an index of the magnitude of the NMDAR component.

Thus, the purpose of analysing the data using two different approaches was to explore the presence of an effect of the in vivo treatments on the ex vivo evaluation, considering the complex dynamics belonging to AMPAR and NMDAR currents.

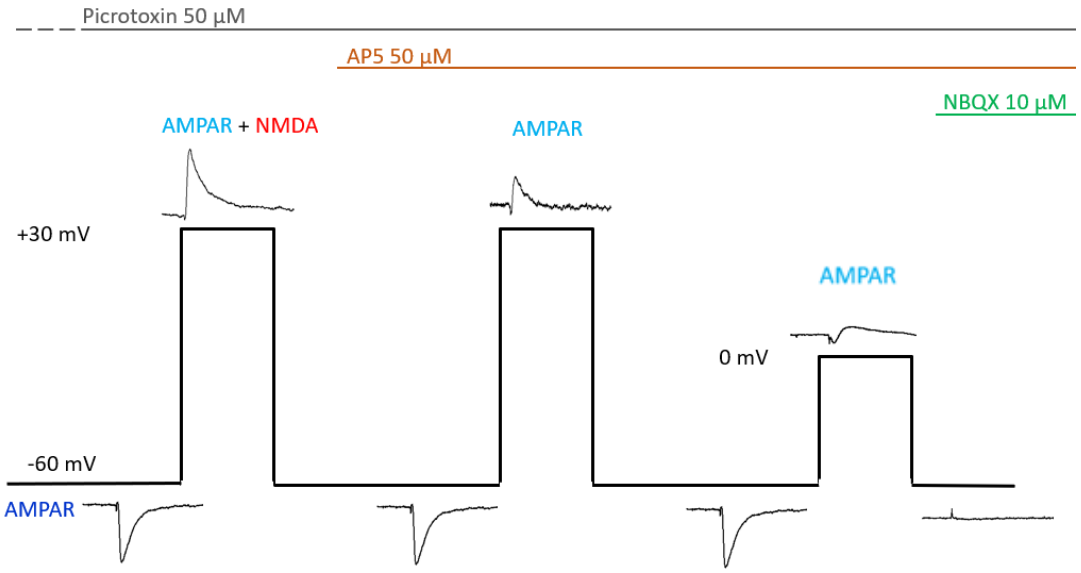

Figure 5.8 - Experimental procedure to detect A/N ratio and RI from the same neuron – Voltage steps have been performed in order to detect AMPAR, NMDAR and $GABA_AR$ component. First, picrotoxin 50 µM was applied at the beginning of the recording. After 6 minutes, the evaluation of the evoked current at -60 mV started. After 2 minutes, the voltage was switched to +30 mV for 1 minute to evaluate the NMDAR component, detectable 50 ms after the stimulation. The voltage was then switched back to -60 mV and 50 µM D-AP5 was applied, and the cell left to stabilise for 5-6 minutes. The voltage was then set at +30 for 1 minute to observe the AMPAR component only. The pure NMDAR component was obtained by subtracting the AMPAR current here earned from the current previously measured at +30 mV in the absence of D-AP5, allowing the assessment of A/N ratio. Also, the AMPAR component measured at this step allowed the comparison between AMPAR at -60 and AMPAR at +30 mV, to obtain the RI. In fact, the voltage was then switched to 0 mV for 1 minute to both verify the effect of picrotoxin on $GABA_AR$ current and to evaluate the AMPAR current to get the RI, as 0 mV is the reversal potential of AMPAR. Finally, at the end of each recording the voltage was brought to -60 mV and the effect of NBQX on the AMPAR current was evaluated, to confirm that the current at that voltage was selectively AMPAR-mediated.

5.2.2 Heroin-conditioned place preference using c-Fos-GFP mice

5.2.2.1 Habituation, acquisition, and extinction

In this experiment, c-Fos-GFP male mice underwent heroin-CPP, in which mice were conditioned with 2 mg/kg heroin and 0.9% saline. The CPP procedure was the same as the one described in Chapter 2 (section 2.4) and Chapter 3 (section 3.2.1). Mice

which had acquired statistically significant preference for the heroin-paired chamber, which was then extinguished after the extinction training, as shown in Figure 5.9.

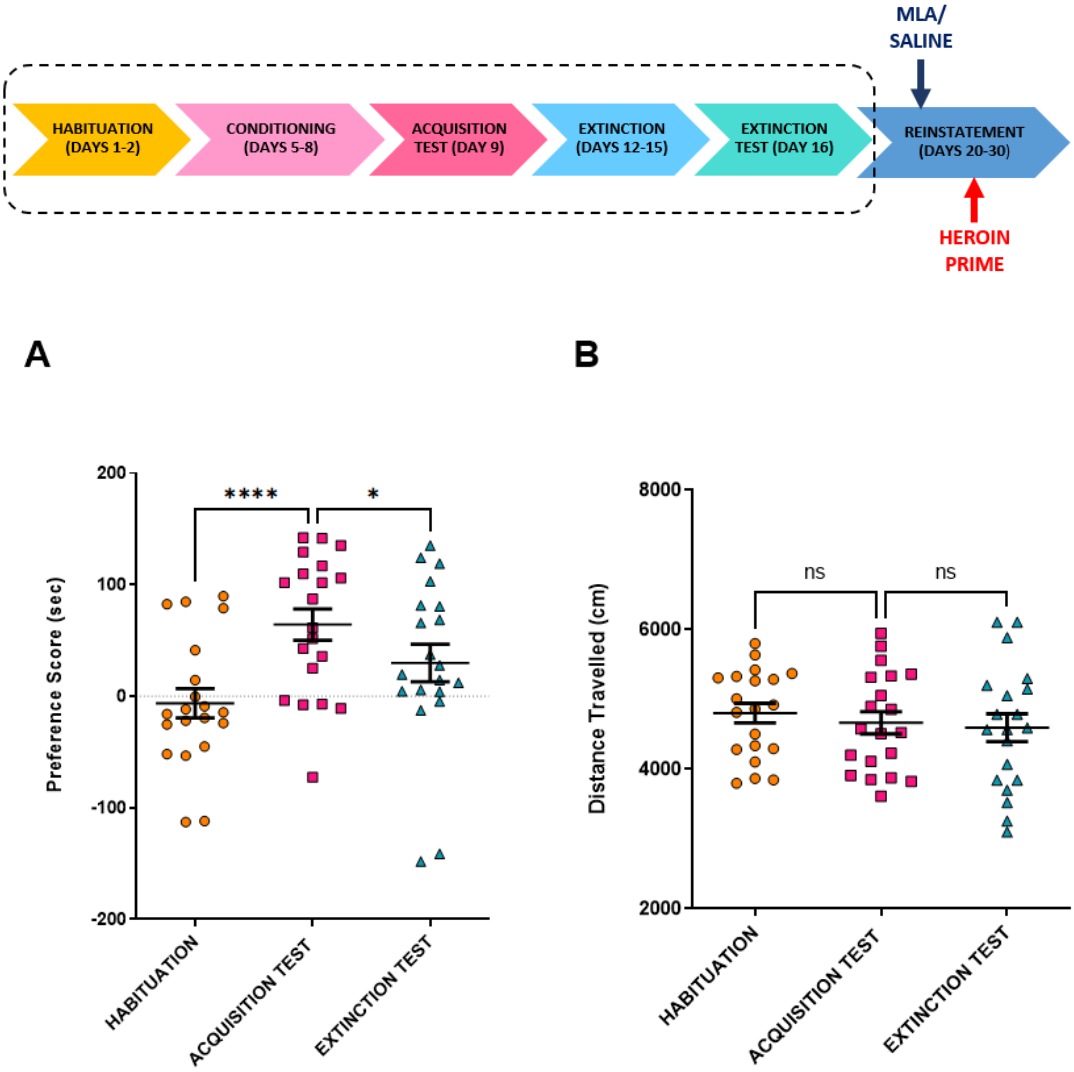

Figure 5.9– Preference scores and locomotor activity on the stages of the heroin-CPP in mice - Top: experimental timeline of the heroin-CPP including all the phases and days. (**A**) Preference scores expressed in seconds across the habituation to obtain a baseline (average from day 1 and day 2), acquisition of the preference (day 9) for the heroin-paired side, induced by a daily injection of heroin 2 mg/kg given in one compartment, and of saline (0.9% i.p.) in the other one, alternately for 4 days; and extinction (day 16), which consisted of daily saline injections (0.9% i.p.) in both compartment in both compartments alternately, for 4 days. During the habituation, acquisition test and extinction test, mice were allowed to freely explore the apparatus. Overall, mice significantly acquired the preference for the heroin-paired compartment, which was then significantly extinguished in comparison with acquisition test. Preference Score is expressed in seconds (sec). One-way ANOVA with Dunnett's Multiple Comparison Test (*post hoc* analysis preference test vs habituation and acquisition test vs extinction), p****<0.0001, p*<0.5. n=20. (**B**) Total distance travelled (cm) along the CPP apparatus during

habituation, preference test and extinction. The analysis of the locomotor activity reported no significant difference across the CPP phases. One-way ANOVA with Dunnett's Multiple Comparison Test (*post hoc* analysis preference test vs habituation and preference test vs extinction), n=20. Data All test sessions were performed in drug free state and tracked via Ethovision XT. Data points are individual mice responses with mean ± SEM overlaid.

Mice acquired statistically significant preference for the heroin-paired chamber, which was then extinguished after the extinction training (Figure 5.9 A). In this experiment, no exclusions were made, as none of the subject reported a score of >200 or <-200 seconds in the habituation phase. During the habituation subjects showed no overall preference for the drug-paired chamber, while the preference for the heroin-paired side appeared uniformly distributed, within the group, confirming the effectiveness of the counterbalanced design (Chapter 2, section 2.4.3.1). Importantly, the preference score was significantly attenuated by the extinction training, which was essential for the further assessment of reinstatement. No differences in locomotion activity were reported at each phase (Figure 5.9 B).

Since CPP had been successfully accomplished, mice were processed for reinstatement and then for the electrophysiological recordings.

5.2.2.2 The effect of MLA on heroin-primed induced reinstatement in c-Fos-GFP mice

Before proceeding with the reinstatement phase, mice were pseudo-randomised and assigned to the SALINE and MLA treatment groups, as shown in Chapter 3, section 3.2.2. This was necessary to guarantee that the preference scores during habituation, preference test and extinction test were all balanced. Figure 5.10 A shows the preference scores during the habituation, acquisition test and extinction test for mice distributed to treatments groups. Student's t-test (unpaired) showed no difference in the preference scores between treatment groups, confirming that the study was balanced.

Once mice were pseudo-randomly distributed to either SALINE or MLA group, the experiment progressed to the priming-induced reinstatement, using the same heroin-priming dose reported in Chapter 3, namely 1 mg/kg. Twenty minutes prior the heroin-primed reinstatement, mice were administered saline or MLA (4 mg/kg s.c.). Unlike the CPP protocols reported in Chapter 3 and Chapter 6, only two mice per day were

tested and then perfused, with NMDG-recovery solution (see Chapter 2, section 2.7.2) 90 minutes after the beginning of the test and the brains processed for electrophysiological recordings. Results of pseudo-randomisation, preference score and locomotor activity during the cocaine-induced reinstatement are displayed below, in Figure 5.10.

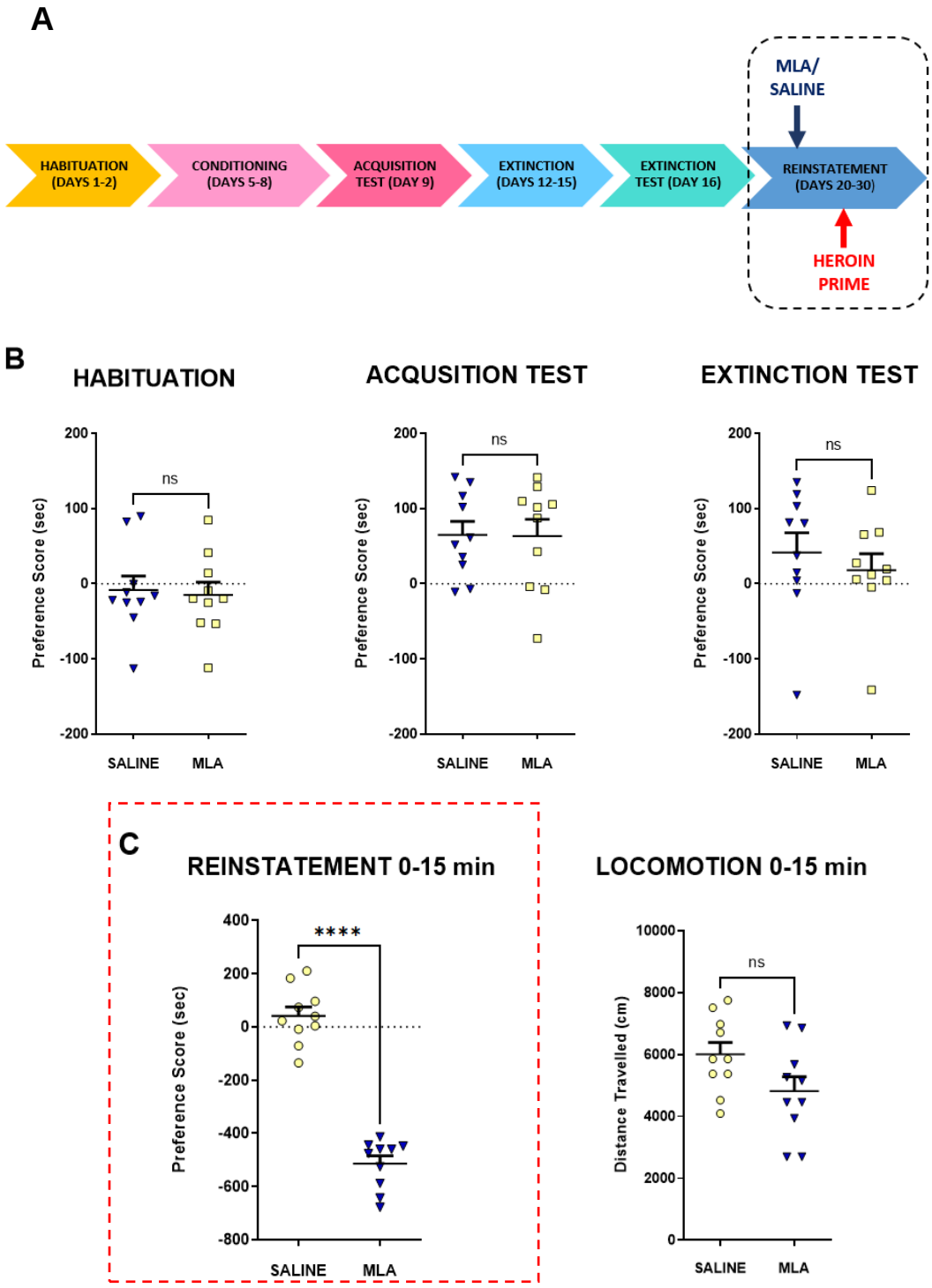

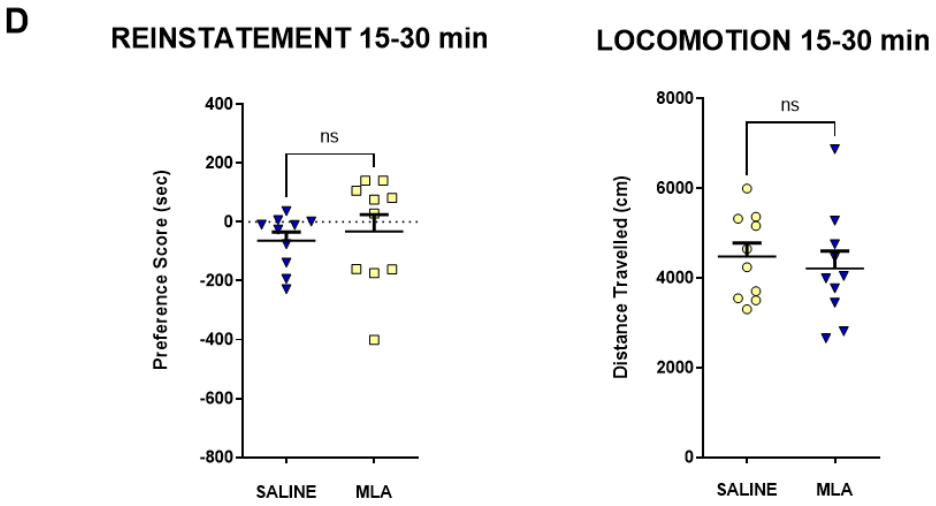

Figure 5.10 - Pseudo-randomisation of preference scores during habituation, acquisition test and extinction test of SALINE and MLA groups and preference score and locomotion from SALINE and MLA groups during the heroin-primed induced reinstatement – (**A**) Time-line of the heroin-CPP, with emphasis on the reinstatement phase. (**B**) Mice were split in two balanced treatment groups, across habituation, acquisition test and extinction test, using the pseudo-randomisation design. Unpaired Student's t-test revealed no difference between assigned groups across the experimental sessions, demonstrating that the treatments groups were balanced and not biased. SALINE=10; MLA=10. (**C**) Preference scores (sec) and Distance travelled (cm) during heroin-primed reinstatement of SALINE and MLA treatment groups. Twenty minutes before the heroin-primed reinstatement, mice were given either SALINE (0.9%, s.c.) or MLA (4 mg/kg, s.c.) and returned to the home cage until the beginning of the test. Mice were the administered a challenge injection of heroin (1 mg/kg, i.p.) and let explore the apparatus for 30 minutes. This amount of time was split in two time-bins of 15 minutes each. As reported in C, MLA treated group reported a significant avoidance for the heroin-paired arena, in comparison with SALINE treated group, which did not show reinstatement. Unpaired Student's t-test, ****$p<0.0001$ SALINE=10, MLA=10. On the right, total distance travelled (cm) across the CPP compartments during the reinstatement test, no difference between groups was reported. Unpaired Student's t-test, SALINE=10, MLA=10. The red, dashed rectangle emphasises the effect of MLA on the first time bin of reinstatement (**D**) There was no statistical difference in SALINE- and MLA-treated mice during the second time bin. Unpaired Student's t-test, **$p<0.05$ SALINE=10, MLA=10. On the right, total distance travelled (cm) across the CPP compartments during the reinstatement test, no difference between groups was reported. Unpaired Student's t-test, SALINE=10, MLA=10. Data points represent individual mice with mean±SEM overlaid.

All animals underwent CPP reinstatement with heroin 1 mg/kg after pre-treatment with either saline or MLA. As displayed in Figure 5.10, surprisingly, saline-pre-treated mice did not report a preference for the heroin-paired compartment, with an average

preference score of 42±33 seconds (n=10) which is not significantly different from these animals' habituation or extinction scores. On the other hand, MLA-treated animals reported a dramatically lower preference score, in comparison to saline control, that was highly statistically significant. Moreover, this effect was only present in the first time-bin, while there is not any significant difference during the second time-bin. This evidence is in contrast with data presented in Chapter 3 (section 3.2.2) and with other studies from our research group (Wright et al., 2019; Palandri et al., 2021), in which however c-Fos-GFP mice were not used.

After the behavioural test, mice were cardio-perfused and brains extracted, sliced and processed for electrophysiological recording, during which AMPA/NMDA ratio, RI, and PPR were investigated. Results from those experiments are reported in the following sections.

5.2.3 Investigating the effect of MLA on the AMPA/NMDA ratio

As reported in Figure 5.8, it was possible to obtain both RI and AMPA/NMDA ratio from the same cell. The experimental aim was to investigate how α7nAChRs modulate synaptic plasticity during salient memory reactivation. Specifically, we tested the hypothesis that α7nAChRs can foster synaptic adaptation that is dependent on the insertion of AMPAR onto the post-synaptic membrane of the vHIP pyramidal neurons. In fact, the cholinergic input from the septum to the hippocampus contributes to memory processing, through the activation of α7nAChRs (Letsinger et al., 2021), which induce synaptic modifications, through Ca^{2+} entrance in the membrane, including c-Fos activation. Hence, patch-clamp recordings were made from both c-Fos+ and c-Fos- neurons, to understand if this potential modification was correlated to c-Fos activation. This approach is very useful to selectively target behaviourally activated cells, in order to reduce the variability due to the direction in which vCA1 neurons project to, sustaining different parallel functions and masking the effect under investigation.

As mentioned in section 5.2.1 data for the AMPA/NMDA ratio were analysed by using two different approaches, in order to verify the presence of a clear effect.

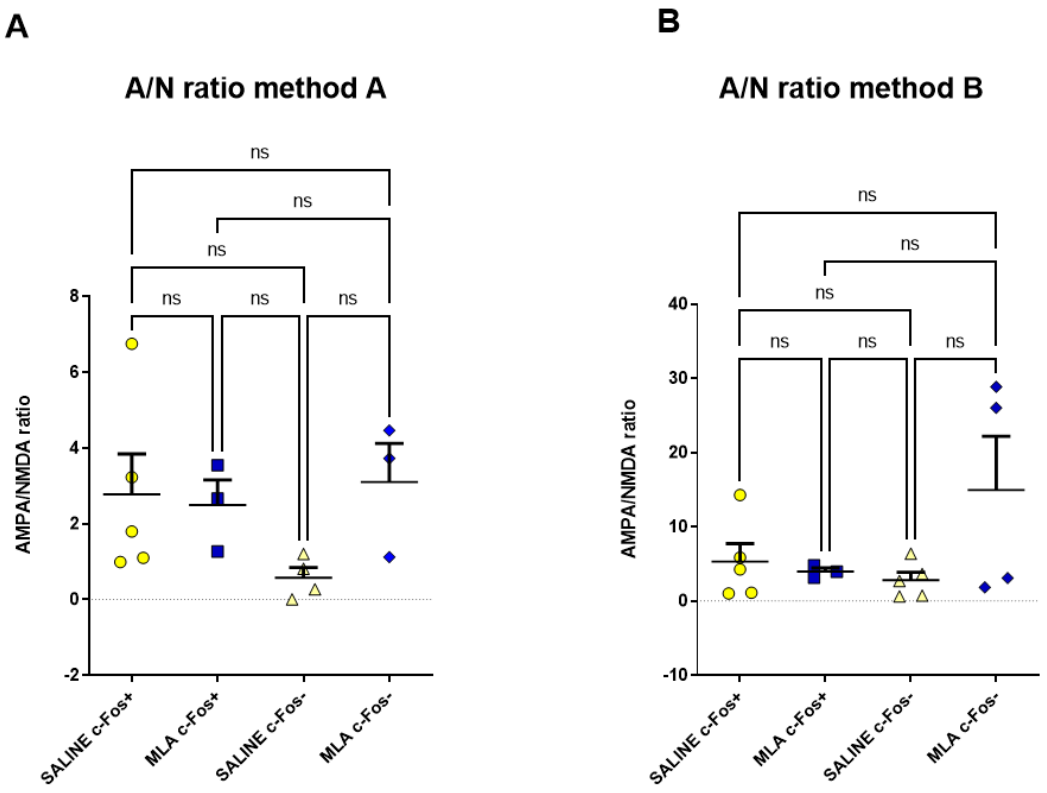

Figure 5.11 - Different approaches to analyse AMPA/NMDA ratios – In both the method for analysing the AMPA/NMDA ratio the AMPAR component was isolated at -60 mV and divided by the NMDAR component, which was defined as follows: (**A**) The NMDAR current at +30 mV was obtained by subtracting the AMPAR-only current at +30 mV, from the AMPA+NMDA combined current at +30 mV, as also described by Figure 5.8. One-way ANOVA, $p>0.05$, two outliers from Grubb's test have been excluded, specifically one subject in SALINE c-Fos- and another in MLA c-Fos-: SALINE c-Fos+=5, MLA c-Fos+, n=3, SALINE c-Fos- n=4, MLA c-Fos, n=3 (**B**) The NMDAR current at +30mV was taken at 60ms after peak current. One-way ANOVA, $p>0.05$. SALINE c-Fos+: n=5, MLA c-Fos+: n=3, SALINE c-Fos: n=5, MLA c-Fos-: n=3

Figure 5.11 shows that there was no overall difference in AMPA/NMDA ratios between treatment groups, and between c-Fos-positive and c-Fos-negative neurons. The analysis of the AMPA/NMDA ratios, using method A, showed that the MLA c-Fos-group had a higher ratio than the SALINE c-Fos-, suggesting that the MLA pre-treatment might induce the insertion of AMPAR on the post-synaptic membrane in c-Fos- neurons (Figure 5.11). However, to deem this effect as real, this result should have been present also when the data were analysed with method B, which was not what is displayed in Figure 5.11 B. In addition, due to the considerable variability and

the small sample size, there are no statistically significant differences and the results here obtained do not allow the verification of the experimental hypothesis.

5.2.4 Rectification index: CP- AMPAR detection in c-Fos+ and c-Fos- neurons

Calcium-permeable AMPARs are involved in modulating different types of synaptic plasticity-LTD dependent, such as LTP1 and LTP2, priming CaMKII and PKA respectively, according to Park and colleagues (2018) (Park et al., 2018). There is a large amount of evidence sustaining the idea that CP-AMPARs are a neural substrate for both opioid and cocaine-context association, in hippocampus and NAc (Billa et al., 2010; Xia et al., 2011; Shukla et al., 2017). On this basis, we investigated if heroin-primed induced reinstatement could induce the insertion of CP-AMPAR on the neurons from vCA1 and that the pre-treatment with MLA could alter this effect, if present. Recordings were made from both c-Fos+ and c-Fos- neurons, to see if this effect is more specific in behaviourally activated neurons. To measure the presence of CP-AMPA, the evoked AMPAR component was isolated and then compared at -60 mV and at +30 mV.

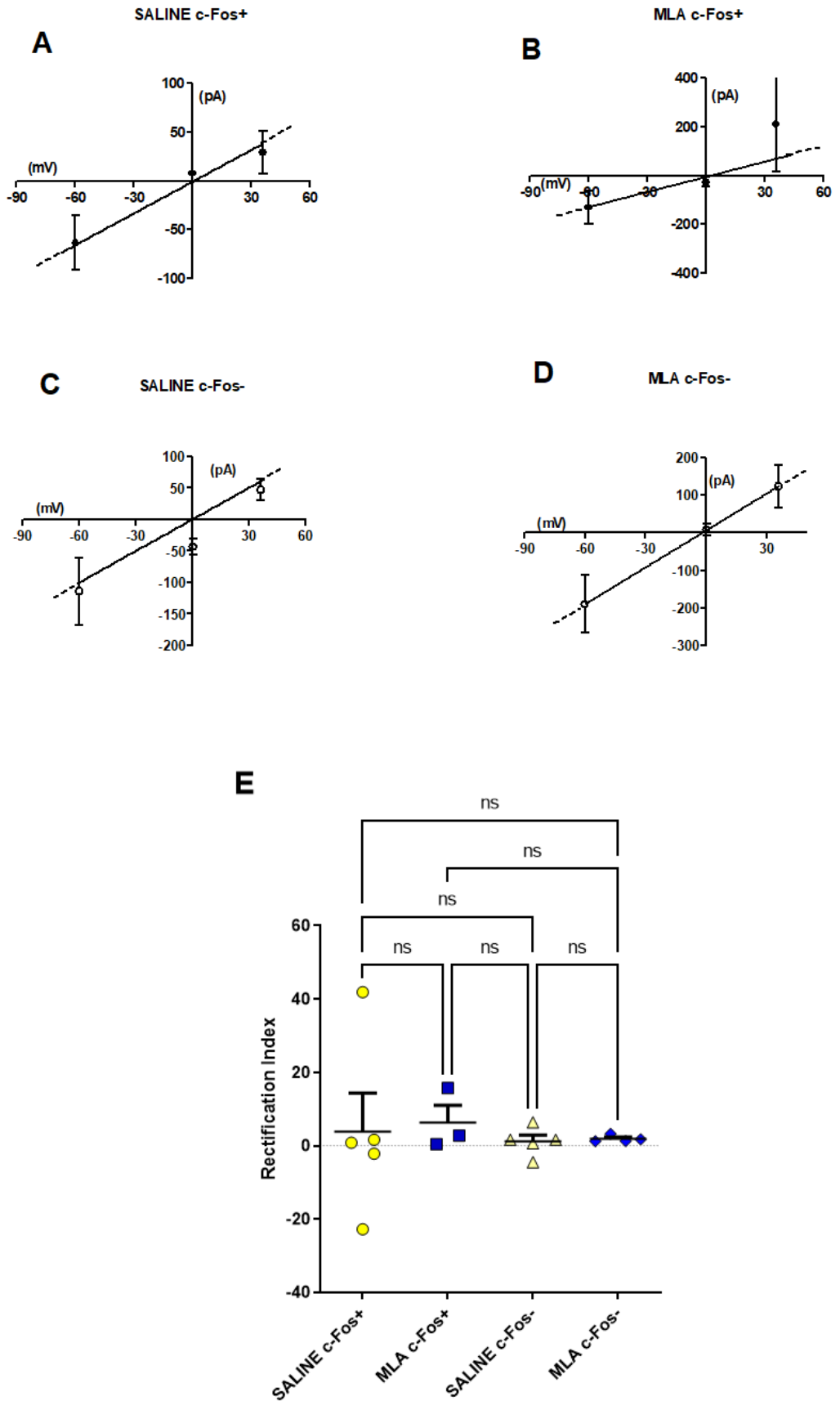
SALINE c-Fos+
A
100
(pA)
50
(mV)
-90
-60
-30
30
60
-50
-100
MLA c-Fos+
B
400
(pA)
200
-90
(mV)
-60
-30
30
60
-200
-400
C
SALINE c-Fos-
100
(pA)
50
(mV)
-90
-60
-30
30
60
-50
-100
-150
-200
D
MLA c-Fos-
200
(pA)
100
(mV)
-90
-60
-30
30
-100
-200
-300
E
ns
ns
ns
ns
ns
ns
60
40
20
0
-20
-40
Rectification Index
SALINE c-Fos+
MLA c-Fos+
SALINE c-Fos-
MLA c-Fos-

Figure 5.12 – AMPAR rectification index from c-Fos+ and c-Fos- neurons of both SALINE- and MLA-treated mice – Above, I-V curves representing AMPAR EPSC evoked at -60 mV, 0 mV and +30 mV. (**A**) SALINE c-Fos+, n=5; (**B**) MLA c-Fos+, n=3; (**C**) SALINE c-Fos-, n=5; (**D**) MLA c-Fos, n=4. At least three measurements for each voltage steps were taken from each cell. (**E**) Summary results showing the RI in each group. RI was calculated by dividing the EPSC peak amplitude at -60 and +30 mV. One-way ANOVA, $p>0.05$.

Overall, there were no statistically significant changes in RI between the treatment groups or between c-Fos-positive and c-Fos-negative neurons, with the majority of neurons showing a linear rectification index, and therefore no indication of inward rectification caused by the presence of CP-AMPARs (Figure 5.12). Overall, the data showed a high degree of variability.

5.2.5 Paired-pulse ratio

The AMPA/NMDA ratio can be used to identify synapses that have undergone synaptic plasticity through postsynaptic changes in AMPAR expression. An alternative method of inducing synaptic plasticity is via presynaptic changes in the probability of neurotransmitter release (Granger & Nicoll, 2014). Neurotransmitter release probability can be assessed by measuring Paired Pulse Ratios (PPR). Rapid and consecutive stimulation of synapses can provoke a higher peak in the second post-synaptic response compared with the first one. This phenomenon is defined as paired-pulse facilitation and PPR is the ratio of the amplitude of the second peak to the first one. This parameter represents the probability of vesicular release from the pre-synaptic site, such that an increase in PPR is seen where there is a decrease in neurotransmitter release probability.

PPR was used to investigate if heroin primed reinstatement of CPP produced synaptic modifications affecting the pre-synaptic neuronal activity and if MLA could prevent these changes. Thus, patch-clamp recording from neurons in the pyramidal layer of the CA1 in the vHIP were performed under a double-pulse stimulation, in order to obtain the PPR, and then the stimulation switched to single-pulse to continue with the rest of the experiment (see above).

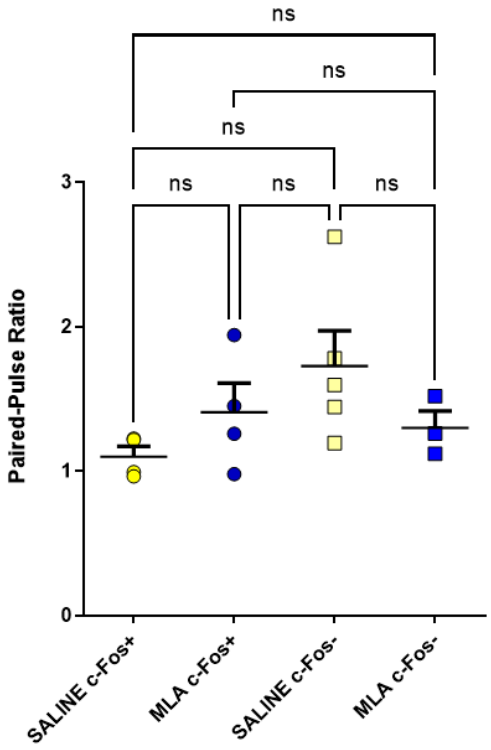

Figure 5.13– PPR of both c-Fos+ and c-Fos- neurons from SALINE- and MLA-treated mice – EPSCs evoked from -60 mV were evoked 50 ms apart and the amplitude of each peak was measured. PPR is the amplitude of the second stimulated EPSC divided by the first stimulated EPSC. Data are presented as mean±SEM. One way ANOVA, p>0.05, SALINE c-Fos+=4, MLA c-Fos+=4, SALINE c-Fos-=5, MLA c-Fos-=3.

The analysis of the PPR, reported in Figure 5.13, did not show any significant difference among treatment groups, from both c-Fos+ and c-Fos- cells. Similar to the AMPA/NMDA ratio studies, sample sizes are small.

5.3 Discussion

The aim of the experiment described in this chapter was to understand to what degree the block of α7nAChRs could affect synaptic changes induced by the heroin-primed reinstatement. Hence, we performed heroin-CPP, from habituation to reinstatement, and subsequent whole cell patch-clamp experiments in order to look at synaptic modifications in vHIP pyramidal cells *ex vivo*. Furthermore, recordings were made from both c-Fos+ and c-Fos- negative neurons by using c-Fos-GFP mice, expressing GFP in c-Fos activated neurons, in order to identify the specific neurons that have

been recruited during the expression of a particular behaviour, in this case heroin-induced reinstatement. No significant differences were seen for AMPA/NMDA ratio, RI and PPR, between animals pre-treated with SALINE or MLA before the heroin-induced reinstatement. in part due to high statistical variability. Possible explanations for unexpected results and methodological issues will be discussed below.

5.3.1 Both SALINE and MLA pre-treatments induced unexpected CPP reinstatement effects

In this experiment using c-Fos-GFP mice the outcome of the reinstatement of the heroin-CPP was different from the findings obtained with C-57 wild type mice shown in Chapter 3. SALINE-treated mice did not show any reinstatement of CPP after the heroin-primed priming, while mice receiving MLA before the priming injection demonstrated, for the first time, an apparent avoidance behaviour for the previously heroin-paired arena. A possible reason for this phenomenon could be that the memory trace was erased throughout the duration of the experiment. Due to the logistics of the experiment, only one or two animals per day were tested and sacrificed during the reinstatement phase, in order to perform patch-clamp recordings on the same day as the behavioural test. As such, some animals had a prolonged time gap between the end of the extinction phase and reinstatement. Moreover. due to this extended length of the experiment, the memory trace may have been undergone other types of changes, thereby altered the behavioural response. On the other hand, the consistency within both SALINE- and MLA-treated groups (Figure 5.11) disconfirms this explanation. Another explanation is that the priming dose of heroin did not provoke any reinstatement in this case, therefore the behavioural output could be lower than the results showed in Chapter 3, and MLA could have just downregulated the response even more deeply. Importantly, previous studies from our lab showed that the MLA pre-treatment had no effect on the reinstatement CPP in saline-primed animals, demonstrating that the MLA alone does not present rewarding or aversive effect (Palandri et al., 2021). On the other hand, rats instead c-Fos-GFP mice were used, therefore a direct comparison is not possible.

Hence, data from this experiment suggest that it is necessary to be careful to address the effect of MLA on the reactivation of reward-related memories, as other mechanisms, not here investigated, may be involved. Moreover, the MLA

pre-treatment did not affect the locomotion (Figure 5.9 B), suggesting that the difference reported in the preference score is not due to a lower exploration in MLA-treated mice.

A critical difference from this study and the ones reported in Chapter 3 and from others (Wright et al., 2019; Palandri et al., 2021) is that here, the c-Fos-GFP mouse was used instead the regular C-57 mouse. This transgenic strain of mice expresses only half of the c-Fos in comparison with wild-type mice (Barth et al., 2004). Thus, it is possible that encoding and reactivation of the reward-associated memory is weakened in c-Fos-GFP mice, because of the lower c-Fos activation, explaining why the SALINE-treated mice might not have reinstated. As reported in Chapter 3, MLA decreased c-Fos expression during heroin-induced reinstatement and this reduction could have affected the already low basal level of c-Fos, inducing and avoidance response. Possible alternatives to repeat this experiment without experiencing this down-stream issue will be discussed in Chapter 7.

5.3.2 How these experiments could be refined?

The analysis of three classical indices of synaptic plasticity: AMPA/NMDA ratio, RI and PPR, did not provide any significant results, preventing the evaluation of the hypothesis. This may be partially due to the complexity of the behavioural part of this experiment. The CPP itself is characterised by different phases, which are all characterised by relatively diverse synaptic adaptations that can be transient or permanent. Hence, the high variability reported by the analysis of these indexes may reflect the complex synaptic architecture formed during the whole experiment. Moreover, the nature of these types of recording is also characterised by a high variability. For example, the RI is obtained from a comparison between the evoked AMPAR currents across different voltage steps and that can be the reason for this considerable variability. Future experiments will provide a larger sample size in order to prevent such statistical issue and so answer to the experimental question.

Methodological problems were also encountered during the electrophysiological recordings. In fact, due to the age of the animals, NMDG-based solutions were used to perfuse animals in order to preserve cellular health (Ting et al., 2018; Sieburg et al.,

2019). However, in some brain slices, this resulted in neurons being very difficult to patch, presenting a very resistant cell surface, probably because of the NMDG itself. This limited the number of successful recordings and the achievement of a larger sample size. Future experiments should follow the approach of the “hot slicing” method (Huang & Uusisaari, 2013). In fact, recent evidence from our lab has shown that 8-10 weeks old mice present a good level of patchable cells by performing the brain slicing in 32º C aCSF. Artefacts normally obtained by low temperature may be prevented by slicing at physiological temperatures, avoiding issues in single-cell and network recordings (Ankri et al., 2014; Eguchi et al., 2020).

Thus, future experiments should be performed by using this approach, in order to obtain a large sample size and higher quality of recordings.

CHAPTER 6
HOW ARE THE PROJECTION AREAS OF THE vHIP INVOLVED IN HEROIN-INDUCED REINSTATEMENT? A NEURONAL-TRACING STUDY

6.1 Introduction

The results presented in Chapter 4 showed that pre-treatment with MLA before heroin-primed induced reinstatement of CPP decreased both drug-associated behaviour and c-Fos expression in vHIP. However, the target areas that receive input from the behaviourally activated vHIP neurons is unknown. The aim of this study was to explore and localise where the c-Fos tagged neurons in vHIP from heroin-primed reinstatement project to and how this is affected by pre-treatment with MLA. Since vHIP mainly projects to PL, NAc Shell and BLA, a retrograde tracing approach was used to investigate the involvement of those areas in drug-associated learning and memory and expand our findings to a "brain connectivity level".

There is evidence that vHIP directly projects to PL (vHIP→PL). A neuronal tracing study using the retrograde tracer Fluorogold (see below) reported a high number of vHIP→PL afferents (Hoover & Vertes, 2007). It has been reported that excitatory input from the vHIP to the PL modulates the contextual fear memory necessary for the fear response in rats (Twining et al., 2020) and it also altered contextual fear conditioning when the associative stimuli were separated in time (Santos et al., 2020). Moreover, the vHIP→PL projections have been shown to play a crucial role in fear extinction and this effect was strongly sustained by the level of activation of vHIP through optogenetic stimulation (Szadzinska et al., 2021). Overall, this supports the idea that vHIP→PL pathway is mainly implicated in fear memory modulation; however, there is also a potential role of this circuit in drug-related behaviour.

Inhibition of α-adrenergic receptors in PL, or the stimulation of both D1 and D2 receptors, promotes the extinction of an amphetamine-CPP (Latagliata et al., 2017;

Latagliata et al., 2020). PL itself is implicated in cue-induced reinstatement of both cocaine and heroin seeking in a polydrug abuse model (Rubio et al., 2019), while context-induced reinstatement of ethanol seeking is possibly due to a hippocampal input involvement (Palombo et al., 2017). Although those studies used an SA model, it is still reasonable to explore the role of vHIP→PL projections in the reinstatement of the heroin-CPP.

As discussed in the introduction (section 1.2.5), the main glutamatergic input to the NAc Shell comes from the vHIP (vHIP→NAc Shell) and this input regulates NAc activity (Britt et al., 2012) and can modulate a series of different functions. A recent study in mice reported that high-frequency activity induced canonical LTP at vHIP→NAc Shell synapses and this LTP drives CPP for a natural reward (LeGates et al., 2018), demonstrating the importance of this pathway in context-reward learning. It has also been found that the vHIP→NAc Shell enhances palatability during optogenetic photo-stimulation time-locked to consumption (Yang et al., 2020). Photo-stimulation of vHIP input was sufficient to induce the conditioning for flavour preference, while its inhibition prevented sucrose-driven flavour preference conditioning, in mice, suggesting that this pathway regulates the hedonic process (Yang et al., 2020). Chronic exposure to ethanol provoked alterations of the vHIP→NAc Shell synapses, in particular at MSN in the NAc expressing D1 receptors, inducing the insertion of Ca^{2+}permeable AMPA receptors, promoting ethanol consumption (Kircher et al., 2019).

This evidence supports the idea that vHIP→NAc Shell projections are deeply implicated in processing different features of reward. However, vHIP→NAc Shell is also thought to regulate spatial and contextual information to the NAc, linking this information to the presence or absence of reward (Van Der Meer & Redish, 2011). Hence, the vHIP→NAc Shell projections perform a crucial role in context-reward associations and context-induced relapse. The functional role of this pathway during the reinstatement of heroin-CPP will be explored here, as well as the impact of the blockade of α7nAChRs during this behaviour.

Direct connections from the vHIP to BLA (vHIP→BLA) have also been identified. Orsini and colleagues (2011) reported that vHIP→BLA projections, as well as projections from PL, are essential in modulating contextual control of fear after extinction (Orsini et al., 2011). Another report showed that both vHIP→PL or vHIP→BLA projecting neurons expressed a high level of c-Fos during fear renewal, suggesting that vHIP neurons with afferents to both areas are important in synchronizing prefrontal-amygdala circuits during fear renewal (Jin & Maren, 2015). The pharmacological inhibition of vHIP and its projections to BLA reduced stress-enhanced reacquisition of nicotine SA in rats, underlying the key role of vHIP→BLA connectivity in modulating stress-induced relapse (Yu and Sharp, 2015). Overall, BLA is thought to modulate reinstatement of drug-seeking. For instance, the blockade of D3 receptors in BLA, prevented the cue-induced reinstatement of nicotine SA (Khaled et al., 2014). Interestingly, it has been found that there are different neuronal ensembles in the BLA underlying memories for nicotine CPP or SA and those ensembles can be also reactivated by priming injections of nicotine (Xue et al., 2017).

There is a large body of evidence that the cholinergic input from basal forebrain to the local nicotinic receptors, including α7nAChRs, play a critical role in regulating physiological homeostasis of the BLA and its functions (Sharp, 2019). Thus, the involvement of vHIP→BLA projecting neurons during heroin-induced reinstatement, and modulation by α7nAChRs, will be explored in this chapter.

As described in Chapter 1 (section 1.2.9), c-Fos expression is a marker of neuronal activation and can be used as a neural correlate for several types of behaviour. From a methodological perspective, it can be co-labelled with different markers to identify different patterns of neuronal activation after an experimental manipulation (McReynolds et al., 2018). This approach is particularly useful for characterising neuronal pathways during a specific behaviour and, to do so, retrograde tracers can be used. When infused into a specific projection area, these molecules are taken up by the axon terminals and are retrogradely transported back to the cell body, from where the neuron projects. With this approach, it is possible to quantify the co-localization

of the retrograde tracer signal and c-Fos expression and analyse the activation pattern (Figure 6.1).

Following local intracerebral injection of retrograde tracer(s), and then behaviour, brain regions are analysed and processed for c-Fos expression, via immunofluorescence. Co-localisation with the retrograde tracer(s) is assessed microscopically. The percentage of co-labelled neurons indicates the rate of activation for that specific pathway.

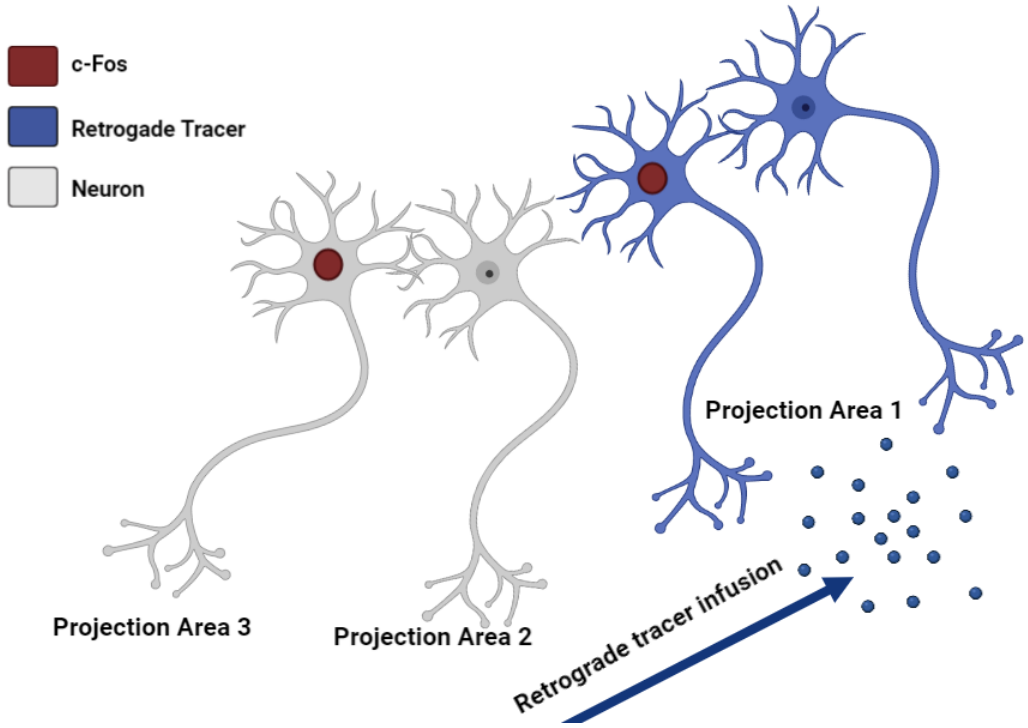

Figure 6.1 – Combining c-Fos and retrograde tracing labelling during a specific behaviour – Example of co-labelling of c-Fos (red) and a retrograde tracer (purple). The double-labelled neuron is an example of neuronal activation and project to a specific brain target, in this case the Area 1, while the neuron projecting to Area 2 is not behaviourally recruited, as there is no c-Fos activation. The other neuron coming from Area 3 is recruited to the observed function but does not project to the same area of the first neuron. (Adapted and modified from McReynolds et al., 2018)

There are several types of retrograde tracers. For this work, cholera toxin subunit B (CTB) and Fluorogold (FG) have been used. New generation CTBs conjugated with Alexa Fluor fluorescent dyes are available, making it possible to identify multiple pathways by fluorescent microscopy. This tracer is compatible with immunohistochemical approaches and other retrograde tracers, such as FG (Yao et al.,

2018). Retrogradely transported CTB is kept in vesicles and appears granular in the soma and therefore does not provide details about the morphology of the cell (for review, see Conte et al., 2009). Even accepting this limitation it is a valuable tool because conjugated CTB transports rapidly, between 2 and 7 days, and has low toxicity (Lanciego & Wouterlood, 2020).

FG is a fluorescent inorganic compound and easily viewable with florescent microscopy, usually with the 'DAPI' fluorescent microscope channel (excitation: ~380 nm / emission: ~450 nm). After absorption into the nerve terminals by fluid phase endocytosis, FG is then transported retrogradely to cell bodies in vesicles and accumulates in the cytoplasm, where it remains detectable for months and is photo-bleach-resistant (Lanciego & Wouterlood, 2020). Considering those advantages, CTB and FG were selected for the experiment documented in this chapter.

The aim of this chapter was to investigate the involvement of the main projecting areas of the vHIP, namely PL, NAc Shell and BLA, during heroin-primed reinstatement of CPP in mice pre-treated with SALINE or MLA. Mice were trained to acquire heroin-CPP, followed by extinction, and then underwent surgery for intracerebral delivery of tracer ligands. After recovery, reinstatement was performed and followed by cardio-perfusion for brain extraction, to proceed with immunofluorescence for c-Fos staining, as reported in Chapter 2 (section 2.6).

6.2 Results

6.2.1 Optimisation of brain infusions of retrograde tracers

Before processing the brain samples from animals that underwent the heroin-CPP experiment, a phase of optimisation on naïve mice was performed. This was to confirm that the retrograde tracers could all be observed in sections of vHIP, and to confirm the correct coordinates for injections into the NAc Shell, PL and BLA. At this stage no other staining, such as c-Fos, was performed.

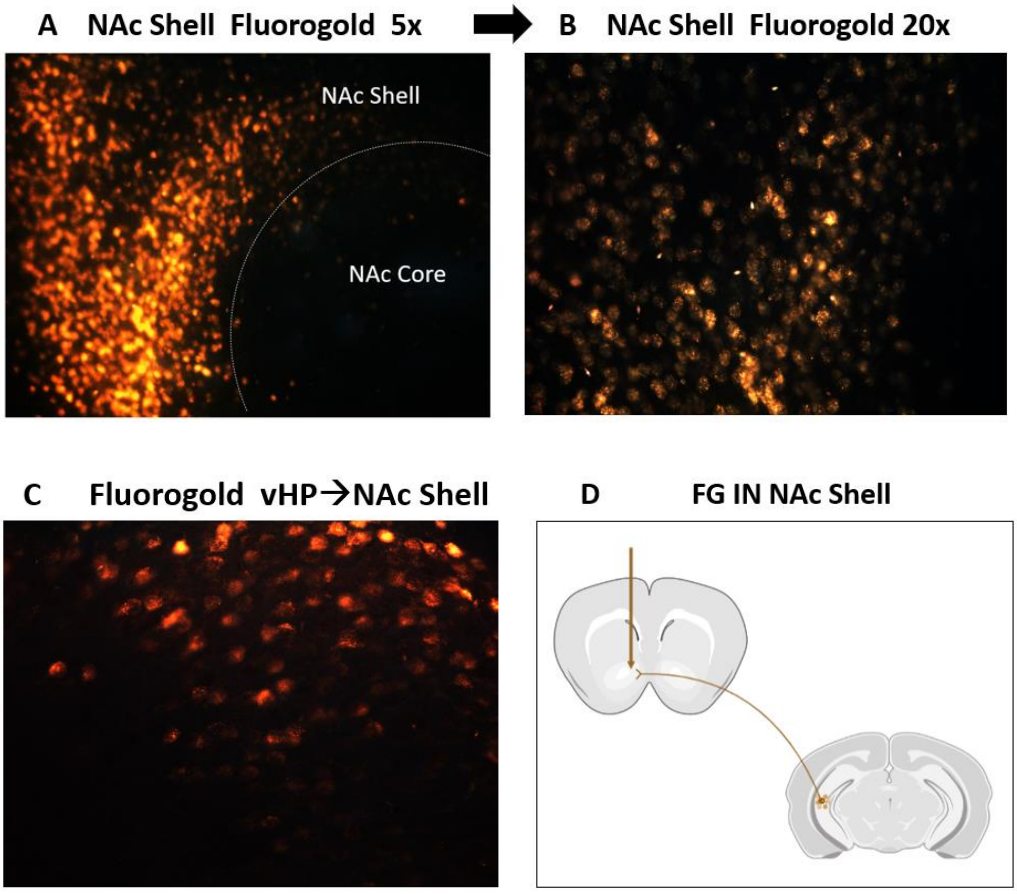

Figure 6.2 – Fluorogold (FG) staining in NAc Shell, from both low (5x) and high (20x) microscope magnification and the vHIP→NAc Shell stained with FG in naïve animal – FG 2% was infused at the flow rate of 0.1 µl/min in the NAc Shell by using the following coordinates: AP +1.34, ML ± 0.5, DV -1.6. (**A**) The staining in NAc Shell from a low magnification (5x), defining the entire region. (**B**) Neurons stained with FG in the NAc Shell. (**C**) Neurons tagged with FG in vHIP confirming that the retrograde tracer FG retro-transported to the area from which those neurons project. (**D**) A schematic diagram representing the FG infusion in NAc Shell (brown line), and retrogradely trafficking to the vHIP (brown neuron and dots).

Preliminary data of FG infusion in NAc Shell are presented in Figure 6.2. Interestingly, FG staining in the injection area was also observed. This is a useful finding because it allows verification of the correct infusion site. FG staining was also detected in ventral hippocampal CA1 neurons (Figure 6.2 C) demonstrating that the correct NAc Shell injection coordinates had been used, that FG retrogradely transported to ventral hippocampal CA1 neurons, and that it can be detected by fluorescence microscopy.

The retrograde tracer CTB 488 was also visualised. This compound is conjugated with the fluorophore Alexa Fluor 488, characterised by a bright, green-fluorescent dye with excitation ideally suited to the 488 nm of the light spectrum. To visualise the CTB 488 staining a L5 microscope channel, with a blue excitation filter, was used.

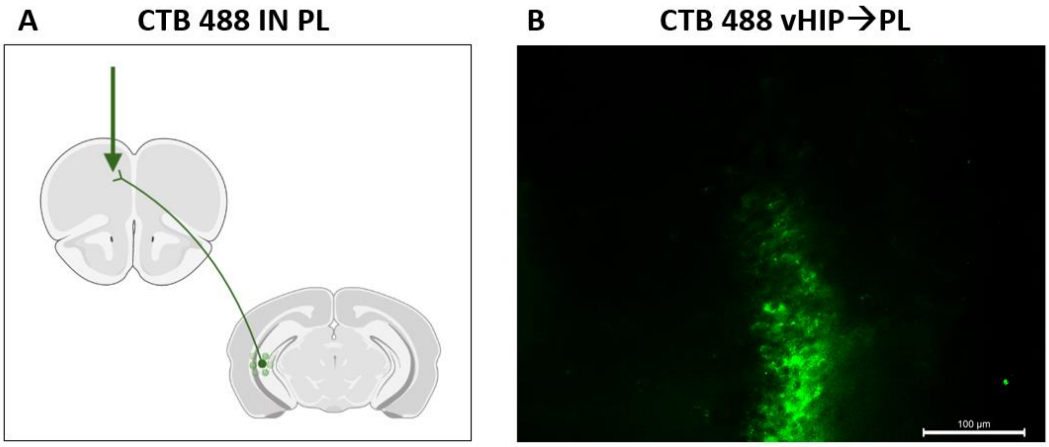

Figure 6.3 – Infusion of CTB 488 in PL and its expression in ventral CA1 in naïve animal – (**A**) A schematic diagram representing the CTB 488 infusion in PL (green arrow), and retrogradely trafficking to the vHIP (green neuron and dots). 0.5% of CTB 488 dissolved in 0.1 M PBS was infused according to the following coordinates: AP +2.8, ML ± 4.8, DV 0.5 (**B**) Ventral CA1 pyramidal neurons expressing CTB 488 tagged neurons projecting to the PL.

Figure 6.3 is an example of CTB 488 detection in vHIP. Differently from FG, no staining in the injection site was detected, so it was not possible to confirm that the injection was correctly located in the PL. However, there was robust expression of the tracer in the pyramidal neurons in the CA1 of the hippocampus.

Finally, the detection of CTB 660 was verified. However, to acquire images with this specific fluorophore (Alexa Fluor 660) a confocal imaging system (Leica LSM800) was required. While for the other fluorophores a fluorescent microscope was sufficient to detect the FG, Alexa Fluor 488 and Alexa Fluor 594 for c-Fos, in this case a fourth channel was needed, in the "far red" range of the spectrum.

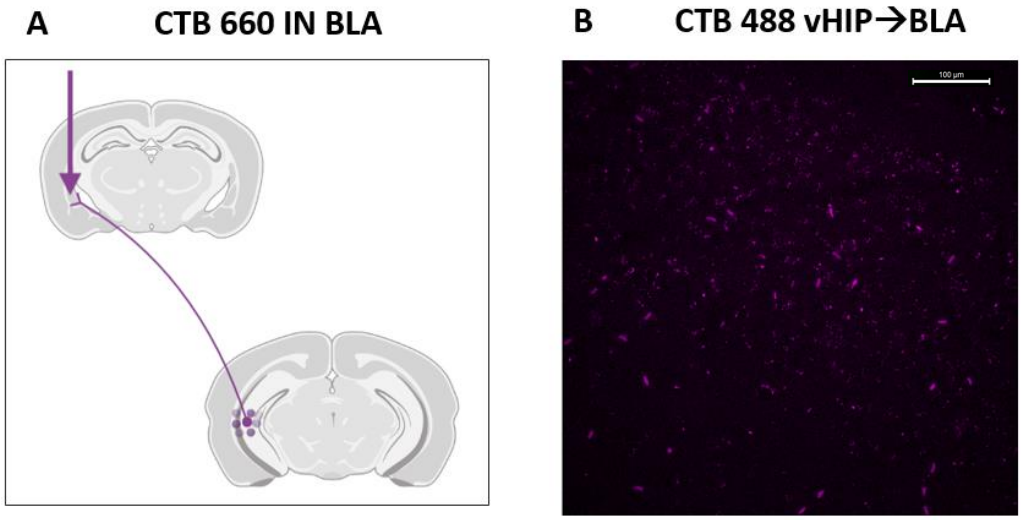

Figure 6.4 – Infusion of CTB 660 in BLA and its expression in ventral CA1 in naïve animal – (**A**) A schematic diagram representing the CTB 660 infusion into the BLA (purple arrow), and retrogradely trafficking to the vHIP (purple neuron and dots). 0.5% of CTB 660 dissolved in 0.1 M PBS was infused according to the following coordinates: AP -1.60, ML ± 3.32, DV -4.9 (**B**) CTB 660-tagged nuclei in the CA1 region of the ventral hippocampus.

Similar to CTB 488, no CTB 600 staining was found at the infusion site, so it was not possible to verify the location of the infusions. However, robust staining was found in the ventral CA1 strongly suggesting that the stereotaxic coordinates for BLA were correct (Figure 6.4 B). Therefore, by using a confocal microscope it was possible to detect the CTB 600 marked nuclei and proceed with the co-staining with c-Fos neurons, obtained via immunofluorescence.

6.2.2 Habituation, acquisition and extinction of the heroin-CPP

Male C-57BL/6 mice underwent heroin-CPP, as shown in Chapter 4 and 5. Mice successfully acquired heroin-CPP, suggesting that the heroin-dose of 2 mg/kg was effective. For this experiment, no exclusions were made based on baseline preference scores, as none of the subjects reported preference score <200 seconds.

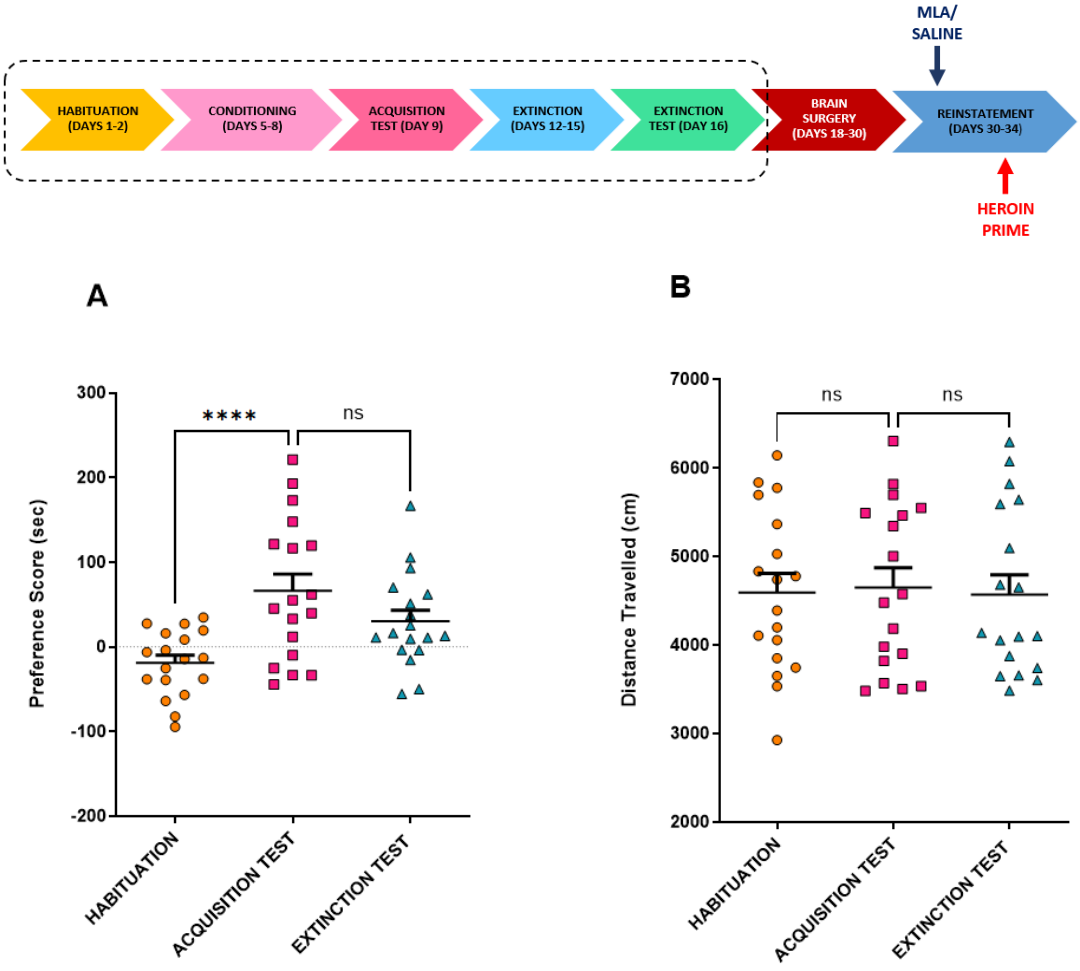

Figure 6.5 – Preference scores and locomotor activity on the stages of the heroin-CPP in mice – Above, experimental timeline of the heroin-CPP including all the phases and days. (**A**) Preference scores expressed in seconds across the habituation to obtain a baseline (average from day 1 and day 2), acquisition of the preference (day 9) for the heroin-paired side, induced by a daily injection of heroin 2 mg/kg given in one compartment, and of saline (0.9% i.p.) in the other one, alternately for 4 days; and extinction (day 16), which consisted of daily saline injections (0.9% i.p.) in both compartment in both compartments alternately, for 4 days. During the habituation, acquisition test and extinction test, mice were allowed to freely explore the apparatus. Overall, mice acquired the preference for the heroin-paired compartment, which was not significantly extinguished. Preference Score is expressed in seconds (sec). One-way ANOVA with Dunnett's Multiple Comparison Test (*post hoc* analysis preference test vs habituation and preference test vs extinction), p***<0.0001, n=18. (**B**) Total distance

travelled (cm) along the CPP apparatus during habituation, preference test and extinction. All test sessions were performed in drug free state and tracked via Ethovision XT. One-way ANOVA with Dunnett's Multiple Comparison Test (*post hoc* analysis preference test vs habituation and preference test vs extinction), n=18. Data points are individual mice responses with mean ± SEM overlaid

In contrast to Chapters 4 and 5, there was no significant difference between means from acquisition test and extinction test scores (p=0.13; Figure 6.5 A). Even though the preferences were spread across a range of positive and negative values, the overall trend was a decrease in preference for the heroin-paired compartment in comparison to the acquisition test. The outcome of the experiment was not due to differences in locomotor activity between the different CPP phases (Figure 6.5 B).

6.2.3 The impact of MLA on heroin-induced reinstatement after brain surgery

After, the extinction test, and before the reinstatement phase, mice underwent the brain surgery session (Wright et al., 2019) where specific retrograde tracers were injected locally into the PL, NAc Shell and BLA. During the 1-week post-surgery recovery, mice were pseudo-randomised and, as reported in Chapter 4 for both heroin- and cocaine-CPP, preference scores were balanced across habituation, preference test and extinction test. Mice were then assigned to either SALINE or MLA groups. Student's t-test (unpaired) reported no difference in the preference scores between treatment groups, across the CPP sessions. Moreover, individual data-points were evenly spread, confirming that this experiment was balanced. In Chapters 3 and 5, 1 mg/kg heroin as a challenge dose was effective in inducing reinstatement of heroin-CPP, hence for this experiment the same dose was used for the reinstatement test. Before the reinstatement, mice were given either saline (s.c) or MLA (4 mg/kg s.c.) 20 minutes before the priming dose of heroin.

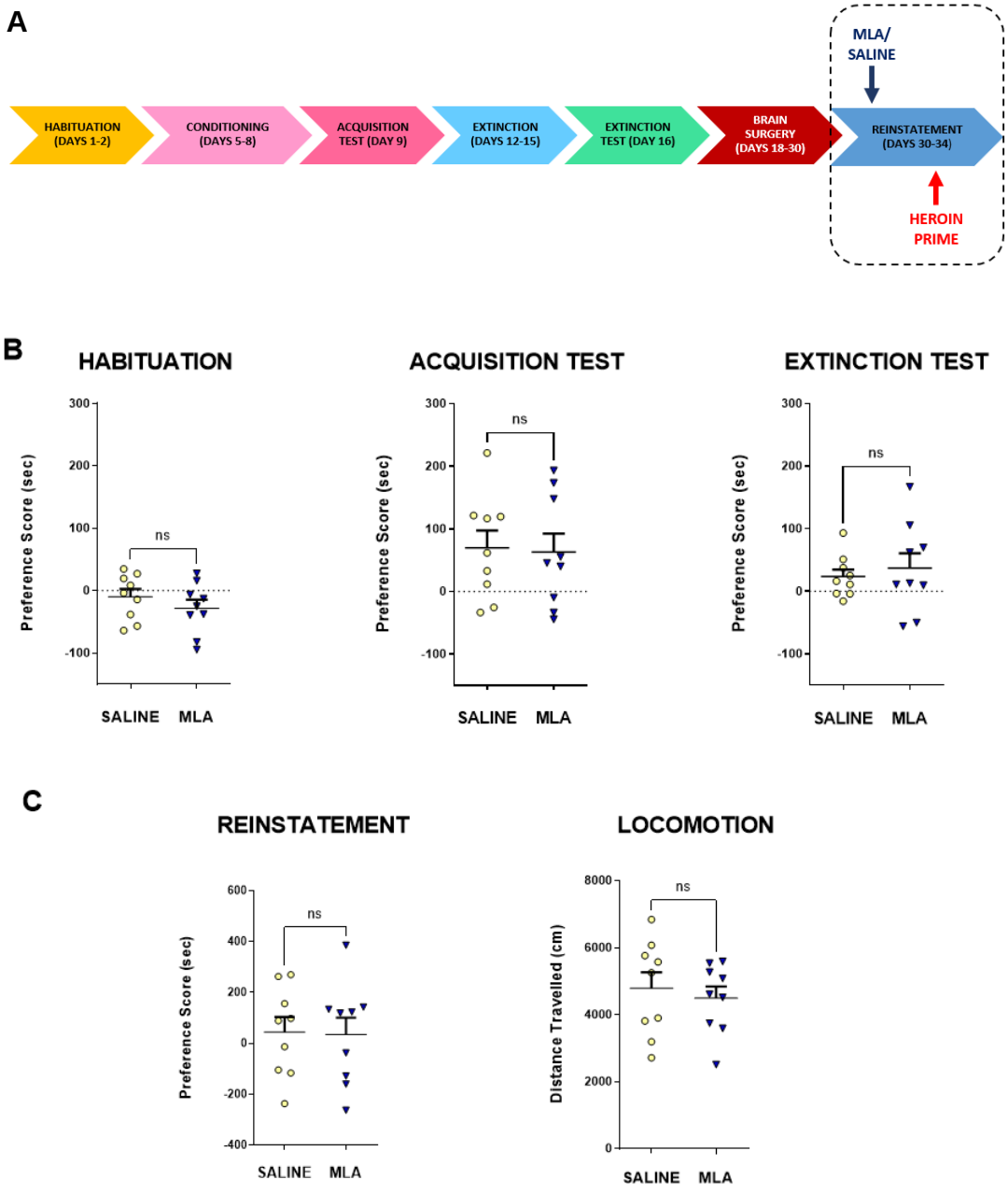

Figure 6.6 - Pseudo-randomisation of preference scores during habituation, acquisition test and extinction test of SALINE and MLA groups and preference score and locomotion from SALINE and MLA groups during the heroin-primed induced reinstatement – (**A**) Timeline of the heroin-CPP, including the surgery phase. (**B**) Mice were split in two balanced treatment groups, across habituation, acquisition test and extinction test, using the pseudo-randomisation design. Unpaired Student's t-test revealed no difference between assigned groups across the experimental sessions, demonstrating that the treatments groups were balanced and not biased. SALINE=9; MLA=9. (**C**) Preference scores (sec) and Distance travelled (cm) during heroin-primed reinstatement of SALINE and MLA treatment groups. Twenty minutes before the heroin-primed reinstatement, mice were given either SALINE (0.9%, s.c.) or MLA (4 mg/kg, s.c.) and returned to the home cage until the beginning

of the test Mice were then administered a challenge injection of heroin (1 mg/kg, i.p.) and allowed to explore the apparatus for 30 minutes. This amount of time was split in two time-bins each of 15 minutes, and only the second one was considered (see Chapter 4). There is no significant difference in the preference score during heroin-induced reinstatement of CPP between SALINE and MLA pre-treated mice. Unpaired Student's t-test, SALINE=9, MLA=9. On the right, total distance travelled (cm) across the CPP compartments during the reinstatement test, no difference between groups was reported. Unpaired Student's t-test, SALINE=9, MLA=9. Data points represent individual mice with mean±SEM overlaid.

Figure 6.6 C shows that in this cohort of mice, the heroin challenge before reinstatement did not produce any reinstatement of drug-seeking behaviour, as the preference for the heroin-paired side was not restored. The major issue with this experiment, however, was that extinction of heroin-induced CPP did not occur (unlike in equivalent experiments shown in Chapters 4 and 5). The reason(s) for this are unknown, but possible explanations are covered in the discussion of this Chapter. Due to time constraints, it was not possible to restart this experiment with a new cohort of mice. Therefore, although it wasn't possible to achieve the original aims of this experiment: to identify the specific neuronal projections from vHIP where c-Fos is expressed following reinstatement of heroin-CPP, the experiment continued with the aim of extending the pilot data (Figures 6.2 – 6.4) and providing proof-of-concept data for future experiments.

6.2.4 Double-labelling of c-Fos marked neurons and retrograde tracers

Ninety minutes after the beginning of the reinstatement test, animals were transcardically perfused with PBS 0.1 M and PFA 4% and brains removed and sectioned for immunofluorescence, as reported in Chapter 2, section 2.6. As shown in Chapter 4, vHIP neurons are involved in processing heroin-primed reinstatement and the block of α7nAChRs, through the selective antagonist MLA 20 minutes before reinstatement, prevented drug-seeking behaviour and c-Fos expression. In this experiment, no effect of MLA on heroin-primed reinstatement was observed, therefore quantification and comparison, between SALINE and MLA groups, of c-Fos+ nuclei was not performed. However, images from microscope slides were acquired, in order to assess the overlap between c-Fos- and retrograde tracer- tagged neurons. For this experiment, all the brains were coronally sliced.

Despite the success of the optimisation experiments, due to unknown technical issues, the quality of the acquired images was lower than expected and, in some microscope slides, no signal could be detected. In order to reduce total numbers of animals used, and to obtain more robust data, in most surgeries, a combination of all 3 tracers were infused into a single animal (1 in each of the 3 projection regions: PL, NAc Shell, BLA), however, in some surgeries only a single tracer was infused. Below are some examples of the images obtained.

6.2.4.1 Multiple brain infusions

The majority of animals in this study received injections with 3 different retrograde tracers in 3 different brain regions. When brains from these animals were taken and processed for immunofluorescence, unforeseen technical problems were observed which meant it was not possible to quantify the data from these experiments.

Figure 6.7 shows sample images from an animal that had undergone to brain infusions of CTB 488 in NAc Shell, CTB 660 in BLA and FG in PL, after the acquisition and extinction phases. After the surgery this animal was administered to MLA pre-treatment, followed by heroin-induced reinstatement. Finally, the brain from this animal was processed for c-Fos immunofluorescence.

The absorption emission spectra of 488 and FG should be well separated, as they are normally detected by different microscope channels. However, Figure 6.7 (A, B and D) shows that there is an overlay of those two tracers, as the activation pattern appears to be the same across Figure 6.7 A and B. One possibility is that there was an interference between the two microscope channels, or that every neuron in the vHIP projecting in the NAc Shell, also projects to PL, although there is no evidence to support this.

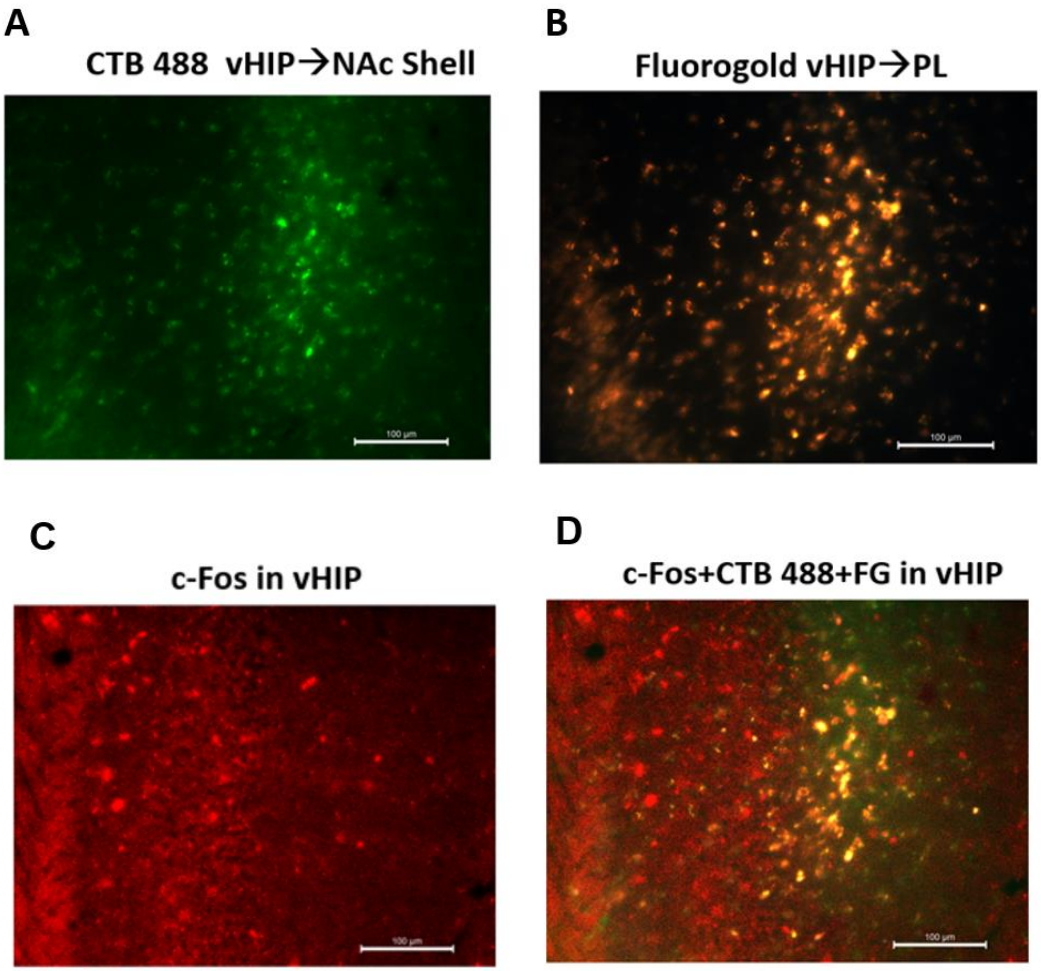

Figure 6.7 – Representative image merging of CTB 488 from NAc Shell and FG from PL on c-Fos positive cells from an MLA-treated mouse – (**A**) Neurons coloured by the CTB 488 retrograde tracer infused in NAc Shell and expressed in the vHIP. The green-coloured neurons are vHIP→NAc Shell. (**B**) Neurons coloured by the FG retrograde tracer infused in PL and expressed in the vHIP. The golden-coloured neurons are vHIP→PL. (**C**) Representative images of c-Fos activated neurons in the vCA1 of mice treated with MLA before reinstatement. (**D**) Merge of A and B showing that the FG and CTB 488 interfered and so preventing the definition of where the behaviourally activated cells (c-Fos) projects to.

The c-Fos secondary antibody is conjugated with Alexa Fluor 568 fluorophore, which can be imaged using to the N2.1 microscope channel, with a green excitation filter. Hence, a clear separation between FG and CTB 488 should have been viewable. However, the number of the neurons activated by both CTB 488, and FG was exactly the same, as shown in Figure 6.7 A and B. In addition, the pattern of c-Fos activation in Figure 6.7 A, which is spread across the ventral CA1, cannot be localised in the

same part of the microscope slide of the CTB 488 and FG, respectively shown in B and C, bringing into question the reliability of this method.
These findings were unexpected and the cause for this interference remains unknown.

The images reported in Figure 6.7 were obtained using a conventional fluorescent microscope, it was however impossible to detect the signal of CTB 660 with this type of microscopy and therefore at confocal microscope was required. Unexpectedly, CTB 660-stained neurons in vHIP could not be detected. As both of the fluorophores conjugated to retrograde tracer and to the c-Fos antibody, 660 and 594 respectively, are relatively close on the wavelength of the fluorescent spectrum, preventing a separation of the channels and the co-labelling between c-Fos nuclei and retrograde tracers.

Theoretically, each tracer was infused in a different brain area, specifically CTB 488 in NAc Shell and FG in PL, and therefore the sets of stained neurons should have been different, as projecting in two different areas. It is possible that processing the brains for immunohistochemistry to detect c-Fos expression may have provoked a destabilisation of the signal, leading to a mixed staining. Further explanations are mentioned in the discussion below.

6.2.4.2 Single brain infusion

The original experimental design was that all animals received infusions of all three retrograde tracers, but during the course of the surgeries some unexpected post-surgical complications occurred (discussed in Section 6.3 below), and the experimental design changed to single infusions per animal. As mentioned in section 6.2.1, the most reliable and strong signal was found when brain structures were infused with FG. Therefore, in a small subset of animals, FG was infused into a single brain region. An example of the merge between c-Fos and FG tagged cells is reported in Fig 6.8 below.

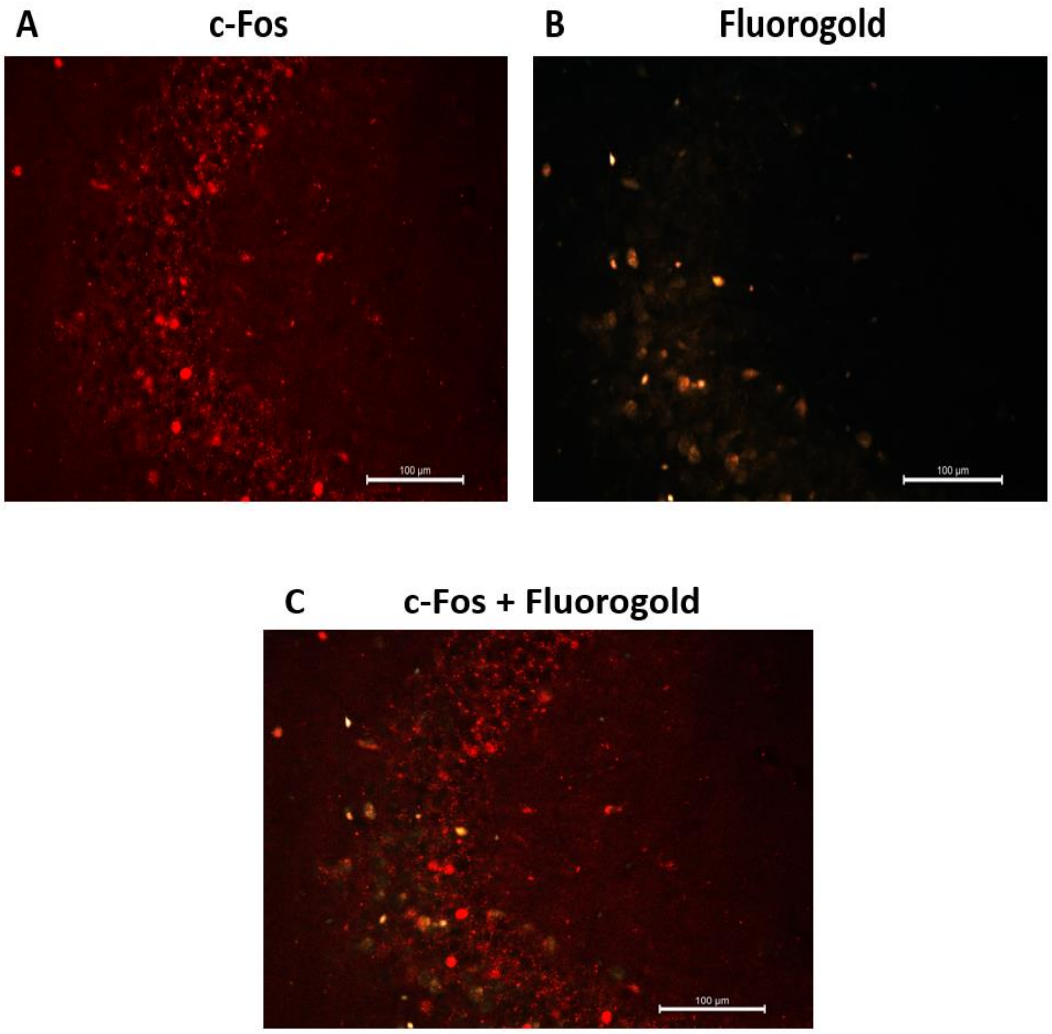

Figure 6.8 – c-Fos activated neurons and FG-marked neurons projecting to NAc Shell after heroin-primed reinstatement – (A) Representative images of c-Fos activated neurons in the vCA1 of mice treated with SALINE before reinstatement. (**B**) Neurons coloured by the FG retrograde tracer infused in NAc Shell and expressed in the vHIP. The golden-coloured neurons are vHIP→NAc Shell. (**C**) Merge of A and B showing few of the c-Fos activated neurons are projecting to the NAc Shell.

Figure 6.8 shows data taken from an animal that had FG infused into the NAc Shell, then underwent heroin-primed CPP reinstatement with a SALINE injection 20 minutes prior to the priming injection. In this case, this animal received just a single fluorophore injection, in order to reduce surgery time and so possible post-surgery complications. The original experimental design was that all animals received infusions of all three retrograde tracers, but during the course of the surgeries some post-surgical complications occurred, and the experimental design changed to single

infusions. This figure demonstrates that in ventral CA1 there are some neurons that project to the NAc Shell, as shown by the FG staining (Figure 6.8 B), as well as cFos-positive neurons (Figure 6.8 A). This microscope image suggests that the two different microscope channels (N2.1 for c-Fos and UV for FG), did not interfere with each other, and allowed imaging that distinguished between c-Fos-positive and FG-positive neurons, at least in animals that only received intracranial infusions of a single retrograde tracer. There is also limited overlap between c-Fos and FG suggesting that c-Fos positive neurons in the vHIP after heroin-primed CPP reinstatement do not project to the NAc Shell.

6.3 Discussion

The aim of this set of experiments was to explore how connectivity between vHIP and its target areas, which specific neuronal pathways are activated during drug-primed reinstatement of heroin CPP and how they are affected by pre-treatment with MLA. It was the first attempt to perform this type of experiment in our laboratory. The data reported here show that this technique may be viable, but it required further refinement and optimisation.

6.3.1 Heroin-CPP and surgeries

The failure of the behavioural part of this study compromised the purpose of this experiment. The fact that data from the heroin-CPP showed no extinction and reinstatement in the SALINE group makes it impossible to draw a comparison with MLA-treated mice. Overall, the behavioural data appeared to be highly variable. The cause of this is not currently known but there are two possibilities.

One possibility is that the during the course of experiment, I noticed that there were issues with the CPP boxes themselves. In some boxes the patterned wall veneers had started to peel off. Subsequent analysis of the videos suggested that mice spent time interacting with these patches of wall, therefore having a considerable impact on time spent in each compartment, masking the true preference scores. As mentioned previously, due to time constraints it was not possible to restart this experiment with a new cohort of animals, having rectified the issues with the CPP boxes themselves.

A second possibility is that the surgical procedure affected the data from the CPP component of this experiment. The surgeries were performed between the extinction and reinstatement test, and this long interruption between the extinction test and the reinstatement test, may have compromised the CPP memory trace. However, similar experiments have been performed in our lab where rats underwent surgery for cannula implantation between opioid-CPP extinction and reinstatement (Wright et al., 2019), and reinstatement was not affected by the surgery. There are, however, significant differences between the experiment described in this Chapter and that described in Wright et al. Firstly, in this study, mice were used whereas rats were used in Wright et al., 2019. Secondly, in this study animals received acute injections of fluorescent tracer during surgery, whereas in Wright et al chronic indwelling cannulae were implanted during surgery. However, both FG and CTB have been reported to not to induce neural damage or general toxic effects (for review see Conte et al., 2009; Saleeba et al., 2019). Finally, in Wright et al, cannulae were implanted into a single brain region (dHIP, vHIP or mPFC) in each animal whereas in the majority of surgeries in this study each animal received an injection into 3 different brain regions (PL, NAc shell, BLA).

6.3.2 Co-label retrograde tracing and c-Fos

During an initial optimisation phase, each tracer was infused singularly in BLA, PL and NAc Shell, and their expression in the vHIP was assessed as successful. However, the co-localisation with c-Fos activated neurons was not possible because the c-Fos signal was barely detectable. The reason(s) for this is not clear but one possibility is that it was caused by the difficulty in focusing during image acquisition due to the absence of fluorescent staining for neuronal cells. The immunofluorescence experiments reported in Chapter 4 were all performed using an antibody against the neuronal marker protein, NeuN, as well as anti-c-Fos antibodies. Using a secondary antibody conjugated to the fluorophore Alexa Fluor 488, NeuN-positive cells can be easily seen in the green channel. Normally, the NeuN signal is very clear and requires minimum times of exposure, around 1.5 seconds, and it allows optimal focusing. Once the “green neurons” have been localised, the microscope filter cube is switched to the red channel, and exposure time is increased, to see the “red c-Fos nuclei”. However, for this experiment the green secondary antibody for detecting neuronal cells could

not be used, as the same channel was required for the green CTB 488. It may be the reason why the c-Fos signal appeared to be weak, and therefore future experiments should consider the use of this antibody.

During the course of this experiment, post-surgery complications were experienced. Following discussions with the Named Animal Care & Welfare Officer, Named Veterinary Surgeon and Home Office Inspector, the experiments continued but the protocol changed so that an individual animal had retrograde tracer infused into 1 brain region (Section 6.2.4.2), rather than 3 different brain regions (Section 6.2.4.1). Although the number of animals that received a single tracer infusion is very small, Figure 6.8 shows initial evidence that with a single tracer infusion it may be possible to observe colocalization between c-Fos and retrograde tracer, although further experiments are required to determine this.

Overall, this experiment brought a new insight in the lab. In fact, through the optimisation of this approach, other studies in the lab have been planned, building on these initial findings, and therefore helping to expand the goals of our research.

CHAPTER 7
DISCUSSION AND CONCLUDING REMARKS

7.1 Summary of findings

This research project has been performed using a multi-disciplinary approach, where different experimental techniques converge to answer the following questions:
Do α7nAChRs in vHIP modulate heroin-primed reinstatement of heroin-induced CPP in mice?
Is cocaine-primed reinstatement of cocaine-induced CPP reinstatement also modulated by α7nAChRs?
How do α7nAChRs impact on neuronal activation, synaptic plasticity and brain circuitry during heroin-primed reinstatement of heroin-induced CPP?

The main results reported in this thesis are:

- Systemic MLA pre-treatment before heroin-primed reinstatement of CPP significantly decreased drug-seeking behaviour and c-Fos expression in vHIP in mice (Chapter 3).
- c-Fos expression in dHIP, PL, NAc Shell and BLA was not affected by systemic administration of MLA to mice after heroin CPP (Chapter 3).
- Cocaine-primed CPP reinstatement and the subsequent c-Fos expression in vHIP were not significantly affected by the systemic administration of MLA (Chapter 3).
- Using patch-clamp electrophysiology, α7nAChRs were shown to be located post-synaptically in both vHIP and dHIP. However, their role in modulating the surrounding neural network remains to be clarified (Chapter 4).
- The contribution of α7nAChRs to regulating LTP-like modifications in vHIP after a heroin-primed CPP reinstatement is still unresolved. The analysis of AMPA/NMDA ratio, RI and PPR did not reveal any significant differences

between c-Fos^{+} and c-Fos^{-} neurons in SALINE and MLA pre-treated mice (Chapter 5).

- A neuronal tracing study demonstrated that neurons in the vHIP project to PL, NAc Shell and BLA, enabling future use of this technique to explore brain pathways involved in CPP reinstatement and other behaviours (Chapter 6).

In this final chapter, these results, their neuropharmacological significance and limitations, will be discussed in the context of the broader literature. Future experiments which may help us in answering the remaining questions will be discussed.

7.2 Measuring relapse-like behaviours with a CPP model

As reported in Chapter 1 and Chapter 3, CPP is considered a Pavlovian model of drug-seeking behaviour, in which contextual stimuli can gain rewarding properties when associated with a reinforcing drug. When compared with SA paradigms, CPP is more simplistic because of the absence of any volitional aspect of drug-taking, and in addition, it does not model human craving (Reiner et al., 2019). CPP however is a valuable paradigm to dissect the different aspects of drug-seeking. In fact, it allows an analysis of the mechanisms that contribute to reinstatement, where reinstatement implies the recovery of conditioned responses, such as drug-seeking, and the restored learning of context-drug association, after extinction. This result presented in the current thesis demonstrated that α7nAChRs in vHIP are selectively involved in modulating heroin-induced CPP reinstatement. This confirms previous evidence for α7nAChRs in morphine- and heroin-primed CPP, extending the observation to mice, and, using c-Fos immunofluorescence, corroborates evidence for the vHIP as a selective locus for MLA's action. This may be due to the role of vHIP in processing emotional episodic memory and its interconnections with other brain areas involved in the reward system (Fanselow & Dong, 2010; McDonald & Mott, 2017). In addition, cholinergic innervation from the basal forebrain sustains memory processing via α7nAChRs which in turn regulates the hippocampal neural network and synaptic plasticity (Letsinger et al., 2021). The findings presented in Chapter 4 demonstrate that there is no apparent difference in α7nAChRs distribution across ventral and dorsal hippocampus highlighting that it might be the circuitry that defines the selectivity of

α7nAChRs in vHIP in modulating heroin-primed reinstatement rather than expression. Viewing the evidence from the scientific literature together with the results presented in this thesis, a hypothetical model of the neurocircuitry underlying heroin-primed reinstatement and the potential role of α7nAChRs will be presented. Initial studies presented in this thesis provide evidence to indicate that α7nAChRs are not involved in reinstatement of cocaine CPP. Although further experiments are required to confirm this hypothesis, this finding suggests that the role of α7nAChRs is dependent on the drug of abuse, and that reinstatement of heroin- and cocaine-CPP may utilise different neurocircuitries., a comparison between CPP and SA models of reinstatement suggests that α7nAChRs may be mainly involved in the processing of drug-context associations, which is essential in triggering reinstatement and well modelled by CPP, rather than in a broader mechanism underling relapse (Palandri et al., 2021).

7.2.1 Mechanisms underlying heroin-primed reinstatement

In Chapter 3, it was demonstrated that a single injection of MLA before heroin-primed reinstatement of CPP significantly reduced the drug-seeking behaviour, in comparison with SALINE controls. Findings from Chapter 4 showed, for the first time, that α7nAChRs are post-synaptically located in both dHIP and vHIP, suggesting that the role of vHIP in modulating reinstatement depends on its interconnections with other brain regions and how the cholinergic system, via its innervation in the hippocampal formation, activated α7nAChRs. It has been widely demonstrated that hippocampal α7nAChRs are also pre-synaptically located on interneurons and glutamatergic terminals (Griguoli et al., 2013; Cheng & Yakel, 2015) thereby influencing the entire hippocampal network and synaptic plasticity. In other words, if the GABAergic interneurons synapse directly onto a pyramidal cell, it will cause inhibition. However, if the GABAergic interneuron expressing α7nAChRs synapses onto another GABAergic interneuron then the effect on the pyramidal cells will be disinhibition (Figure 7.1). Hence, α7nAChRs can modulate the interplay within the hippocampal network, affecting the theta rhythm required for LTP. Hippocampal theta oscillations are thought to be essential in many cognitive processes (Stoiljkovic et al., 2015; Gu et al., 2020), which may include the processing of drug-associated contexts and cues. The block of α7nAChRs, through administration of MLA, may reduce the sustained excitatory transmission, occurring during the heroin-primed reinstatement, in the vHIP

and so affecting the theta rhythm required for LTP and the expression of drug-seeking behaviour.

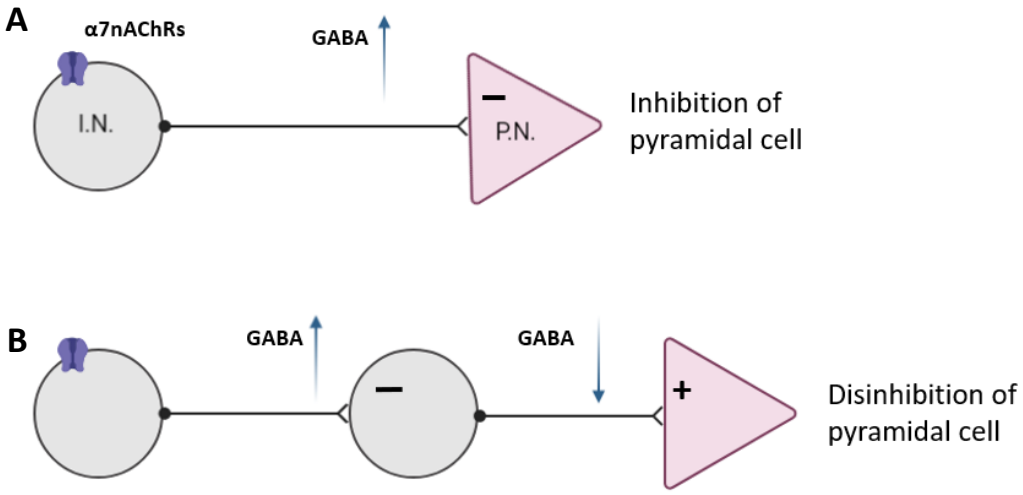

Figure 7.1 - α7nAChRs can provoke inhibition or disinhibition of the pyramidal cell – (**A**) α7nAChRs on a GABAergic interneuron (I.N.) tends to hyperpolarise (-) the post-synaptic cell. If this is a pyramidal neuron (P.N.) then its activity will be reduced and so inhibited. (**B**) If the postsynaptic cell is another interneuron that in turn synapses onto a pyramidal cell, the second interneuron will be inhibited and release less GABA so the pyramidal neuron will be disinhibited (+).

MLA given systemically can influence the neurochemical equilibrium of other brain regions which interact with the vHIP, and the neurocircuitry underlying this phenomenon has been hypothesised. During conditioning, heroin stimulates μOR on GABAergic neurons in the VTA reducing GABA release leading to disinhibition of DA neurons and subsequently to DA release in NAc. There are also other brain regions involved in reinstatement, as schematically illustrated in Figure 7.2. According to the proposed circuitry, interplay between glutamatergic, cholinergic and GABAergic transmission induces synaptic modifications thereby increasing AMPA receptor responsiveness to glutamate (Kauer & Malenka, 2007).

These changes have been shown not only in VTA, but also in NAc and PFC, depending on the phase of drug-consumption and drug-seeking (van Huijstee & Mansvelder, 2014). The hippocampus is also implicated in addiction-related memories. Thus, it has been shown that extinction training induces further changes, abolishing LTP (Portugal et al., 2014) and inducing a new and active memory trace (Bouton, 2004). An earlier

study reported that administration of the priming dose during CPP reinstatement enhanced glutamatergic and dopaminergic signalling promoting synaptic modifications underlying LTP in hippocampus (Morón et al., 2007). Importantly, research from our laboratory has shown that infusion of MLA in vHIP, but not in dHIP or mPFC, blocked morphine-induced reinstatement, highlighting the importance of vHIP in drug-seeking behaviours. Moreover, it has been proposed that a heroin challenge can enhance the cholinergic tone in the striatum and hippocampus (Pych et al., 2005; Goldberg & Reynolds, 2011). α7nAChRs would then be activated by the cholinergic input, increasing level of intracellular Ca^{2+}, at both pre- and post-synaptic sites promoting glutamatergic transmission and so enhancing post-synaptic excitability to provoke reinstatement of CPP.

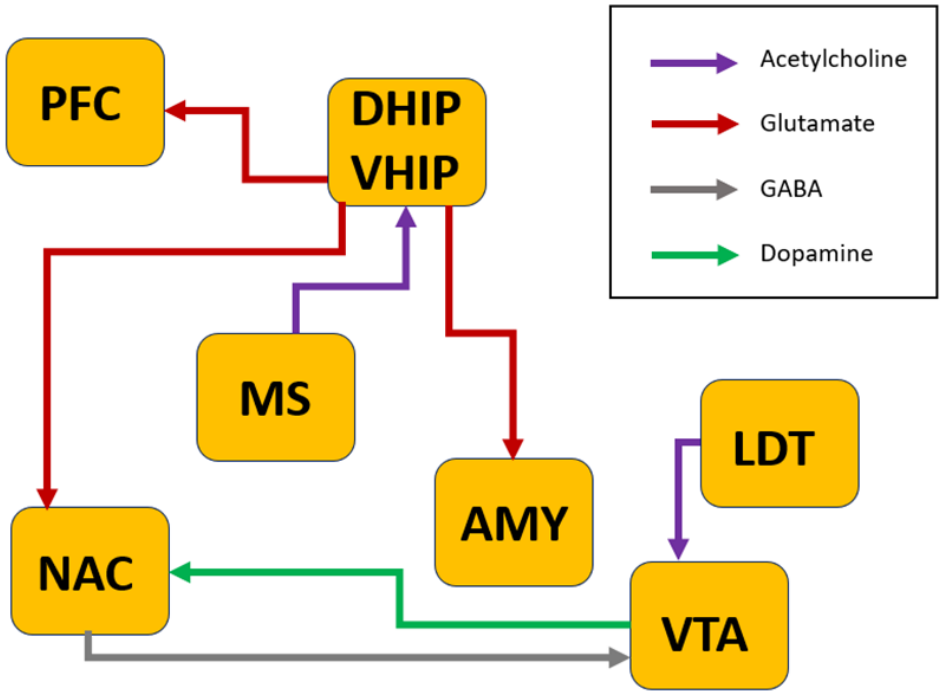

Figure 7.2 – Neurocircuitry underlying heroin-induced reinstatement – During reinstatement, the administration of a priming dose of heroin provokes an increase of dopaminergic and glutamatergic transmissions, leading to synaptic modifications which may restore LTP, previously induced by the conditioning and attenuated by extinction (not shown). The drug-related memory is then "reinstated", leading to drug-seeking behaviour. The inhibition of α7nAChRs via MLA attenuates the reactivation of the drug-associated memory and therefore inhibiting the expression of the conditioned response.

7.2.2 What about cocaine-CPP?

Processes similar to those discussed in the previous section may occur during the development of cocaine-induced CPP including reinstatement of the response even if the neurochemistry underlying cocaine and heroin seeking is different (Badiani et al., 2011). Thus, the aim of the cocaine-CPP experiment, reported in Chapter 3, was to examine whether the findings from heroin-CPP could be generalised to other drugs of abuse.

Acutely, cocaine potentiates DA transmission, directly activating the VTA→NAc pathway, as well as the excitatory glutamatergic transmission, facilitating mechanisms of synaptic plasticity not only in NAc, but also in other brain regions (van Huijstee & Mansvelder, 2014; Kutlu & Gould, 2016; Zhou et al., 2019). The cholinergic system may impact on the neurocircuitry underlying the cocaine-CPP similarly to the diagram illustrated in Figure 7.2. However, in this work MLA was ineffective in preventing reinstatement of cocaine-CPP. However, there are caveats to this conclusion. As discussed in Chapter 3, it was possible that the cocaine dose used for the reinstatement was too high, masking the effect of MLA on drug-seeking behaviour. Alternatively, it is also possible that α7nAChRs may not be involved in processing cocaine-related memories. Pastor and colleagues (2021) recently showed that infusion of MLA in mPFC, either before CPP acquisition or preference test, prevented both acquisition and expression of the cocaine-CPP. On the other hand, when infusion of MLA in mPFC occurred directly after the end of the conditioning it did not affect consolidation of the CPP (Pastor et al., 2021), possibly because this function is processed by other brain areas, such as the hippocampus or amygdala. The authors suggest that α7nAChRs may interfere with reward-processing in the NAc, as α7nAChRs are expressed in cortex layer V pyramidal neurons projecting to NAc (Gabbott et al., 2005). Hence, considering that α7nAChRs modulate synaptic plasticity and that cocaine-CPP induces synaptic changes, it is possible the α7 blockade, via MLA, could affect cocaine-induced synaptic plasticity in layer V neurons projecting to the NAc (Pastor et al., 2021). Importantly, in this report the impact of MLA on cocaine-induced reinstatement was not investigated and so, future experiments are required to certainly determine that MLA has no effect on this CPP-phase. Therefore, results from Pastor and colleagues (2021) and our lab (Wright et al., 2019; Palandri et al., 2021) suggest

that the effect of MLA might be completely different between opioids and psychostimulants. Wright and colleagues (2019) reported that MLA had no effect on acquisition or expression of a morphine-CPP, but it selectively affected reinstatement. Moreover, the work from Pastor (2021) demonstrates the importance of α7nAChRs in mPFC, as an infusion of MLA into this brain region prevented the acquisition and retrieval of the cocaine-CPP, while Wright and colleagues (2019), showed that local infusion of MLA in mPFC did not prevent the reinstatement of the morphine-CPP, showing that α7nAChRs in mPFC are not involved in opioid reinstatement. This latter finding is also in accordance results reported in Chapter 3, section 3.2.3. There was no statistical difference in c-Fos expression between MLA- and SALINE- pre-treated mice, before heroin-induced reinstatement in prelimbic cortex (PL), which is an integral part of the mPFC.

Taken together, the findings suggest that α7nAChRs are implicated in processing drug-related memories across different stages of the development of CPP, that recruit discrete brain regions not only at different stages of the establishment, maintenance, extinction and reinstatement of the response, but also depending on the pharmacological mechanism of the drug of abuse. Results from Chapter 3 suggest that α7nAChRs are not involved in cocaine-induced CPP reinstatement, as systemic administration of MLA was ineffective in blocking drug-seeking behaviour and c-Fos expression. On the other hand, this result cannot be considered conclusive, due to the relatively small sample size. Therefore, future studies, enlarging the sample size as a first step, are required to confirm these results.

7.2.3 α7nAChRs in reinstatement: CPP vs SA studies

The contribution of α7nAChRs in reinstatement has been largely unexplored, even if they are highly involved in modulating drug-context learning and memory. Moreover, depending on the type of reward task, it is possible to obtain different, sometimes opposite, results (Green & Bardo, 2020). Research findings from our laboratory showed that blockade of α7nAChRs by systemic administration of MLA prevents heroin-primed CPP reinstatement, but not reinstatement in a SA paradigm induced by combined drug-priming and cue exposure (Palandri et al., 2021). One explanation is that drug-priming requires different neural mechanisms from the cue-induced

reinstatement, as described in Chapter 1, sections 1.2.6 and 1.2.7, even if the roles of α7nAChR in those mechanisms remain to be clarified. Other studies investigating the role of α7nAChRs in reinstatement, using SA models, report variable results (see below). This evidence reflects the different mechanism underlying drug-associative learning models, and understanding this difference is essential to frame our results and propose further experiments. The most important difference between CPP and SA is that the first one is a classical Pavlovian model of drug-context association, while the latter requires an operant behaviour, in other words animals need to make an "effort" to receive the drugs, via lever pressing or nose poking. Moreover, terms like "reward", "seeking", "reinstatement" are normally associated to CPP model, whereas "reinforce", "craving" and "relapse" are more attributable to SA paradigms, highlighting different aspects of addiction. Hence, those two models explore different functions and the results obtained from those two models may not be convergent (for review, see Green & Bardo, 2020).

In respect of α7nAChRs, Liu (2014) demonstrated that pre-treatment with the α7nAChRs antagonist MLA, but not the α4β2-selective antagonist dihydro-β-erythroidine (DHβE), significantly reduced the cue-induced reinstatement of responses in a model of nicotine SA, highlighting the relevance of α7nAChRs in nicotine relapse (Liu, 2014). On the other hand, this experiment did not investigate different classes of drugs of abuse and the reinstatement was induced by cues, not drug priming, recruiting different brain pathways.

Secci et al. (2017) showed that blocking the metabolism of kynurenic acid, a tryptophan metabolite generally known as a glutamatergic antagonist, but also as an α7nAChR inhibitor (Albuquerque & Schwarcz, 2013), provoked a decrease in nicotine SA in rats. This effect which was not however reversed by the α7 PAM PNU-120596, strongly suggesting that this effect was not, in fact α7nAChRs-mediated. On the other hand, the authors reported that kynurenic acid inhibitor Ro61-8048 reduced nicotine-primed reinstatement of nicotine seeking in squirrel monkeys and cue-induced reinstatement of nicotine seeking in both rats and squirrel monkeys and cocaine-primed reinstatement cocaine seeking in monkeys. This effect was reversed by the α7 PAM PNU-120596, suggesting an α7-mediated effect for relapse-like

behaviour. Even though the authors suggested the involvement of α7nAChRs in this process, there was no clear explanation of how these receptors modulate this phenomenon (Secci et al., 2017). The veracity of this interpretation is debatable, as a recent comprehensive review casts doubt on the role of kynurenic acid as a putative α7nAChR blocker, and having any direct nicotinic actions (Stone, 2021).

The role of α7nAChRs in SA reinstatement models is still to be clarified. The clear results on the effect of MLA on drug-induced CPP reinstatement suggest that these receptors, specifically in vHIP, might be more involved in modulating, specifically, drug-context association. In other words, α7nAChRs may be selectively implicated in modulating drug-context memories triggered by drug challenges, as shown by the present CPP experiments, rather than generally impacting on craving or relapse.

7.3 vHIP, but not dHIP, is involved in processing drug-related memories

7.3.1 How do α7nAChRs in vHIP regulate neuronal activation underlying heroin-induced reinstatement?

In Chapter 3 it was shown that pre-treatment with MLA before heroin-induced CPP reinstatement decreased c-Fos expression only in vHIP, out of all of the areas where the expression of this marker was explored. As c-Fos expression is an index of neuronal activity, its evaluation in both dHIP and vHIP helps in understanding the relative contributions of those two brain sub-regions. The result supports the hypothesis that the α7nAChRs in vHIP, but not in dHIP, are involved in opioid-induced CPP reinstatement. This result is consistent with previous reports from our laboratory showing that local infusion of MLA in vHIP, but not in dHIP, inhibited the reinstatement of a morphine-CPP in rats, suggesting those two sub-regions play different roles in drug-related memories (Wright et al., 2019).

One possible explanation for this phenomenon is that α7nAChRs may be differently distributed across vHIP and dHIP, for example that α7nAChRs are expressed in vHIP but not dHIP. However, as demonstrated by the results presented in Chapter 4, α7nAChRs are expressed post-synaptically in both those sub-regions, provoking a considerable inward current when stimulated. A crucial feature of α7nAChRs is their interaction with the glutamatergic system (Cheng & Yakel, 2014), where they enhance

glutamate release and the consequential signalling cascades underlying the mechanisms of synaptic modifications. Once glutamate is released, it activates AMPA receptors inducing depolarisation and the subsequent release of the magnesium block on NMDA receptors, allowing Ca^{2+} influx. The increased intracellular Ca^{2+} in the post-synaptic compartment acts as a second messenger, leading to the activation of ERK/MAPK or protein kinase A (PKA) molecular pathways both of which directly activate the cAMP response element binding (CREB), which is highly expressed in the hippocampus (Tully et al., 2003; Kandel, 2012). CREB attracts particular interest, as it influences gene expression for immediate early genes, like c-Fos (Cruz et al., 2015), which is commonly used as a marker of neuronal activation in memory and learning (for review see Gallo et al., 2018). Figure 7.3 shows a possible mechanism though which the interaction between α7nAChRs and glutamatergic system may induce c-Fos expression in ventral hippocampus during heroin-induced CPP reinstatement.

c-Fos expression in projection areas of the vHIP, namely PL, NAc Shell and BLA (Britt et al., 2012; Kim & Cho, 2017; Twining et al., 2020) was also explored, to examine whether α7nAChRs in those areas have a role in modulating drug-induced reinstatement. It has been widely reported that PL, NAc Shell and BLA are involved in reinstatement of opioid-seeking behaviour (Karimi et al., 2014; Rubio et al., 2019; Madayag et al., 2019), and α7nAChRs in these regions play an important role in network excitability neurotransmission and synaptic plasticity (Pidoplichko et al., 2013; Maex et al., 2014; Udakis et al., 2016). In contrast to this hypothesis, results presented in Chapter 3 found no differences between SALINE- and MLA-treated mice in c-Fos activation in these brain regions, during heroin-primed reinstatement. The contribution of α7nAChRs in drug-induced reinstatement in these regions is still to be explored, and the current work is the first attempt investigating the role of α7 in heroin-induced reinstatement.

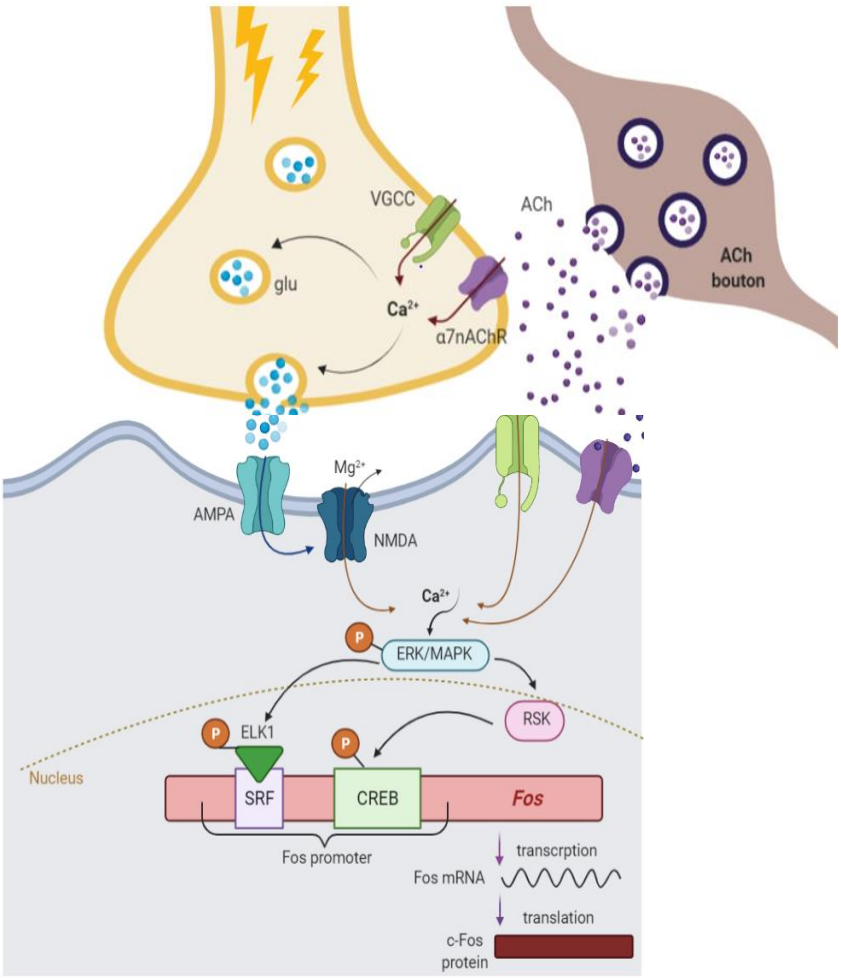

Figure 7.3 – Interaction of α7nAChRs with the glutamatergic system initiates c-Fos expression – The action potential (yellow lightning bolts) provoked by reactivation of the drug-related memory depolarises the presynaptic terminals of pyramidal neurons in the vHIP opening of the voltage-gated calcium channels and inducing Ca^{2+} influx. This action is potentiated by the activation of the pre-synaptic α7nAChRs by the cholinergic input from the septum, allowing further Ca^{2+} entrance at the pre-synaptic site, potentiating glutamate release. Once the glutamate activates AMPAR, which removes the Mg^{2+} block from NMDAR, further Ca^{2+} enters at the post-synaptic site thereby acting as a second messenger. Further Ca^{2+} influx accompanies the activation of extra-synaptic α7nAChRs, stimulated by the septal cholinergic bouton. The level of intracellular Ca^{2} will trigger ERK/MAPK via the Ras-Raf-MEKK pathway and leading to phosphorylation of Elk-1, associated with serum response factor (SRF) as well as phosphorylation of CREB via ribosomal S6 kinase (RSK). The complex Elk-1/SRF and CREB are transcription factors which, when phosphorylated can provoke transcription of the coding sequence for c-Fos. Transcribed c-Fos mRNA and the translated protein product Fos can be interpreted as an index of strongly activated neurons (image adapted from Cruz et al., 2015).

Remarkably, these results are consistent with previous findings from our laboratory. Wright and colleagues (2019) showed that AMPA binding measured by autoradiography was increased exclusively in the vHIP after morphine-induced CPP reinstatement in mice, and this increase was significantly attenuated by pre-treatment with MLA (Wright et al., 2019). Taken together, these results highlight the interplay between α7nAChRs and glutamatergic signalling within the vHIP, during opioid-induced CPP reinstatement.

7.3.2 Beyond c-Fos: other IEGs involved in drug-related behaviours

As discussed in Chapter 1, IEGs are used as indirect markers of neuronal activity and they are often influenced by the rewarding effects of drugs of abuse. This project selectively investigated c-Fos activation in several brain areas underpinning drug prime reinstatement of CPP. The results showed that this response can be prevented by blocking α7nAChRs with MLA, suggesting that c-Fos plays a critical role in memory reactivation. However, c-Fos isn't the only IEG and in future studies it would be interesting to look at the effects of α7nAChRs on others such as Egr1 and Arc.

Together with c-Fos, Egr1 and Arc are associated with learning and memory, sustaining long-term memory formation and maintenance. Compared with c-Fos, Egr1 presents a different pattern of expression in the brain and mediates the function of some late-response genes implicated in neuronal events, such as growth control and synaptic modification (for review, see Gallo 2018). Depletion of Egr1, also known as zif268, provokes performance impairment over a wide range of behavioural paradigms that are dependent on different brain areas. For instance, in Egr1 mutant-mice short-term memory remained intact, while long-term memory was affected in several tasks such as taste aversion memory, object-place recognition memory, object recognition and social transmission of food preference (Jones et al., 2001; Bozon et al., 2003; Davis et al., 2010). Administration of opioids induces Egr1 expression in several brain areas such as the NAc Core and Shell, dorsal striatum and cortical regions of mouse brain, while the hippocampus was not investigated (El Rawas et al., 2009). Nonetheless, the expression of Egr1 in the hippocampus has been widely demonstrated. For example, Katche and colleagues (2012) found that fear learning in an inhibitory avoidance task required at least two waves of Egr1 in the hippocampus,

which also initiated the mechanisms of LTP (Katche et al., 2012). it has also been reported that isoflurane exposure adversely affects subsequent fear memory formation in mice, reducing also the Egr1 expression in the hippocampus (Yang et al., 2017).

The cytoskeletal protein Arc is believed to be involved in consolidation of several types of memory. Differently from c-Fos and Egr1, Arc codes for synaptic proteins and is an effector for the brain-derived neurotrophic factor (BDNF). Importantly, the formation of new synapses and the maintenance of old ones are sustained by Arc, due to its involvement in mechanisms of synaptic plasticity such as LTP and LTD and it is also thought to be implicated in experience-dependent dendritic reconfiguration (for review, see Gallo 2018). From a behavioural perspective, increased Arc levels have been found in hippocampal regions following Morris water maze and fear conditioning (Lonergan et al., 2010; Barry et al., 2016). Another study reported that the inactivation of the dorsal CA1 inhibited the Morris water maze performance which was also associated to a reduction of the expression of Arc in the retrosplenial cortex (Kubik et al., 2012). Guzowski et al. (2006) showed that Arc expression in CA1 neurons correlated with the recency of behavioural history of the animal. In fact, when the animals were exposed repeatedly to the new context, Arc expression in the CA1 region was diminished (Guzowski et al., 2006). Furthermore, Arc expression is also elicited by the consumption of drugs of abuse. An early report showed that cocaine infusions can increase both Fos and Arc mRNA levels in the mesocorticolimbic regions (Samaha et al., 2004). Increased levels of Arc were observed also during cocaine self-administration, suggesting a role of Arc in neuroplastic modifications underlying addiction (Gao et al., 2017). Finally, both Egr1 and Arc were found to be upregulated in the hippocampal DG during morphine-withdrawal memory retrieval, suggesting these IEGs could be involved in the synaptic plasticity events underlying morphine-related contextual memories (García-Pérez et al., 2016).

Egr1 and Arc underpin different aspects of synaptic plasticity underlying reward and, memory and learning and they can also be expressed differently across brain regions. Thus, in future experiments, the investigation of these IEGs, in addition to c-Fos, can contribute to better understanding the neuronal activation changes observed in this work.

7.3.4 Is the dHIP also involved in reinstatement?

In this study, we found that systemic administration of MLA before heroin-primed CPP reinstatement did not affect the neuronal activation in dHIP. Conversely, as reported in Chapter 4, α7nAChRs were found post-synaptically in both dHIP and vHIP, suggesting that the region-specific effect of MLA to inhibit opioid CPP is due to differences in networks involving vHIP and dHIP rather than α7nAChR expression in those regions. On the other hand, this evidence does not exclude the possibility that this hippocampal sub-region can still be implicated in relapse-like behaviours. In fact, it has been found that the dHIP is critical for contextual representation and its inactivation impaired the context-induced reinstatement of cocaine-seeking, in a SA model (Fuchs et al., 2005). Selective block of GluR1 receptors in the dHIP prevented context-induced reinstatement of extinguished cocaine-seeking behaviour (Xie et al., 2010). Furthermore, synaptic inhibition in the dHIP has been shown to attenuate the reinstatement of alcohol self-administration, in rats, supporting the involvement of dHIP in relapse-like behaviours (Felipe et al., 2021). However, the agent used to inhibit synapses in this study was cobalt chloride, a non-selective synaptic inhibitor which is likely to have other off-targets effects.

It has been demonstrated that dHIP projections to the lateral septum (LS), quantified by identification of CTB+ neurons, showed increased c-Fos expression during context-induced, but not cue-induced reinstatement, in a SA model of cocaine (McGlinchey & Aston-Jones, 2018). The same report showed that chemogenetic inhibition of dHIP, but not vHIP, afferents to lateral septum, specifically decreased context-induced reinstatement of cocaine-seeking, underlying the importance of dHIP→LS in mediating selectively context-induced reinstatement (McGlinchey & Aston-Jones, 2018). Those studies are however all performed via SA tasks, which recruit different mechanisms in respect of α7nAChRs, as reported in section 7.2.3.

Taken together, these findings support the idea that the dorsal portion of the hippocampus is involved in different aspects of reinstatement, such as processing of the context. Accordingly, the dHIP appears to mediate spatial memory, as demonstrated by early works reporting that lesions of dHIP, but not vHIP, impaired spatial learning in maze paradigms (Moser et al., 1995; Pothuizen et al., 2004). As

reported in Chapter 1 (section 1.2.5), dHIP appears to be more connected with "navigation" functions, while the vHIP shows major connectivity with "emotional" regions. the distinct connectivity of those two sub-regions might explain the reason why dHIP and vHIP differently contribute to relapse-like behaviours. Research described in this thesis and other work from our laboratory (Wright et al., 2019) has demonstrated the importance of the vHIP in modulating drug-induced reinstatement. In this project, we have not studied context-induced reinstatement or whether α7nAChRs in the dHIP are involved in this type of behaviour. Based on the discussion above, it would be an interesting area for future research.

7.3.5 α7nAChRs in vHIP and dHIP: what does make the difference?

The different connectivity characterising the two sub-regions of the hippocampus has been explored and discussed throughout this thesis. This work demonstrated that α7nAChRs were found on the post-synaptic sites in both vHIP and dHIP, while the presence of hippocampal pre-synaptic α7 receptors in the hippocampus has been demonstrated by others (Gu et al., 2012). It is possible that there are region-specific differences in presynaptic expression of α7nAChRs taking part to the functional difference between vHIP and dHIP. ACh could be released mostly in vHIP and not in dHIP during priming-induced reinstatement, activating the two regions differently. Intracerebral microdialysis studies might be useful to explore this hypothesis; however, this technique may be not sensitive enough in terms of temporal resolution. Novel approaches such as rapid amperometric detection of cholinergic transmission or optogenetics to target and modulate a specific neuronal population (Parikh et al., 2004; Gritton et al., 2016) might be more appropriate techniques to explore this hypothesis.

The different extrinsic connectivity of both vHIP and dHIP, which involves other areas and different neurotransmitters, must be also considered. For example, it has been reported that the vHIP, but not the dHIP, can regulate neurotransmission in mesolimbic areas (Valenti et al., 2011; Kramar et al., 2017) and early reports showed that DA axons from the VTA mainly innervate the ventral portion of the hippocampus (Verney et al., 1985; Nyakas et al., 1987), emphasising the pivotal connection of the vHIP with the mesolimbic system. Moreover, serotonergic afferents in the vHIP were

found to be denser in comparison to dHIP (Gage & Thompson, 1980). These vHIP afferents have been found to be critical for in anxiety-like and goal-directed behaviour (Tu et al., 2014; Yoshida et al., 2019). On the other hand, similar level of NA innervations have been found across the hippocampal formation (Haring & Davis, 1985), suggesting that the entire hippocampal formation is involved in stress-induced responses (Osborne et al., 2015).

Finally, the relative contributions of dHIP and vHIP to context conditioning could depend on the type of contextual representation. In fact, there is evidence demonstrating that contexts characterised by spatio-temporal cues may require mostly dHIP (for review see Bannerman et al., 2004), while a context paired with non-spatial cues, such as emotional or interoceptive stimuli, may engage the vHIP (Levita & Muzzio, 2010; Bertagna et al., 2021). This evidence is in line with that reported from our lab, as mice were reinstated with a challenge dose of heroin, or morphine (Wright et al., 2019), inducing euphoria and general rewarding sensations. The aim of Chapter 6 was to explore the connectivity of the vHIP, in order to define a brain pathway underying the drug-induced reinstatement in respect of α7nAChRs. Due to technical difficulties, it was impossible to obtain robust findings from this set of experiment, except to confirm that vHIP pyramidal neurons project to PL, NAc Shell and BLA. Potential future works are discussed in section 7.4.2.

7.4 Future perspectives

Possible future experiments to extend the results obtained have been discussed throughout this thesis. In some experiments the verification of the hypothesis through new approaches for the lab could not be possible due to unexpected technical issues. However, the optimisation of new techniques has been an important step forward, not only for experiments related to this thesis, but also for other projects in our lab, helping to respond to other experimental questions aimed to enlarge scientific knowledge.
Hence, in this section alternative protocols to improve and repeat some experiments will be discussed, in order to extend the results here obtained, but also possible new experiments that can extend and enforce those results.

7.4.1 α7nAChRs and synaptic plasticity in vHIP after heroin-CPP

Previous studies have shown that α7nAChRs are present on the nerve terminals of glutamatergic neurons in the hippocampus, modulating neurotransmission when stimulated via cholinergic input. One of the aims of Chapter 4 was to explore the action of α7nAChRs in modulating glutamatergic transmission and clarify their role in synaptic plasticity mechanisms in both vHIP and dHIP. Technical issues did not allow this investigation. As discussed in Chapter 4 (section 4.3), there are other approaches to study pre-synaptic α7nAChRs and future experiments could apply these approaches to investigate possible differences in the roles of the pre-synaptic α7nAChRs in vHIP and dHIP. For example, blocking pre-synaptic α7 receptors with MK-801 or pharmacologically inhibiting AMPA receptors to examine GABAergic IPSCs and see how they are affected by a α7 agonists, and vice versa for the EPSC. In this way, it would be possible to investigate any possible difference between vHIP and dHIP in presynaptic α7nAChR expression and function.

Post-synaptic α7nAChRs would be expected to modulate signalling cascades when activated by afferent ACh volume input. This hippocampal cholinergic- glutamatergic interaction is essential for memory and learning regulation (Aigner, 1995). In this thesis the neural activity marker c-Fos was used as a possible correlate of the interplay between cholinergic and glutamatergic transmission. However, the changes observed in c-Fos expression vHIP, in SALINE- and MLA-treated mice during heroin-induced CPP reinstatement cannot be interpreted directly as synaptic plasticity modifications. Therefore, the aim of Chapter 5 was to investigate if the block of α7nAChRs during heroin-primed CPP reinstatement could have altered synaptic plasticity, measured through AMPA/NMDA ratio, CP-AMPA and PPR. However, due to technical issues and peculiar behavioural results, the investigation of these indices was unsuccessful. The c-Fos-GFP mouse is a good approach to isolate behaviourally recruited neurons, but there are more selective approaches that could be considered for repeating this experiment. Studies investigating neuronal ensembles, patterns of neurons showing coordinated firing, have demonstrated that many behaviours are mediated by just the 3% of neurons in a specific brain area (Bossert et al., 2011; Cruz et al., 2014). Neuronal ensembles, composed of c-Fos neurons and also defined as engrams, have been found in many brain regions, including the hippocampus (for review, see Josselyn et al.,

2015). An engram is defined as persistent modification in the brain that derives from a specific experience or event which could be expressed during retrieval cues, such as sensory input, ongoing behaviours or motivated actions. From a synaptic perspective, multiple changes are required for engram formation, localisation, learning. In addition, mechanisms of LTP impacting on spine morphology, have been recognised to be essential for the engram (Moser et al., 1994; Muller et al., 2000; Bosch & Hayashi, 2012). In addition, other cellular modifications have been found to be essential for the engram definition, including changes in DNA structure (Day & Sweatt, 2011), post-translational kinases, such as CamKII (Lisman et al., 2002) which enhances AMPA and NMDA function in synaptic strength (Kristensen et al., 2011), activation of IEGs, such as c-Fos and Arc (Guzowski, 2002; Horn, 2004) and alteration in hippocampal in neuronal excitability (Oh et al., 2003). Alternative strategies aimed at "capturing" the engram have been used to mark those neurons active during encoding leading to the visualization of those at time-points after initial consolidation, when the engram is more stable. Many approaches have been used to confine the tagging activity to a specific moment. In the TetTag mice genetic model, tetracycline regulates the capture of activated neurons, via a self-activating tTA–TetO system in, and the window of activity targeting is opened by withdrawing mice from a diet based on the tetracycline derivative, also called doxycycline (Reijmers et al., 2007). The target recombination in active populations (TRAP) requires genetic model of mice expressing the Cre recombinase which can be activated by tamoxifen which, when administered systemically (Guenthner et al., 2013; Denny et al., 2014). The advantage of these capture strategies is that the neuronal pattern active during memory formation is also active during the recall test demonstrating that the neurons forming an engram are supporting a specific memory.

These techniques can also be used for finding the engram in other memory phases, such as reinstatement, and then perform electrophysiological recordings from the engram neurons to investigate synaptic modifications underling a specific behaviour (Pignatelli et al., 2019). Thus, it would be promising to use one of the above approaches for future experiments, to investigate how the α7nAChRs modulate synaptic modifications underlying heroin-primed reinstatement of CPP.

7.4.2 Re-thinking and improving the neuroanatomical tracing study

The aim of the retrograde tracing study reported in Chapter 6 was to investigate the involvement of the target areas of the vHIP, namely PL, BLA and NAC Shell, and to extend the results obtained in Chapter 3. The behavioural part of this experiment was unsuccessful thereby preventing the quantification of c-Fos positive neurons.

To reduce the number of animals used, three different retrograde tracers were infused in the three vHIP projection areas, so that the tracer-tagged neurons would have been co-labelled with c-Fos activated neurons, to explore where the c-Fos activated neurons mostly project to, during heroin-primed reinstatement. However, no reliable images could be obtained from either form of CTB, therefore, the co-labelling was not possible. Unexpectedly, the three tracers did not allow a separation of each microscope channel, preventing any co-labelling study. On the other hand, in some mice, only FG was infused, which was easily visible and allowed co-labelling with c-Fos. Therefore, sole use of FG would be better for future retrograde tracing experiments, as it is visible and allows co-labelling with c-Fos neurons, as well as permitting imaging of neurons themselves with anti-NeuN antibodies (as mentioned in Chapter 6). However, this approach of only labelling one neuronal pathway per animal would require a higher number of animals overall to achieve the experimental objectives. Also, it would not allow identification of vHIP neurons projecting to all 3 brain regions – in the same brain section – as originally envisaged. To achieve this, other retrograde tracers, or changes to the protocol used here, could be considered. CTB has been shown to be successful in many publications, hence it is possible that in this case, some more dilution studies are required. Here, a volume of 0.5 nL per minute, 0.5% of CTB for 3 minutes, was infused, via infusion pump, it is however possible that this quantity was not enough to acquire a stable fluorescence signal. Alternatively, fluorescent retrobeads are also considered a good tool for retrograde tracing studies, allowing co-labelling for IEGs using immunofluorescence (Leyrer-Jackson et al., 2021) and electrophysiological recordings in tagged neurons (McGarry & Carter, 2017). Their main advantage is their resistance to fading and ability to maintain long-term labelling. Retrobeads are generally recognised as stable fluorescence dyes with minimal diffusion from the infusion site, with a precise retrograde travelling, tested as non-toxic to neuron and suitable for extended experiments (for review see Saleeba et

al., 2019). Another alternative would be to use adeno-associated viruses (AAV). For instance, infusion of an AAV9 vector, expressing Cre-dependent fluorescent marker only in hippocampal pyramidal cells in the CA2 region of transgenic mice expressing Cre-recombinase, allowed the mapping of a neuronal pathway that may be involved in learning and memory (Kohara et al., 2014). The recent development of synthetic AAV capsid that can lead to retrograde tracing with particularly high efficiency and selectivity has been described (Tervo et al., 2016). This AAV-retro capsid behaves similarly to classical retrograde tracers, such as FG, as it is compatible with small injection volumes, and is not associated with significant toxicity (Sun et al., 2019).

In summary, the wide choice of good retrograde tracers makes it worth re-designing the experiment presented in Chapter 6. the use of different fluorescent retrobeads appears to be the most promising and without requiring any transgenic model of mouse, such as Cre-recombinase strain. in this way, it would be possible to use less animals and compare the c-Fos and retrobeads co-labelling in different brain areas and within the same animal.

7.4.3 How can we further extend the current work?

This work demonstrated the pivotal relationship between α7nAChR function in vHIP and reward-related memories. There is evidence that vHIP is also involved in modulating recognition memory (Titulaer et al., 2021), The novel object recognition test (NOR) is a hippocampal-dependent task (Ledonne et al., 2018), in which rodents explore novel items and the difference in time spent in exploring the presented items is a measure of recognition memory (Cohen & Stackman, 2015). To investigate whether α7nAChRs within the vHIP are also implied in modulating spatial memory, it would be interesting to locally administer MLA directly in this area, via canula implantation, during a novel object recognition task. Modulation of α7 and α2β4nAChRs, by systemic administration of the agonists, PNU-282987 and RJR-2403, increased NOR in female rats (McLean et al., 2016). In addition, systemic administration of the α7 PAM PNU-120596 improved recognition memory and cognitive flexibility in rats (Nikiforuk et al., 2015). However, those studies are purely behavioural. Exploring the effect of MLA selectively in vHIP on this type of memory,

would clarify whether α7nAChRs are implicated in processing different types of memory.

It has been proposed that the vHIP is mainly involved in emotional regulation including formation of stress responses and anxiety (Fanselow & Dong, 2010; Strange et al., 2014). Projections from the vHIP to the amygdala, including the BLA, mediate contextual fear memory retrieval (Xu et al., 2016) and the optogenetic silencing of vHIP→mPFC glutamatergic afferents reduced anxiety behaviours measured with elevated-plus maze and open field (Padilla-Coreano et al., 2016). On the other hand, infusion of MLA in dHIP reduced anxiety-like behaviours, measured through tail suspension and forced swimming stress-models, in male but not female mice (Mineur et al., 2018). This evidence suggests that ACh transmission via α7nAChRs in the hippocampus plays a critical role in modulating anxiety-like behaviours when ACh release enhanced, as can happen during stressful tasks. This evidence prompts the idea that α7nAChRs in dHIP are implicated in modulating mood fluctuations, which are also relevant in triggering drug-seeking. Therefore, investigating the contribution α7nAChRs in vHIP in modulating aversive stimuli, for example through a conditioned place aversion or contextual fear conditioning, would be helpful to understand the involvement of α7nAChRs in processing emotional memories.

Finally, exploring sex differences is another an important factor to consider for future experiments. The above-mentioned finding from Mineur et al. (2018) is an example of how the response obtained in males and females can be different for the same type of behavioural and molecular stimulation. There is a large body of evidence showing that there are sex differences in terms of acquisition of CPP (reviewed in Pogun et al., 2017; Cullity et al., 2021), its extinction (Hilderbrand & Lasek, 2014) and reinstatement (Thanos et al., 2016). In this thesis, experiments were conducted only in male mice. Thus, exploring the effect of MLA on drug-induced CPP reinstatement in female mice is an important step to establish the impact of sex differences on the action of α7nAChRs in reinstatement.

The importance of the cholinergic system in modulating several hippocampal functions has been well studied. For example, early milestones from research in behavioural neuroscience found that lesions to the hippocampal formation provoked deficits in several types of learning and memory, including sensory discrimination, spatial learning, working memory, and conditional or contextual associations (Gray & McNaughton 1983). Rawlins and colleagues demonstrated, through complex lesions studies, that the theta rhythms in the hippocampus depend on the integrity of the medial septum (Rawlins et al., 1979). Winocur (1987) and colleagues reported that lesions in the rat hippocampus prevented the formation of Pavlovian conditioning, in which a CS predicted a shock. However, these animals showed a high conditioning to the context even when the shock was anticipated by the CS, suggesting that the hippocampus could be implicated in the stimulus choice during conditioned learning (Winocur et al., 1987). Moreover, chronic ethanol intake induced cognitive deficits in rats, showing impaired learning and performance of the radial maze. However, those impairments were restored by administration of a cholinergic agonist, and by cholinergic-rich fetal neuronal transplants in the cortex and/or hippocampus, demonstrating the key role of the hippocampal cholinergic system in learning and memory (Arendt et al., 1989).

Remarkably, the crosstalk between nAChRs and noradrenergic transmission in the rat hippocampus has been demonstrated (Kennet et al., 2012). In fact, chronic, but not acute, administration of nicotine enhanced the activity of tyrosine hydroxylase only in the hippocampus, where the most diffuse catecholamine is noradrenaline. This evidence implies the role of hippocampal nAChRs, among α7nAChRs, in modulating different classes of neurotransmitters deeply implicated in emotional responses (Gray et al., 1990). Intriguingly, it has been demonstrated that noradrenaline is profoundly implicated in regulating theta rhythms in the hippocampus. In fact, the application of minor tranquillisers such as ethanol, chlordiazepoxide and Δ9-tetrahydrocannabinol, inhibits the septally-controlled theta rhythms in the hippocampus, and this impairment could partially explain the behavioural effect of anxiolytic drugs (Gray et al., 1975). The interplay between α7nAChRs and other catecholaminergic inputs to the hippocampus could be an interesting avenue for studying conditioned memories and drug-related behaviours.

However, most of those studies do not investigate the difference between dorsal and ventral hippocampus. Therefore, considering novel approaches and early milestones exploring the complexity of hippocampus it will be possible to answer, at least in part, the questions arising from this thesis.

7.5 Conclusions

These experiments provide evidence for a critical role of α7nAChRs in vHIP in selectively processing reinstatement of heroin-CPP. This work demonstrated that the changes in c-Fos expression, a neuronal marker implicated in synaptic plasticity mechanisms, in the ventral CA1, suggesting α7nAChRs, via their Ca^{2+} permeability, take part in synaptic modifications underlying heroin-CPP reinstatement. Further experiments are required to confirm the role α7nAChRs of cocaine CPP-reinstatement and to improve and repeat experiments aimed at studying the precise role of α7nAChRs in synaptic plasticity in vHIP and the neurocircuitry underlying reinstatement. On the other hand, it is possible to suggest that MLA affects opioid-related learning, but not cocaine-related learning.

Heroin and cocaine induce important synaptic plasticity changes in the hippocampus, which may be responsible for the drug-context memories which trigger the individual to relapse. The mesocorticolimbic dopaminergic system has been massively investigated to clarify the neural basis of drug-addiction but the answers coming from those studies are not definitive, and sometimes contradictory. Therefore, the study of other neurotransmitters and receptors, such as ACh and α7nAChRs, may help us in understanding how changes in the reward circuitry, including the ventral hippocampus, contribute to reward-related memories which drive motivated behaviours.

REFERENCES

Aguilar, M. A., Rodriguez-Arias, M., & Minarro, J. (2009). Neurobiological mechanisms of the reinstatement of drug-conditioned place preference. Brain Res Rev, 59(2), 253-277. doi:10.1016/j.brainresrev.2008.08.002

Aigner, T. G. (1995). Pharmacology of memory: cholinergic-glutamatergic interactions. Curr Opin Neurobiol, 5(2), 155-160. doi:10.1016/0959-4388(95)80021-2

Albuquerque, E. X., & Schwarcz, R. (2013). Kynurenic acid as an antagonist of α7 nicotinic acetylcholine receptors in the brain: facts and challenges. Biochem Pharmacol, 85(8), 1027-1032. doi:10.1016/j.bcp.2012.12.014

Alkondon, M., & Albuquerque, E. X. (2001). Nicotinic acetylcholine receptor α7 and α4β2 subtypes differentially control GABAergic input to CA1 neurons in rat hippocampus. J Neurophysiol, 86(6), 3043-3055.

Alkondon, M., Albuquerque, E. X., & Pereira, E. F. (2013). Acetylcholinesterase inhibition reveals endogenous nicotinic modulation of glutamate inputs to CA1 stratum radiatum interneurons in hippocampal slices. Neurotoxicol 36, 72-81.

Almonte, A. G., Ewin, S. E., Mauterer, M. I., Morgan, J. W., Carter, E. S., & Weiner, J. L. (2017). Enhanced ventral hippocampal synaptic transmission and impaired synaptic plasticity in a rodent model of alcohol addiction vulnerability. Sci Rep, 7(1), 12300. doi:10.1038/s41598-017-12531-z

Alvandi, M. S., Bourmpoula, M., Homberg, J. R., & Fathollahi, Y. (2017). Association of contextual cues with morphine reward increases neural and synaptic plasticity in

the ventral hippocampus of rats. Addict Biol, 22(6), 1883-1894. doi:10.1111/adb.12547

Amador, M., & Dani, J. A. (1991). MK-801 inhibition of nicotinic acetylcholine receptor channels. Synapse, 7(3), 207-215.

Andersen, N., Corradi, J., Sine, S. M., & Bouzat, C. (2013). Stoichiometry for activation of neuronal α7 nicotinic receptors. PNAS, 110(51), 20819-20824.

Andersen, N. D., Nielsen, B. E., Corradi, J., Tolosa, M. F., Feuerbach, D., Arias, H. R., & Bouzat, C. (2016). Exploring the positive allosteric modulation of human α7 nicotinic receptors from a single-channel perspective. Neuropharmacol, 107, 189-200.

Ankri, L., Yarom, Y., & Uusisaari, M. Y. (2014). Slice it hot: acute adult brain slicing in physiological temperature. JoVE, 92.

Arendt, T., Allen, Y., Marchbanks, R. M., Schugens, M. M., Sinden, J., Lantos, P. L., & Gray, J. A. (1989). Cholinergic system and memory in the rat: effects of chronic ethanol, embryonic basal forebrain brain transplants and excitotoxic lesions of cholinergic basal forebrain projection system. Neurosci, 33(3), 435-462.

Atkins, A. L., Mashhoon, Y., & Kantak, K. M. (2008). Hippocampal regulation of contextual cue-induced reinstatement of cocaine-seeking behavior. Pharmacol Biochem Behav, 90(3), 481-491. doi:10.1016/j.pbb.2008.04.007

Azam, L., Winzer-Serhan, U., & Leslie, F. (2003). Co-expression of α7 and β2 nicotinic acetylcholine receptor subunit mRNAs within rat brain cholinergic neurons. Neurosci, 119(4), 965-977.

Badiani, A., Belin, D., Epstein, D., Calu, D., & Shaham, Y. (2011). Opiate versus psychostimulant addiction: the differences do matter. Nat Rev Neurosci, 12(11), 685-700. doi:10.1038/nrn3104

Bailey, A., Metaxas, A., Al-Hasani, R., Keyworth, H. L., Forster, D. M., & Kitchen, I. (2010). Mouse strain differences in locomotor, sensitisation and rewarding effect of heroin; association with alterations in MOP-r activation and dopamine transporter binding. Eur J Neurosci, 31(4), 742-753. doi:10.1111/j.1460-9568.2010.07104.x

Balfour, D. J. (2004). The neurobiology of tobacco dependence: a preclinical perspective on the role of the dopamine projections to the nucleus. Nicotine Tob Res, 6(6), 899-912.

Banerjee, J., Alkondon, M., & Albuquerque, E. X. (2012). Kynurenic acid inhibits glutamatergic transmission to CA1 pyramidal neurons via α7 nAChR-dependent and-independent mechanisms. Biochem Pharmacol, 84(8), 1078-1087.

Banerjee, J., Alkondon, M., Albuquerque, E. X., & Pereira, E. F. (2013). Contribution of CA3 and CA1 pyramidal neurons to the tonic α7 nAChR-dependent glutamatergic input to CA1 pyramidal neurons. Neurosci Lett, 554, 167-171. doi:10.1016/j.neulet.2013.08.025

Bannerman, D. M., Rawlins, J. N., McHugh, S. B., Deacon, R. M., Yee, B. K., Bast, T., Zhang, W. N., Pothuizen, H. H., & Feldon, J. (2004). Regional dissociations within the hippocampus--memory and anxiety. Neurosci Biobehav Rev, 28(3), 273-283. doi:10.1016/j.neubiorev.2004.03.004

Barak, S., Arad, M., De Levie, A., Black, M. D., Griebel, G., & Weiner, I. (2009). Pro-cognitive and antipsychotic efficacy of the α 7 nicotinic partial agonist SSR180711 in pharmacological and neurodevelopmental latent inhibition models of schizophrenia. Neuropsychopharmacol, 34(7), 1753-1763.

Bardo, M., & Bevins, R. A. (2000). Conditioned place preference: what does it add to our preclinical understanding of drug reward? Psychopharmacol, 153(1), 31-43.

Barry, D. N., Coogan, A. N., & Commins, S. (2016). The time course of systems consolidation of spatial memory from recent to remote retention: A comparison of the

Immediate Early Genes Zif268, c-Fos and Arc. Neurobiol Learn Mem, 128, 46-55. doi:10.1016/j.nlm.2015.12.010

Barth, A. L., Gerkin, R. C., & Dean, K. L. (2004). Alteration of neuronal firing properties after in vivo experience in a FosGFP transgenic mouse. J Neurosci, 24(29), 6466-6475.

Benke, T. A., Lüthi, A., Isaac, J. T., & Collingridge, G. L. (1998). Modulation of AMPA receptor unitary conductance by synaptic activity. Nature, 393(6687), 793-797.

Berretta, N., & Jones, R. (1996). Tonic facilitation of glutamate release by presynaptic N-methyl-D-aspartate autoreceptors in the entorhinal cortex. Neurosci, 75(2), 339-344.

Berridge, K. C., & Robinson, T. E. (2003). Parsing reward. Trends Neurosci, 26(9), 507-513.

Bertagna, N. B., Dos Santos, P. G. C., Queiroz, R. M., Fernandes, G. J. D., Cruz, F. C., & Miguel, T. T. (2021). Involvement of the ventral, but not dorsal, hippocampus in anxiety-like behaviors in mice exposed to the elevated plus maze: participation of CRF1 receptor and PKA pathway. Pharmacol Rep, 73(1), 57-72. doi:10.1007/s43440-020-00182-3

Bertrand, D., & Gopalakrishnan, M. (2007). Allosteric modulation of nicotinic acetylcholine receptors. Biochem Pharmacol, 74(8), 1155-1163.

Besson, M., David, V., Baudonnat, M., Cazala, P., Guilloux, J. P., Reperant, C., Cloez-Tayarani, I., Changeux, J. P., Gardier, A. M., & Granon, S. (2012). Alpha7-nicotinic receptors modulate nicotine-induced reinforcement and extracellular dopamine outflow in the mesolimbic system in mice. Psychopharmacol, 220(1), 1-14. doi:10.1007/s00213-011-2422-1

Billa, S. K., Liu, J., Bjorklund, N. L., Sinha, N., Fu, Y., Shinnick-Gallagher, P., & Moron, J. A. (2010). Increased insertion of glutamate receptor 2-lacking alpha-amino-3-hydroxy-5-methyl-4-isoxazole propionic acid (AMPA) receptors at hippocampal synapses upon repeated morphine administration. Mol Pharmacol, 77(5), 874-883. doi:10.1124/mol.109.060301

Blagbrough, I. S., Coates, P. A., Hardick, D. J., Lewis, T., Rowan, M. G., Wonnacott, S., & Potter, B. V. L. (1994). Acylation of lycoctonine: semi-synthesis of inuline, delsemine analogues and methyllycaconitine. Tetrahedron Lett, 35(46), 8705-8708.

Blake, M. G., Krawczyk, M. C., Baratti, C. M., & Boccia, M. M. (2014). Neuropharmacology of memory consolidation and reconsolidation: Insights on central cholinergic mechanisms. J Physiology, 108(4-6), 286-291. doi:10.1016/j.jphysparis.2014.04.005

Boccia, M. M., Blake, M. G., Krawczyk, M. d. C., & Baratti, C. M. (2010). Hippocampal alpha7 nicotinic receptors modulate memory reconsolidation of an inhibitory avoidance task in mice. Neurosci, 171(2), 531-543.

Bosch, M., & Hayashi, Y. (2012). Structural plasticity of dendritic spines. Curr Opin Neurobiol, 22(3), 383-388.

Bossert, J. M., Stern, A. L., Theberge, F. R., Cifani, C., Koya, E., Hope, B. T., & Shaham, Y. (2011). Ventral medial prefrontal cortex neuronal ensembles mediate context-induced relapse to heroin. Nat Neurosci, 14(4), 420-422. doi:10.1038/nn.2758

Bouton, M. E. (2004). Context and behavioral processes in extinction. Learn Mem, 11(5), 485-494.

Bouton, M. E. (2014). Why behavior change is difficult to sustain. Prev Med, 68, 29-36. doi:10.1016/j.ypmed.2014.06.010

Bouzat, C., Bartos, M., Corradi, J., & Sine, S. M. (2008). The interface between extracellular and transmembrane domains of homomeric Cys-loop receptors governs open-channel lifetime and rate of desensitization. J Neurosci, 28(31), 7808-7819.

Bouzat, C. (2012). New insights into the structural bases of activation of Cys-loop receptors. J Physiol, 106(1-2), 23-33.

Bouzat, C., Lasala, M., Nielsen, B. E., Corradi, J., & Esandi, M. D. C. (2018). Molecular function of alpha7 nicotinic receptors as drug targets. J Physiol, 596(10), 1847-1861. doi:10.1113/JP275101

Bouzat, C., & Sine, S. M. (2018). Nicotinic acetylcholine receptors at the single-channel level. Brit J Pharmacol, 175(11), 1789-1804.

Bozon, B., Davis, S., & Laroche, S. (2003). A requirement for the immediate early gene zif268 in reconsolidation of recognition memory after retrieval. Neuron, 40(4), 695-701. doi:10.1016/s0896-6273(03)00674-3

Briggs, C. A., & McKenna, D. G. (1996). Effect of MK-801 at the human α7 nicotinic acetylcholine receptor. Neuropharmacol, 35(4), 407-414.

Britt, J. P., Benaliouad, F., McDevitt, R. A., Stuber, G. D., Wise, R. A., & Bonci, A. (2012). Synaptic and behavioral profile of multiple glutamatergic inputs to the nucleus accumbens. Neuron, 76(4), 790-803. doi:10.1016/j.neuron.2012.09.040

Brown, M. T., Tan, K. R., O'Connor, E. C., Nikonenko, I., Muller, D., & Lüscher, C. (2012). Ventral tegmental area GABA projections pause accumbal cholinergic interneurons to enhance associative learning. Nature, 492(7429), 452-456.

Bürli, T., Baer, K., Ewers, H., Sidler, C., Fuhrer, C., & Fritschy, J. M. (2010). Single particle tracking of alpha7 nicotinic AChR in hippocampal neurons reveals regulated confinement at glutamatergic and GABAergic perisynaptic sites. PLoS One, 5(7), e11507. doi:10.1371/journal.pone.0011507

Cahill, E., Salery, M., Vanhoutte, P., & Caboche, J. (2014). Convergence of dopamine and glutamate signaling onto striatal ERK activation in response to drugs of abuse. Front Pharmacol, 4, 172. doi:10.3389/fphar.2013.00172

Cave, C. B., & Squire, L. R. (1991). Equivalent impairment of spatial and nonspatial memory following damage to the human hippocampus. Hippocampus, 1(3), 329-340.

Celentano, M., Caprioli, D., Dipasquale, P., Cardillo, V., Nencini, P., Gaetani, S., & Badiani, A. (2009). Drug context differently regulates cocaine versus heroin self-administration and cocaine- versus heroin-induced Fos mRNA expression in the rat. Psychopharmacol, 204(2), 349-360. doi:10.1007/s00213-009-1467-x

Cenquizca, L. A., & Swanson, L. W. (2007). Spatial organization of direct hippocampal field CA1 axonal projections to the rest of the cerebral cortex. Brain Res Rev, 56(1), 1-26.

Chatzidaki, A., & Millar, N. S. (2015). Allosteric modulation of nicotinic acetylcholine receptors. Biochem Pharmacol, 97(4), 408-417.

Cheng, H., & Lederer, W. (2008). Calcium sparks. Physiological reviews, 88(4), 1491-1545.

Cheng, Q., & Yakel, J. L. (2014). Presynaptic alpha7 nicotinic acetylcholine receptors enhance hippocampal mossy fiber glutamatergic transmission via PKA activation. J Neurosci, 34(1), 124-133. doi:10.1523/JNEUROSCI.2973-13.2014

Cheng, Q., & Yakel, J. L. (2015). The effect of alpha7 nicotinic receptor activation on glutamatergic transmission in the hippocampus. Biochem Pharmacol, 97(4), 439-444. doi:10.1016/j.bcp.2015.07.015

Chiba, T. (2000). Collateral projection from the amygdalo–hippocampal transition area and CA1 to the hypotus and medial prefrontal cortex in the rat. Neurosci Res, 38(4), 373-383.

Childress, A. R., Mozley, P. D., McElgin, W., Fitzgerald, J., Reivich, M., & O'Brien, C. P. (1999). Limbic activation during cue-induced cocaine craving. Am J Psychiatry, 156(1), 11-18. doi:10.1176/ajp.156.1.11

Childs, E., & de Wit, H. (2009). Amphetamine-induced place preference in humans. Biol Psychiatry, 65(10), 900-904.

Chilton, M., Mastropaolo, J., Rosse, R. B., Bellack, A. S., & Deutsch, S. I. (2004). Behavioral consequences of methyllycaconitine in mice: a model of α7 nicotinic acetylcholine receptor deficiency. Life Sci, 74(25), 3133-3139.

Christie, M. (2008). Cellular neuroadaptations to chronic opioids: tolerance, withdrawal and addiction. Brit J Pharmacol, 154(2), 384-396.

Cohen, S. J., & Stackman, R. W., Jr. (2015). Assessing rodent hippocampal involvement in the novel object recognition task. A review. Behav Brain Res, 285, 105-117. doi:10.1016/j.bbr.2014.08.002

Conte, W. L., Kamishina, H., & Reep, R. L. (2009). Multiple neuroanatomical tract-tracing using fluorescent Alexa Fluor conjugates of cholera toxin subunit B in rats. Nat Protoc, 4(8), 1157-1166. doi:10.1038/nprot.2009.93

Corrie, J. B., & Sine, S. M. (2013). Stoichiometry for drug potentiation of a pentameric ion channel. PNAS, 110(16), 6595-6600.

Cruz, F. C., Koya, E., Guez-Barber, D. H., Bossert, J. M., Lupica, C. R., Shaham, Y., & Hope, B. T. (2013). New technologies for examining the role of neuronal ensembles in drug addiction and fear. Nat Rev Neurosci, 14(11), 743-754. doi:10.1038/nrn3597

Cruz, F. C., Babin, K. R., Leao, R. M., Goldart, E. M., Bossert, J. M., Shaham, Y., & Hope, B. T. (2014). Role of nucleus accumbens shell neuronal ensembles in context-induced reinstatement of cocaine-seeking. J Neurosci, 34(22), 7437-7446. doi:10.1523/JNEUROSCI.0238-14.2014

Cruz, F. C., Javier Rubio, F., & Hope, B. T. (2015). Using c-fos to study neuronal ensembles in corticostriatal circuitry of addiction. Brain Res, 1628(Pt A), 157-173. doi:10.1016/j.brainres.2014.11.005

Cullity, E. R., Guerin, A. A., Perry, C. J., & Kim, J. H. (2021). Examining sex differences in conditioned place preference or aversion to methamphetamine in adolescent and adult mice. Front Pharmacol, 12, 770614. doi:10.3389/fphar.2021.770614

Cunningham, C. L., Gremel, C. M., & Groblewski, P. A. (2006). Drug-induced conditioned place preference and aversion in mice. Nat Protoc, 1(4), 1662-1670.

Cutsuridis, V., & Wennekers, T. (2009). Hippocampus, microcircuits and associative memory. Neural Netw, 22(8), 1120-1128. doi:10.1016/j.neunet.2009.07.009

daCosta, C. J. B., Free, C. R., Corradi, J., Bouzat, C., & Sine, S. M. (2011). Single-channel and structural foundations of neuronal α7 acetylcholine receptor potentiation. J Neurosci, 31(39), 13870-13879. doi:10.1523/jneurosci.2652-11.2011

Dajas-Bailador, F., & Wonnacott, S. (2004). Nicotinic acetylcholine receptors and the regulation of neuronal signalling. Trends Pharmacol Sci, 25(6), 317-324. doi:10.1016/j.tips.2004.04.006

Dajas-Bailador, F., Soliakov, L., & Wonnacott, S. (2002). Nicotine activates the extracellular signal-regulated kinase 1/2 via the α7 nicotinic acetylcholine receptor and protein kinase A, in SH-SY5Y cells and hippocampal neurones. J Neurochem, 80(3), 520-530.

Dalley, J. W., Everitt, B. J., & Robbins, T. W. (2011). Impulsivity, compulsivity, and top-down cognitive control. Neuron, 69(4), 680-694.

Dani, J. A., & Bertrand, D. (2007). Nicotinic acetylcholine receptors and nicotinic cholinergic mechanisms of the central nervous system. Annu. Rev. Pharmacol. Toxicol., 47, 699-729.

Daumas, S., Halley, H., Francés, B., & Lassalle, J. M. (2005). Encoding, consolidation, and retrieval of contextual memory: differential involvement of dorsal CA3 and CA1 hippocampal subregions. Learn Mem, 12(4), 375-382. doi:10.1101/lm.81905

Davis, S., Renaudineau, S., Poirier, R., Poucet, B., Save, E., & Laroche, S. (2010). The formation and stability of recognition memory: what happens upon recall? Front Behav Neurosci, 4, 177. doi:10.3389/fnbeh.2010.00177

Day, J. J., & Sweatt, J. D. (2011). Epigenetic mechanisms in cognition. Neuron, 70(5), 813-829.

Denny, C. A., Kheirbek, M. A., Alba, E. L., Tanaka, K. F., Brachman, R. A., Laughman, K. B., Tomm, N. K., Turi, G. F., Losonczy, A., & Hen, R. (2014). Hippocampal memory traces are differentially modulated by experience, time, and adult neurogenesis. Neuron, 83(1), 189-201.

Dickinson, J. A., Hanrott, K. E., Mok, M. S., Kew, J. N., & Wonnacott, S. (2007). Differential coupling of α7 and non-α7 nicotinic acetylcholine receptors to calcium-induced calcium release and voltage-operated calcium channels in PC12 cells. J Neurochem, 100(4), 1089-1096.

Dong, H. W., & Swanson, L. W. (2006). Projections from bed nuclei of the stria terminalis, anteromedial area: cerebral hemisphere integration of neuroendocrine, autonomic, and behavioral aspects of energy balance. J Comp Neurol, 494(1), 142-178.

Dong, Y., Taylor, J. R., Wolf, M. E., & Shaham, Y. (2017). Circuit and synaptic plasticity mechanisms of drug relapse. J Neurosci, 37(45), 10867-10876. doi:10.1523/JNEUROSCI.1821-17.2017

Dunlop, J., Lock, T., Jow, B., Sitzia, F., Grauer, S., Jow, F., Kramer, A., Bowlby, M. R., Randall, A., & Kowal, D. (2009). Old and new pharmacology: positive allosteric modulation of the α7 nicotinic acetylcholine receptor by the 5-hydroxytryptamine2B/C receptor antagonist SB-206553 (3, 5-dihydro-5-methyl-N-3-pyridinylbenzo [1, 2-b: 4, 5-b′] di pyrrole-1 (2H)-carboxamide). J Pharmacol Expl Ther, 328(3), 766-776.

Eguchi, K., Velicky, P., Hollergschwandtner, E., Itakura, M., Fukazawa, Y., Danzl, J. G., & Shigemoto, R. (2020). Advantages of acute brain slices prepared at physiological temperature in the characterization of synaptic functions. Front Cell Neurosci, 14, 63.

El Rawas, R., Thiriet, N., Lardeux, V., Jaber, M., & Solinas, M. (2009). Environmental enrichment decreases the rewarding but not the activating effects of heroin. Psychopharmacol, 203(3), 561-570. doi:10.1007/s00213-008-1402-6

Elnagar, M. R., Walls, A. B., Helal, G. K., Hamada, F. M., Thomsen, M. S., & Jensen, A. A. (2018). Functional characterization of α7 nicotinic acetylcholine and NMDA receptor signaling in SH-SY5Y neuroblastoma cells in an ERK phosphorylation assay. Eur J Pharmacol, 826, 106-113.

Everitt, B. J., Dickinson, A., & Robbins, T. W. (2001). The neuropsychological basis of addictive behaviour. Brain Res Rev, 36(2-3), 129-138. doi:10.1016/s0165-0173(01)00088-1

Everitt, B. J., & Robbins, T. W. (2005). Neural systems of reinforcement for drug addiction: from actions to habits to compulsion. Nat Neurosci, 8(11), 1481-1489.

Exley, R., & Cragg, S. (2008). Presynaptic nicotinic receptors: a dynamic and diverse cholinergic filter of striatal dopamine neurotransmission. Brit J Pharmacol, 153(S1), S283-S297.

Fabian-Fine, R., Skehel, P., Errington, M. L., Davies, H. A., Sher, E., Stewart, M. G., & Fine, A. (2001). Ultrastructural distribution of the α7 nicotinic acetylcholine receptor subunit in rat hippocampus. J Neurosci, 21(20), 7993-8003.

Fanselow, M. S., & Poulos, A. M. (2005). The neuroscience of mammalian associative learning. Annu. Rev. Psychol., 56, 207-234.

Fanselow, M. S., & Dong, H. W. (2010). Are the dorsal and ventral hippocampus functionally distinct structures? Neuron, 65(1), 7-19. doi:10.1016/j.neuron.2009.11.031

Fayuk, D., & Yakel, J. L. (2007). Dendritic Ca2+ signalling due to activation of α7-containing nicotinic acetylcholine receptors in rat hippocampal neurons. J Physiol, 582(2), 597-611.

Felipe, J. M., Palombo, P., Bianchi, P. C., Zaniboni, C. R., Anésio, A., Yokoyama, T. S., Engi, S. A., Carneiro-de-Oliveira, P. E., Planeta, C. D. S., Leão, R. M., & Cruz, F. C. (2021). Dorsal hippocampus plays a causal role in context-induced reinstatement of alcohol-seeking in rats. Behav Brain Res, 398, 112978. doi:10.1016/j.bbr.2020.112978

Feng, B., Xing, J. H., Jia, D., Liu, S. B., Guo, H. J., Li, X. Q., He, X. S., & Zhao, M. G. (2011). Blocking alpha4beta2 and alpha7 nicotinic acetylcholine receptors inhibits the reinstatement of morphine-induced CPP by drug priming in mice. Behav Brain Res, 220(1), 100-105. doi:10.1016/j.bbr.2011.01.040

Frankland, P. W., Bontempi, B., Talton, L. E., Kaczmarek, L., & Silva, A. J. (2004). The involvement of the anterior cingulate cortex in remote contextual fear memory. Sci, 304(5672), 881-883.

Freund, T. F., & Buzsáki, G. (1996). Interneurons of the hippocampus. Hippocampus, 6(4), 347-470.

Fuchs, R. A., Evans, K. A., Ledford, C. C., Parker, M. P., Case, J. M., Mehta, R. H., & See, R. E. (2005). The role of the dorsomedial prefrontal cortex, basolateral amygdala, and dorsal hippocampus in contextual reinstatement of cocaine seeking in rats. Neuropsychopharmacol, 30(2), 296-309.

Fuchs, R. A., Eaddy, J. L., Su, Z. I., & Bell, G. H. (2007). Interactions of the basolateral amygdala with the dorsal hippocampus and dorsomedial prefrontal cortex regulate drug context-induced reinstatement of cocaine-seeking in rats. Eur J Neurosci, 26(2), 487-498. doi:10.1111/j.1460-9568.2007.05674.x

Fuchs, R. A., Higginbotham, J. A., & Lyons, C. E. (2017). Hippocampal contributions to dopamine receptor-mediated effects of cocaine. In The Neuroscience of Cocaine (pp. 449-459).

Fucile, S. (2004). Ca2+ permeability of nicotinic acetylcholine receptors. Cell Calcium, 35(1), 1-8. doi:10.1016/j.ceca.2003.08.006

Gabbott, P. L., Warner, T. A., Jays, P. R., Salway, P., & Busby, S. J. (2005). Prefrontal cortex in the rat: projections to subcortical autonomic, motor, and limbic centers. J Comp Neurol, 492(2), 145-177. doi:10.1002/cne.20738

Gage, F. H., & Thompson, R. G. (1980). Differential distribution of norepinephrine and serotonin along the dorsal-ventral axis of the hippocampal formation. Brain Res Bull, 5(6), 771-773. doi:10.1016/0361-9230(80)90220-8

Gallagher, M., & Colombo, P. J. (1995). Ageing: the cholinergic hypothesis of cognitive decline. Curr Opin Neurobiol, 5(2), 161-168. doi:10.1016/0959-4388(95)80022-0

Gallo, F. T., Katche, C., Morici, J. F., Medina, J. H., & Weisstaub, N. V. (2018). Immediate early genes, memory and psychiatric disorders: focus on c-Fos, Egr1 and Arc. Front Behav Neurosci, 12, 79.

Gao, P., Limpens, J. H., Spijker, S., Vanderschuren, L. J., & Voorn, P. (2017). Stable immediate early gene expression patterns in medial prefrontal cortex and striatum after long-term cocaine self-administration. Addict Biol, 22(2), 354-368.

García-Pérez, D., Ferenczi, S., Kovács, K. J., Laorden, M. L., Milanés, M. V., & Núñez, C. (2016). Different contribution of glucocorticoids in the basolateral amygdala to the formation and expression of opiate withdrawal-associated memories. Psychoneuroendocrinol, 74, 350-362.

Ge, S., & Dani, J. A. (2005). Nicotinic acetylcholine receptors at glutamate synapses facilitate long-term depression or potentiation. J Neurosci, 25(26), 6084-6091.

Glasgow, S. D., McPhedrain, R., Madranges, J. F., Kennedy, T. E., & Ruthazer, E. S. (2019). Approaches and limitations in the investigation of synaptic transmission and plasticity. Front Synaptic Neurosci, 11, 20. doi:10.3389/fnsyn.2019.00020

Gotti, C., & Clementi, F. (2004). Neuronal nicotinic receptors: from structure to pathology. Prog Neurobiol, 74(6), 363-396.

Granger, A. J., & Nicoll, R. A. (2014). Expression mechanisms underlying long-term potentiation: a postsynaptic view, 10 years on. Philos Trans R Soc Lond B Biol Sci, 369(1633), 20130136.

Gray, J. A., McNaughton, N., James, D. T. D., & Kelly, P. H. (1975). Effect of minor tranquillisers on hippocampal θ rhythm mimicked by depletion of forebrain noradrenaline. Nature, 258(5534), 424-425.

Gray, J. A., & McNaughton, N. (1983). Comparison between the behavioural effects of septal and hippocampal lesions: a review. Neurosci BiobehavRev, 7(2), 119-188.

Green, T. A., & Bardo, M. T. (2020). Opposite regulation of conditioned place preference and intravenous drug self-administration in rodent models: Motivational and non-motivational examples. Neurosci Biobehav Rev, 116, 89-98. doi:10.1016/j.neubiorev.2020.06.006

Griguoli, M., Cellot, G., & Cherubini, E. (2013). In hippocampal oriens interneurons anti-Hebbian long-term potentiation requires cholinergic signaling via alpha7 nicotinic acetylcholine receptors. J Neurosci, 33(3), 1044-1049. doi:10.1523/JNEUROSCI.1070-12.2013

Gritton, H. J., Howe, W. M., Mallory, C. S., Hetrick, V. L., Berke, J. D., & Sarter, M. (2016). Cortical cholinergic signaling controls the detection of cues. PNAS, 113(8), E1089-E1097.

Grybko, M. J., Hahm, E. t., Perrine, W., Parnes, J. A., Chick, W. S., Sharma, G., Finger, T. E., & Vijayaraghavan, S. (2011). A transgenic mouse model reveals fast nicotinic transmission in hippocampal pyramidal neurons. Eur J Neurosci, 33(10), 1786-1798.

Gu, Z., & Yakel, J. L. (2011). Timing-dependent septal cholinergic induction of dynamic hippocampal synaptic plasticity. Neuron, 71(1), 155-165.

Gu, Z., Lamb, P. W., & Yakel, J. L. (2012). Cholinergic coordination of presynaptic and postsynaptic activity induces timing-dependent hippocampal synaptic plasticity. J Neurosci, 32(36), 12337-12348. doi:10.1523/JNEUROSCI.2129-12.2012

Gu, Z., Smith, K. G., Alexander, G. M., Guerreiro, I., Dudek, S. M., Gutkin, B., Jensen, P., & Yakel, J. L. (2020). Hippocampal interneuronal α7 nAChRs modulate theta oscillations in freely moving mice. Cell Rep, 31(10), 107740.

Gubbins, E. J., Gopalakrishnan, M., & Li, J. (2010). α7 nAChR-mediated activation of MAP kinase pathways in PC12 cells. Brain Res, 1328, 1-11.

Guenthner, C. J., Miyamichi, K., Yang, H. H., Heller, H. C., & Luo, L. (2013). Permanent genetic access to transiently active neurons via TRAP: targeted recombination in active populations. Neuron, 78(5), 773-784.

Guzowski, J. F. (2002). Insights into immediate-early gene function in hippocampal memory consolidation using antisense oligonucleotide and fluorescent imaging approaches. Hippocampus, 12(1), 86-104.

Guzowski, J. F., Miyashita, T., Chawla, M. K., Sanderson, J., Maes, L. I., Houston, F. P., Lipa, P., McNaughton, B. L., Worley, P. F., & Barnes, C. A. (2006). Recent behavioral history modifies coupling between cell activity and Arc gene transcription in hippocampal CA1 neurons. PNAS, 103(4), 1077-1082. doi:10.1073/pnas.0505519103

Haam, J., Zhou, J., Cui, G., & Yakel, J. L. (2018). Septal cholinergic neurons gate hippocampal output to entorhinal cortex via oriens lacunosum moleculare interneurons. PNAS, 115(8), E1886-E1895.

Hajos, M., Hurst, R., Hoffmann, W., Krause, M., Wall, T., Higdon, N., & Groppi, V. (2005). The selective α7 nicotinic acetylcholine receptor agonist PNU-282987 [N-[(3R)-1-azabicyclo [2.2. 2] oct-3-yl]-4-chlorobenzamide hydrochloride] enhances GABAergic synaptic activity in brain slices and restores auditory gating deficits in anesthetized rats. J Pharmacol Expl Ther, 312(3), 1213-1222.

Haring, J. H., & Davis, J. N. (1985). Differential distribution of locus coeruleus projections to the hippocampal formation: anatomical and biochemical evidence. Brain Res, 325(1-2), 366-369. doi:10.1016/0006-8993(85)90342-7

Harker, K. T., & Whishaw, I. Q. (2004). Impaired place navigation in place and matching-to-place swimming pool tasks follows both retrosplenial cortex lesions and cingulum bundle lesions in rats. Hippocampus, 14(2), 224-231.

Harris, K. M. (2020). Structural LTP: from synaptogenesis to regulated synapse enlargement and clustering. Curr Opin Neurobiol, 63, 189-197. doi:10.1016/j.conb.2020.04.009

Hasselmo, M. E. (2006). The role of acetylcholine in learning and memory. Curr Opin Neurobiol, 16(6), 710-715. doi:10.1016/j.conb.2006.09.002

Heal, D. J., Gosden, J., & Smith, S. L. (2014). Dopamine reuptake transporter (DAT)"inverse agonism"–a novel hypothesis to explain the enigmatic pharmacology of cocaine. Neuropharmacol, 87, 19-40.

Heal, D. J., & Smith, S. (2021). Evidence against the involvement of increased dopamine signalling in the abuse potential of mu opioid agonists. College on Problems of Drug Dependence 83rd Annual Virtual Meeting.

Hearing, M. C., Jedynak, J., Ebner, S. R., Ingebretson, A., Asp, A. J., Fischer, R. A., Schmidt, C., Larson, E. B., & Thomas, M. J. (2016). Reversal of morphine-induced cell-type-specific synaptic plasticity in the nucleus accumbens shell blocks reinstatement. PNAS, 113(3), 757-762. doi:10.1073/pnas.1519248113

Hebb, D. O. (1949). The organization of behavior: a neuropsychological theory: Science editions.

Henke, P. G. (1990). Hippocampal pathway to the amygdala and stress ulcer development. Brain Res Bull, 25(5), 691-695.

Hilderbrand, E. R., & Lasek, A. W. (2014). Sex differences in cocaine conditioned place preference in C57BL/6J mice. Neurorep, 25(2), 105-109. doi:10.1097/wnr.0000000000000053

Hoover, W. B., & Vertes, R. P. (2007). Anatomical analysis of afferent projections to the medial prefrontal cortex in the rat. Brain Struct Funct, 212(2), 149-179. doi:10.1007/s00429-007-0150-4

Horn, G. (2004). Pathways of the past: the imprint of memory. Nat Rev Neurosci, 5(2), 108-120.

Huang, L. T., Sherwood, J. L., Sun, Y. J., Lodge, D., & Wang, Y. (2010). Activation of presynaptic α7 nicotinic receptors evokes an excitatory response in hippocampal CA3 neurones in anaesthetized rats: an in vivo iontophoretic study. Brit J Pharmacol, 159(3), 554-565.

Huang, S., & Uusisaari, M. Y. (2013). Physiological temperature during brain slicing enhances the quality of acute slice preparations. Front Cell Neurosci, 7, 48.

Hunter, B. E., Christopher, M., Papke, R. L., Kem, W. R., & Meyer, E. M. (1994). A novel nicotinic agonist facilitates induction of long-term potentiation in the rat hippocampus. Neurosci Lett, 168(1-2), 130-134.

Hurst, R. S., Hajós, M., Raggenbass, M., Wall, T. M., Higdon, N. R., Lawson, J. A., Rutherford-Root, K. L., Berkenpas, M. B., Hoffmann, W., & Piotrowski, D. W. (2005). A novel positive allosteric modulator of the α7 neuronal nicotinic acetylcholine receptor: in vitro and in vivo characterization. J Neurosci, 25(17), 4396-4405.

Hurst, R. S., Rollema, H., & Bertrand, D. (2013). Nicotinic acetylcholine receptors: from basic science to therapeutics. Pharm Ther, 137(1), 22-54.

Hyer, M., Shaw, G., Goswamee, P., Dyer, S., Burns, C., Soriano, E., Sanchez, C., Rowson, S., McQuiston, A., & Neigh, G. (2021). Chronic adolescent stress causes sustained impairment of cognitive flexibility and hippocampal synaptic strength in female rats. Neurobiol Stress, 14, 100303.

Hyman, S. E., Malenka, R. C., & Nestler, E. J. (2006). Neural mechanisms of addiction: the role of reward-related learning and memory. Annu Rev Neurosci, 29, 565-598. doi:10.1146/annurev.neuro.29.051605.113009

Ikemoto, S. (2010). Brain reward circuitry beyond the mesolimbic dopamine system: a neurobiological theory. Neurosci Biobehav Rev, 35(2), 129-150. doi:10.1016/j.neubiorev.2010.02.001

Ito, H. T., & Schuman, E. M. (2008). Frequency-dependent signal transmission and modulation by neuromodulators. Front Neurosci, 2(2), 138-144. doi:10.3389/neuro.01.027.2008

Jentsch, J. D., & Taylor, J. R. (1999). Impulsivity resulting from frontostriatal dysfunction in drug abuse: implications for the control of behavior by reward-related stimuli. Psychopharmacol, 146(4), 373-390.

Ji, D., & Dani, J. A. (2000). Inhibition and disinhibition of pyramidal neurons by activation of nicotinic receptors on hippocampal interneurons. J Neurophyisiol, 83(5), 2682-2690.

Ji, D., Lape, R., & Dani, J. A. (2001). Timing and location of nicotinic activity enhances or depresses hippocampal synaptic plasticity. Neuron, 31(1), 131-141.

Jin, J., & Maren, S. (2015). Fear renewal preferentially activates ventral hippocampal neurons projecting to both amygdala and prefrontal cortex in rats. Sci Rep, 5, 8388. doi:10.1038/srep08388

Jones, M. W., Errington, M. L., French, P. J., Fine, A., Bliss, T. V., Garel, S., Charnay, P., Bozon, B., Laroche, S., & Davis, S. (2001). A requirement for the immediate early gene Zif268 in the expression of late LTP and long-term memories. Nat Neurosci, 4(3), 289-296. doi:10.1038/85138

Jones, M. W., & Wilson, M. A. (2005). Theta rhythms coordinate hippocampal–prefrontal interactions in a spatial memory task. PLoS Biol, 3(12), e402.

Joseph, M. H., Peters, S. L., Prior, A., Mitchell, S. N., Brazell, M. P., & Gray, J. A. (1990). Chronic nicotine administration increases tyrosine hydroxylase selectivity in the rat hippocampus. Neurochemistry international, 16(3), 269-273.

Josselyn, S. A., Köhler, S., & Frankland, P. W. (2015). Finding the engram. Nat Rev Neurosci, 16(9), 521-534.

Jung, M. W., Wiener, S. I., & McNaughton, B. L. (1994). Comparison of spatial firing characteristics of units in dorsal and ventral hippocampus of the rat. J Neurosci, 14(12), 7347-7356.

Kabbani, N., Nordman, J. C., Corgiat, B. A., Veltri, D. P., Shehu, A., Seymour, V. A., & Adams, D. J. (2013). Are nicotinic acetylcholine receptors coupled to G proteins? Bioessays, 35(12), 1025-1034.

Kandel, E. R. (2012). The molecular biology of memory: cAMP, PKA, CRE, CREB-1, CREB-2, and CPEB. Mol Brain, 5(1), 1-12.

Kaneda, K. (2019). Neuroplasticity in cholinergic neurons of the laterodorsal tegmental nucleus contributes to the development of cocaine addiction. Eur J Neurosci, 50(3), 2239-2246. doi:10.1111/ejn.13962

Karasinska, J. M., George, S. R., Cheng, R., & O'Dowd, B. F. (2005). Deletion of dopamine D1 and D3 receptors differentially affects spontaneous behaviour and cocaine-induced locomotor activity, reward and CREB phosphorylation. Eur J Neurosci, 22(7), 1741-1750. doi:10.1111/j.1460-9568.2005.04353.x

Karimi, S., Attarzadeh-Yazdi, G., Yazdi-Ravandi, S., Hesam, S., Azizi, P., Razavi, Y., & Haghparast, A. (2014). Forced swim stress but not exogenous corticosterone could induce the reinstatement of extinguished morphine conditioned place preference in rats: involvement of glucocorticoid receptors in the basolateral amygdala. Behav Brain Res, 264, 43-50.

Katche, C., Goldin, A., Gonzalez, C., Bekinschtein, P., & Medina, J. H. (2012). Maintenance of long-term memory storage is dependent on late posttraining Egr-1 expression. Neurobiol Learn Mem, 98(3), 220-227. doi:10.1016/j.nlm.2012.08.001

Kauer, J. A., & Malenka, R. C. (2007). Synaptic plasticity and addiction. Nat Rev Neurosci, 8(11), 844-858. doi:10.1038/nrn2234

Kennett, A., Heal, D. J., & Wonnacott, S. (2012). Pharmacological differences between rat frontal cortex and hippocampus in the nicotinic modulation of noradrenaline release implicate distinct receptor subtypes. Nicotine Tob Res, 14(11), 1339-1345.

Khaled, M. A., Pushparaj, A., Di Ciano, P., Diaz, J., & Le Foll, B. (2014). Dopamine D3 receptors in the basolateral amygdala and the lateral habenula modulate cue-induced reinstatement of nicotine seeking. Neuropsychopharmacol, 39(13), 3049-3058. doi:10.1038/npp.2014.158

Kim, J. J., & Fanselow, M. S. (1992). Modality-specific retrograde amnesia of fear. Sci, 256(5057), 675-677.

Kim, W. B., & Cho, J. H. (2017). Synaptic targeting of double-projecting ventral CA1 hippocampal neurons to the medial prefrontal cortex and basal amygdala. J Neurosci, 37(19), 4868-4882. doi:10.1523/JNEUROSCI.3579-16.2017

King, J. R., Nordman, J. C., Bridges, S. P., Lin, M.-K., & Kabbani, N. (2015). Identification and characterization of a G protein-binding cluster in α7 nicotinic acetylcholine receptors. J Biol Chem, 290(33), 20060-20070.

Kircher, D. M., Aziz, H. C., Mangieri, R. A., & Morrisett, R. A. (2019). Ethanol experience enhances glutamatergic ventral hippocampal inputs to D1 receptor-expressing medium spiny neurons in the nucleus accumbens shell. J Neurosci, 39(13), 2459-2469. doi:10.1523/jneurosci.3051-18.2019

Kishi, T., Tsumori, T., Ono, K., Yokota, S., Ishino, H., & Yasui, Y. (2000). Topographical organization of projections from the subiculum to the hypothalamus in the rat. J Comp Neurol, 419(2), 205-222.

Klausberger, T., & Somogyi, P. (2008). Neuronal diversity and temporal dynamics: the unity of hippocampal circuit operations. Sci, 321(5885), 53-57. doi:10.1126/science.1149381

Koch, M., Schmid, A., & Schnitzler, H. U. (2000). Role of muscles accumbens dopamine D1 and D2 receptors in instrumental and Pavlovian paradigms of conditioned reward. Psychopharmacol, 152(1), 67-73. doi:10.1007/s002130000505

Koenig, G., Palfreyman, M., Chesworth, R., Shapiro, G., Prickaerts, J., & Reneerkens, O. (2009). EVP-6124, a novel and potent α7 nicotinic acetylcholine receptor agonist, improves memory acquisition, retention and retrieval and reverses scopolamine-induced memory deficits. Soc Neurosci, Abst, 887, 1-4.

Kohara, K., Pignatelli, M., Rivest, A. J., Jung, H.-Y., Kitamura, T., Suh, J., Frank, D., Kajikawa, K., Mise, N., & Obata, Y. (2014). Cell type–specific genetic and optogenetic tools reveal hippocampal CA2 circuits. Nat Neurosci, 17(2), 269-279.

Koob, G. F., & Le Moal, M. (1997). Drug abuse: hedonic homeostatic dysregulation. Sci, 278(5335), 52-58.

Koob, G. F. (2017). Antireward, compulsivity, and addiction: seminal contributions of Dr. Athina Markou to motivational dysregulation in addiction. Psychopharmacol, 234(9-10), 1315-1332.

Kouhen, R. E., Hu, M., Anderson, D., Li, J., & Gopalakrishnan, M. (2009). Pharmacology of α7 nicotinic acetylcholine receptor mediated extracellular signal-regulated kinase signalling in PC12 cells. Brit J Pharmacol, 156(4), 638-648.

Koya, E., Cruz, F. C., Ator, R., Golden, S. A., Hoffman, A. F., Lupica, C. R., & Hope, B. T. (2012). Silent synapses in selectively activated nucleus accumbens neurons following cocaine sensitization. Nat Neurosci, 15(11), 1556-1562.

Kramar, C., Loureiro, M., Renard, J., & Laviolette, S. R. (2017). Palmitoylethanolamide modulates GPR55 receptor signaling in the ventral hippocampus to regulate mesolimbic dopamine activity, social interaction, and memory processing. Cannabis Cannabinoid Res, 2(1), 8-20.

Kristensen, A. S., Jenkins, M. A., Banke, T. G., Schousboe, A., Makino, Y., Johnson, R. C., Huganir, R., & Traynelis, S. F. (2011). Mechanism of Ca 2+/calmodulin-dependent kinase II regulation of AMPA receptor gating. Nat Neurosci, 14(6), 727-735.

Kroker, K. S., Rast, G., & Rosenbrock, H. (2011). Differential effects of subtype-specific nicotinic acetylcholine receptor agonists on early and late hippocampal LTP. Eur J Pharmacol, 671(1-3), 26-32.

Kubik, S., Miyashita, T., Kubik-Zahorodna, A., & Guzowski, J. F. (2012). Loss of activity-dependent Arc gene expression in the retrosplenial cortex after hippocampal inactivation: interaction in a higher-order memory circuit. Neurobiol Learn Mem, 97(1), 124-131. doi:10.1016/j.nlm.2011.10.004

Kutlu, M. G., & Gould, T. J. (2016). Effects of drugs of abuse on hippocampal plasticity and hippocampus-dependent learning and memory: contributions to development and maintenance of addiction. Learn Mem, 23(10), 515-533. doi:10.1101/lm.042192.116

Labiner, D. M., Butler, L. S., Cao, Z., Hosford, D., Shin, C., & McNamara, J. (1993). Induction of c-fos mRNA by kindled seizures: complex relationship with neuronal burst firing. J Neurosci, 13(2), 744-751.

Lammel, S., Lim, B. K., & Malenka, R. C. (2014). Reward and aversion in a heterogeneous midbrain dopamine system. Neuropharmacol, 76, 351-359.

Lanciego, J. L., & Wouterlood, F. G. (2020). Neuroanatomical tract-tracing techniques that did go viral. Brain Struct Funct, 225(4), 1193-1224. doi:10.1007/s00429-020-02041-6

Lasseter, H. C., Xie, X., Ramirez, D. R., & Fuchs, R. A. (2010). Sub-region specific contribution of the ventral hippocampus to drug context-induced reinstatement of cocaine-seeking behavior in rats. Neurosci, 171(3), 830-839. doi:10.1016/j.neuroscience.2010.09.032

Latagliata, E. C., Lo Iacono, L., Chiacchierini, G., Sancandi, M., Rava, A., Oliva, V., & Puglisi-Allegra, S. (2017). Single prazosin infusion in prelimbic cortex fosters extinction of amphetamine-induced conditioned place preference. Front Pharmacol, 8, 530.

Latagliata, E. C., Coccia, G., Chiacchierini, G., Milia, C., & Puglisi-Allegra, S. (2020). Concomitant D1 and D2 dopamine receptor agonist infusion in prelimbic cortex is required to foster extinction of amphetamine-induced conditioned place preference. Behav Brain Res, 392, 112716.

Leão, R. N., Mikulovic, S., Leão, K. E., Munguba, H., Gezelius, H., Enjin, A., Patra, K., Eriksson, A., Loew, L. M., & Tort, A. B. (2012). OLM interneurons differentially modulate CA3 and entorhinal inputs to hippocampal CA1 neurons. Nat Neurosci, 15(11), 1524-1530.

Ledonne, A., Mango, D., Latagliata, E. C., Chiacchierini, G., Nobili, A., Nisticò, R., D'Amelio, M., Puglisi-Allegra, S., & Mercuri, N. B. (2018). Neuregulin 1/ErbB signalling modulates hippocampal mGluRI-dependent LTD and object recognition memory. Pharmacol Res, 130, 12-24. doi:10.1016/j.phrs.2018.02.003

LeGates, T. A., Kvarta, M. D., Tooley, J. R., Francis, T. C., Lobo, M. K., Creed, M. C., & Thompson, S. M. (2018). Reward behaviour is regulated by the strength of hippocampus-nucleus accumbens synapses. Nature, 564(7735), 258-262. doi:10.1038/s41586-018-0740-8

Leri, F., & Rizos, Z. (2005). Reconditioning of drug-related cues: a potential contributor to relapse after drug reexposure. Pharmacol Biochem Behav, 80(4), 621-630. doi:10.1016/j.pbb.2005.01.013

Leshner, A. I. (1997). Addiction is a brain disease, and it matters. Sci, 278(5335), 45-47.

Letsinger, A. C., Gu, Z., & Yakel, J. L. (2021). α7 nicotinic acetylcholine receptors in the hippocampal circuit: taming complexity. Trends Neurosci.

Levin, E. D. (2013). Complex relationships of nicotinic receptor actions and cognitive functions. Biochem Pharmacol, 86(8), 1145-1152.

Levita, L., & Muzzio, I. A. (2010). Role of the hippocampus in goal-oriented tasks requiring retrieval of spatial versus non-spatial information. Neurobiol Learn Mem, 93(4), 581-588. doi:10.1016/j.nlm.2010.02.006

Leyrer-Jackson, J. M., Hood, L. E., & Olive, M. F. (2021). Alcohol consumption preferentially activates a subset of pro-opiomelanocortin (POMC) producing neurons targeting the amygdala. Neuropharmacol, 195, 108674. doi:10.1016/j.neuropharm.2021.108674

Li, Y. J., Ping, X. J., Qi, C., Shen, F., Sun, L. L., Sun, X. W., Ge, F. F., Xing, G. G., & Cui, C. L. (2017). Re-exposure to morphine-associated context facilitated long-term potentiation in the vSUB-NAc glutamatergic pathway via GluN2B-containing receptor activation. Addict Biol, 22(2), 435-445.

Lisman, J., Schulman, H., & Cline, H. (2002). The molecular basis of CaMKII function in synaptic and behavioural memory. Nat Rev Neurosci, 3(3), 175-190.

Lisman, J. E., & Grace, A. A. (2005). The hippocampal-VTA loop: controlling the entry of information into long-term memory. Neuron, 46(5), 703-713. doi:10.1016/j.neuron.2005.05.002

Livingstone, P. D., & Wonnacott, S. (2009). Nicotinic acetylcholine receptors and the ascending dopamine pathways. Biochem Pharmacol, 78(7), 744-755. doi:10.1016/j.bcp.2009.06.004

Livingstone, P. D., Dickinson, J. A., Srinivasan, J., Kew, J. N., & Wonnacott, S. (2010). Glutamate-dopamine crosstalk in the rat prefrontal cortex is modulated by Alpha7 nicotinic receptors and potentiated by PNU-120596. J Mol Neurosci, 40(1-2), 172-176. doi:10.1007/s12031-009-9232-5

Lonergan, M. E., Gafford, G. M., Jarome, T. J., & Helmstetter, F. J. (2010). Time-dependent expression of Arc and zif268 after acquisition of fear conditioning. Neural Plast, 2010, 139891. doi:10.1155/2010/139891

Luo, A. H., Tahsili-Fahadan, P., Wise, R. A., Lupica, C. R., & Aston-Jones, G. (2011). Linking context with reward: a functional circuit from hippocampal CA3 to ventral tegmental area. Sci, 333(6040), 353-357. doi:10.1126/science.1204622

Luscher, C., & Malenka, R. C. (2011). Drug-evoked synaptic plasticity in addiction: from molecular changes to circuit remodeling. Neuron, 69(4), 650-663. doi:10.1016/j.neuron.2011.01.017

Lutas, A., Kucukdereli, H., Alturkistani, O., Carty, C., Sugden, A. U., Fernando, K., Diaz, V., Flores-Maldonado, V., & Andermann, M. L. (2019). State-specific gating of salient cues by midbrain dopaminergic input to basal amygdala. Nat Neurosci, 22(11), 1820-1833.

Ma, L., Turner, D., Zhang, J., Wang, Q., Wang, M., Shen, J., Zhang, S., & Wu, J. (2014). Deficits of synaptic functions in hippocampal slices prepared from aged mice null α7 nicotinic acetylcholine receptors. Neurosci Lett, 570, 97-101.

Madayag, A. C., Gomez, D., Anderson, E. M., Ingebretson, A. E., Thomas, M. J., & Hearing, M. C. (2019). Cell-type and region-specific nucleus accumbens AMPAR plasticity associated with morphine reward, reinstatement, and spontaneous withdrawal. Brain Struct Funct, 224(7), 2311-2324.

Maldonado, C., Rodriguez-Arias, M., Castillo, A., Aguilar, M., & Minarro, J. (2007). Effect of memantine and CNQX in the acquisition, expression and reinstatement of cocaine-induced conditioned place preference. Prog Neuropsychopharmacol Bio, 31(4), 932-939.

Malenka, R. C., & Nicoll, R. A. (1999). Long-term potentiation--a decade of progress? Sci, 285(5435), 1870-1874.

Malinow, R., Mainen, Z. F., & Hayashi, Y. (2000). LTP mechanisms: from silence to four-lane traffic. Curr Opin Neurobiol, 10(3), 352-357.

McDonald, A. J., & Mott, D. D. (2017). Functional neuroanatomy of amygdalohippocampal interconnections and their role in learning and memory. J Neurosci Res, 95(3), 797-820. doi:10.1002/jnr.23709

McGarry, L. M., & Carter, A. G. (2017). Prefrontal cortex drives distinct projection neurons in the basolateral amygdala. Cell Rep, 21(6), 1426-1433.

McGlinchey, E. M., & Aston-Jones, G. (2018). Dorsal hippocampus drives context-induced cocaine seeking via inputs to lateral septum. Neuropsychopharmacol, 43(5), 987-1000. doi:10.1038/npp.2017.144

McKay, B. E., Placzek, A. N., & Dani, J. A. (2007). Regulation of synaptic transmission and plasticity by neuronal nicotinic acetylcholine receptors. Biochem Pharmacol, 74(8), 1120-1133.

McKinney, M., Coyle, J. T., & Hedreen, J. C. (1983). Topographic analysis of the innervation of the rat neocortex and hippocampus by the basal forebrain cholinergic system. J Comp Neurol, 217(1), 103-121. doi:10.1002/cne.902170109

McLean, S. L., Grayson, B., Marsh, S., Zarroug, S. H., Harte, M. K., & Neill, J. C. (2016). Nicotinic α7 and α4β2 agonists enhance the formation and retrieval of recognition memory: Potential mechanisms for cognitive performance enhancement in neurological and psychiatric disorders. Behav Brain Res, 302, 73-80. doi:10.1016/j.bbr.2015.08.037

McReynolds, J. R., Taylor, A., Vranjkovic, O., Ambrosius, T., Derricks, O., Nino, B., Kurtoglu, B., Wheeler, R. A., Baker, D. A., & Gasser, P. J. (2017). Corticosterone potentiation of cocaine-induced reinstatement of conditioned place preference in mice is mediated by blockade of the organic cation transporter 3. Neuropsychopharmacol, 42(3), 757-765.

McReynolds, J. R., Christianson, J. P., Blacktop, J. M., & Mantsch, J. R. (2018). What does the Fos say? Using Fos-based approaches to understand the contribution of stress to substance use disorders. Neurobiol Stress, 9, 271-285. doi:10.1016/j.ynstr.2018.05.004

Means, L. W., Holsten, R. D., Long, M., & High, K. M. (1996). Scopolamine-and morphine-induced deficits in water maze alternation: failure to attenuate with glucose. Neurobiol Learn Mem, 66(2), 167-175.

Mesulam, M. M., Mufson, E. J., Wainer, B. H., & Levey, A. I. (1983). Central cholinergic pathways in the rat: an overview based on an alternative nomenclature (Ch1-Ch6). Neurosci, 10(4), 1185-1201. doi:10.1016/0306-4522(83)90108-2

Miles, R., Tóth, K., Gulyás, A. I., Hájos, N., & Freund, T. F. (1996). Differences between somatic and dendritic inhibition in the hippocampus. Neuron, 16(4), 815-823. doi:10.1016/s0896-6273(00)80101-4

Mineur, Y. S., Mose, T. N., Blakeman, S., & Picciotto, M. R. (2018). Hippocampal alpha7 nicotinic ACh receptors contribute to modulation of depression-like behaviour in C57BL/6J mice. Brit J Pharmacol, 175(11), 1903-1914. doi:10.1111/bph.13769

Miyamoto, E. (2006). Molecular mechanism of neuronal plasticity: induction and maintenance of long-term potentiation in the hippocampus. J Pharmacol Sci, 100(5), 433-442.

Mogenson, G. J., Jones, D. L., & Yim, C. Y. (1980). From motivation to action: functional interface between the limbic system and the motor system. Prog Neurobiol, 14(2-3), 69-97.

Montanari, C., Stendardo, E., De Luca, M. T., Meringolo, M., Contu, L., & Badiani, A. (2015). Differential vulnerability to relapse into heroin versus cocaine-seeking as a function of setting. Psychopharmacol, 232(13), 2415-2424. doi:10.1007/s00213-015-3877-2

Morón, J. A., Abul-Husn, N. S., Rozenfeld, R., Dolios, G., Wang, R., & Devi, L. A. (2007). Morphine administration alters the profile of hippocampal postsynaptic density-associated proteins: a proteomics study focusing on endocytic proteins. Mol Cel Proteomics, 6(1), 29-42.

Morris, R. G., Garrud, P., Rawlins, J. a., & O'Keefe, J. (1982). Place navigation impaired in rats with hippocampal lesions. Nature, 297(5868), 681-683.

Moser, M.-B., Trommald, M., & Andersen, P. (1994). An increase in dendritic spine density on hippocampal CA1 pyramidal cells following spatial learning in adult rats suggests the formation of new synapses. PNAS, 91(26), 12673-12675.

Moser, M.-B., Moser, E. I., Forrest, E., Andersen, P., & Morris, R. (1995). Spatial learning with a minislab in the dorsal hippocampus. PNAS, 92(21), 9697-9701.

Moser, M. B., & Moser, E. I. (1998). Functional differentiation in the hippocampus. Hippocampus, 8(6), 608-619.

Muller, D., Toni, N., & Buchs, P. A. (2000). Spine changes associated with long-term potentiation. Hippocampus, 10(5), 596-604.

Nair, A. B., & Jacob, S. (2016). A simple practice guide for dose conversion between animals and human. JBCP, 7(2), 27.

Napier, T. C., Herrold, A. A., & de Wit, H. (2013). Using conditioned place preference to identify relapse prevention medications. Neurosci Biobehav Rev, 37(9 Pt A), 2081-2086. doi:10.1016/j.neubiorev.2013.05.002

Nestler, E. J. (2005). The neurobiology of cocaine addiction. Sci Pract Perspect, 3(1), 4-10. doi:10.1151/spp05314

Neves, G., Cooke, S. F., & Bliss, T. V. (2008). Synaptic plasticity, memory and the hippocampus: a neural network approach to causality. Nat Rev Neurosci, 9(1), 65-75.

Nikiforuk, A., Kos, T., Potasiewicz, A., & Popik, P. (2015). Positive allosteric modulation of alpha 7 nicotinic acetylcholine receptors enhances recognition memory and cognitive flexibility in rats. Eur Neuropsychopharmacol, 25(8), 1300-1313. doi:10.1016/j.euroneuro.2015.04.018

Nyakas, C., Luiten, P. G., Spencer, D. G., & Traber, J. (1987). Detailed projection patterns of septal and diagonal band efferents to the hippocampus in the rat with emphasis on innervation of CA1 and dentate gyrus. Brain Res Bull, 18(4), 533-545. doi:10.1016/0361-9230(87)90117-1

O'Brien, C. P., Childress, A. R., McLellan, A. T., & Ehrman, R. (1992). Classical conditioning in drug-dependent humans. Ann N Y Acad Sci, 654, 400-415. doi:10.1111/j.1749-6632.1992.tb25984.x

O'Keefe, J., & Dostrovsky, J. (1971). The hippocampus as a spatial map: preliminary evidence from unit activity in the freely-moving rat. Brain Res.

O'Keefe, J., & Speakman, A. (1987). Single unit activity in the rat hippocampus during a spatial memory task. Exp Brain Res, 68(1), 1-27.

Oh, M. M., Kuo, A. G., Wu, W. W., Sametsky, E. A., & Disterhoft, J. F. (2003). Watermaze learning enhances excitability of CA1 pyramidal neurons. J Neurophysiol, 90(4), 2171-2179.

Orlandi, C., La Via, L., Bonini, D., Mora, C., Russo, I., Barbon, A., & Barlati, S. (2011). AMPA receptor regulation at the mRNA and protein level in rat primary cortical cultures. PLoS One, 6(9), e25350.

Orr-Urtreger, A., Göldner, F. M., Saeki, M., Lorenzo, I., Goldberg, L., De Biasi, M., Dani, J. A., Patrick, J. W., & Beaudet, A. L. (1997). Mice Deficient in the α7 Neuronal Nicotinic Acetylcholine Receptor Lack α-Bungarotoxin Binding Sites and Hippocampal Fast Nicotinic Currents. J Neurosci, 17(23), 9165-9171. doi:10.1523/jneurosci.17-23-09165.1997

Orsini, C. A., Kim, J. H., Knapska, E., & Maren, S. (2011). Hippocampal and prefrontal projections to the basal amygdala mediate contextual regulation of fear after extinction. J Neurosci, 31(47), 17269-17277. doi:10.1523/JNEUROSCI.4095-11.2011

Osborne, D. M., Pearson-Leary, J., & McNay, E. C. (2015). The neuroenergetics of stress hormones in the hippocampus and implications for memory. Front Neurosci, 9, 164. doi:10.3389/fnins.2015.00164

Padilla-Coreano, N., Bolkan, S. S., Pierce, G. M., Blackman, D. R., Hardin, W. D., Garcia-Garcia, A. L., Spellman, T. J., & Gordon, J. A. (2016). Direct Ventral Hippocampal-Prefrontal Input Is Required for Anxiety-Related Neural Activity and Behavior. Neuron, 89(4), 857-866. doi:10.1016/j.neuron.2016.01.011

Palandri, J., Smith, S. L., Heal, D. J., Wonnacott, S., & Bailey, C. P. (2021). Contrasting effects of the α7 nicotinic receptor antagonist methyllycaconitine in different rat models of heroin reinstatement. J Psychopharmacol, 0269881121991570.

Pałczyńska, M. M., Jindrichova, M., Gibb, A. J., & Millar, N. S. (2012). Activation of α7 nicotinic receptors by orthosteric and allosteric agonists: influence on single-channel kinetics and conductance. Mol Pharmacol, 82(5), 910-917.

Palombo, P., Leao, R. M., Bianchi, P. C., de Oliveira, P. E. C., Planeta, C. D. S., & Cruz, F. C. (2017). Inactivation of the Prelimbic Cortex Impairs the Context-Induced Reinstatement of Ethanol Seeking. Front Pharmacol, 8, 725. doi:10.3389/fphar.2017.00725

Panagis, G., Kastellakis, A., Spyraki, C., & Nomikos, G. (2000). Effects of methyllycaconitine (MLA), an α 7 nicotinic receptor antagonist, on nicotine-and cocaine-induced potentiation of brain stimulation reward. Psychopharmacol, 149(4), 388-396.

Papke, R. L., Kem, W. R., Soti, F., Lopez-Hernandez, G. Y., & Horenstein, N. A. (2009). Activation and desensitization of nicotinic α7-type acetylcholine receptors by benzylidene anabaseines and nicotine. J Pharmacol Expl Ther, 329(2), 791-807.

Papke, R. L., & Lindstrom, J. M. (2020). Nicotinic acetylcholine receptors: Conventional and unconventional ligands and signaling. Neuropharmacol, 168, 108021.

Parikh, V., Pomerleau, F., Huettl, P., Gerhardt, G. A., Sarter, M., & Bruno, J. P. (2004). Rapid assessment of in vivo cholinergic transmission by amperometric detection of changes in extracellular choline levels. Eur J Neurosci, 20(6), 1545-1554.

Park, P., Kang, H., Sanderson, T. M., Bortolotto, Z. A., Georgiou, J., Zhuo, M., Kaang, B. K., & Collingridge, G. L. (2018). The role of calcium-permeable AMPARs in long-term potentiation at principal neurons in the rodent hippocampus. Front Synaptic Neurosci, 10, 42. doi:10.3389/fnsyn.2018.00042

Pascoli, V., Terrier, J., Espallergues, J., Valjent, E., O'Connor, E. C., & Luscher, C. (2014). Contrasting forms of cocaine-evoked plasticity control components of relapse. Nature, 509(7501), 459-464. doi:10.1038/nature13257

Pastor, V., Díaz, F. C., Sanabria, V. C., Dalto, J. F., Antonelli, M. C., & Medina, J. H. (2021). Prefrontal cortex nicotinic receptor inhibition by methyllycaconitine impaired cocaine-associated memory acquisition and retrieval. Behav Brain Res, 406, 113212.

Paul, S., Jeon, W. K., Bizon, J. L., & Han, J.-S. (2015). Interaction of basal forebrain cholinergic neurons with the glucocorticoid system in stress regulation and cognitive impairment. Frontiers Aging Neurosci, 7, 43.

Paxinos, G., & Franklin, K. B. J. (2004). The Mouse Brain in Stereotaxic Coordinates: Academic Press.

Penn, A. C., Zhang, C. L., Georges, F., Royer, L., Breillat, C., Hosy, E., Petersen, J. D., Humeau, Y., & Choquet, D. (2017). Hippocampal LTP and contextual learning require surface diffusion of AMPA receptors. Nature, 549(7672), 384-388. doi:10.1038/nature23658

Perry, C. J., Zbukvic, I., Kim, J. H., & Lawrence, A. J. (2014). Role of cues and contexts on drug-seeking behaviour. Brit J Pharmacol, 171(20), 4636-4672.

Pesti, K., Szabo, A. K., Mike, A., & Vizi, E. S. (2014). Kinetic properties and open probability of α7 nicotinic acetylcholine receptors. Neuropharmacol, 81, 101-115.

Picciotto, M. R., Zoli, M., Rimondini, R., Léna, C., Marubio, L. M., Pich, E. M., Fuxe, K., & Changeux, J.-P. (1998). Acetylcholine receptors containing the β2 subunit are involved in the reinforcing properties of nicotine. Nature, 391(6663), 173-177.

Picciotto, M. R., Higley, M. J., & Mineur, Y. S. (2012). Acetylcholine as a neuromodulator: cholinergic signaling shapes nervous system function and behavior. Neuron, 76(1), 116-129. doi:10.1016/j.neuron.2012.08.036

Pignatelli, M., & Bonci, A. (2015). Role of dopamine neurons in reward and aversion: a synaptic plasticity perspective. Neuron, 86(5), 1145-1157.

Pignatelli, M., Ryan, T. J., Roy, D. S., Lovett, C., Smith, L. M., Muralidhar, S., & Tonegawa, S. (2019). Engram cell excitability state setermines the efficacy of memory retrieval. Neuron, 101(2), 274-284 e275. doi:10.1016/j.neuron.2018.11.029

Pitkänen, A., Pikkarainen, M., Nurminen, N., & Ylinen, A. (2000). Reciprocal connections between the amygdala and the hippocampal formation, perirhinal cortex, and postrhinal cortex in rat: a review. Ann N Y Acad Sci, 911(1), 369-391.

Pogun, S., Yararbas, G., Nesil, T., & Kanit, L. (2017). Sex differences in nicotine preference. J Neurosci Res, 95(1-2), 148-162. doi:10.1002/jnr.23858

Pontieri, F. E., Calò, L., Di Grezia, R., Orzi, F., & Passarelli, F. (1997). Functional correlates of heroin sensitization in the rat brain. Eur J Pharmacol, 335(2-3), 133-137. doi:10.1016/s0014-2999(97)01195-3

Portugal, G. S., Al-Hasani, R., Fakira, A. K., Gonzalez-Romero, J. L., Melyan, Z., McCall, J. G., Bruchas, M. R., & Moron, J. A. (2014). Hippocampal long-term potentiation is disrupted during expression and extinction but is restored after

reinstatement of morphine place preference. J Neurosci, 34(2), 527-538. doi:10.1523/JNEUROSCI.2838-13.2014

Preston, C. J., & Wagner, J. J. (2021). Withdrawal from cocaine conditioning progressively alters AMPA receptor-mediated transmission in the ventral hippocampus. Addict Biol, e1310

Proctor, W. R., Dobelis, P., Moritz, A. T., & Wu, P. H. (2011). Chronic nicotine treatment differentially modifies acute nicotine and alcohol actions on GABA(A) and glutamate receptors in hippocampal brain slices. Brit J Pharmacol, 162(6), 1351-1363. doi:10.1111/j.1476-5381.2010.01141.x

Puglisi-Allegra, S., & Ventura, R. (2012). Prefrontal/accumbal catecholamine system processes emotionally driven attribution of motivational salience. Rev Neurosci, 23(5-6), 509-526.

Radcliffe, K. A., Fisher, J. L., Gray, R., & Dani, J. A. (1999). Nicotinic modulation of glutamate and GABA synaptic transmission in hippocampal neurons. Ann N Y Acad Sci, 868(1), 591-610.

Ramirez, D. R., Bell, G. H., Lasseter, H. C., Xie, X., Traina, S. A., & Fuchs, R. A. (2009). Dorsal hippocampal regulation of memory reconsolidation processes that facilitate drug context-induced cocaine-seeking behavior in rats. Eur J Neurosci, 30(5), 901-912.

Ramirez, S., Tonegawa, S., & Liu, X. (2013). Identification and optogenetic manipulation of memory engrams in the hippocampus. Front Behav Neurosci, 7, 226. doi:10.3389/fnbeh.2013.00226

Rawlins, J. N. P., Feldon, J., & Gray, J. A. (1979). Septo-hippocampal connections and the hippocampal theta rhythm. Exp Brain Res, 37(1), 49-63.

Reijmers, L. G., Perkins, B. L., Matsuo, N., & Mayford, M. (2007). Localization of a stable neural correlate of associative memory. Sci, 317(5842), 1230-1233.

Reiner, D. J., Fredriksson, I., Lofaro, O. M., Bossert, J. M., & Shaham, Y. (2019). Relapse to opioid seeking in rat models: behavior, pharmacology and circuits. Neuropsychopharmacol, 44(3), 465-477. doi:10.1038/s41386-018-0234-2

Robinson, T. E., & Berridge, K. C. (1993). The neural basis of drug craving: an incentive-sensitization theory of addiction. Brain Res Rev, 18(3), 247-291.

Rogers, J. L., & See, R. E. (2007). Selective inactivation of the ventral hippocampus attenuates cue-induced and cocaine-primed reinstatement of drug-seeking in rats. Neurobiol Learn Mem, 87(4), 688-692.

Roncarati, R., Scali, C., Comery, T. A., Grauer, S. M., Aschmi, S., Bothmann, H., Jow, B., Kowal, D., Gianfriddo, M., & Kelley, C. (2009). Procognitive and neuroprotective activity of a novel α7 nicotinic acetylcholine receptor agonist for treatment of neurodegenerative and cognitive disorders. J Pharmacol Exp Therap, 329(2), 459-468.

Rosenblum, K., Futter, M., Voss, K., Erent, M., Skehel, P. A., French, P., Obosi, L., Jones, M. W., & Bliss, T. V. (2002). The role of extracellular regulated kinases I/II in late-phase long-term potentiation. J Neurosci, 22(13), 5432-5441. doi:10.1523/jneurosci.22-13-05432.2002

Roy, D. S., Kitamura, T., Okuyama, T., Ogawa, S. K., Sun, C., Obata, Y., Yoshiki, A., & Tonegawa, S. (2017). Distinct neural circuits for the formation and retrieval of episodic memories. Cell, 170(5), 1000-1012 e1019. doi:10.1016/j.cell.2017.07.013

Royer, S., Sirota, A., Patel, J., & Buzsáki, G. (2010). Distinct representations and theta dynamics in dorsal and ventral hippocampus. J Neurosci, 30(5), 1777-1787. doi:10.1523/jneurosci.4681-09.2010

Rubio, F. J., Quintana-Feliciano, R., Warren, B. L., Li, X., Witonsky, K. F. R., Valle, F. S. D., Selvam, P. V., Caprioli, D., Venniro, M., Bossert, J. M., Shaham, Y., & Hope, B. T. (2019). Prelimbic cortex is a common brain area activated during cue-induced reinstatement of cocaine and heroin seeking in a polydrug self-administration rat model. Eur J Neurosci, 49(2), 165-178. doi:10.1111/ejn.14203

Ruediger, S., Spirig, D., Donato, F., & Caroni, P. (2012). Goal-oriented searching mediated by ventral hippocampus early in trial-and-error learning. Nat Neurosci, 15(11), 1563-1571. doi:10.1038/nn.3224

Russo, S. J., & Nestler, E. J. (2013). The brain reward circuitry in mood disorders. Nat Rev Neurosci, 14(9), 609-625.

Sakimoto, Y., Mizuno, J., Kida, H., Kamiya, Y., Ono, Y., & Mitsushima, D. (2019). Learning promotes subfield-specific synaptic diversity in hippocampal CA1 neurons. Cereb Cortex, 29(5), 2183-2195. doi:10.1093/cercor/bhz022

Salamone, J. D., & Correa, M. (2012). The mysterious motivational functions of mesolimbic dopamine. Neuron, 76(3), 470-485.

Saleeba, C., Dempsey, B., Le, S., Goodchild, A., & McMullan, S. (2019). A student's guide to neural circuit tracing. Front Neurosci, 13, 897. doi:10.3389/fnins.2019.00897

Samaha, A. N., Mallet, N., Ferguson, S. M., Gonon, F., & Robinson, T. E. (2004). The rate of cocaine administration alters gene regulation and behavioral plasticity: implications for addiction. J Neurosci, 24(28), 6362-6370. doi:10.1523/jneurosci.1205-04.2004

Santos, T. B., Wallau, A. E., Kramer-Soares, J. C., & Oliveira, M. G. M. (2020). Functional interaction of ventral hippocampal CA1 region and prelimbic cortex contributes to the encoding of contextual fear association of stimuli separated in time. Neurobiol Learn Mem, 171, 107216. doi:10.1016/j.nlm.2020.107216

Sarter, M., Parikh, V., & Howe, W. M. (2009). Phasic acetylcholine release and the volume transmission hypothesis: time to move on. Nat Rev Neurosci, 10(5), 383-390. doi:10.1038/nrn2635

Schuster, C. R., & Thompson, T. (1969). Self administration of and behavioral dependence on drugs. Annu Rev Pharmacol, 9(1), 483-502.

Secci, M. E., Auber, A., Panlilio, L. V., Redhi, G. H., Thorndike, E. B., Schindler, C. W., Schwarcz, R., Goldberg, S. R., & Justinova, Z. (2017). Attenuating nicotine reinforcement and relapse by enhancing endogenous brain levels of kynurenic acid in rats and squirrel monkeys. Neuropsychopharmacol, 42(8), 1619-1629. doi:10.1038/npp.2017.21

Semyanov, A., & Kullmann, D. M. (2000). Modulation of GABAergic signaling among interneurons by metabotropic glutamate receptors. Neuron, 25(3), 663-672.

Sgambato, V., Abo, V., Rogard, M., Besson, M., & Deniau, J. (1997). Effect of electrical stimulation of the cerebral cortex on the expression of the Fos protein in the basal ganglia. Neurosci, 81(1), 93-112.

Shaham, Y., Shalev, U., Lu, L., De Wit, H., & Stewart, J. (2003). The reinstatement model of drug relapse: history, methodology and major findings. Psychopharmacol, 168(1), 3-20.

Shalev, U., Grimm, J. W., & Shaham, Y. (2002). Neurobiology of relapse to heroin and cocaine seeking: a review. Pharmacol Rev, 54(1), 1-42. doi:10.1124/pr.54.1.1

Sharma, G., Grybko, M., & Vijayaraghavan, S. (2008). Action potential-independent and nicotinic receptor-mediated concerted release of multiple quanta at hippocampal CA3–mossy fiber synapses. J Neurosci, 28(10), 2563-2575.

Sharp, B. M. (2019). Basolateral amygdala, nicotinic cholinergic receptors, and nicotine: Pharmacological effects and addiction in animal models and humans. Eur J Neurosci, 50(3), 2247-2254. doi:10.1111/ejn.13970

Shen, J. X., & Yakel, J. L. (2009). Nicotinic acetylcholine receptor-mediated calcium signaling in the nervous system. Acta Pharmacol Sin, 30(6), 673-680. doi:10.1038/aps.2009.64

Shen, L., Cui, W. Y., Chen, R. Z., & Wang, H. (2016). Differential modulation of GABAA and NMDA receptors by alpha7-nicotinic receptor desensitization in cultured rat hippocampal neurons. Acta Pharmacol Sin, 37(3), 312-321. doi:10.1038/aps.2015.106

Shukla, A., Beroun, A., Panopoulou, M., Neumann, P. A., Grant, S. G., Olive, M. F., Dong, Y., & Schluter, O. M. (2017). Calcium-permeable AMPA receptors and silent synapses in cocaine-conditioned place preference. EMBO J, 36(4), 458-474. doi:10.15252/embj.201695465

Sieburg, M. C., Ziminski, J. J., Margetts-Smith, G., Reeve, H. M., Brebner, L. S., Crombag, H. S., & Koya, E. (2019). Reward devaluation attenuates cue-evoked sucrose seeking and is sssociated with the elimination of excitability differences between ensemble and non-ensemble neurons in the nucleus accumbens. eNeuro, 6(6). doi:10.1523/ENEURO.0338-19.2019

Sine, S. M., & Engel, A. G. (2006). Recent advances in Cys-loop receptor structure and function. Nature, 440(7083), 448-455.

Singh, P. K., & Lutfy, K. (2017). Nicotine pretreatment reduced cocaine-induced CPP and its reinstatement in a sex-and dose-related manner in adult C57BL/6J mice. Pharmacol Biochem and Behav, 159, 84-89.

Smith, J. E., Guerin, G. F., Co, C., Barr, T. S., & Lane, J. D. (1985). Effects of 6-OHDA lesions of the central medial nucleus accumbens on rat intravenous morphine self-administration. Pharmacol Biochem Beh, 23(5), 843-849.

Solinas, M., Scherma, M., Fattore, L., Stroik, J., Wertheim, C., Tanda, G., Fratta, W., & Goldberg, S. R. (2007). Nicotinic alpha 7 receptors as a new target for treatment of cannabis abuse. J Neurosci, 27(21), 5615-5620. doi:10.1523/jneurosci.0027-07.2007

Stoiljkovic, M., Kelley, C., Nagy, D., & Hajos, M. (2015). Modulation of hippocampal neuronal network oscillations by alpha7 nACh receptors. Biochem Pharmacol, 97(4), 445-453. doi:10.1016/j.bcp.2015.06.031

Stone, T. W. (2021). Relationships and Interactions between Ionotropic Glutamate Receptors and Nicotinic Receptors in the CNS. Neurosci, 468, 321-365. doi:10.1016/j.neuroscience.2021.06.007

Stramiello, M., & Wagner, J. J. (2010). Cocaine enhancement of long-term potentiation in the CA1 region of rat hippocampus: lamina-specific mechanisms of action. Synapse, 64(8), 644-648.

Strange, B. A., Witter, M. P., Lein, E. S., & Moser, E. I. (2014). Functional organization of the hippocampal longitudinal axis. Nat Rev Neurosci, 15(10), 655-669. doi:10.1038/nrn3785

Sun, L., Tang, Y., Yan, K., Yu, J., Zou, Y., Xu, W., Xiao, K., Zhang, Z., Li, W., & Wu, B. (2019). Differences in neurotropism and neurotoxicity among retrograde viral tracers. Mol Neurodegener, 14(1), 1-24.

Swerdlow, N. R., Gilbert, D., & Koob, G. F. (1989). Conditioned drug effects on spatial preference. Psychopharmacol (pp. 399-446)

Szabo, A. K., Pesti, K., Mike, A., & Vizi, E. S. (2014). Mode of action of the positive modulator PNU-120596 on α7 nicotinic acetylcholine receptors. Neuropharmacol, 81, 42-54.

Szadzinska, W., Danielewski, K., Kondrakiewicz, K., Andraka, K., Nikolaev, E., Mikosz, M., & Knapska, E. (2021). Hippocampal inputs in the prelimbic cortex curb fear after extinction. J Neurosci, 41(44), 9129-9140. doi:10.1523/JNEUROSCI.0764-20.2021

Taly, A., Corringer, P. J., Guedin, D., Lestage, P., & Changeux, J. P. (2009). Nicotinic receptors: allosteric transitions and therapeutic targets in the nervous system. Nat Rev Drug Discov, 8(9), 733-750. doi:10.1038/nrd2927

Tang, B., Luo, D., Yang, J., Xu, X.-Y., Zhu, B.-L., Wang, X.-F., Yan, Z., & Chen, G.-J. (2015). Modulation of AMPA receptor mediated current by nicotinic acetylcholine receptor in layer I neurons of rat prefrontal cortex. Sci Rep, 5(1), 1-14.

Taube, J. S. (2007). The head direction signal: origins and sensory-motor integration. Annu. Rev. Neurosci., 30, 181-207.

Teles-Grilo Ruivo, L. M., & Mellor, J. R. (2013). Cholinergic modulation of hippocampal network function. Front Synaptic Neurosci, 5, 2. doi:10.3389/fnsyn.2013.00002

Tervo, D. G. R., Hwang, B.-Y., Viswanathan, S., Gaj, T., Lavzin, M., Ritola, K. D., Lindo, S., Michael, S., Kuleshova, E., & Ojala, D. (2016). A designer AAV variant permits efficient retrograde access to projection neurons. Neuron, 92(2), 372-382.

Thanos, P. K., Malave, L., Delis, F., Mangine, P., Kane, K., Grunseich, A., Vitale, M., Greengard, P., & Volkow, N. D. (2016). Knockout of p11 attenuates the acquisition and reinstatement of cocaine conditioned place preference in male but not in female mice. Synapse, 70(7), 293-301. doi:10.1002/syn.21904

Thomas, M. J., Beurrier, C., Bonci, A., & Malenka, R. C. (2001). Long-term depression in the nucleus accumbens: a neural correlate of behavioral sensitization to cocaine. Nat Neurosci, 4(12), 1217-1223. doi:10.1038/nn757

Thomsen, M., Mikkelsen, J., Timmermann, D., Peters, D., Hay-Schmidt, A., Martens, H., & Hansen, H. (2008). The selective α7 nicotinic acetylcholine receptor agonist A-582941 activates immediate early genes in limbic regions of the forebrain: Differential effects in the juvenile and adult rat. Neurosci, 154(2), 741-753.

Tian, L., Akerboom, J., Schreiter, E. R., & Looger, L. L. (2012). Neural activity imaging with genetically encoded calcium indicators. Prog Brain Res, 196, 79-94.

Timmermann, D. B., Grønlien, J. H., Kohlhaas, K. L., Nielsen, E. Ø., Dam, E., Jørgensen, T. D., Ahring, P. K., Peters, D., Holst, D., & Chrsitensen, J. K. (2007). An allosteric modulator of the α7 nicotinic acetylcholine receptor possessing cognition-enhancing properties in vivo. J Pharmacol Expl Ther, 323(1), 294-307.

Ting, J. T., Lee, B. R., Chong, P., Soler-Llavina, G., Cobbs, C., Koch, C., Zeng, H., & Lein, E. (2018). Preparation of acute brain slices using an optimized N-Methyl-D-glucamine protective recovery method. JoVE, 132. doi:10.3791/53825

Titulaer, J., Björkholm, C., Feltmann, K., Malmlöf, T., Mishra, D., Bengtsson Gonzales, C., Schilström, B., & Konradsson-Geuken, Å. (2021). The importance of ventral hippocampal dopamine and norepinephrine in recognition memory. Front Behav Neurosci, 15, 667244. doi:10.3389/fnbeh.2021.667244

Titus, D. J., Johnstone, T., Johnson, N. H., London, S. H., Chapalamadugu, M., Hogenkamp, D., Gee, K. W., & Atkins, C. M. (2019). Positive allosteric modulation of the α7 nicotinic acetylcholine receptor as a treatment for cognitive deficits after traumatic brain injury. PLoS One, 14(10), e0223180.

Torquatto, K. I., Menegolla, A. P., Popik, B., Casagrande, M. A., & de Oliveira Alvares, L. (2019). Role of calcium-permeable AMPA receptors in memory consolidation, retrieval and updating. Neuropharmacol, 144, 312-318.

Tramullas, M., Martínez-Cué, C., & Hurlé, M. A. (2008). Chronic administration of heroin to mice produces up-regulation of brain apoptosis-related proteins and impairs spatial learning and memory. Neuropharmacol, 54(4), 640-652.

Tropea, T. F., Kosofsky, B. E., & Rajadhyaksha, A. M. (2008). Enhanced CREB and DARPP-32 phosphorylation in the nucleus accumbens and CREB, ERK, and GluR1 phosphorylation in the dorsal hippocampus is associated with cocaine-conditioned place preference behavior. J Neurochem, 106(4), 1780-1790.

Truett, G. E., Heeger, P., Mynatt, R. L., Truett, A. A., Walker, J. A., & Warman, M. L. (2000). Preparation of PCR-quality mouse genomic DNA with Hot Sodium Hydroxide and Tris (HotSHOT). BioTechniques, 29(1), 52-54. doi:10.2144/00291bm09

Tu, W., Cook, A., Scholl, J. L., Mears, M., Watt, M. J., Renner, K. J., & Forster, G. L. (2014). Serotonin in the ventral hippocampus modulates anxiety-like behavior during amphetamine withdrawal. Neurosci, 281, 35-43. doi:10.1016/j.neuroscience.2014.09.019

Tully, T., Bourtchouladze, R., Scott, R., & Tallman, J. (2003). Targeting the CREB pathway for memory enhancers. Nat Rev Drug Discov, 2(4), 267-277.

Twining, R. C., Lepak, K., Kirry, A. J., & Gilmartin, M. R. (2020). Ventral hippocampal input to the prelimbic cortex dissociates the context from the cue association in trace fear memory. J Neurosci, 40(16), 3217-3230. doi:10.1523/JNEUROSCI.1453-19.2020

Tzschentke, T. M. (2007). Review on CPP: Measuring reward with the conditioned place preference (CPP) paradigm: update of the last decade. Addict Biol, 12(3-4), 227-462.

Udakis, M., Wright, V. L., Wonnacott, S., & Bailey, C. P. (2016). Integration of inhibitory and excitatory effects of alpha7 nicotinic acetylcholine receptor activation in the prelimbic cortex regulates network activity and plasticity. Neuropharmacol, 105, 618-629. doi:10.1016/j.neuropharm.2016.02.028

Uteshev, V. V. (2012). α7 nicotinic ACh receptors as a ligand-gated source of Ca 2+ ions: the search for a Ca 2+ optimum. Calcium Signal, 603-638.

Valenti, O., Lodge, D. J., & Grace, A. A. (2011). Aversive stimuli alter ventral tegmental area dopamine neuron activity via a common action in the ventral hippocampus. J Neurosci, 31(11), 4280-4289.

Van den Oever, M. C., Goriounova, N. A., Wan Li, K., Van der Schors, R. C., Binnekade, R., Schoffelmeer, A. N., Mansvelder, H. D., Smit, A. B., Spijker, S., & De Vries, T. J. (2008). Prefrontal cortex AMPA receptor plasticity is crucial for cue-induced relapse to heroin-seeking. Nat Neurosci, 11(9), 1053-1058.

Van Der Meer, M. A., & Redish, A. D. (2011). Theta phase precession in rat ventral striatum links place and reward information. J Neurosci, 31(8), 2843-2854.

van Goethem, N. P., Paes, D., Puzzo, D., Fedele, E., Rebosio, C., Gulisano, W., Palmeri, A., Wennogle, L. P., Peng, Y., & Bertrand, D. (2019). Antagonizing α7 nicotinic receptors with methyllycaconitine (MLA) potentiates receptor activity and memory acquisition. Cell Signal, 62, 109338.

Van Groen, T., & Wyss, J. M. (2003). Connections of the retrosplenial granular b cortex in the rat. J Comp Neurol, 463(3), 249-263.

van Huijstee, A. N., & Mansvelder, H. D. (2014). Glutamatergic synaptic plasticity in the mesocorticolimbic system in addiction. Front Cell Neurosci, 8, 466. doi:10.3389/fncel.2014.00466

Vanderschuren, L. J., & Everitt, B. J. (2004). Drug seeking becomes compulsive after prolonged cocaine self-administration. Sci, 305(5686), 1017-1019.

Ventura, R., Alcaro, A., & Puglisi-Allegra, S. (2005). Prefrontal cortical norepinephrine release is critical for morphine-induced reward, reinstatement and dopamine release in the nucleus accumbens. Cereb Cortex, 15(12), 1877-1886.

Wallace, T. L., Callahan, P. M., Tehim, A., Bertrand, D., Tombaugh, G., Wang, S., Xie, W., Rowe, W. B., Ong, V., & Graham, E. (2011). RG3487, a novel nicotinic α7 receptor partial agonist, improves cognition and sensorimotor gating in rodents. J Pharmacol Expl Ther, 336(1), 242-253.

Wallace, T. L., & Porter, R. H. (2011). Targeting the nicotinic alpha7 acetylcholine receptor to enhance cognition in disease. Biochem Pharmacol, 82(8), 891-903. doi:10.1016/j.bcp.2011.06.034

Wang, D., Noda, Y., Tsunekawa, H., Zhou, Y., Miyazaki, M., Senzaki, K., & Nabeshima, T. (2007). Behavioural and neurochemical features of olfactory bulbectomized rats resembling depression with comorbid anxiety. Behav Brain Res, 178(2), 262-273. doi:10.1016/j.bbr.2007.01.003

Ward, J. M., Cockcroft, V. B., Lunt, G. G., Smillie, F. S., & Wonnacott, S. (1990). Methyllycaconitine: a selective probe for neuronal alpha-bungarotoxin binding sites. FEBS Lett, 270(1-2), 45-48. doi:10.1016/0014-5793(90)81231-c

Warren, B. L., Mendoza, M. P., Cruz, F. C., Leao, R. M., Caprioli, D., Rubio, F. J., Whitaker, L. R., McPherson, K. B., Bossert, J. M., Shaham, Y., & Hope, B. T. (2016). Distinct Fos-expressing neuronal ensembles in the ventromedial prefrontal cortex

mediate food reward and extinction memories. J Neurosci, 36(25), 6691-6703. doi:10.1523/JNEUROSCI.0140-16.2016

Whitaker, L. R., de Oliveira, P. E. C., McPherson, K. B., Fallon, R. V., Planeta, C. S., Bonci, A., & Hope, B. T. (2016). Associative learning drives the formation of silent synapses in neuronal ensembles of the nucleus accumbens. Biol Psychiatry, 80(3), 246-256.

Whitaker, L. R., & Hope, B. T. (2018). Chasing the addicted engram: identifying functional alterations in Fos-expressing neuronal ensembles that mediate drug-related learned behavior. Learn Mem, 25(9), 455-460. doi:10.1101/lm.046698.117

White, N. M. (2011). Reward: what is it? How can it be inferred from behavior? Neurobiol Sens Reward, 45-60.

Wills, L., Ables, J. L., Braunscheidel, K. M., Caligiuri, S. P. B., Elayouby, K. S., Fillinger, C., Ishikawa, M., Moen, J. K., & Kenny, P. J. (2022). Neurobiological mechanisms of nicotine reward and aversion. Pharmacol Rev, 74(1), 271-310. doi:10.1124/pharmrev.121.000299

Winocur, G., Rawlins, J. N., & Gray, J. A. (1987). The hippocampus and conditioning to contextual cues. Behav Neurosci, 101(5), 617.

Wise, R. A. (2008). Dopamine and reward: the anhedonia hypothesis 30 years on. Neurotox Res, 14(2-3), 169-183. doi:10.1007/bf03033808

Wise, R. A., & Koob, G. F. (2014). The development and maintenance of drug addiction. Neuropsychopharmacol, 39(2), 254-262. doi:10.1038/npp.2013.261

Wise, R. A., & Robble, M. A. (2020). Dopamine and Addiction. Annu Rev Psychol, 71, 79-106. doi:10.1146/annurev-psych-010418-103337

Witten, I. B., Lin, S.-C., Brodsky, M., Prakash, R., Diester, I., Anikeeva, P., Gradinaru, V., Ramakrishnan, C., & Deisseroth, K. (2010). Cholinergic interneurons control local circuit activity and cocaine conditioning. Sci, 330(6011), 1677-1681.

Wright, V. L., Georgiou, P., Bailey, A., Heal, D. J., Bailey, C. P., & Wonnacott, S. (2019). Inhibition of alpha7 nicotinic receptors in the ventral hippocampus selectively attenuates reinstatement of morphine-conditioned place preference and associated changes in AMPA receptor binding. Addict Biol, 24(4), 590-603. doi:10.1111/adb.12624

Xia, Y., Portugal, G. S., Fakira, A. K., Melyan, Z., Neve, R., Lee, H. T., Russo, S. J., Liu, J., & Moron, J. A. (2011). Hippocampal GluA1-containing AMPA receptors mediate context-dependent sensitization to morphine. J Neurosci, 31(45), 16279-16291. doi:10.1523/JNEUROSCI.3835-11.2011

Xie, X., Ramirez, D. R., Lasseter, H. C., & Fuchs, R. A. (2010). Effects of mGluR1 antagonism in the dorsal hippocampus on drug context-induced reinstatement of cocaine-seeking behavior in rats. Psychopharmacol, 208(1), 1-11. doi:10.1007/s00213-009-1700-7

Xu, C., Krabbe, S., Gründemann, J., Botta, P., Fadok, J. P., Osakada, F., Saur, D., Grewe, B. F., Schnitzer, M. J., Callaway, E. M., & Lüthi, A. (2016). Distinct hippocampal pathways mediate dissociable roles of context in memory retrieval. Cell, 167(4), 961-972.e916. doi:10.1016/j.cell.2016.09.051

Xue, Y. X., Chen, Y. Y., Zhang, L. B., Zhang, L. Q., Huang, G. D., Sun, S. C., Deng, J. H., Luo, Y. X., Bao, Y. P., Wu, P., Han, Y., Hope, B. T., Shaham, Y., Shi, J., & Lu, L. (2017). Selective inhibition of amygdala neuronal ensembles encoding nicotine-associated memories inhibits nicotine preference and relapse. Biol Psychiatry, 82(11), 781-793. doi:10.1016/j.biopsych.2017.04.017

Yang, A. K., Mendoza, J. A., Lafferty, C. K., Lacroix, F., & Britt, J. P. (2020). Hippocampal input to the nucleus accumbens shell enhances food palatability. Biol Psychiatry, 87(7), 597-608. doi:10.1016/j.biopsych.2019.09.007

Yang, X., Li, G., Xue, Q., Luo, Y., Wang, S., Xia, Y., Zhuang, L., & Yu, B. (2017). Calcineurin/P-ERK/Egr-1 pathway is involved in fear memory impairment after isoflurane exposure in mice. Sci Rep, 7(1), 13947. doi:10.1038/s41598-017-13975-z

Yao, F., Zhang, E., Gao, Z., Ji, H., Marmouri, M., & Xia, X. (2018). Did you choose appropriate tracer for retrograde tracing of retinal ganglion cells? The differences between cholera toxin subunit B and Fluorogold. PLoS One, 13(10), e0205133.

Yoshida, K., Drew, M. R., Mimura, M., & Tanaka, K. F. (2019). Serotonin-mediated inhibition of ventral hippocampus is required for sustained goal-directed behavior. Nat Neurosci, 22(5), 770-777. doi:10.1038/s41593-019-0376-5

Zanetti, L., de Kerchove D'Exaerde, A., Zanardi, A., Changeux, J. P., Picciotto, M. R., & Zoli, M. (2006). Inhibition of both alpha7* and beta2* nicotinic acetylcholine receptors is necessary to prevent development of sensitization to cocaine-elicited increases in extracellular dopamine levels in the ventral striatum. Psychopharmacol, 187(2), 181-188. doi:10.1007/s00213-006-0419-y

Zanetti, L., Picciotto, M. R., & Zoli, M. (2007). Differential effects of nicotinic antagonists perfused into the nucleus accumbens or the ventral tegmental area on cocaine-induced dopamine release in the nucleus accumbens of mice. Psychopharmacol, 190(2), 189-199.

Zappettini, S., Grilli, M., Salamone, A., Fedele, E., & Marchi, M. (2010). Pre-synaptic nicotinic receptors evoke endogenous glutamate and aspartate release from hippocampal synaptosomes by way of distinct coupling mechanisms. Brit J Pharmacol, 161(5), 1161-1171.

Zappettini, S., Grilli, M., Olivero, G., Chen, J., Padolecchia, C., Pittaluga, A., Tomé, A. R., Cunha, R. A., & Marchi, M. (2014). Nicotinic α7 receptor activation selectively potentiates the function of NMDA receptors in glutamatergic terminals of the nucleus accumbens. Front Cell Neurosci, 8, 332.

Zhao, Y., Araki, S., Wu, J., Teramoto, T., Chang, Y.-F., Nakano, M., Abdelfattah, A. S., Fujiwara, M., Ishihara, T., & Nagai, T. (2011). An expanded palette of genetically encoded Ca2+ indicators. Sci, 333(6051), 1888-1891.

Zhou, Y., Zhu, H., Liu, Z., Chen, X., Su, X., Ma, C., Tian, Z., Huang, B., Yan, E., Liu, X., & Ma, L. (2019). A ventral CA1 to nucleus accumbens core engram circuit mediates conditioned place preference for cocaine. Nat Neurosci, 22(12), 1986-1999. doi:10.1038/s41593-019-0524-y

Ziminski, J. J., Sieburg, M. C., Margetts-Smith, G., Crombag, H. S., & Koya, E. (2018). Regional differences in striatal neuronal ensemble excitability following cocaine and extinction memory retrieval in Fos-GFP mice. Neuropsychopharmacol, 43(4), 718-727. doi:10.1038/npp.2017.101

Zoli, M., Jansson, A., Syková, E., Agnati, L. F., & Fuxe, K. (1999). Volume transmission in the CNS and its relevance for neuropsychopharmacology. Trends Pharmacol Sci, 20(4), 142-150.